

processes

Special Issue Reprint

Fermentation and Bioprocess Engineering Processes

Edited by
Ali Demirci, Irfan Turhan and Ehsan Mahdinia

mdpi.com/journal/processes



Fermentation and Bioprocess Engineering Processes

Fermentation and Bioprocess Engineering Processes

Guest Editors

Ali Demirci

Irfan Turhan

Ehsan Mahdinia



Basel • Beijing • Wuhan • Barcelona • Belgrade • Novi Sad • Cluj • Manchester

Guest Editors

Ali Demirci
Department of Agricultural
and Biological Engineering
Pennsylvania State University
University Park
USA

Irfan Turhan
Department of Food
Engineering
Akdeniz University
Antalya
Türkiye

Ehsan Mahdinia
Pharma & Biotech
Mettler-Toledo Process
Analytics Inc.
Billerica
USA

Editorial Office

MDPI AG
Grosspeteranlage 5
4052 Basel, Switzerland

This is a reprint of the Special Issue, published open access by the journal *Processes* (ISSN 2227-9717), freely accessible at: <http://www.mdpi.com>.

For citation purposes, cite each article independently as indicated on the article page online and as indicated below:

Lastname, A.A.; Lastname, B.B. Article Title. <i>Journal Name</i> Year , <i>Volume Number</i> , Page Range.
--

ISBN 978-3-7258-3491-4 (Hbk)

ISBN 978-3-7258-3492-1 (PDF)

<https://doi.org/10.3390/books978-3-7258-3492-1>

Cover illustration design by Xinyi Huang

© 2025 by the authors. Articles in this book are Open Access and distributed under the Creative Commons Attribution (CC BY) license. The book as a whole is distributed by MDPI under the terms and conditions of the Creative Commons Attribution-NonCommercial-NoDerivs (CC BY-NC-ND) license (<https://creativecommons.org/licenses/by-nc-nd/4.0/>).

Contents

About the Editors vii

Ali Demirci, Irfan Turhan and Ehsan Mahdinia
Fermentation and Bioprocess Engineering Processes
Reprinted from: *Processes* 2025, 13, 598, <https://doi.org/10.3390/pr13030598> 1

Julius G. Akinbomi, Regina J. Patinvoh, Omotoyosi S. Atunrase, Benjamin C. Onyenuwe, Chibuike N. Emereonye, Joshua F. Ajeigbe and Mohammad J. Taherzadeh
Evaluating Potentials of Activated Carbon, Inoculum Diversity, and Total Solids Content for Improved Digestate Quality in Anaerobic Food Waste Treatment
Reprinted from: *Processes* 2025, 13, 382, <https://doi.org/10.3390/pr13020382> 4

Fujunzhu Zhao, Zhiwu Wang and Haibo Huang
Physical Cell Disruption Technologies for Intracellular Compound Extraction from Microorganisms
Reprinted from: *Processes* 2024, 12, 2059, <https://doi.org/10.3390/pr12102059> 19

Mariana Albino, Carina L. Gargalo, Gisela Nadal-Rey, Mads O. Albæk, Ulrich Krühne and Krist V. Gernaey
Hybrid Modeling for On-Line Fermentation Optimization and Scale-Up: A Review
Reprinted from: *Processes* 2024, 12, 1635, <https://doi.org/10.3390/pr12081635> 46

Rahul Thunuguntla, Hasan K. Atiyeh, Raymond L. Huhnke and Ralph S. Tanner
Characterizing Novel Acetogens for Production of C2–C6 Alcohols from Syngas
Reprinted from: *Processes* 2024, 12, 142, <https://doi.org/10.3390/pr12010142> 64

Ilias Diamantis, Seraphim Papanikolaou, Savvoula Michou, Vassilios Anastasopoulos and Panagiota Diamantopoulou
Yeast Lipids from Crude Glycerol Media and Utilization of Lipid Fermentation Wastewater as Maceration Water in Cultures of Edible and Medicinal Mushrooms
Reprinted from: *Processes* 2023, 11, 3178, <https://doi.org/10.3390/pr11093178> 81

Xin Tang, Bulei Wang, Bingyong Mao, Jianxin Zhao, Guangrong Liu, Kaiye Yang and Shumao Cui
Screening of Microbial Strains Used to Ferment *Dendrobium officinale* to Produce Polysaccharides, and Investigation of These Polysaccharides' Skin Care Effects
Reprinted from: *Processes* 2023, 11, 2563, <https://doi.org/10.3390/pr11092563> 100

Kubra Tarhan Kuzu, Gamze Aykut, Serap Tek, Ercan Yatmaz, Mustafa Germec, Ibrahim Yavuz and Irfan Turhan
Production and Characterization of Kombucha Tea from Different Sources of Tea and Its Kinetic Modeling
Reprinted from: *Processes* 2023, 11, 2100, <https://doi.org/10.3390/pr11072100> 113

Neha Lal, Mostafa Seifan and Aydin Berenjian
Fermentation of Menaquinone-7: The Influence of Environmental Factors and Storage Conditions on the Isomer Profile
Reprinted from: *Processes* 2023, 11, 1816, <https://doi.org/10.3390/pr11061816> 129

Attia Iram, Ali Ozcan, Irfan Turhan and Ali Demirci
Production of Value-Added Products as Food Ingredients via Microbial Fermentation
Reprinted from: *Processes* 2023, 11, 1715, <https://doi.org/10.3390/pr11061715> 145

Can Liu, Ahamed Ullah, Xin Gao and Jian Shi

Synergistic Ball Milling–Enzymatic Pretreatment of Brewer’s Spent Grains to Improve Volatile Fatty Acid Production through Thermophilic Anaerobic Fermentation

Reprinted from: *Processes* **2023**, *11*, 1648, <https://doi.org/10.3390/pr11061648> **172**

About the Editors

Ali Demirci

Dr. Ali Demirci is a Professor of Agricultural and Biological Engineering at The Pennsylvania State University, USA. He received his Ph.D. in Food Science and Technology with a minor in Chemical Engineering at Iowa State University, USA, in 1992. He joined The Pennsylvania State University in 1999, and today, he is serving as the Professor-in-Charge of the CSL Behring Fermentation Facility at Penn State. His research involves bioprocessing/fermentation processes for the production of value-added products via microbial fermentation as well as inactivation/control of pathogenic microorganisms in foods and the environment by novel non-thermal processing methods. He holds two U.S. patents and has authored or co-authored over 180 refereed journal articles and 40 book chapters, and has edited 3 books. He has delivered numerous presentations at regional, national, and international conferences.

Irfan Turhan

Dr. Irfan Turhan received his Ph.D. in Food Engineering from Akdeniz University, Türkiye, in 2009. He worked as a Research Assistant in the Department of Food Engineering at Akdeniz University between 2005 and 2009. He was a visiting scholar at The Pennsylvania State University, USA, between 2007 and 2008. After graduating from the same university, he then worked in the same department as an Assistant/Associate Professor. He was later promoted to Professor in 2021. His teaching and research focus on Bioprocess Engineering includes the fermentation of fruit and vegetables or its waste, fermentor design, enzyme technology, bioprocess separations, scale-up of analytical separation methods, conversion of batch processes to continuous processes, and integrated fermentation/recovery systems. He has authored or co-authored around 90 refereed journal articles, numerous conference papers, and one book chapter, translated one technical book, and delivered numerous presentations at regional, national, and international conferences.

Ehsan Mahdinia

Dr. Ehsan Mahdinia is responsible for Global Industry Management for Pharma, Biotech, Cosmetics, and Flavors and Fragrances at Mettler-Toledo Process Analytics. Ehsan holds a Ph.D. in Microbiological Engineering awarded by the Agricultural and Biological Engineering Department of The Pennsylvania State University, USA. He also earned a master's degree in Biotechnology from the Department of Chemical and Petroleum Engineering of the Sharif University of Technology, Iran. Previously, he was the Director of the Masters of Biomanufacturing and Bioprocessing program at the Stack Family Center for Biopharmaceutical Education and Training (CBET), where he also helped lay the foundations as one of the founding faculty members for CBET. Ehsan simultaneously served as an Assistant Professor at the Departments of Basic and Clinical Sciences and Pharmaceutical Sciences at the Albany College of Pharmacy and Health Sciences before joining Mettler-Toledo Process Analytics, Inc.

Fermentation and Bioprocess Engineering Processes

Ali Demirci ^{1,*}, Irfan Turhan ² and Ehsan Mahdinia ³

¹ Department of Agricultural and Biological Engineering, Pennsylvania State University, University Park, PA 16802, USA

² Department of Food Engineering, Akdeniz University, Antalya 07058, Türkiye; iturhan@akdeniz.edu.tr

³ Pharma & Biotech, Mettler-Toledo Process Analytic Inc., 900 Middlesex Turnpike, Building 8, Billerica, MA 01821, USA; ehsan.mahdinia@mt.com

* Correspondence: demirci@psu.edu

Valorization of waste materials into valuable resources through biotechnological methods has received great attention in recent years due to sustainability and environmental concerns. This approach is also compatible with the principles of the circular economy, where waste is seen as a potential raw material for the production of high-value products. The early stages of these approaches usually involve processes such as fermentation and microbial transformation, which offer promising solutions to environmental problems. The term fermentation refers to practices that employ microbial cells as factories to produce value-added products, and the practical application of fermentation goes back as far as the beginnings of human-recorded history; long before cells were even discovered as units of life!

However, microbial bioprocesses are still sometimes considered modern inventions since the advanced biomanufacturing industry is now utilizing recombinant technologies that emerged in the 80s and the bioreactor designs in large-scale stainless-steel vessels that came about shortly before that. Today, after only a few decades, microbial fermentation has become the foundation of a thriving biotech industry with production at an impressive large scale.

Many food or agricultural wastes are converted into biogas through anaerobic digestion. Similarly, syngas fermentation utilizes microbial electrocatalysts to convert gasified biomass into alcohols. Thus, a suitable alternative path for sustainable biofuel production emerges. It is part of a growing trend to utilize microbial fermentation to recycle waste substrates, such as fatty acids from wastewater and organic residues in mushroom cultivation, into useful products.

Additionally, the production of bioactive compounds such as polysaccharides, menaquinone-7, and natural flavors through microbial fermentation shows that fermentation technology can be used in many areas. This method offers environmentally friendly production routes that support the food, pharmaceutical, and cosmetic industries. Techniques such as thermophilic anaerobic fermentation and online fermentation optimization reflect advances in bioprocess efficiency by adapting fermentation conditions in real time to accommodate industrial scale-up.

This Special Issue has, therefore, been undertaken to provide some updates in this area. As a result, several novel approaches and cutting-edge research are featured, all at the frontiers of different sectors of biotech and employing microbial fermentation.

- Across Agricultural Biotech (Green Biotechnology), studies here have investigated physicochemical methods to improve efficiency of anaerobic digestors employed for food waste valorization and the production of biofertilizers. Other researchers looked

Received: 10 February 2025

Revised: 14 February 2025

Accepted: 17 February 2025

Published: 20 February 2025

Citation: Demirci, A.; Turhan, I.; Mahdinia, E. Fermentation and Bioprocess Engineering Processes. *Processes* **2025**, *13*, 598. <https://doi.org/10.3390/pr13030598>

Copyright: © 2025 by the authors. Licensee MDPI, Basel, Switzerland. This article is an open access article distributed under the terms and conditions of the Creative Commons Attribution (CC BY) license (<https://creativecommons.org/licenses/by/4.0/>).

into wastewater valorization of mushroom cultures to enhance lipid fermentation in yeast. Complementing their efforts, another study illustrated the benefits of pretreating brewers' spent grain to improve volatile fatty acid production through thermophilic anaerobic fermentation [1–3].

- Looking into Industrial Biotech (White Biotechnology), our colleagues characterized novel acetogens to produce C2–C6 alcohols from syngas [4,5].
- In Food Biotech (Yellow Biotechnology), the research teams produced and characterized Kombucha tea from different sources of tea and were able to model kinetics of its production [6–8].
- As an effort in Nutraceuticals Biotech (Orange Biotechnology), fermentation of Menaquinone-7 (vitamin K2) was reviewed and the influence of environmental factors and storage conditions on the isomer profile was highlighted [9,10].
- And finally, in Pharma Biotech (Red Biotechnology) researchers screened *Bacillus* strains to ferment *Dendrobium officinale* into polysaccharides and, furthermore, investigate these polysaccharides for skincare applications [11,12].

This convergence of waste utilization and microbial synthesis demonstrates the potential for innovation in the field of biotechnology that promotes resource efficiency and environmental sustainability. Through optimized fermentation strategies and bioprocessing technologies, the aim is to facilitate the creation of value-added products, increase economic sustainability and reduce our ecological footprint. Ongoing research and development in these areas holds the promise of transforming industries by increasing resilience in the face of global sustainability challenges.

Conflicts of Interest: The authors declare no conflict of interest.

List of Contributions

1. Akinbomi, J.G.; Patinvoh, R.J.; Atunrase, O.S.; Onyenuwe, B.C.; Emereonye, C.N.; Ajeigbe, J.F.; Taherzadeh, M.J. Evaluating Potentials of Activated Carbon, Inoculum Diversity, and Total Solids Content for Improved Digestate Quality in Anaerobic Food Waste Treatment. *Processes* **2025**, *13*, 382. <https://doi.org/10.3390/pr13020382>.
2. Thunuguntla, R.; Atiyeh, H.K.; Huhnke, R.L.; Tanner, R.S. Characterizing Novel Acetogens for Production of C2–C6 Alcohols from Syngas. *Processes* **2024**, *12*, 142. <https://doi.org/10.3390/pr12010142>.
3. Diamantis, I.; Papanikolaou, S.; Michou, S.; Anastasopoulos, V.; Diamantopoulou, P. Yeast Lipids from Crude Glycerol Media and Utilization of Lipid Fermentation Wastewater as Maceration Water in Cultures of Edible and Medicinal Mushrooms. *Processes* **2023**, *11*, 3178. <https://doi.org/10.3390/pr11113178>.
4. Tang, X.; Wang, B.; Mao, B.; Zhao, J.; Liu, G.; Yang, K.; Cui, S. Screening of Microbial Strains Used to Ferment *Dendrobium officinale* to Produce Polysaccharides, and Investigation of These Polysaccharides' Skin Care Effects. *Processes* **2023**, *11*, 2563. <https://doi.org/10.3390/pr11092563>.
5. Tarhan Kuzu, K.; Aykut, G.; Tek, S.; Yatmaz, E.; Germec, M.; Yavuz, I.; Turhan, I. Production and Characterization of Kombucha Tea from Different Sources of Tea and Its Kinetic Modeling. *Processes* **2023**, *11*, 2100. <https://doi.org/10.3390/pr11072100>.
6. Lal, N.; Seifan, M.; Berenjian, A. Fermentation of Menaquinone-7: The Influence of Environmental Factors and Storage Conditions on the Isomer Profile. *Processes* **2023**, *11*, 1816. <https://doi.org/10.3390/pr11061816>.
7. Liu, C.; Ullah, A.; Gao, X.; Shi, J. Synergistic Ball Milling–Enzymatic Pretreatment of Brewers' Spent Grains to Improve Volatile Fatty Acid Production through Thermophilic Anaerobic Fermentation. *Processes* **2023**, *11*, 1648. <https://doi.org/10.3390/pr11061648>.
8. Zhao, F.; Wang, Z.; Huang, H. Physical Cell Disruption Technologies for Intracellular Compound Extraction from Microorganisms. *Processes* **2024**, *12*, 2059. <https://doi.org/10.3390/pr12102059>.

9. Albino, M.; Gargalo, C.L.; Nadal-Rey, G.; Albæk, M.O.; Krühne, U.; Gernaey, K.V. Hybrid Modeling for On-Line Fermentation Optimization and Scale-Up: A Review. *Processes* **2024**, *12*, 1635. <https://doi.org/10.3390/pr12081635>.
10. Iram, A.; Ozcan, A.; Turhan, I.; Demirci, A. Production of Value-Added Products as Food Ingredients via Microbial Fermentation. *Processes* **2023**, *11*, 1715. <https://doi.org/10.3390/pr11061715>.

References

1. Sekar, M.; Mathimani, T.; Alagumalai, A.; Chi, N.T.L.; Duc, P.A.; Bhatia, S.K.; Brindhadevi, K.; Pugazhendhi, A. A review on the pyrolysis of algal biomass for biochar and bio-oil—Bottlenecks and scope. *Fuel* **2021**, *283*, 119190. [CrossRef]
2. Shin, T.S.; Yoo, S.Y.; Kang, I.K.; Kim, N.; Kim, S.; Lim, H.B.; Choe, K.; Lee, J.C.; Yang, H.I. Analysis of Hydrothermal Solid Fuel Characteristics Using Waste Wood and Verification of Scalability through a Pilot Plant. *Processes* **2022**, *10*, 2315. [CrossRef]
3. Sun, X.; Atiyeh, H.K.; Zhang, H.; Tanner, R.S.; Huhnke, R.L. Enhanced ethanol production from syngas by *Clostridium ragsdalei* in continuous stirred tank reactor using medium with poultry litter biochar. *Appl. Energy* **2019**, *236*, 1269–1279. [CrossRef]
4. Doyle, D.A.; Smith, P.R.; Lawson, P.A.; Tanner, R.S. *Clostridium muellerianum* sp. nov., a carbon monoxide-oxidizing acetogen isolated from old hay. *Int. J. Syst. Evol. Microbiol.* **2022**, *72*, 005297. [CrossRef] [PubMed]
5. Ratledge, C.; Cohen, Z. Microbial and algal oils: Do they have a future for biodiesel or as commodity oils. *Lipid Technol.* **2008**, *20*, 155–160. [CrossRef]
6. Qin, L.; Liu, L.; Zeng, A.-P.; Wei, D. From low-cost substrates to single cell oils synthesized by oleaginous yeasts. *Bioresour. Technol.* **2017**, *245*, 1507–1519. [CrossRef] [PubMed]
7. Yu, G.; Xie, Q.; Su, W.; Dai, S.; Deng, X.; Gu, Q.; Liu, S.; Yun, J.; Xiang, W.; Xiong, Y. Improvement of antioxidant activity and active ingredient of *Dendrobium officinale* via microbial fermentation. *Front. Microbiol.* **2023**, *14*, 1061970. [CrossRef] [PubMed]
8. Greenwalt, C.; Steinkraus, K.; Ledford, R. Kombucha, the fermented tea: Microbiology, composition, and claimed health effects. *J. Food Prot.* **2000**, *63*, 976–981. [CrossRef] [PubMed]
9. Berenjian, A.; Mahanama, R.; Talbot, A.; Biffin, R.; Regtop, H.; Valtchev, P.; Kavanagh, J.; Dehghani, F. Efficient media for high menaquinone-7 production: Response surface methodology approach. *New Biotechnol.* **2011**, *28*, 665–672. [CrossRef] [PubMed]
10. Mahdinia, E.; Demirci, A.; Berenjian, A. Production and application of menaquinone-7 (vitamin K2): A new perspective. *World J. Microbiol. Biotechnol.* **2017**, *33*, 2. [CrossRef] [PubMed]
11. Nfor, B.K.; Ahamed, T.; van Dedem, G.W.; van der Wielen, L.A.; van de Sandt, E.J.; Eppink, M.H.; Ottens, M. Design strategies for integrated protein purification processes: Challenges, progress and outlook. *J. Chem. Technol. Biotechnol.* **2008**, *83*, 124–132. [CrossRef]
12. Pigou, M.; Morchain, J. Investigating the interactions between physical and biological heterogeneities in bioreactors using compartment, population balance and metabolic models. *Chem. Eng. Sci.* **2015**, *126*, 267–282. [CrossRef]

Disclaimer/Publisher’s Note: The statements, opinions and data contained in all publications are solely those of the individual author(s) and contributor(s) and not of MDPI and/or the editor(s). MDPI and/or the editor(s) disclaim responsibility for any injury to people or property resulting from any ideas, methods, instructions or products referred to in the content.

Article

Evaluating Potentials of Activated Carbon, Inoculum Diversity, and Total Solids Content for Improved Digestate Quality in Anaerobic Food Waste Treatment

Julius G. Akinbomi¹, Regina J. Patinvoh¹, Omotoyosi S. Atunrase¹, Benjamin C. Onyenuwe¹, Chibuikwe N. Emereonye¹, Joshua F. Ajeigbe¹ and Mohammad J. Taherzadeh^{2,*}

¹ Department of Chemical Engineering, Faculty of Engineering, Lagos State University Ojo, Lagos 100268, Nigeria; julius.akinbomi@lasu.edu.ng (J.G.A.); queenpat6@gmail.com (R.J.P.); omotoyosiaturase@gmail.com (O.S.A.); onyenuweben@gmail.com (B.C.O.); emereonyenoel50@gmail.com (C.N.E.); ajeigbef@gmail.com (J.F.A.)

² Swedish Centre for Resource Recovery, University of Borås, 50190 Borås, Sweden

* Correspondence: mohammad.taherzadeh@hb.se; Tel.: +46-(0)33-435-5908

Abstract: The potential presence of toxic compounds in the digestate obtained from the anaerobic digestion of biodegradable waste restricts its application as a biofertilizer for soil conditioning and plant growth enhancement. The aim of this study was to assess digestate quality in terms of plant nutrient composition by evaluating the effects of activated carbon supplementation, inoculum source, and total solids content in the anaerobic digestion medium. The anaerobic digestion of food waste was conducted over a 60-day period at 25 °C in a 2.5 L bioreactor. The results demonstrated that inoculum diversity significantly impacted the digestate composition, particularly the zinc nutrient, with a *p*-value of 0.0054. This suggests that microbial diversity influences the valorization of organic waste into biofertilizer. However, the effects of inoculum diversity on other nutrients, aside from zinc, were not significant due to substantial interaction effects. Furthermore, assessing the impact of activated carbon supplementation proved challenging, as it was analyzed as part of a subset of the other two factors. The results of the digestate composition analysis indicated that activated carbon supplementation exhibited some influence on nutrient composition, necessitating further research to elucidate its significance. The findings of this study may contribute to enhancing the quality of digestate as a biofertilizer.

Keywords: anaerobic digestion; food wastes; total solids; activated carbon; digestates; toxicity; biofertilizer

Academic Editors: Ali Demirci, Irfan Turhan and Ehsan Mahdinia

Received: 31 December 2024

Revised: 24 January 2025

Accepted: 27 January 2025

Published: 30 January 2025

Citation: Akinbomi, J.G.; Patinvoh, R.J.; Atunrase, O.S.; Onyenuwe, B.C.; Emereonye, C.N.; Ajeigbe, J.F.; Taherzadeh, M.J. Evaluating

Potentials of Activated Carbon, Inoculum Diversity, and Total Solids Content for Improved Digestate Quality in Anaerobic Food Waste Treatment. *Processes* **2025**, *13*, 382.

<https://doi.org/10.3390/pr13020382>

Copyright: © 2025 by the authors. Licensee MDPI, Basel, Switzerland. This article is an open access article distributed under the terms and conditions of the Creative Commons Attribution (CC BY) license (<https://creativecommons.org/licenses/by/4.0/>).

1. Introduction

The global food production rate is approaching a critical juncture where it will no longer be able to sustain the exponential population growth. This situation presents a significant risk of widespread hunger and malnutrition, affecting a large portion of the global population. According to the United Nations' 2030 Agenda for Sustainable Development Goals (SDGs), approximately 821 million people worldwide were chronically undernourished in 2017, while 148 million children were malnourished in 2022 [1–4]. By 2030, it is projected that around 600 million people globally will face acute hunger [1–4]. This alarming statistic can be directly attributed to the adverse effects of environmental degradation, drought, and biodiversity loss. The mismanagement of generated waste and the excessive use of inorganic or synthetic fertilizers can lead to environmental degradation, drought, and biodiversity loss, which negatively impact the social, economic, and

environmental sustainability of a country. Burning or landfilling waste is a common yet environmentally harmful method that many developing countries use for waste disposal. Additionally, farmers heavily rely on synthetic or inorganic fertilizers for soil conditioning to enhance plant growth and productivity. While the use of synthetic fertilizers can increase food production, excessive application is associated with adverse effects such as soil and crop degradation, human health risks, groundwater contamination from leached nutrients, and increased crop susceptibility to diseases. Clearly, burning and landfilling waste, along with the excessive use of synthetic fertilizers, are unsustainable practices that hinder the achievement of sustainable development in any country [5].

One sustainable technique for addressing the challenges mentioned above is the adoption of anaerobic digestion (AD) technology [6,7]. AD is a process that breaks down biodegradable or organic waste in the absence of oxygen through microbial activity. This process produces biogas and digestate, which can be used for energy and soil conditioning, respectively. Anaerobic digestion technology can effectively serve as a waste management solution, converting waste into valuable resources such as biogas (an energy source) and digestate (as a biofertilizer). Anaerobic digestate is the liquid residue from the anaerobic digestion of organic materials. It contains undigested feedstock, microbial biomass, and their metabolites. Organic materials, such as food waste, contain nutrients (both macro- and micronutrients) that are released and stored as digestate components during the digestion process. Therefore, applying digestate as a biofertilizer offers several benefits, including soil amendments and improved crop productivity, without the associated health risks. Utilizing digestate as a biofertilizer also conserves resources that would otherwise be used in the production of inorganic chemical fertilizers. Unlike inorganic fertilizers, digestate is an organic alternative that enhances soil organic matter and microbial content, improves soil bulk density and fertility, and increases the nutrient and water absorption capacity of plants. Additionally, applying digestate for soil conditioning supports carbon sequestration, contributing to the mitigation of global warming.

The nutrient composition of soil plays a crucial role in the effectiveness of soil fertilization and crop productivity. Plants require a total of eighteen essential elements to support their growth, development, and overall health. These elements include both non-mineral nutrients, such as carbon, hydrogen, and oxygen, which plants acquire directly from atmospheric carbon dioxide and water, and various mineral nutrients absorbed from soil. These essential elements are categorized based on the quantities needed by plants: primary macronutrients, secondary or major nutrients, and micronutrients. The primary macronutrients—nitrogen (N), phosphorus (P), and potassium (K)—are required in the largest amounts and are fundamental to several key physiological processes. Nitrogen is vital for protein synthesis, chlorophyll formation, and overall plant growth; phosphorus is essential for energy transfer via ATP (adenosine triphosphate), root development, and photosynthesis; and potassium is necessary for regulating various metabolic processes, including carbohydrate and starch synthesis, enzyme activation, and maintaining water balance within plant cells [8].

Secondary or major nutrients include calcium (Ca), magnesium (Mg), and sulfur (S). Although these elements are required in smaller quantities than primary macronutrients, they are equally important. Calcium contributes to soil improvement by facilitating soil aggregation and enhancing nutrient uptake and cell wall development within the plant. Magnesium is a central component of the chlorophyll molecule, which is essential for photosynthesis, and also acts as a cofactor in numerous enzymatic reactions. Sulfur is involved in the synthesis of amino acids, proteins, and vitamins and plays a role in enzyme function and chlorophyll formation. Micronutrients include elements such as boron (B), chlorine (Cl), copper (Cu), iron (Fe), manganese (Mn), molybdenum (Mo), cobalt (Co),

nickel (Ni), and zinc (Zn), which are required only in trace amounts but are indispensable for various biochemical and physiological functions. For example, iron is crucial for chlorophyll synthesis and acts as a catalyst in several enzymatic reactions; zinc plays a role in protein synthesis, growth regulation, and hormone production; and manganese is involved in photosynthesis, nitrogen metabolism, and the formation of essential enzymes. These nutrients are absorbed from soil through the plant's root system, and for optimal plant growth, it is essential that all macronutrients are present in adequate quantities and balanced proportions. Sufficient nitrogen levels, for example, ensure robust vegetative growth; adequate phosphorus supports strong root systems and efficient energy transfer; and sufficient potassium enhances the plant's ability to synthesize carbohydrates and starches, which are critical for energy storage and structural integrity [9]. While secondary nutrients are needed in smaller amounts, they still play a significant role in plant health by facilitating processes such as soil acidification (calcium), photosynthetic efficiency (magnesium), and protein synthesis (sulfur). Micronutrients, though required only in trace amounts [10], are vital for specific enzymatic activities and overall plant metabolism. Given the complexity and interdependence of these nutrients, it is crucial that any fertilizer used—whether synthetic or organic, including digestate—contains the appropriate concentrations of these essential elements. This ensures that plants receive a balanced supply of nutrients necessary for healthy growth, optimal agricultural productivity, and soil health maintenance. Effective nutrient management through balanced fertilization is fundamental to sustainable farming practices and helps prevent nutrient deficiencies or toxicities that can negatively affect plant health and crop yields.

Meanwhile, the inorganic nutrients (such as nitrogen, phosphorus, and potassium) present in the digestate after the anaerobic digestion process are often the same as those found in the feedstock used during digestion, since microorganisms primarily degrade the organic or carbon component of the feedstock. As a result, the quality of digestate as a biofertilizer depends on its composition, which in turn is influenced by both the feedstock composition and the conditions of the anaerobic digestion process. However, it is important to note that digestate may contain toxic compounds, such as heavy metals (e.g., palladium, cadmium, chromium, nickel, copper, and zinc) and organic contaminants (e.g., monocyclic aromatics, polychlorinated dibenzodioxins, polychlorinated dibenzofurans, phthalic acid esters, organochlorinated pesticides, chlorobenzenes, amines, nitrosamines, and phenols). Ideally, digestate should be free from toxic substances that could lead to soil degradation or impede crop growth. Therefore, it is crucial to minimize the release of toxic substances from both the feedstock and the anaerobic digestion process. As a result, various techniques have been employed in previous studies to enhance digestate quality, including the use of specialized digesters [11], nitrification processes [12,13], struvite precipitation [14] to reduce high levels of ammonium ions (NH_4^+), and dilution or biochar methods to mitigate sodium chloride and NH_4^+ toxicity [15–17] in digestate products.

The activated carbon supplementation of the digestion media or vermicomposting of the digestate prior to its application as a biofertilizer can effectively remove toxic compounds from the digestate, thereby ensuring that humans and animals are not exposed to contaminated plants and water. Activated carbon has been extensively studied for its ability to adsorb inhibitory compounds. It has also been shown that activated carbon supplementation enhances the stability of anaerobic digestion operations, increases methane production, and improves the removal of color from digestates produced during the digestion process [18–21]. Additionally, the solid content, or total solids, of the biodegradable substrate is a crucial factor that influences anaerobic digestion. The total solids content in biodegradable wastes can range from low to high, depending on whether it is less than or equal to 10% or greater than or equal to 20%, respectively [22]. While low-solid anaerobic

digestion is commonly practiced, high-solid anaerobic digestion is becoming more popular due to its associated benefits, such as water conservation and a smaller digester footprint. However, high-solid AD processes can affect stability and performance if not properly managed. The success of the AD process depends on how well various influencing factors are managed, including temperature, pressure, pH, inhibitors, organic loading rate, retention time, and others. Furthermore, the importance of inoculum in the anaerobic digestion process cannot be overstated, as it provides the microorganisms necessary for improving substrate biodegradability and converting it into products like digestate [23,24].

Limited research has been conducted on the influence of inoculum diversity, digestion type (high- or low-solid digestion), and activated carbon supplementation on the reduction in toxicity (specifically high heavy metal content) in digestate products. Therefore, the primary objectives of this study were to assess the feasibility of using either low- or high-solid anaerobic digestion processes for the valorization of food waste into biofertilizer, investigate the impact of activated carbon supplementation, and examine the effects of various inoculum sources on the digestion process, with a specific focus on improving the quality of the digestate produced. This study investigated how variations in feedstock total solids, inoculum source, and activated carbon supplementation affect digestate quality, particularly in terms of reducing heavy metal content. It is hypothesized that activated carbon, due to its porous structure and capacity to adsorb substances, can help mitigate the concentration of toxic compounds in digestate. Typically, farmers are reluctant to use digestate as a biofertilizer due to concerns that it may contain toxic compounds, such as heavy metals and certain organic substances, which could negatively impact crop growth. The presence of these toxic compounds presents a challenge for the widespread use of digestate as a biofertilizer. Therefore, the findings from this study are expected to help develop standard techniques for minimizing digestate toxicity, thereby enhancing its commercial application as a biofertilizer for soil conditioning and crop growth improvement.

2. Materials and Methods

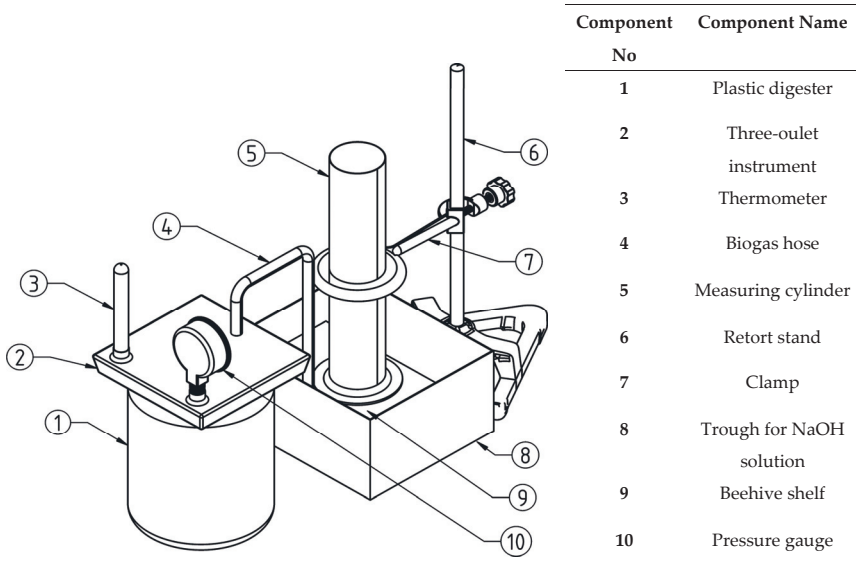
2.1. Materials

The food waste mixture, consisting of vegetable leftovers, rice, and cassava flour, was the main feedstock used for anaerobic digestion. The food waste was collected from various local restaurants around Lagos State University (Epe, Lagos, Nigeria), while the chicken dung used as inoculum was obtained from a local poultry farm. After collection, the food waste was blended and stored in a refrigerator at 4 °C until it was used. Before samples were taken from the food waste and inoculum for experimentation, they were thoroughly mixed to ensure homogeneity. The materials and equipment used in this experiment included a 2.5 L reactor, a 10 L capacity container for initial digestion, a furnace, pressure gauges, gas pipes, hose connectors, gas valves, a blender, measuring bottles, a pH meter, 1 L measuring cylinders, beakers, an oven, desiccators, a beehive shelf, a retort stand, a mixing container, a weighing balance, a trough for holding carbon dioxide (CO₂) solution for gas absorption, Topgit gum, sodium hydroxide (NaOH), and hydrochloric acid (HCl) reagents (Figure 1).

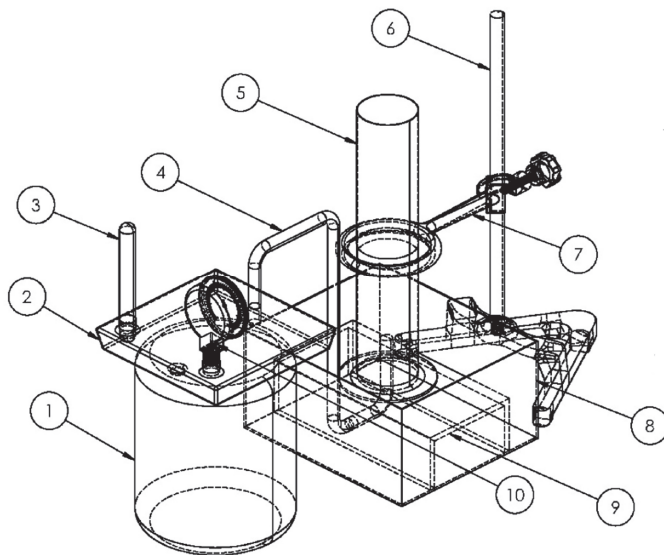
2.2. Experimental Methods

The experimental procedure involved the anaerobic digestion of food waste at 25 °C in a 2.5 L reactor with an active volume of 1.5 L. Three experimental setups—blank, control, and activated carbon supplementation—were studied for comparative analysis. The blank setup contained a fixed mixture of inoculum and water only; the control setup had a fixed mixture of inoculum, food waste, and water; and the activated carbon supplementation setup [25] included a fixed mixture of inoculum, food waste, activated carbon, and water

(Table 1). This study investigated the effects of three factors: total solids, inoculum source, and activated carbon supplementation. Three types of inoculums were used during this experiment: chicken dung, partially digested food waste, and a mixture of chicken dung and partially digested food waste. The partially digested food waste was prepared by placing the waste in a covered 10 L plastic container and allowing it to undergo anaerobic digestion for 30 days.



(a)



(b)

Figure 1. Experimental setup (a) without internals and (b) with internals.

Table 1. Experimental setup measurements.

Inoculum Diversity	Experimental Setups	Low-Solid Anaerobic Digestion				High-Solid Anaerobic Digestion					
		Chicken Dung	Partially Digested Food Waste	Substrate (Food Waste) Mass (g)	Mass Concentration of Activated Carbon (g/dm ³)	Total Solids in Reactor (%)	Chicken Dung	Partially Digested Food Waste	Substrate (Food Waste) Mass (g)	Mass Concentration of Activated Carbon (g/dm ³)	Total Solids in Reactor (%)
(A) With chicken dung as inoculum	with activated carbon	1034.19	0	256.86	15	15.01	1034.19	0	256.86	15	23.97
	without activated carbon	1034.19	0	256.86	0	15.01	1034.19	0	256.86	0	23.97
	blank (inoculum and water)	1034.19	0	0	0	15.03	1034.19	0	0	0	23.75
(B) With chicken dung and partially digested food waste as inoculum	with activated carbon	517.09	316.20	256.86	15	15.00	517.09	316.20	256.86	15	24.12
	without activated carbon	517.09	316.20	256.86	0	15.00	517.09	316.20	256.86	0	24.12
	blank (inoculum and water)	517.09	316.20	0	0	15.03	517.09	316.20	0	0	24.12
(C) With partially digested food waste as inoculum	with activated carbon	0	632.40	256.86	15	14.96	0	632.40	256.86	15	24.16
	without activated carbon	0	632.40	256.86	0	14.96	0	632.40	256.86	0	24.16
	blank (inoculum and water)	0	632.40	0	0	15.07	0	632.40	0	0	24.08

The activated carbon used in this experiment was obtained by chemically activating the carbon black residue from rubber tire pyrolysis. The carbon black produced during the pyrolysis of discarded rubber tires was ground into pellets and subjected to chemical activation using a 2 M potassium hydroxide (KOH) solution. Approximately 200 g of the ground carbon was impregnated with 200 g of 2 M KOH in a 1000 mL measuring cylinder at room temperature for 24 h. After this period, the impregnated material was packed into plastic containers. The digestion medium was supplemented with activated carbon at a mass concentration of 15 g/dm³. The amount of activated carbon used was based on the optimal value used in a research study by Zhang et al. [25]. The surface area of the activated carbon was determined using the Brunauer–Emmett–Teller (BET) equation to calculate the nitrogen quantity required to form a monolayer on the activated carbon surface. Initial contaminants, including water and carbon dioxide (CO₂), on the activated carbon surface were removed by pretreating the carbon with heat and vacuum. After pretreatment, carbon was cooled to cryogenic temperatures under vacuum by dosing it with liquid nitrogen in controlled increments while allowing the pressure to equilibrate [26]. The pore volume and pore size distribution were determined by gradually increasing the gas pressure until all the pores on the activated carbon were filled with liquid. The gas pressure was then reduced to evaporate the condensed gas from the activated carbon. Pore volume and pore size were calculated using methods such as BJH (Barrett–Joyner–Halenda) or DFT (Density Functional Theory) to evaluate the adsorption and desorption isotherms [26].

The components of the different experimental setups were thoroughly mixed and poured into their respective 2.5 L reactors. The total solids in the reactor volume for each experimental setup were approximately 15% for the low-solid anaerobic digestion process and 24% for the high-solid anaerobic digestion process. The pH of each reactor was adjusted to 7.0 using 2 M sodium hydroxide (NaOH) and hydrochloric acid (HCl) solutions. A specialized instrument with three spouts—one for the inlet feed hose, one for the pressure gauge, and one for the gas hose—was used to seal each reactor and ensure airtight connections without any leakage. The gas hose was directed into a 1000 mL measuring cylinder containing distilled water, which was supported by a beehive shelf placed over the cylinder's mouth. The measuring cylinder was carefully inverted and placed in a trough containing a molar NaOH solution. The anaerobic digestion of food waste was conducted as a semi-continuous process for 60 days at 25 °C in a 2.5 L plastic reactor vessel with an active volume of 1.5 L. The experimental assays, which were triplicated for each observation, were allowed to settle for three days before gas production was measured. At specific intervals, gas valves were opened to allow biogas buildup in the digester to escape through the hose into the cylinder. The biogas generated in the reactor passed through the beehive shelf into the cylinder, displacing a corresponding amount of water. The amount of water displaced in the cylinder was equal to the volume of methane gas produced. Since the primary focus of this study was on digestate production, biogas was neither measured nor stored.

2.3. Analytical Methods

The procedure for analyzing the experimental samples was conducted in two phases. The first phase involved the collection of samples of food waste (substrate), inoculum, and carbon black in sample bottles for Brunauer–Emmett–Teller (BET) analysis, Scanning Electron Microscopy–Energy-Dispersive X-ray (SEM-EDX; Thermo Fischer, Waltham, MA, USA) analysis, and proximate analysis, prior to the commencement of the anaerobic digestion process. BET analysis, using a BET surface area analyzer (Quantachrome NOvaWin 1994–2013, version 11.03, UK), was performed to determine the specific surface area, pore size, and pore volume of the activated carbon used [27]. SEM-EDX analysis was employed

to assess the elemental composition of the activated carbon before its supplementation in this experiment [28]. Proximate analysis was conducted to determine the percentage concentration of moisture, ash, ether extract (EE), crude fiber (CF), crude protein (CP), cellulose, hemicellulose, lignin, and total solids content in the inoculum and food waste [29].

The second phase involved the collection of digestate products from the various experimental setups for plant nutrient composition analysis. Analyses for BET, SEM-EDX, and proximate compositions were carried out at the National Animal Production Research Institute, Ahmadu Bello University (Zaria, Nigeria), while plant nutrient composition analysis was performed at Amalab Laboratory Services Limited (Ibadan, Oyo State, Nigeria).

2.4. Statistical Analyses

A two-way ANOVA (analysis of variance) was performed using Excel software (Microsoft® Excel® 2016 MSO, version 2501 Build 16.0.18429.20044) to analyze the results obtained from the experimental work. For the activated carbon factor, there were two levels: with activated carbon (1) and without activated carbon (0). For the total solids content factor, there were two levels: high solid content and low solid content. For the inoculum diversity factor, there were two types of inocula based on the total solids content. For high solid content, the inoculum types were either chicken dung or a mixture of chicken dung and partially digested food waste. For low solid content, the inoculum types were either a mixture of chicken dung and partially digested food waste or just partially digested food waste.

The two-way ANOVA was used to determine whether total solids content or inoculum diversity influenced differences in digestate nutrient composition and to identify any interaction effects between the two factors. Total solids content and inoculum diversity were the two main factors analyzed, while the third factor (activated carbon supplementation) was treated as a subset of the other two factors. A pre-determined alpha (α)-level of 0.05 was selected as the criterion for determining whether the effect of each factor was significant. If the p -value was less than or equal to the alpha (α)-level of 0.05, the effect of the factor was considered significant, indicating that the means for that factor were significantly different. Conversely, if the p -value was greater than 0.05, the effect of the factor was deemed not significant. Additionally, if the interaction effect was significant ($p < 0.05$), this suggested that the effects of each factor were different at varying levels of the other factor, meaning the individual effects were not independent.

3. Results and Discussion

The primary objective of this study was to determine the influence of total solids content, inoculum source, and activated carbon supplementation on the quality of digestate products, with a specific focus on the composition of plant nutrients.

3.1. Effects of Total Solids on Digestate Composition

The effects of total solids content, inoculum source, and activated carbon supplementation on digestate quality in relation to plant nutrient compositions were evaluated through a semi-continuous anaerobic digestion process of food waste over a 60-day period at 25 °C in a 2.5 L plastic reactor vessel with an active volume of 1.5 L. The analysis used to determine the percentage concentration of moisture, ash, ether extract, crude fiber, crude protein, cellulose, hemicellulose, lignin, and total solids content of the inoculum and food waste is presented in Figure 2. The results showed that food waste comprised both organic and inorganic components. The organic component consisted of the digestible portion (volatile solids: 29.70% and ether extract or crude lipids: 22.18%), while the non-digestible portion included crude fiber (2.70%), cellulose (2.23%), hemicellulose (1.66%), and lignin

(1.30%). The inorganic component included crude protein (total nitrogen: 4.25%) and ash (1.13%). The total solids content in the food waste was 31.38%, indicating a substantial amount of substrate available for conversion into valuable resources, such as digestate (biofertilizer). The digestate products included both digested and undigested feedstock components, as well as microbial biomass produced during the anaerobic digestion process.

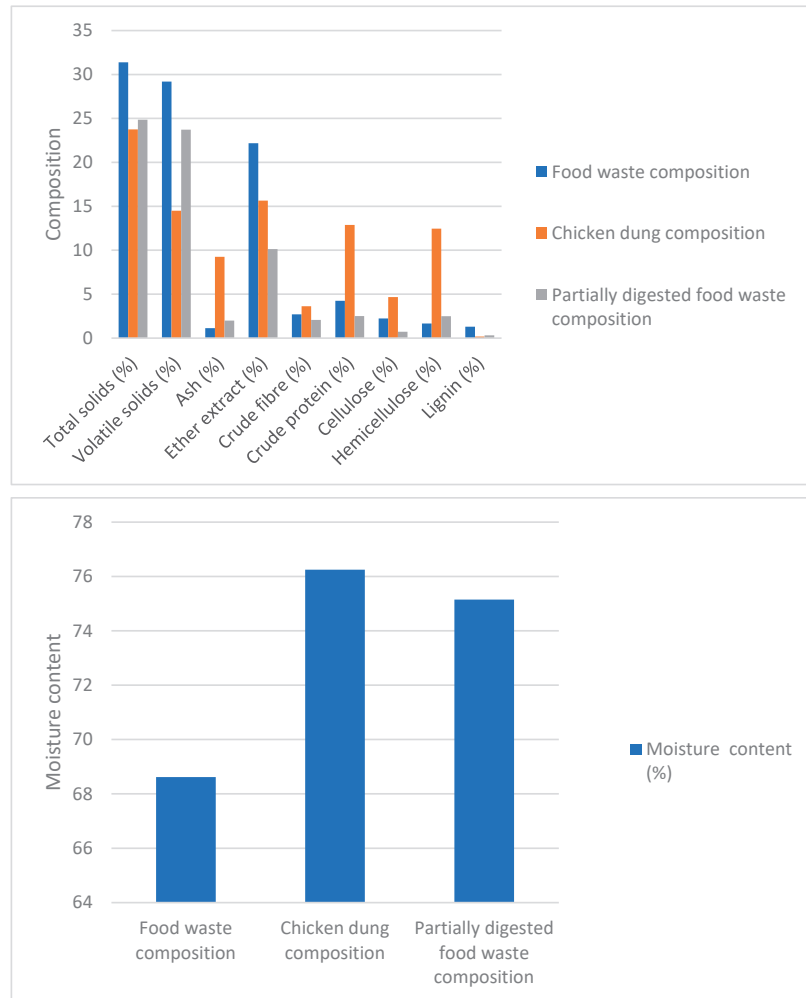


Figure 2. Compositions of food waste and inoculum used in this study.

Table 2 presents the nutrient compositions of the digestate products obtained from the anaerobic digestion of food waste. To assess the impact of low and high solid contents on the feedstock, a two-way ANOVA was employed to determine the significance of these factors in digestate nutrient composition (Table 3). Using a pre-determined α -level of 0.05 as the criterion for statistical significance, it is evident from Table 3 that the interaction effects of the factors on digestate nutrient composition are significant for all nutrients except for zinc, which showed an interaction effect with a p -value of 0.295415. This p -value exceeds the pre-determined α -level of 0.05, indicating that the interaction effects are not statistically significant. As a result, the effects of each factor are considered relevant. However, the results in Table 3 indicate that the effect of total solids content on the digestate

zinc composition was not significant, as the p -value of 0.951393 is greater than the pre-determined α -level of 0.05.

Table 2. Triplicated values of digestate nutrient compositions from anaerobic digestion of food wastes at different total solid contents.

S/N	Inoculum Type	Digestion Media	N (g/kg)	P (g/kg)	K (g/kg)	Ca (g/kg)	Mg (g/kg)	Na (g/kg)	Mn (g/kg)	Fe (g/kg)	Cu (g/kg)	Zn (g/kg)	
(A) High-Solid Digestion													
1	With chicken dung and partially digested food waste as inoculum	Food wastes with activated carbon	R1	16.90	23.80	12.90	87.00	11.10	7.91	0.20	2.92	0.07	1.18
			R2	17.20	24.10	13.10	89.20	9.80	8.32	0.41	2.62	0.13	1.20
			R3	16.90	24.10	13.00	90.80	9.10	8.07	0.29	2.86	0.10	1.22
		Food wastes without activated carbon (control)	R1	15.70	20.80	10.80	73.00	7.90	7.01	0.32	2.72	0.05	1.01
			R2	16.10	21.30	11.20	75.20	11.20	7.25	0.27	2.66	0.04	0.99
			R3	16.20	20.90	11.00	76.80	10.90	6.74	0.31	2.72	0.03	1.00
2	With chicken dung as inoculum	Food wastes with activated carbon	R1	13.80	36.80	47.80	143.00	15.70	12.54	0.64	5.13	0.43	0.73
			R2	14.30	37.20	48.20	145.20	16.10	12.13	0.60	5.31	0.05	0.66
			R3	13.90	37.00	48.00	146.80	16.20	11.33	0.56	5.16	0.12	0.71
		Food wastes without activated carbon (control)	R1	16.90	35.90	16.80	144.00	15.10	5.55	0.48	4.53	0.09	0.39
			R2	17.30	36.30	17.30	146.10	16.20	5.67	0.48	4.61	0.12	0.41
			R3	16.80	35.80	16.90	147.90	16.70	6.48	0.54	4.66	0.72	0.40
(B) Low-Solid Digestion													
1	With chicken dung and partially digested food waste as inoculum	Food wastes with activated carbon	R1	19.70	9.00	7.90	24.80	0.00	12.10	0.08	0.29	0.00	1.44
			R2	20.40	10.20	8.20	25.20	2.00	11.97	0.13	0.31	0.00	0.87
			R3	19.90	10.80	7.90	25.00	1.00	11.63	0.09	0.30	0.00	0.97
		Food wastes without activated carbon (control)	R1	19.90	11.90	5.70	28.70	0.00	12.89	0.19	0.19	0.00	0.29
			R2	20.20	12.30	6.20	29.10	3.00	13.10	0.01	0.22	0.00	0.29
			R3	19.90	11.80	6.10	29.20	0.00	13.01	0.10	0.19	0.00	0.32
2	With partially digested food waste as inoculum	Food wastes with activated carbon	R1	14.70	18.70	34.8	96.80	11.00	14.22	0.39	3.30	0.00	2.65
			R2	15.30	19.40	35.3	97.20	13.20	14.44	0.39	3.34	0.00	2.74
			R3	15.00	18.90	34.9	97.00	14.80	15.12	0.42	3.26	0.00	2.71
		Food wastes without activated carbon (Control)	R1	17.90	26.70	21.8	99.80	11.00	13.77	0.38	3.15	0.11	0.38
			R2	18.20	27.20	22.3	102.00	12.30	14.02	0.42	3.07	0.11	0.39
			R3	17.90	27.10	21.9	98.20	12.70	13.61	0.40	3.08	0.08	0.43

R1—experimental assay 1; R2—experimental assay 2 (replicate); R3—experimental assay 3 (replicate). N = nitrogen; P = phosphorus; K = potassium; Ca = calcium; Mg = magnesium; Na = sodium; Mn = manganese; Fe = iron; Cu = copper; Zn = zinc.

3.2. Effects of Activated Carbon Supplementation on Digestate Composition

Activated carbon was added to the anaerobic digestion media to mitigate inhibitory compounds that could impair process performance and affect the quality of the digestate products. The activated carbon used had a surface area, pore volume, and pore size of 627.50 m²/g, 0.221 cm³/g, and 65.38 Å, respectively. The elemental composition analysis of the activated carbon showed that it contained aluminum (33.01%), carbon (15.73%), silicon (12.99%), sulfur (12.67%), potassium (9.77%), calcium (3.62%), silver (2.82%), chlorine (1.98%), sodium (1.93%), oxygen (1.52%), magnesium (1.50%), phosphorus (1.46%), and titanium (1.01%). The presence of other elements alongside carbon may have originated from pyrolyzed rubber tires and the activating agent (KOH) used in the production of activated carbon. The digestion medium in the reactor's working volume was supplemented with 15 g/dm³ of activated carbon, based on the optimal amount used in a study by Zhang et al. [22].

The effects of activated carbon supplementation on digestate nutrient composition were difficult to assess directly, as total solids content and inoculum diversity were the two main factors analyzed, with activated carbon supplementation as a subset of these factors. However, the results in Table 2 indicate that, in the high-solid anaerobic digestion process, the augmented media (with activated carbon) had significantly higher concentrations of nutrients, including nitrogen, phosphorus, potassium, calcium, iron, copper, and zinc. Conversely, in the low-solid anaerobic digestion process, only potassium, iron, and zinc had higher concentrations in the augmented media compared to the non-augmented media.

Table 3. Significant effects of activated carbon supplementation, inoculum diversity and total solids content on digestate nutrient composition.

1. NITROGEN (N)													
Source of variation	SS	df	MS	F	p-value	F-crit	Source of variation	SS	df	MS	F	p-value	F-crit
Sample	22.57344	3	7.524479	5.473592	0.008793	3.238872	Sample	45.42003	3	15.14001	4.902333	0.013276	3.238872
Columns	2033.836	3	677.9453	493.1632	5.7×10^{-16}	3.238872	Columns	739.5315	3	246.5105	79.82005	7.68×10^{-10}	3.238872
Interaction	28.38531	9	3.153924	2.294284	0.070624	2.537667	Interaction	68.11175	9	7.567973	2.450508	0.056521	2.537667
Within	21.995	16	1.374688				Within	49.41325	16	3.088328			
Total	2106.79	31					Total	902.4765	31				
2. PHOSPHORUS (P)													
Sample	690.645	3	230.215	46.00849	4.31×10^{-8}	3.238872	Sample	1.520184	3	0.506728	3.953505	0.027592	3.238872
Columns	3873.415	3	1291.138	258.0341	9.36×10^{-14}	3.238872	Columns	15.67043	3	5.223478	40.7537	1.02×10^{-7}	3.238872
Interaction	638.555	9	70.95056	14.17948	4.81×10^{-6}	2.537667	Interaction	2.911553	9	0.323506	2.524001	0.050966	2.537667
Within	80.06	16	5.00375				Within	2.05075	16	0.128172			
Total	5282.675	31					Total	22.15292	31				
3. POTASSIUM (K)													
Sample	934.9034	3	311.6345	4.384066	0.019645	3.238872	Sample	26.9995	3	8.999833	56.61385	9.68×10^{-9}	3.238872
Columns	2827.808	3	942.6028	13.26051	0.000132	3.238872	Columns	27.24643	3	9.082142	57.13162	9.06×10^{-9}	3.238872
Interaction	921.0253	9	102.3361	1.439662	0.25138	2.537667	Interaction	22.32998	9	2.481108	15.60752	2.5×10^{-6}	2.537667
Within	1137.335	16	71.08344				Within	2.5435	16	0.158969			
Total	5821.072	31					Total	79.1194	31				
4. CALCIUM (Ca)													
Sample	14.282.85	3	4760.95	331.0023	1.33×10^{-14}	3.238872	Sample	1.266075	3	0.422025	3.251661	0.049453	3.238872
Columns	60.075.27	3	20,025.09	1392.232	1.5×10^{-19}	3.238872	Columns	20.05063	3	6.683542	51.49604	1.92×10^{-8}	3.238872
Interaction	14,104.51	9	1567.168	108.9564	1.22×10^{-12}	2.537667	Interaction	2.8217	9	0.313522	2.415658	0.05938	2.537667
Within	230.135	16	14.38344				Within	2.0766	16	0.129788			
Total	88,692.76	31					Total	26.213	31				
5. MAGNESIUM (Mg)													
Sample	235.0525	3	78.35083	136.4106	1.32×10^{-11}	3.238872	Sample	0.175263	3	0.058421	0.112718	0.951393	3.238872
Columns	592.605	3	197.535	343.9129	9.81×10^{-15}	3.238872	Columns	9.616413	3	3.205471	6.18466	0.005408	3.238872
Interaction	223.3275	9	24.81417	43.20203	1.53×10^{-9}	2.537667	Interaction	6.212713	9	0.690301	1.331873	0.295415	2.537667
Within	9.19	16	0.574375				Within	8.2927	16	0.518294			
Total	1060.175	31					Total	24.29709	31				

Table Legend: SS: sum of squares; df: degrees of freedom; MS: mean sum of squares; F: F value from the F-test; F-crit: F-critical value; Sample: total solids content factor; Columns: inoculum diversity factor.

The application of activated carbon supplementation to digestate composition may have a positive impact on the anaerobic digestion process. This could lead to improvements in the process and a more effective management of the factors that influence it. Activated carbon supplementation has the potential to enhance the quality of digestate as a biofertilizer due to its high surface area, which enables it to adsorb toxic compounds. Additionally, it facilitates the microbial degradation of food waste during digestion, improves soil water retention, and prevents nutrient leaching during soil fertilization [30].

3.3. Effects of Inoculum Source on Digestate Composition

The significance of inoculum activity in anaerobic processes cannot be overstated, as it acts as a catalyst to enhance anaerobic digestion. Inoculum from diverse sources may exhibit varying effects during the digestion process due to species differences. Therefore, investigating the impact of inoculum source on digestate composition is essential. The findings from this study, as shown in Table 3, indicate that the effects of inoculum diversity on digestate nutrient composition are significant only for the digestate zinc composition. Notably, the interaction effects of the factors involved were not significant. The results show that the effects of inoculum diversity on digestate zinc composition were significant, with a p -value of 0.005408.

A further enhancement in digestate quality, as demonstrated in this study, will make digestate suitable for use as an organic fertilizer, as it contains a substantial concentration of essential elements necessary for plant growth. Additional research findings [30–32] also support the potential of digestates from food waste and other organic substances to be used as biofertilizers for soil amendments and crop production improvement. Several studies have elucidated the impact of various factors, such as inoculum source or type [33], substrate solubility [34–37], and activated carbon supplementation [38], on enhancing the stability of the anaerobic digestion process. This, in turn, leads to improvements in the quality of digestate products. Beyond its utility as a soil fertilizer, the application of digestate can help mitigate the depletion of resources required for the production of inorganic chemical fertilizers, thus promoting sustainability and environmental protection [39,40].

4. Conclusions and Future Work

This study explored the feasibility of utilizing feedstock total solids content, inoculum species diversity, and activated carbon supplementation to enhance the quality of digestate products derived from the anaerobic digestion of food waste. Statistical analysis revealed that using a diverse inoculum species significantly impacted digestate quality, specifically regarding zinc composition. The p -value for the influence of inoculum diversity on zinc composition was 0.005408, indicating substantial effects. In contrast, the influence of total solids on digestate nutrient composition was not significant for zinc composition, as the p -value was 0.951393, which is greater than the pre-determined α -level of 0.05. The effects of activated carbon supplementation were inconclusive, as it was considered as a subset of the other two factors (inoculum diversity and total solids content). However, the digestate nutrient composition table suggested that activated carbon supplementation did have some impact on nutrient compositions, showing higher concentrations of certain nutrients when compared to non-augmented media, especially under both low- and high-solid anaerobic digestion conditions. This suggests that activated carbon supplementation may influence digestate nutrient compositions, warranting further investigation into its significance. Future research will focus on maximizing the effects of activated carbon supplementation and total solids content while exploring other techniques (including the use of vermicompost digestate as a biofertilizer) to enhance digestate quality. This will help make the process more economically, socially, and environmentally sustainable. Such efforts will facilitate the widespread adoption of digestate as a biofertilizer, contributing to environmental, social, and economic well-being.

Author Contributions: Conceptualization—J.G.A., R.J.P. and M.J.T.; methodology—J.G.A., R.J.P., O.S.A., B.C.O. and C.N.E.; formal analysis—J.G.A., R.J.P., O.S.A., B.C.O. and C.N.E.; investigation—J.G.A., R.J.P., O.S.A., B.C.O. and C.N.E.; resources—J.G.A., R.J.P., O.S.A., B.C.O. and C.N.E.; data curation—J.G.A., R.J.P., O.S.A., B.C.O. and C.N.E.; statistical analysis and drawing—J.G.A. and J.F.A.; writing (initial draft)—J.G.A.; writing and editing—J.G.A. and M.J.T.; project administration—J.G.A., R.J.P. and M.J.T.; funding acquisition—J.G.A. and M.J.T. All authors have read and agreed to the published version of the manuscript.

Funding: This research was funded by Tertiary Education Trust Fund (TETFUND), NIGERIA, under grant number LASU/VC/DSI/RP/23/028 and Swedish Research Council FORMAS under grant number 2021-02458.

Data Availability Statement: The original contributions presented in this study are included in the article. Further inquiries can be directed to the corresponding author.

Acknowledgments: The authors would like to express their gratitude to the University of Borås (Sweden) and Lagos State University (Lagos, Nigeria) for their invaluable support during this research study and in the publication of the results from this study. Adenike Adetayo, Lukman Olabanjo, and George Isiguzo are also acknowledged for their assistance during this research study.

Conflicts of Interest: The authors declare no conflicts of interest.

Abbreviations

AD	Anaerobic digestion
ANOVA	Analysis of variance
ATP	Adenosine triphosphate
BET	Brunauer–Emmett–Teller
BJH	Barrett–Joyner–Halenda
Ca	Calcium
CF	Crude fiber
CO ₂	Carbon (iv) oxide
CP	Crude protein
Cu	Copper
DFT	Density Functional Theory
EE	Ether extract
dF	Degrees of freedom
F	F value from the F-test
F-crit	F-critical value
Fe	Iron
HCl	Hydrochloric acid
K	Potassium
KOH	Potassium hydroxide
Mg	Magnesium
Mn	Manganese
MS	Mean sum of squares
Na	Sodium
NaOH	Sodium hydroxide
N	Nitrogen
P	Phosphorus
R1	Experimental assay 1
R2	Experimental assay 2 (replicate)
R3	Experimental assay 3 (replicate)
SDGs	Sustainable Development Goals
SEM-EDX	Scanning Electron Microscopy–Energy-Dispersive X-ray
SS	Sum of squares
Zn	Zinc

References

- United Nations. The Sustainable Development Goals Report 2023: Special Edition. Department of Economic and Social Affairs Statistics Division: A High-Level Event Call to Action. Available online: <https://unstats.un.org/sdgs/report/2023> (accessed on 30 December 2024).
- Wackernagel, M.; Hanscom, L.; Lin, D. Making the sustainable development goals consistent with sustainability. *Front. Energy Res.* **2017**, *5*, 18. [CrossRef]
- Kim, R.E. Augment the SDG indicator framework. *Environ. Sci.* **2023**, *142*, 62–67. [CrossRef]
- Bhattacharya, A.; Ivanyina, M.; Oman, W.; Stern, N. Climate action to unlock the inclusive growth story of the 21st century. *IMF Work. Pap.* **2021**, *147*, 1.
- Jote, C.A. The Impacts of Using Inorganic Chemical Fertilizers on the Environment and Human Health. *Org. Med. Chem.* **2023**, *13*, 555864.
- Daniel-Gromke, J.; Rensberg, N.; Denysenko, V.; Stinner, W.; Schmalhub, T.; Scheftelowitz, M.; Nelles, M.; Liebetrau, J. Current developments in production and utilization of biogas and biomethane in Germany. *Chem. Ing. Tech.* **2017**, *90*, 17–35. [CrossRef]
- Wainaina, S.; Lukitawesa-Awashthi, M.K.; Taherzadeh, M.J. Bioengineering of anaerobic digestion for volatile fatty acids, hydrogen or methane production: A critical review. *Bioengineered* **2019**, *10*, 437–458. [CrossRef]
- Viancelli, A.; Schneider, T.M.; Demczuk, T.; Delmoral, A.P.G.; Petry, B.; Collato, M.M.; Michelin, W. Unlocking the value of biomass: Exploring microbial strategies for biogas and volatile fatty acids generation. *Bioresour. Technol. Rep.* **2023**, *23*, 101552. [CrossRef]
- Barlog, P.; Hlisenkovsky, L.; Kunzova, E. Effect of digestate on soil organic carbon and plant-available nutrient content compared to cattle slurry and mineral fertilization. *Agronomy* **2020**, *10*, 379. [CrossRef]
- Arachchige, U.; Ranaweera, S.; Ampemohotti, T.; Weliwaththage, S.R.G. Development of an organic fertilizer. *J. Res. Technol. Eng.* **2020**, *1*, 1–7.
- Erraji, H.; Afilat, M.E.; Asehraou, A.; Azim, K. Biogas and digestate production from food wastes: A case study of dome digester in Morocco. *Biomass Convers. Biorefinery* **2021**, *13*, 10771–10780. [CrossRef]
- Pelayo-Lind, O.; Hultberg, M.; Bergstrand, K.J.; Larsson-Jönsson, H.; Caspersen, S.; Asp, H. Biogas digestate in vegetable hydroponic production: pH dynamics and pH management by controlled nitrification. *Waste Biomass Valori.* **2021**, *12*, 123–133. [CrossRef]
- Weimers, K.; Bergstrand, K.J.; Hultberg, M.; Asp, H. Liquid anaerobic digestate as sole nutrient source in soilless horticulture—Or spiked with mineral nutrients for improved plant growth. *Front. Plant Sci.* **2022**, *13*, 443. [CrossRef] [PubMed]
- Ryu, H.D.; Lim, D.Y.; Kim, S.J.; Baek, U.I.; Chung, E.G.; Kim, K.; Lee, J.K. Struvite precipitation for sustainable recovery of nitrogen and phosphorus from anaerobic digestion effluents of swine manure. *Sustainability* **2020**, *12*, 8574. [CrossRef]
- Song, S.; Lim, J.W.; Lee, J.T.; Cheong, J.C.; Hoy, S.H.; Hu, Q.; Tan, J.K.; Chiam, Z.; Arora, S.; Lum, T.Q. Food-waste anaerobic digestate as a fertilizer: The agronomic properties of untreated digestate and biochar-filtered digestate residue. *Waste Manag.* **2021**, *136*, 143–152. [CrossRef]
- Cheong, J.C.; Lee, J.T.; Lim, J.W.; Song, S.; Tan, J.K.; Chiam, Z.Y.; Yap, K.Y.; Lim, E.Y.; Zhang, J.; Tan, H.T. Closing the food waste loop: Food waste anaerobic digestate as fertilizer for the cultivation of the leafy vegetable, xiao bai cai (*Brassica rapa*). *Sci. Total Environ.* **2020**, *715*, 136789. [CrossRef]
- Ali, S.; Rizwan, M.; Qayyum, M.F.; Ok, Y.S.; Ibrahim, M.; Riaz, M.; Arif, M.S.; Hafeez, F.; Al-Wabel, M.I.; Shahzad, A.N. Biochar soil amendment on alleviation of drought and salt stress in plants: A critical review. *Environ. Sci. Pollut. Res.* **2017**, *24*, 12700–12712. [CrossRef]
- Ko, J.H.; Wang, N.; Yuan, T.; Lu, F.; He, P.; Xu, Q. Effect of nickel containing activated carbon on food waste anaerobic digestion. *Bioresour. Technol.* **2018**, *266*, 516–523. [CrossRef]
- Zhang, J.; Zhang, L.; Loh, K.-C.; Dai, Y.; Tong, Y.-W. Enhanced anaerobic digestion of food waste by adding activated carbon: Fate of bacterial pathogens and antibiotic resistance genes. *Biochem. Eng. J.* **2017**, *128*, 19–25. [CrossRef]
- Teklit, G.A.; Rene, E.R.; Nizami, A.-S.; Dupont, C.; Vaccari, M.; van-Hullebusch, E.D. Beneficial role of biochar addition on the anaerobic digestion of food waste: A systematic and critical review of the operational parameters and mechanisms. *J. Environ. Manag.* **2021**, *290*, 112537.
- Kaarela, O.E.; Harkki, H.A.; Palmtoth, M.R.T.; Tuhkanen, T.A. Bacterial diversity and active biomass in full-scale granular activated carbon filters operated at low water temperatures. *Environ. Technol.* **2015**, *36*, 681–692. [CrossRef]
- Akinbomi, J.G.; Patinvoth, R.J.; Taherzadeh, M.J. Current challenges of high solid anaerobic digestion and possible measures for its effective applications: A review. *Biotechnol. Biofuels Bioprod.* **2022**, *15*, 52. [CrossRef] [PubMed]
- Cordoba, V.; Fernandez, M.; Santalla, E. The effect of different inoculums on anaerobic digestion of swine wastewater. *J. Environ. Chem. Eng.* **2016**, *4*, 115–122. [CrossRef]
- Demichelis, F.; Tommasi, T.; Deorsola, F.A.; Marchisio, D.; Fino, D. Effect of inoculum origin and substrate-inoculum ratio to enhance the anaerobic digestion of organic fraction municipal solid waste (OFMSW). *J. Clean. Prod.* **2022**, *351*, 131539. [CrossRef]

25. Zhang, L.; Zhang, J.; Loh, K.-C. Activated carbon enhanced anaerobic digestion of food waste—Laboratory-scale and Pilot-scale operation. *Waste Manag.* **2018**, *5*, 270–279. [CrossRef]
26. Kacan, E. Optimum BET surface areas for activated carbon produced from textile sewage sludges and its application as dye removal. *J. Environ. Manag.* **2016**, *166*, 116–123. [CrossRef]
27. Li, G.; Lakunkov, A.; Boulanger, N.; Lazar, O.A.; Enachescu, M.; Grinm, A.; Talyzin, A.V. Activated carbons with extremely high surface area produced from cones, bark and wood using the same procedure. *R. Soc. Chem. Adv.* **2023**, *21*, 14543–14553. [CrossRef]
28. Mopoung, S.; Moonsri, P.; Palas, W.; Khumpai, S. Characterization and properties of activated carbon prepared from Tamarind seeds by KOH Activation for Fe(III) adsorption from aqueous solution. *Sci. World J.* **2015**, *2015*, 415961. [CrossRef]
29. Lawal, I.M.; Ndagi, A.; Mohammed, A.; Saleh, Y.Y.; Shuaibu, A.; Hassan IAbubakar, S.; Soja, U.B.; Jagaba, A.H. Proximate analysis of waste-to-energy potential of municipal solid waste for sustainable renewable energy generation. *Ain. Shams. Eng. J.* **2024**, *15*, 102357. [CrossRef]
30. Ries, J.; Chen, Z.; Park, Y. Potential applications of food waste based anaerobic digestate for sustainable crop production practice. *Sustainability* **2023**, *15*, 8520. [CrossRef]
31. Hafner, F.; Hartung, J.; Moller, K. Digestate composition affecting N fertilizer value and C mineralization. *Waste Biomass Valor.* **2022**, *13*, 3445–3462. [CrossRef]
32. Horf, M.; Gibbers, R.; Vogel, S.; Ostermann, M.; Piepel, M.; Olfs, H. Determination of nutrients in liquid manures and biogas digestates by portable energy-dispersive x-ray fluorescence spectrometry. *Sensors* **2021**, *21*, 3892. [CrossRef] [PubMed]
33. Wi, J.; Lee, S.; Ahn, H. Influence of dairy manure as inoculum source on anaerobic digestion of swine manure. *Bioengineering* **2023**, *10*, 432. [CrossRef] [PubMed]
34. Wang, Z.; Jiang, Y.; Wang, Y.; Zhang, Y.; Hu, Y.; Hu, Z.; Wu, G.; Zhan, X. Impact of total solids content on anaerobic co-digestion of pig manure and food waste insight into shifting of the methanogenesis pathway. *Waste Manag.* **2020**, *14*, 96–106. [CrossRef] [PubMed]
35. Zhang, X.-F.; Yuan, Y.-Q.; Chen, Q.-K.; Li, Q.; Huang, Y.; Li, L. Effect of total solids contents on the performance of anaerobic digester treating food waste and kinetics evaluation. *E3S Web Conf.* **2021**, *272*, 01226.
36. Ahmadi-Pirtlou, M.; Gundoshmian, T.-M. The effect of substrate ratio and total solids in biogas production from anaerobic co-digestion of municipal solid waste and sewage sludge. *J. Mater. Cycles Waste Manag.* **2021**, *23*, 1938–1946. [CrossRef]
37. Johnravendar, D.; Kaur, G.; Liang, J.; Lou, L.; Zhao, J.; Manu, M.K.; Kumar, R.; Varjani, S.; Wong, J.W.C. Impact of total solids content on biochar amended co-digestion of food waste and sludge microbial community dynamics, methane production and digestate quality assessment. *Bioresour. Technol.* **2022**, *361*, 127682.
38. Cueloz, M.J.; Martinez, E.J.; Moreno, R.; Gonzalez, R.; Otero, M.; Gomez, X. Enhancing anaerobic digestion of poultry blood using activated carbon. *J. Adv. Res.* **2017**, *8*, 297–307.
39. Bergstrand, K.J. Organic fertilizers in greenhouse production systems: A review. *Sci. Hortic.* **2022**, *295*, 110855. [CrossRef]
40. Mican, B.S.; Ren, A.T.; Buhlmann, C.H.; Cihadouani, A.; Solaiman, Z.M.; Jenkins, S.; Pang, J.; Ryan, M.H. Closing the circle for urban food waste anaerobic digestion. The use of digestate and biochar on plant growth in potting soil. *J. Clean. Prod.* **2022**, *347*, 131071. [CrossRef]

Disclaimer/Publisher’s Note: The statements, opinions and data contained in all publications are solely those of the individual author(s) and contributor(s) and not of MDPI and/or the editor(s). MDPI and/or the editor(s) disclaim responsibility for any injury to people or property resulting from any ideas, methods, instructions or products referred to in the content.

Review

Physical Cell Disruption Technologies for Intracellular Compound Extraction from Microorganisms

Fujunzhu Zhao ¹, Zhiwu Wang ² and Haibo Huang ^{1,*}¹ Department of Food Science & Technology, Virginia Tech, Blacksburg, VA 24061, USA; fzhao179@vt.edu² Department of Biological Systems Engineering, Virginia Tech, Blacksburg, VA 24061, USA; wzw@vt.edu

* Correspondence: huang151@vt.edu

Abstract: This review focuses on the physical disruption techniques in extracting intracellular compounds, a critical step that significantly impacts yield and purity. Traditional chemical extraction methods, though long-established, face challenges related to cost and environmental sustainability. In response to these limitations, this paper highlights the growing shift towards physical disruption methods—high-pressure homogenization, ultrasonication, milling, and pulsed electric fields—as promising alternatives. These methods are applicable across various cell types, including bacteria, yeast, and algae. Physical disruption techniques achieve relatively high yields without degrading the bioactivity of the compounds. These techniques, utilizing physical forces to break cell membranes, offer promising extraction efficiency, with reduced environmental impacts, making them attractive options for sustainable and effective intracellular compound extraction. High-pressure homogenization is particularly effective for large-scale extracting of bioactive compounds from cultivated microbial cells. Ultrasonication is well-suited for small to medium-scale applications, especially for extracting heat-sensitive compounds. Milling is advantageous for tough-walled cells, while pulsed electric field offers gentle, non-thermal, and highly selective extraction. This review compares the advantages and limitations of each method, emphasizing its potential for recovering various intracellular compounds. Additionally, it identifies key research challenges that need to be addressed to advance the field of physical extractions.

Keywords: cell disruption; microorganisms; extraction; milling; high-pressure homogenization; ultrasound; pulsed electric field

Citation: Zhao, F.; Wang, Z.; Huang, H. Physical Cell Disruption Technologies for Intracellular Compound Extraction from Microorganisms. *Processes* **2024**, *12*, 2059. <https://doi.org/10.3390/pr12102059>

Academic Editor: Vijaya Raghavan

Received: 3 August 2024

Revised: 17 September 2024

Accepted: 20 September 2024

Published: 24 September 2024



Copyright: © 2024 by the authors. Licensee MDPI, Basel, Switzerland. This article is an open access article distributed under the terms and conditions of the Creative Commons Attribution (CC BY) license (<https://creativecommons.org/licenses/by/4.0/>).

1. Introduction

Intracellular compounds, ranging from proteins to lipids to pigments, are crucial in various industries, including biotechnology, biofuels, and pharmaceuticals [1–4]. These compounds are essential for producing bio-based products that serve as key ingredients in animal feed, food, and medical applications. For instance, proteins derived from algal proteins are increasingly used as nutritional supplements or as animal feed ingredients [5]. The extraction of intracellular compounds from microbial cells, particularly those produced through fermentation processes, is a critical step that determines the yield, purity, and functionality of the final products. In fermentation, microorganisms like bacteria, yeast, and algae are cultured to produce a wide array of intracellular compounds. These compounds have diverse applications, from biofuels, where algal lipids are converted into renewable energy sources, to pharmaceuticals, where intracellular proteins contribute to the development of therapeutic agents [6]. Furthermore, pigments synthesized intracellularly through fermentation are used in various sectors, including food and cosmetics, underscoring the broad utility of these bio-derived substances [7]. Efficient recovery of these compounds is, therefore, vital to both the functionality of the final product and the efficacy and sustainability of biomanufacturing processes [6].

Downstream processing, which involves the recovery and purification of intracellular compounds, is a crucial phase to ensure product yield and quality [8]. However, traditional chemical methods for intracellular compound extraction often struggle to achieve both recovery efficiency and the preservation of compound integrity. Solvent extraction, a widely used approach, can degrade sensitive intracellular compounds, compromising their stability and functionality. Moreover, the environmental impact of solvent use—along with the high operational costs associated with solvent recovery, waste management, and disposal—pose significant sustainability and economic challenges [9]. Furthermore, scalability poses an additional barrier, as techniques that work well at a laboratory scale may not be transferable to industrial-scale applications [10,11]. To address some of these limitations, biological approaches such as the enzymatic disruption of cell walls are also employed for intracellular compound extraction. Enzymes offer a more selective and gentler approach to cell disruption, targeting specific cell walls or membrane components to release desired intracellular compounds. One of the key advantages of enzymatic methods is their environmentally friendly nature, requiring lower energy inputs and reducing the need for harsh chemicals. Moreover, they are highly effective at preserving the functionality and structure of intracellular compounds. However, enzymatic processes are hindered by their slow reaction rates and high operation costs. Their efficacy can be inconsistent, varying with different cell types [12], and the need for precise control over reaction conditions, such as temperature and pH, adds to the complexity and cost of the process [13]. Moreover, enzymatic extraction faces challenges in scaling up for industrial applications. The cost and limited availability of certain enzymes, along with the difficulty of replicating optimal process conditions required for enzymes, can further restrict their application in large-scale operations.

Given the limitations of chemical and enzymatic methods, there has been a growing focus on the development of physical disruption techniques for intracellular compound extraction. These methods, which include high-pressure homogenization, ultrasonication, mechanical milling, and pulsed electric field, primarily apply physical forces to disrupt the cell wall or membrane, allowing the release of intracellular products. They offer a promising alternative to conventional chemical and biological approaches [14–19]. The shift toward physical methods is driven by their potential to enhance extraction efficiency, reduce operational costs, and minimize environmental impacts [20]. Ultrasonication, for example, uses high-frequency sound waves to induce cavitation phenomena in the liquid medium and within cells. When these bubbles collapse, they generate localized shear forces that can break open microbial cells, making this method particularly effective for disrupting a wide range of cell types [14]. High-pressure homogenization, on the other hand, forces cell suspensions through a narrow orifice at extremely high pressure, causing intense high shear forces that rupture the cells [16]. These methods offer a viable path to cost-effective and environmentally friendly intracellular compound extraction. These methods have also been shown to achieve high yields of target valuable intracellular compounds while preserving their bioactivity. This makes them ideal for industries that rely on the recovery of functional proteins, lipids, pigments, and other high-value products from microbial cells. As industries continue to prioritize green technologies, physical disruption methods present a viable path toward large-scale, sustainable, and cost-effective intracellular product recovery.

In this review, we delve into the principles and applications of various physical cell disruption techniques for the recovery of intracellular compounds. By investigating methods like high-pressure homogenization, ultrasonication, milling, and pulsed electric fields, we aim to highlight how these physical approaches are transforming the field of intracellular compound extraction and being investigated for different applications. Unlike chemical and biological methods, which have been extensively studied and applied, physical methods have received comparatively less attention in the literature. Our review uniquely fills this gap by providing an in-depth analysis of the mechanisms underlying each method, as well as exploring their diverse potential applications across various microorganisms and intracellular compounds. This review also offers critical insights into how these methods

work at a fundamental level and the advantages and limitations of each technique, paying special attention to the conditions under which they excel. By integrating the latest research and technological advancements, we provide a comprehensive understanding on how these methods can be implemented in small and industrial scales. Ultimately, this review underscores the transformative potential of physical cell description techniques, positioning them as critical tools for advancing intracellular compound extraction in a sustainable, scalable, and cost-effective manner.

2. Physical Methods for Intracellular Compound Extraction

2.1. High-Pressure Homogenization

High-pressure homogenization (HPH) is a widely used method to disrupt cells for recovering intracellular materials [16]. A schematic diagram of high-pressure homogenizer is presented in Figure 1. In this process, a cell suspension is forced through a narrow valve under a high pressure, typically ranging from 10 to 300 MPa. When the cell suspension exits the valve, it experiences an intense pressure drop. As the velocity of the cell suspension changes, shear force is generated, breaking cell walls. High turbulence is generated by the high-speed flow through the narrow valve. Cavitation releases energy, creating mechanical damage to cell walls [21–24]. The combination of high turbulence, shear force, and cavitation breaks cells and releases intracellular contents. The cell disruption using high-pressure homogenization allows for the extraction and isolation of valuable substances from intracellular space. This method is efficient, scalable, and can be precisely controlled to maximize yield and preserve the functionality of the extracted compounds.

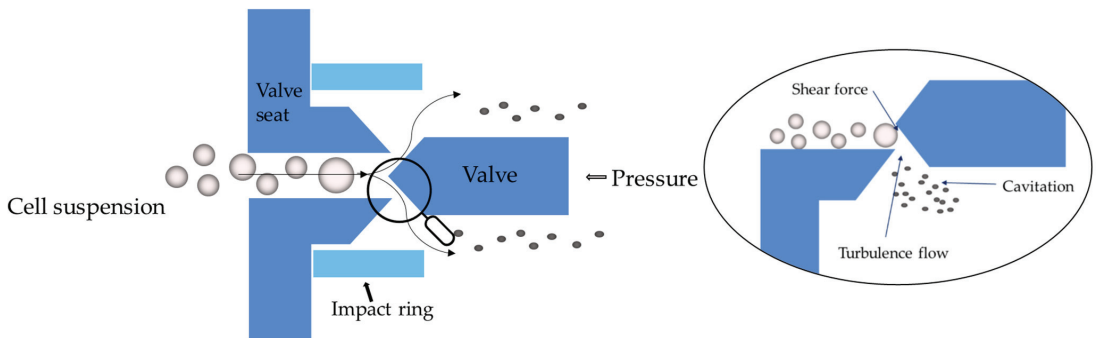


Figure 1. A schematic diagram of high-pressure homogenization to disrupt cells. The cell suspension exits the valve and it experiences an intense pressure drop, generating high turbulence, shear force, and cavitation to break cells.

Many studies have reported using HPH to break microalgae cells for extracting various intracellular compounds (Table 1). For instance, high-pressure homogenization was used to break the cellular and chloroplast membranes of the microalgae *Porphyridium cruentum* to release B-Phycoerythrin, an intracellular pigment, and proteins [25]. The study explored various pressures and the number of homogenizations passes. A critical pressure point was identified at 100 MPa. Below this threshold, the chloroplasts membrane was only slightly damaged, resulting in a low B-Phycoerythrin and protein release. In contrast, pressures above 100 MPa effectively broke the cells, releasing significantly more B-Phycoerythrin. This is because pigments like B-Phycoerythrin are confined to chloroplasts, while other water-soluble proteins are also found in the cytoplasm. Operating at lower pressures may cause plasma membrane penetration, releasing proteins from the cytoplasm but not as effectively breaking down the chloroplasts. In the study of Zhang et al., HPH was applied to the microalgae *Parachlorella kessleri*, which is known for its high content of proteins, carbohydrates, and lipids, to recover intracellular compounds [26]. The microalgal suspension was passed through a high-pressure homogenizer at various pressures of

40, 80, and 120 MPa, for breaking cell walls. The study showed that the amount of protein released significantly increased with higher pressures and more passes through the high-pressure homogenizer. At 40 MPa, the protein concentration released increased from 250 to 919 mg/L after 10 passes. At 80 MPa, it rose from 500 to 2352 mg/L, and at 120 MPa, from 1375 to 3656 mg/L. In another study, HPH was demonstrated effective cell disruption for cells with recalcitrant cell walls, like *Nannochloropsis* microalgae, facilitating the extraction of proteins, lipids, and sugars [27]. The study found that the extraction efficiency of these compounds using high-pressure homogenization was affected by the age of microalgae cells since the cell wall thickness increased as the cell age. For microalgae, the pressure required for HPH varies based on cell wall thickness and composition. The cell walls of red algae, such as *Porphyridium cruentum*, are made of cellulose, xylan, or mannan fibrils and extensive matrix polysaccharides, making them particularly tough and thicker. In contrast, green algae like *Parachlorella kessleri* have cell walls primarily composed of cellulose, along with other proteins. This complexity of red algae requires a higher pressure to effectively disrupt red algae cell walls compared to green algae [28].

Besides microalgae, HPH has also been employed to extract intracellular compounds from yeast cells. In a study performed by Liu et al., high-pressure homogenizer was applied for breaking *Saccharomyces cerevisiae* yeast cells to release protein [29]. The study found that HPH at 80 MPa caused significant cell wall disruption and effectively extracted 50 µg intracellular protein from 1 g of yeast. In another study, Shynkaryk et al. investigated the potential synergistic effects of pulsed electric fields and high-voltage electric discharge with HPH to break *Saccharomyces cerevisiae* yeast cell walls [30]. The study found that high voltage electric discharge before HPH was effective for cell disruption. The shock waves generated by high voltage electric discharge impacted the physical integrity of the yeast cell walls, resulting in more disruption of the cells. In addition to the laboratory scale, high-pressure homogenizer was also tested at a pilot scale for extracting poly-β-hydroxybutyrate from recombinant *Escherichia coli* (*E.coli*) cells [31]. By using 55 MPa, the processes efficiently extracted poly-β-hydroxybutyrate (PHB) from the cell. With 20 L processing amount, the recovery rate reached 75% without chemical additives, while the green chemical assist extraction using sodium hypochlorite achieved a recovery rate of 80% and a purity of 95%. While HPH is suitable for a variety of cell types, the pressure required depends on the cell characteristics. Microalgae, with their thicker cell walls, demand a higher pressure input compared to bacterial and yeast cells. Yeast cell walls are primarily composed of a complex network of polysaccharides, mainly β-glucans along with chitin. Bacterial cell walls, on the other hand, consist mainly of peptidoglycan, making them less resistant to mechanical force. Therefore, among these three cell types, microalgae require the highest pressure for effective disruption, followed by yeast, with bacteria requiring the least [32].

Among an array of physical methods, HPH offers several significant advantages in intracellular compound recovery. One of the primary advantages of HPH is its high efficiency and yield. The technique generates mechanical forces—such as shear, cavitation, and turbulence—that are effective in breaking the cell walls of microorganisms, including tough cell types like bacteria, yeast, and algae. This leads to high recovery yields of intracellular compounds such as proteins, lipids, and enzymes, making HPH invaluable in industries like biotechnology, pharmaceuticals, and biofuels, where maximizing product recovery is crucial to ensuring cost-effective production. Another key benefit of HPH is its scalability. The technique can process large volumes of microbial cultures in a continuous operation, making it particularly well-suited for industrial-scale applications [33]. This ability to maintain efficiency even when scaled up is one of the reasons why HPH is favored in large-volume industries like food and beverage industry. For example, most milk is currently treated with HPH to enhance its microbial and physiochemical shelf life [34]. More importantly, HPH is highly versatile and able to break down diverse types of microbial cells, from bacteria and yeast to more resilient microalgae, through adjusting its pressure and number of passes. This versatility allows engineers to tune the process conditions (e.g., pressure, passes) to optimize extraction for different microorganisms.

Despite its clear advantages, high-pressure homogenization has several limitations that need to be addressed to fully optimize its performance. One of the primary drawbacks is heat generation. The mechanical forces involved in HPH generate significant amounts of heat, especially when high pressure forces are applied to viscosity liquids. The generated heat can elevate substrate temperature and potentially degrade heat-sensitive intracellular compounds, such as enzymes and essential oils. Although integrating cooling systems with HPH can partially solve this limitation, it adds the process complexity and cost to the process. Another limitation is the high energy consumption. Although HPH is relatively energy efficient at scale compared to other methods, operating HPH can be energy intensive, particularly at high pressure and with the multi-passes required for breaking thick cell walls like those of gram-positive bacteria and microalgae. One way to alleviate this challenge is to add an pretreatment, such as high-voltage electric discharge, to partially break cells before HPH, allowing HPH operate at low-pressure conditions [30]. Additionally, the shear forces generated during the process can fragment intracellular compounds or denature proteins [35].

Given its advantages and limitations, HPH is particularly well-suited for a number of practical applications in various industries. One of its key applications is the recovery of therapeutic proteins and enzymes from microbial cells like *E. coli* and yeast [36–38]. The ability of HPH to maintain the bioactivity of sensitive molecules while efficiently extracting them from cells makes it indispensable in the production of biologics, such as recombinant proteins and vaccines. In the biofuel industry, HPH is widely proposed to break the cell walls of microalgae to release lipid, which can be used to produce biodiesels [39,40]. Furthermore, HPH also plays an important role in the functional food industry, where it is used to extract bioactive compounds like proteins, enzymes, and vitamins from cultivated microbial cells.

Table 1. Summary of studies on high-pressure homogenization techniques extracting intracellular compound.

Microorganism	Target Compounds	Pressure	Recovery	Key Finding	Source
<i>Porphyridium cruentum</i>	B-Phycocyanin and protein	270 MPa	Near 100%	100 MPa is a critical pressure point. Below the 100 MPa threshold, the chloroplast membrane was slightly damaged. Above 100 MPa, the cells were effectively broken, releasing significantly more B-Phycocyanin.	[25]
<i>Parachlorella kessleri</i>	Proteins, carbohydrates	120 MPa/10 passes	3656 mg/L proteins	The concentration of released compounds significantly increases with higher pressures and more passes through the high-pressure homogenizer.	[41]
<i>Nannochloropsis</i>	proteins, lipids, and carbohydrates	125 MPa/6 passes	50.4 mg/g	The extraction efficiency of these compounds using high-pressure homogenization was affected by the age of microalgae.	[27]
<i>Saccharomyces cerevisiae</i>	Protein	80 MPa	50 µg protein/1 g of yeast	High-pressure homogenization resulted in almost complete damage of yeast cell walls.	[29]
<i>Saccharomyces cerevisiae</i>	bio-products	30–200 MPa	Near 100%	High-voltage electric discharge proved to have synergistic enhancement with high-pressure homogenizer.	[30]
<i>Escherichia coli</i>	poly-β-hydroxybutyrate	55 MPa	75%	The recovery rate reached 75% without chemical additives.	[31]

2.2. Ultrasonication

Ultrasonication is emerging technique for extracting intracellular materials using ultrasound waves at frequencies between 20 kHz and 10 MHz. The ultrasound waves, generating through converting electrical energy into physical vibrations, transmit into a fluid and create pressure waves [42]. As these waves travel through a cell suspension, they generate compressible microbubbles that respond to the pressure waves. This phenomenon, known as cavitation, involves the microbubbles undergoing cycles of expansion and contraction [43,44]. Cavitation can occur in two forms: (1) stable cavitation at lower ultrasonic intensities, where bubbles oscillate without collapsing, and (2) inertial cavitation at higher intensities, where bubbles implode, causing significant biophysical effects (Figure 2). During the low-acoustic pressure cycles, stable cavitation is formed by microbubbles within the liquid. As the acoustic pressure increases, the cavitation bubbles collapse violently, generating intense physical, thermal, and chemical effects. These effects collectively contribute to cell disruption, membrane permeabilization, and the release of intracellular contents [45,46]. The severity of these effects depends on factors such as ultrasonic intensity, frequency, and exposure time.

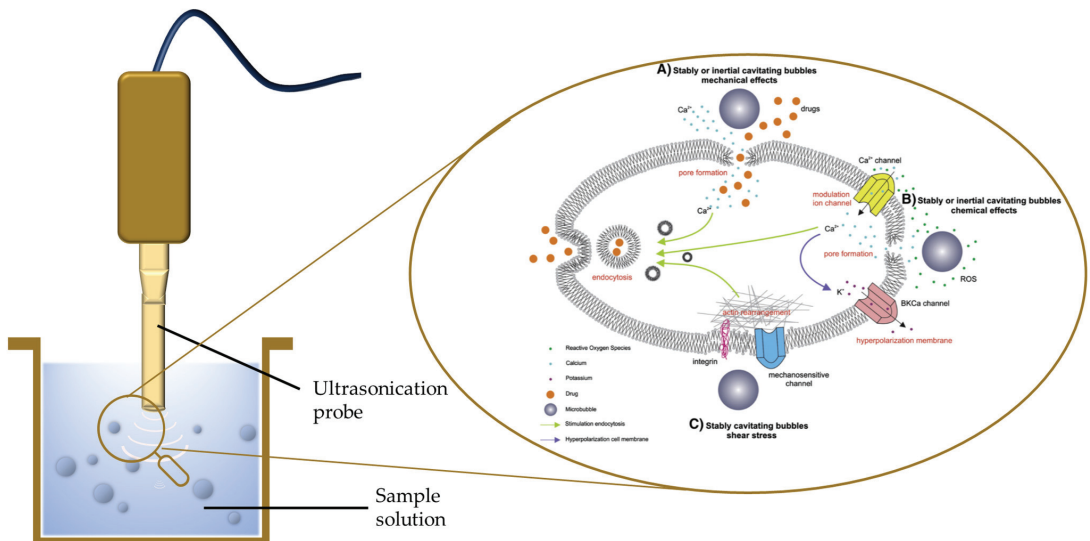


Figure 2. A schematic representation of the cavitation phenomenon in the ultrasonication mechanism, where microbubbles undergo cycles of expansion and contraction. Cavitation can occur in stable cavitation at lower ultrasonic intensities, and inertial cavitation at higher intensities. Reproduced with permission [43].

Ultrasonication has been used to disrupt diverse types of cells (Table 2). The study done by Liu et al. demonstrated that ultrasonication is effective to extract intracellular protein from yeast [14]. They found that increased acoustic power and duty cycles enhanced cell disruption and protein release. The study also compared horn-type sonication to bath-type sonication for yeast cell disruption. A horn-type sonicator consists of a probe that directly contacts the sample and transmits ultrasonic energy into the medium, while a bath-type sonicator generates ultrasonic waves within a tank filled with liquid (usually water). The sample is placed in a container, which is submerged in the bath. The ultrasonic waves are transmitted through the liquid, creating cavitation in the sample container indirectly. They revealed that horn-typed sonication is more effective to disrupt yeast cells. In another study, Wu et al. investigated the mechanisms of ultrasonic disruption in yeast cells (*Saccharomyces cerevisiae*), analyzing how different processing parameters impact the

release of cell wall polysaccharides and intracellular proteins [47]. Their study revealed that at low acoustic intensities (10 W/cm^2), cell wall disruption occurs more rapidly, resulting in a quicker release of cell wall polysaccharides compared to intracellular proteins. However, at higher intensities (24 and 39 W/cm^2), this pattern reverses, with proteins being released more rapidly than polysaccharides. Moreover, an increased processing temperature, more cell wall polysaccharides but few intracellular proteins were released. The findings suggested that ultrasonic cell disruption initiates with the breakdown of the cell wall, followed by the cell membrane.

Ultrasonication has also been applied to disrupt microalgae cells. A study investigated how ultrasonic intensity, duration, temperature, culture time, and ethanol concentration affected the extraction of polysaccharides from *Chlorella pyrenoidosa* [48]. The researchers optimized the extraction process using an orthogonal design and found that the highest polysaccharide yield, 44.8 g/kg , was achieved with an ultrasound intensity of 400 W ultrasound for 800 s , followed by incubation at $100 \text{ }^\circ\text{C}$ for 4 h in 80% ethanol. The study also presented a straightforward method for isolating polysaccharides from the crude extracts using column chromatography purification. Aouira et al. investigated the extraction of phycobiliproteins from microalgae *Spirulina platensis* using ultrasound technologies [49]. The study compared the yield and purity of phycobiliproteins extracted by ultrasound to those obtained using the pulsed electric field method. The pulsed electric field method, conducted at 38 kV/cm for 0.03 s , resulted in the highest yields of phycocyanin (0.084 g/L), allophycocyanin (0.065 g/L), and phycoerythrin (0.024 g/L). In contrast, ultrasound technology achieved similar yields by treating the samples at 35 kHz , 750 W for 90 min . Despite producing comparable yields, ultrasound demanded significantly longer treatment and higher energy input, making it a less efficient and less preferable method for extracting phycobiliproteins from *Spirulina platensis* compared to the pulsed electric field method.

In addition to extracting polysaccharides and proteins, ultrasonication can also be used to extract intracellular lipid. Natarajan et al. applied continuous ultrasonication to disrupt two marine microalgae species for lipid extraction [50]. The authors found that fatty acids release patterns differed between different microalgae species. Lipids in microalgae with rigid cell walls were easily released to the liquid after cell disruption, whereas lipids in microalgae having flexible cell membranes tend to be retained on membranes after disruption. In general, cell disruption and lipid release efficiencies correlate with ultrasound energy consumption. In the Ronald Halim et al. study, the researchers demonstrated that the ultrasonication effectively extracted all available intracellular lipids [51]. Their result also indicated that higher initial cell concentration promoted faster spread of the shock wave generated by the microbubble implosion but reduced the amount of energy received by each cell. When the initial cell concentration was low, the effect of increasing the transmission rate was dominant. However, beyond a certain threshold, the effect of the energy reduction outweighs the effect of the increase in the transmission rate. Lipids recovered from disrupted microalgae cells with 30 min of ultrasonication were found to have similar triglyceride profiles, but the higher degree of unsaturation ($61.6 \text{ wt}\%$ of triglyceride had more than eight double bonds) compared to the lipids in intact microalgal cells ($24.4 \text{ wt}\%$ of triglyceride had more than eight double bonds). A possible explanation for the changes in triglyceride composition could be the liberation of neutral lipids located inside cells or associated with membranes.

Ultrasonication offers distinct advantages for extracting various intracellular compounds, particularly in small- to medium-scale applications where control and precision are essential. One of the main strengths of ultrasonication is its tunability (e.g., adjusting frequency, intensity, duration, and configurations) to achieve selective and controlled cell disruption through the phenomenon of acoustic activation [47]. This high-level of tunability is not seen in other physical methods, such as HPH and mechanical bead milling. Moreover, the localized shear forces generated during cavitation can effectively break down microbial cell walls while preserving the integrity of sensitive intracellular compounds like proteins, enzymes, and nucleic acids. This makes ultrasonication especially applicable in the high-

value products, such as pharmaceuticals and nutraceuticals, where the preservation of bioactivity is critical. In addition, although ultrasound generates heat during cavitation, the heat generation is localized and relatively mild compared with HPH and mechanical bead milling, which generates significant heat due to mechanical force. This makes the ultrasound method more suitable for heat-sensitive and high-value compounds.

Scalability is perhaps the biggest challenge of the ultrasound method in academia and industry. While the ultrasound method excels at small- and medium-scale processing, it becomes less efficient in large-scale processing [52]. As the volume of liquid medium increases, the energy of the sound waves attenuates, leading to incomplete or uneven cell disruption, especially for those cells far away from the ultrasound generator. Another known limitation of ultrasonication is that it is less effective to process high-viscosity liquids. When the viscosity of the medium increases, the ability of sound waves to propagate uniformly is hindered. This reduced wave propagation dampens the formation of cavitation bubbles, which are essential for cell disruption. Consequently, cavitation occurs less uniformly, resulting in lower mechanical forces and less efficient cell breakage [53]. In addition, it was reported that the ultrasound-induced cavitation can generate free radicals in the liquid medium [54,55], which may cause undesirable oxidative reaction between the free radicals and intracellular compounds, thus degrading the product quality.

Overall, ultrasound is particularly suitable for small- to medium-scale applications in the industries like functional foods and pharmaceuticals, where controlled, gentle cell disruption is necessary to keep the integrity and bioactivity of the targeted compounds. Moreover, users need to be particularly careful about using the ultrasound method to process high-viscosity liquid medium. If needed, mechanical stirring and dilution can be combined with ultrasonication to alleviate the viscosity effect.

Table 2. Summary of studies on ultrasonication techniques extracting intracellular compound.

Microorganism	Target Compounds	Key Finding	Source
<i>Saccharomyces cerevisiae</i>	Protein	The intracellular protein release followed first-order kinetics. The horn-type sonication was proved more effective than bath-type sonication for yeast cell disruption.	[14]
<i>Saccharomyces cerevisiae</i>	Polysaccharides, proteins	At low acoustic intensities, the release of cell wall polysaccharides was quicker. At higher intensities proteins, were released more rapidly than polysaccharides.	[47]
<i>Chlorella pyrenoidosa</i>	Polysaccharides	The highest polysaccharide yield, 44.8 g/kg, was achieved with an ultrasound intensity of 400 W ultrasound for 800 s, followed by incubation at 100 °C for 4 h in 80% ethanol.	[48]
<i>Spirulina platensis</i>	Phycobiliproteins	Ultrasound required significantly longer treatment times and higher energy input, making it less efficient and less preferable for extracting phycobiliproteins compared to the pulsed electric field method.	[49]
Marine microalga	Fatty acids	The fatty acid release pattern varied among different microalgae species.	[50]
Microalga	Lipids	Higher initial cell concentration promoted faster spread of the shock wave generated by the microbubble implosion but reduced the amount of energy received by each cell.	[51]

2.3. Mechanical Milling

Mechanical milling (also referred to as ‘beating’ in some sources) is a simple and effective method for breaking cell walls to release intracellular compounds. This technique applies mechanical forces through the use of small, hard beads (usually made of steel, ceramic) to break down cell structures [56]. Two typical pieces of milling equipment used to disrupt cells are bead mills and ball mills. In both pieces of equipment, cells are disrupted by grinding them between beads or balls within a closed container. The beads or balls agitate

and collide with the cells, causing physical shear forces that break apart the cell walls and release their contents. The radial acceleration of beads or balls results in different velocity generating high shear forces (Figure 3) [57]. In bead mills, kinetic energy is transferred to the grinding media by stirring shafts in vertical or horizontal configurations. Depending on the intensity of the stress applied, different particle size reduction mechanisms can occur. At low stress, surface abrasion leads to the removal of fine particles from the parent particles, resulting in most of the particles being close in size to the parent particles. At relatively intense stress, particle cleavage occurs, producing fragments slightly smaller than the parent particles. At rapidly intense stress, fracture leads to the production of small particles with a wide particle size distribution [58]. Ball milling, on the other hand, operates within a rotating container where the balls generate forces including impact, abrasion, and corrosion forces. Impact results from repeated high-energy impacts causing surface cracking. Corrosion wear involves galvanic interactions between the cell and the balls or between different abraded and unabraded points on the balls' surface [59]. When cells are crushing and grinding in the milling, the ball size distribution, and rotation speed both determine disintegration ability [60,61]. Between the two, bead mills are generally the preferred choice because of their greater efficiency in breaking down microbial cells due to their smaller bead size generating higher shear force. Overall, the milling method offers several advantages, including continuous operation, relatively low capital costs, and suitability for applications ranging from the laboratory scale to the industrial scale [60,62].

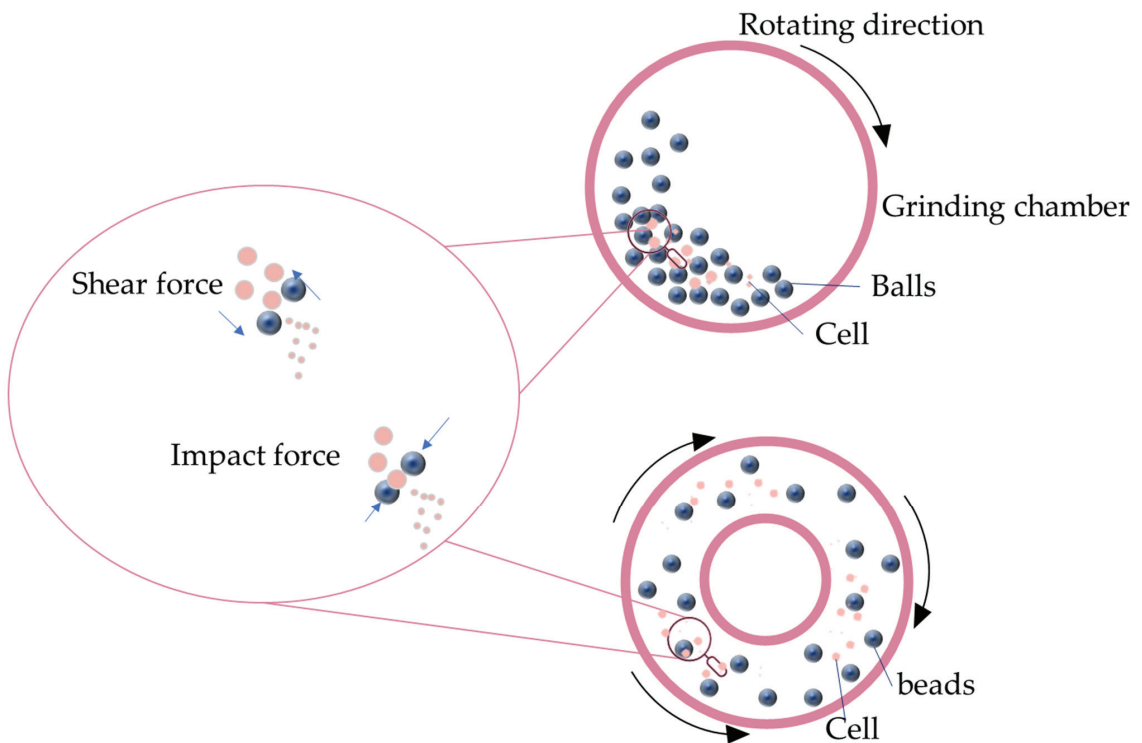


Figure 3. A schematic diagram of ball mill (upper one) and bead mill (lower one). In both equipment types, cells are disrupted by grinding them between beads or balls within a closed container. The beads or balls agitate and collide with the cells, causing physical shear forces and impact forces that break apart the cell walls and release their intracellular contents.

Milling technology has been used to disrupt bacterial cell walls. Tamer et al. applied a continuous flow high-speed bead mill to recover intracellular poly(b-hydroxybutyric acid) (PHB) from *Alcaligenes latus* cells [63]. Without any chemical involved, an 85% loaded bead achieved over a 50% improvement compared to an 80% loaded bead, which had a disruption rate constant of 0.44. The results also indicated that PHB purity increased with the number of passes. However, extreme physical disruption could result in a micronization phenomenon occurring to PHB, resulting in loss of PHB. Although bead milling alone does not achieve higher extraction efficiency than solvent extraction, it offers better energy efficiency since highly concentrated slurries can be processed in bead mills. Another study done by the same group studied how different bead milling parameters affect the protein extraction from *Alcaligenes latus* cells [18]. Their study showed that the mean diameter of the beads (512 to 945 μm) did not affect the disruption rate of *Alcaligenes latus* cells, since the bacterial cell size was too small (0.5–1.0 μm in diameter). With a mean diameter of 512- μm beads, complete disruption was achieved by the eighth pass at an 85% bead loading, whereas a reduced loading of 75% did not release all the cellular protein even after 16 passes. The biomass concentration was not a dependent factor for bead mill disruption effectiveness. Another study investigated the extraction of intracellular enzymes from *Arthrobacter* sp. DSM 3747 by examining the effects of various operational parameters of the stirred ball mill on disintegration results [60]. They found that, under the same operating conditions, achieving a disintegration rate of 50% with 1.28 mm beads requires 20 times higher energy compared to smaller beads of 0.2 mm. The optimized operational parameters combination was small grinding beads (0.3 mm) with a moderate-to-high cell concentration in the suspension (about 50%) and operating at low-to-moderate agitator speeds (6 m/s circumferential speed of agitator disks).

In addition, bead milling was applied to algae for cell disruption. A study investigated the optimization of bead milling for microalgae cell disruption, focusing on how different bead sizes affect the process efficiency, energy consumption, and the release of proteins and carbohydrates [64]. The result indicated that smaller bead size, which induces more shearing forces, improved extraction yield with a lower energy consumption. Specifically, the bead size range of 0.3–0.4 mm was determined as optimal bead size for balancing cell disruption efficiency and energy consumption for microalgae. In another study, researchers employed bead milling to disrupt cells for isolating proteins from the green microalga *Tetraselmis* sp. [65]. The microalgae were milled by bead milling to release proteins, followed by centrifugation and ion exchange chromatography to purify the proteins. The resulting algae-soluble isolate comprised 64% protein and had a clear appearance with 100% solubility at pH above 5.5, making it a potential food ingredient. In a study, Loureiro et al. studied five cell-disruption methods including freeze–thaw cycles, bead milling, high-speed homogenization, microwave, and sonication to disrupt microalgae (*Coelastrella* sp.) for releasing intracellular biochemical compounds [66]. They found that sonication showed the highest efficiency in the release of proteins, carbohydrates, and lipids, followed by bead milling. However, considering the balance of the extraction efficiency and energy consumption, bead milling can be considered the most efficient method. Another study examined the effects of nitrogen depletion on bead-milling performance for releasing cellular components from *Neochloris oleabundans* [67]. Under the same bead-milling operation condition, the study revealed that nitrogen-depleted cells had significantly higher release rates of biomass and biochemical components, with a release ratio of 0.57, compared to 0.38 for nitrogen-replete cells. Nitrogen-depleted conditions enhanced the release intracellular compounds, achieving up to 68% carbohydrate, 59% protein, and 56% lipids (*w/w*) release. Additionally, the energy consumption per kilogram of released product was lower for nitrogen-depleted cells, indicating more efficient cell disruption.

Several studies examined the disruption of yeast cells using bead milling to release glucose 6-phosphate dehydrogenase. One study used a vertical bead mill to extract glucose 6-phosphate dehydrogenase [68]. Their results identified 2300 rpm for 6 min as optimal conditions for yeast disruption, achieving higher proportion of glucose 6-phosphate de-

hydrogenase release in total proteins without heat denaturation. Another study used a horizontal bead mill in continuous recycle mode to extract glucose 6-phosphate dehydrogenase [69]. The result indicated that optimal total protein release (37.3 mg/mL) was achieved with a 24 h/L feeding rate and 50% (*w/v*) initial biomass concentration. However, a higher biomass concentration loading generated heat, which decreased glucose 6-phosphate dehydrogenase activity. To balance optimal yield, minimal glucose 6-phosphate dehydrogenase degradation, and manageable viscosity during afterward centrifugation, the study concluded that a 20% (*w/v*) biomass load was optimal. This reduced heat generation and maintained enzyme bioactivity while facilitating easier separation after milling.

Milling has been demonstrated to be useful in extracting proteins and lipids from various cell types (Table 3). It has particularly advantageous for tough-walled cells, such as microalgae, due to the high mechanical forces generated by the grinding media, which can effectively disrupt rigid cell walls with relatively low energy consumption [70]. Additionally, milling systems are scalable from laboratory to industrial scale, and bead milling can be adapted for continuous processing of viscous and highly concentrated cell suspensions, making it beneficial for industrial applications [71]. In addition, mechanical milling provides consistent and uniform cell disruption, which is critical for maximizing the recovery of intracellular compounds.

However, mechanical milling methods come with certain limitations. One primary concern is the significant heat generation due to the friction between beads/balls during the milling process [72,73]. The generated heat is difficult to remove from the container and it could damage heat-sensitive intracellular compounds. This requires careful management of heat removal by additional cooling system. Moreover, compared to other physical methods like ultrasonication or high-pressure homogenization, mechanical milling provides less precise control over the disruption process, potentially leading to the co-extraction of unwanted cell debris, complicating downstream purification processes. Additionally, there is a risk of contamination from the grinding media, as the beads and balls can wear down over time due to the mechanical forces of impact, abrasion, and attrition, releasing particles into the samples. For applications requiring high purity, such as pharmaceuticals or fine chemicals, this contamination can be problematic and may require additional filtration or purification steps [59].

Overall, due to its versatility, mechanical milling is widely used in industrial-scale bioprocessing, particularly for breaking tough cell types like yeast, microalgae, and fungi. Its scalability and cost-effectiveness make it suitable for large-scale operations where high throughput and uniform cell disruption are critical. However, due to its high heat generation, it is less ideal for recovering thermolabile compounds, where more precise methods like ultrasonication may be preferred.

Table 3. Summary of studies on milling techniques extracting intracellular compound.

Microorganism	Target Compounds	Recovery	Parameters	Key Finding	Source
<i>Alcaligenes latus</i>	poly(b-hydroxybutyric acid)	44% disruption rate, 1.2 kg PHB/kg pellet	512 µm mean bead diameter, 80% bead loading	The extreme mechanical disruption could result in micronization phenomenon to poly(b-hydroxybutyric acid).	[63]
<i>Alcaligenes latus</i>	Proteins	Near 100%	512 to 945 µm bead diameter, 85% bead loading	The mean diameter of the beads did not affect the disruption rate of <i>Alcaligenes latus</i> cells. Biomass concentration did not influence the effectiveness of bead mill disruption.	[18]
<i>Arthrobacter</i> sp.	Proteins	50% disintegration rate	300 µm bead diameter, 80% dead loading	Cell disruption correlates with energy input.	[60]

Table 3. Cont.

Microorganism	Target Compounds	Recovery	Parameters	Key Finding	Source
microalgae	Proteins and carbohydrates	30–50% proteins, 10–30% carbohydrates	300–400 μm bead diameter, 65% bead loading	The bead size range of 0.3–0.4 mm was determined as optimal balancing cell disruption efficiency and low energy consumption.	[64]
<i>Tetraselmis</i> sp.	Proteins	64% proteins	400–600 μm bead diameter, 65% bead loading	Bead milling followed by centrifugation and ion exchange chromatography resulted algae-soluble isolate comprised 64% protein and 100% solubility at pH levels above 5.5.	[65]
<i>Coelastrella</i> sp.	biochemical compounds	94% disruption efficiency	500 μm bead diameter, 32% bead loading	Considering the balance of the extraction efficiency and energy consumption, bead milling can be considered the most efficient method.	[66]
<i>Neochloris oleabundans</i>	Carbohydrate, protein, and lipids	68% carbohydrate, 59% protein, and 56% lipids	400–600 μm bead diameter	Nitrogen depletion can enhance the cost-effectiveness of microalgal biomass processing by bead milling.	[67]
<i>Saccharomyces cerevisiae</i>	glucose 6-phosphate dehydrogenase	15 mg/mL protein	500 μm bead diameter	The vertical bead mill at 2300 rpm for 6 min was optimal conditions for yeast disruption and glucose 6-phosphate dehydrogenase release without heat denaturation.	[68]
<i>Saccharomyces cerevisiae</i>	glucose 6-phosphate dehydrogenase	37.3 mg/mL protein	300 μm bead diameter	In a horizontal bead mill operating in continuous recycle mode, the optimal total protein release was achieved with a 24 h/L feeding rate and a 50% (<i>w/v</i>) initial biomass concentration.	[69]

2.4. Pulsed Electric Field

Pulsed electric field is an emerging and non-thermal method used for intracellular compound extraction, primarily in the biotechnology, food, and pharmaceutical industries. It disrupts cell walls or membranes by applying short and high-voltage electrical pulses (10–80 kVcm^{-1}), creating temporary or irreversible pores or gaps in the cell membrane, allowing molecules, ions, or other substances to pass through that would normally be restricted [74]. The electrical pulses alter the transmembrane potential, causing the formation of nanopores in the cell membrane's phospholipid layer. These nanopores arise from the reorganization and destabilization of lipid molecules induced by the electric field. This process, known as electroporation or electropermeabilization, is influenced by several key electrical parameters, including the field strength, pulse shape and duration, number of pulses, and specific energy used in treatment [75]. As shown in Figure 4, this electroporation can be reversible or irreversible based on the strength of the applied electrical field. When the applied external electrical field (E_e) is higher than the critical electrical field strength of the cell membrane (E_c), membrane permeabilization takes place but the cell membrane can recover after the exposure is performed. When the E_e further increases, the E_e is much higher than E_c to the certain point that the permeabilization is not able to be recovered. The release of intracellular substance resulting from pulsed electric field is a relatively gentle cell-disintegration process, typically performed at ambient temperatures and without introducing additional impurities [76]. The mild treatment avoids heat

degradation of the targeted intracellular materials while releasing them. Additionally, the disruption process is rapid, occurring within a few seconds.

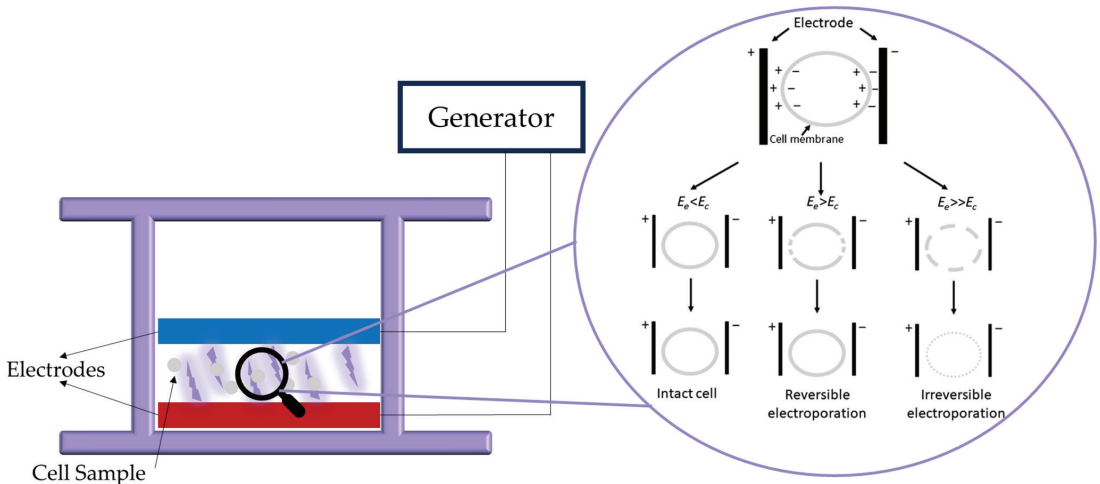


Figure 4. A schematic diagram illustrating the electroporation mechanism of pulsed electric fields. This technique disrupts cell membranes by applying short or high-voltage electrical pulses, creating temporary or irreversible pores in the cell membrane. These pores allow molecules, ions, or other substances to pass through that would normally be restricted. Reproduced with permission [74].

The pulsed electric field made the cell membrane permeable, as demonstrated by the percentage propidium iodine fluorescent dye up taken by cells, which can only pass through the non-intact membrane. Luengo et al. examined the impact of pulsed electric field treatments on the permeabilization of *Chlorella vulgaris* and the extraction of pigments [77]. The study found that after 150 μs of pulsed electric field treatment, it caused irreversible electroporation resulting in 100% cell death of *Chlorella vulgaris*. The application of 20 kVcm^{-1} for 75 μs increased pigment extraction yields by 1.2 to 2.1 times after 1 h incubation compared to immediate extraction, which were 1100 μg carotenoids, 2500 μg chlorophyll a, and 1100 μg chlorophyll b per g of culture. In another study, Lam et al. investigated the release of protein from microalgae using two sets of pulsed electric field: (i) batch pulsed electric field with electric field strength between 7.5 and 30 kV cm^{-1} , and (ii) continuous flow pulsed electric field treatment with electric field strength of 20 kV cm^{-1} with 13 mL min^{-1} flow rate [19]. They found that with increased pulsed electric field energy, the relative ion release increased, indicating that the pulsed electric field made the microalgae membrane more permeable. However, a low protein yield was obtained as intracellular proteins remained entrapped. One study examined how the pulsed electric field treatment energy and electric field strength and biomass concentration affected cell disruption using the microalgae *Auxenochlorella protothecoides* [76]. It was observed that the disruption efficiency increased as specific treatment energy increased, while the field strength had a minimal impact. For pigments and proteins extraction from *Parachlorella kessleri* microalgae, high-voltage electrical discharges were found effective for extracting ionic components and carbohydrates but less so for proteins and pigments, achieving a maximum protein extraction of only 750 mg/L , which was about 15% of the total protein content [26].

Coustets et al. developed a pulsed electric field-based process to extract cytoplasmic proteins from three microalgae species: *Nannochloropsis salina*, *Chlorella vulgaris*, and *Haematococcus pluvialis* [78]. The study examined various electric field strengths, pulse durations, and incubation conditions, finding that optimal extraction conditions were species-dependent. *Nannochloropsis salina* required a stronger electric field (6 kV cm^{-1}) for effective release of 25 μg protein/ mL culture. For *Chlorella vulgaris* and *Haematococcus pluvialis*, milder conditions

(4.5 kV cm⁻¹) sufficed to release 30 µg protein/mL culture due to their larger cell sizes. *Nanochloropsis salina*, with higher field strength needed, had extraction improved significantly after a second cycle of 15 bipolar pulses, while *Chlorella vulgaris* did not benefit from an additional cycle. The study also demonstrated a linear relationship between cell concentration and extracted protein concentration, indicating that higher cell densities directly increased the amount of protein extracted. Postma et al. observed a synergistic effect between pulsed electric field and temperature treatments to disrupt microalgae *Chlorella vulgaris* [79]. They demonstrated that applying pulsed electric field at temperatures between 25 °C and 65 °C increased cell permeability and selectively enhanced the release of carbohydrates, achieving up to 39% carbohydrate extraction while retaining over 95% of the proteins within the cells. This synergistic effect was most pronounced at 55 °C, particularly for carbohydrate release. The combined pulsed electric field and temperature treatment effectively released small, water-soluble molecules but was less efficient for protein extraction compared to bead milling. Luengo et al. compared the effects of millisecond- and microsecond-pulsed electric field treatments on the permeabilization and extraction of pigments from microalgae *Chlorella vulgaris* [80]. The study found that permanently electroporation occurred at 4 kV cm⁻¹ with millisecond pulses, while microsecond pulses required 10 kV cm⁻¹. Electroporation effectiveness was linked to pulse duration and frequency: millisecond pulses needed 20 pulses at 5 kV cm⁻¹, whereas microsecond pulses required shorter treatment times but higher electric field strengths (≥15 kV cm⁻¹). To achieve a similar degree of permanent electroporation, a reduction in pulse duration from milliseconds to microseconds required a three-fold increase in electric field strength. For effective pigment extraction, microsecond pulses proved more energy-efficient, consuming 30 kJ/L compared to 150 kJ/L for millisecond pulses. Additionally, microsecond pulses (15 kV cm⁻¹, 25 pulses) yielded higher pigment extraction, with concentrations of carotenoids and chlorophylls a and b at 1.09, 3.95, and 2.17 mg/L of culture, respectively. In contrast, millisecond pulses (5 kV cm⁻¹, 20 pulses) resulted in yields of 1.06, 2.90, and 1.69 mg/L of culture for the same pigments. These findings indicate that microsecond pulses offer a more energy-efficient and effective method for pigment extraction from microalgae.

Studies were also conducted to apply pulsed electric field for extracting protein from *Saccharomyces cerevisiae*, which is rich in intracellular proteins and other bioactive compounds. Ganeva et al. assessed the effect of medium pH on the protein release from yeast by pulsed electric field treatment [81]. The result indicated that the more alkalic condition increased the intracellular protein release. Cell concentration also influenced protein release efficiency—a higher cell concentration reduces optimal field strength. About 90% of the total soluble protein release occurred only after dilution and incubation of the permeabilized cells in buffer with pH 8–9. Fincan et al. explored the efficacy of pulsed electric field treatment in enhancing the extraction of red pigment from red beetroot [82]. By applying 270 rectangular pulses at 1 kV cm⁻¹, the research achieved approximately 90% total red coloring and ionic content release after 1 h aqueous extraction. It offers a low-energy alternative for the extraction of valuable compounds from plant tissues. The pulsed electric field treatment significantly led to a higher release of pigment and ionic species into the solution, compared to the traditional freezing and thawing method.

One of the major advantages of pulsed electric field is its gentle, non-invasive nature. Unlike mechanical milling or HPH, pulsed electric field does not generate a large amount of heat due to friction, making it ideal for extracting heat-sensitive compounds, such as pigments, enzymes, and functional proteins (Table 4). Another clear advantage of pulsed electric field is its selectivity. It selectively disrupts the cell membrane without causing extensive damage to other cellular components, thus enhancing the product purity and simplifying downstream purification by reducing the co-extraction of undesirable cell debris. In addition, with operation times ranging from microseconds to milliseconds, pulsed electric field is a rapid and efficient method. Additionally, the process can be precisely controlled.

Pulsed electric field has some challenges to overcome. First, unlike mechanical milling, which can be universally used with similar operations, the pulsed electric field technique

depends heavily on the optimization of process parameters like electric field strength, pulse duration, and the conductivity of the medium for each type of microbial cells and liquid medium. Failing to optimize these parameters will likely cause incomplete extraction of intracellular compounds or excessive cell damage. Second, although this technology is highly scalable to the industrial level, it requires specialized equipment, which usually leads to high capital investment to purchase and install the equipment and auxiliary facility to initiate the process. Additionally, the viscosity of the suspension can impact the uniformity of the electric field. In high-density broths or non-conductive media, cells may not experience uniform field exposure, leading to incomplete disruption [74].

As an emerging technology, the pulsed electric field technology is still largely in the research and pilot-scale stage for many applications, although there are some industrial uses for the purpose of extending shelf-life of liquid foods (like fruit juices). The motioned challenges, including the need for process optimization, specialized equipment, and limitation with breaking down tough cell types like fungi, have slowed the wide industrial adoption of this technique for intracellular extraction. However, there is a tremendous interest in commercializing this technique for the recovering of high-value protein and enzymes from microbial cells in the pharmaceutical and biotechnology industry, due to its capability to preserve bioactivity and ensure purity of the target compounds.

Table 4. Summary of studies on pulsed electric field techniques extracting intracellular compound.

Microorganism	Target Compounds	Electrical Field Strength	Key Finding	Source
<i>Chlorella vulgaris</i>	Carotenoids and Chlorophylls a and b	20 kVcm ⁻¹	After 150 μs of pulsed electric field treatment, it caused irreversible electroporation resulting the <i>Chlorella vulgaris</i> cell 100% death.	[77]
<i>Chlorella vulgaris</i> and <i>Neochloris oleoabundans</i>	Protein	20–30 kVcm ⁻¹	Increased pulsed electric field energy enhanced membrane permeability in microalgae. However, protein yield remained low, as intracellular proteins were still trapped.	[19]
<i>Auxenochlorella protothecoides</i>	Intracellular valuables	23–43 kVcm ⁻¹	The efficiency of disruption increased as specific treatment energy increased, while the field strength had minimal impact.	[76]
<i>Parachlorella kessleri</i>	Protein and pigment	40 kVcm ⁻¹	High-voltage electrical discharge was found effective for extracting ionic components.	[26]
<i>Nannochloropsis salina</i> , <i>Chlorella vulgaris</i> , and <i>Haematococcus pluvialis</i>	Protein	4.5 and 6 kVcm ⁻¹	A linear relationship between cell concentration and extracted protein concentration was found. Optimal extraction conditions were species dependent.	[78]
<i>Chlorella vulgaris</i>	Protein and carbohydrates	17.1 kVcm ⁻¹	A synergistic effect between pulsed electric field and temperature treatments increased cell permeability and released small, water-soluble molecules.	[79]
<i>Chlorella vulgaris</i>	Pigments	5–15 kVcm ⁻¹	Microsecond pulses offer a more energy-efficient and effective method than millisecond pulses for pigment extraction from microalgae.	[80]
<i>Saccharomyces cerevisiae</i>	Protein	2.5–5.5 kVcm ⁻¹	More alkalic conditions increased the intracellular protein release. A higher cell concentration reduced optimal field strength.	[81]
Red beetroot	Red pigment	1 kVcm ⁻¹	Pulsed electric field treatment significantly led to a higher release of pigment and ionic species into solution, compared to traditional freezing and thawing method.	[82]

Physical cell disruption methods include high-pressure homogenization, ultrasonication, milling, and pulsed electric fields. These methods can also be combined with chemical and biological approaches. Each technique has its own advantages and disadvantages, and their application depends on the target compounds and specific processing requirements (Figure 5).

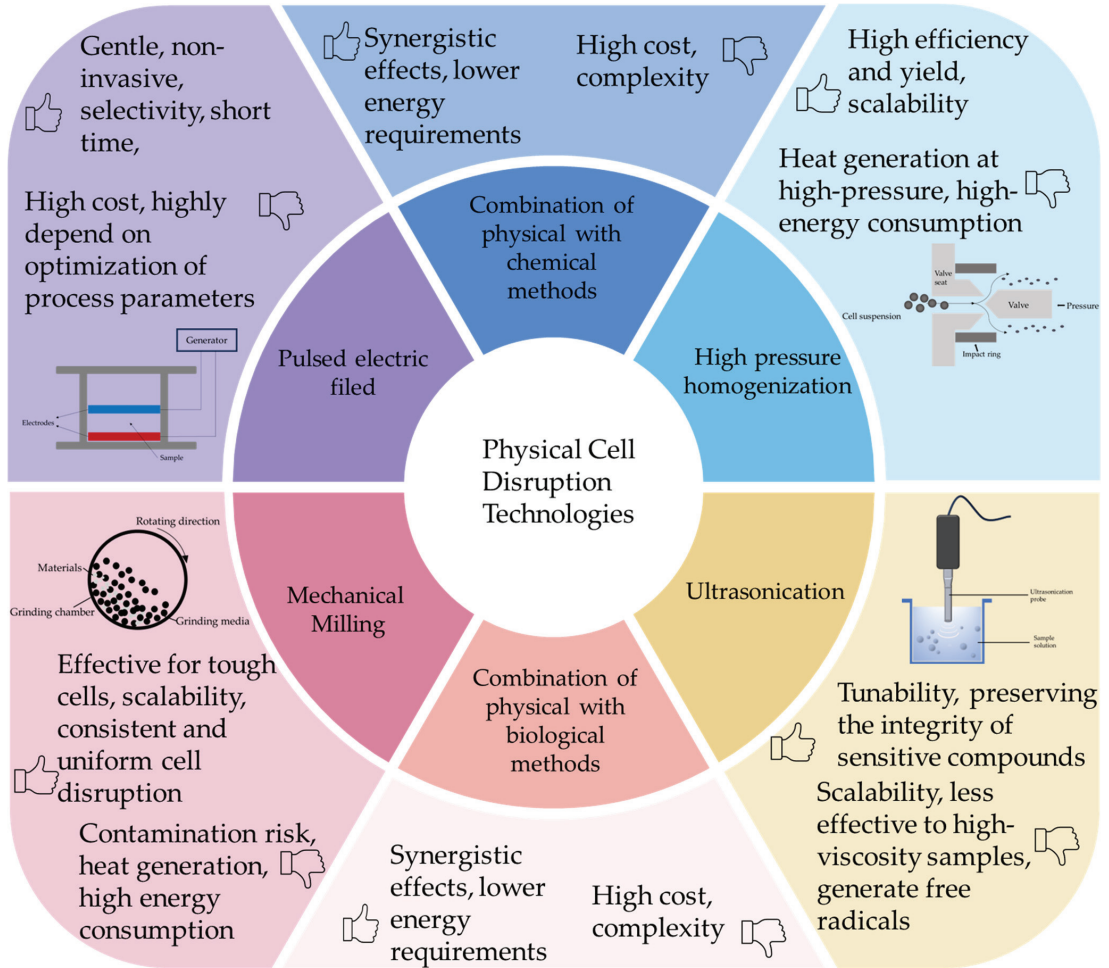


Figure 5. Physical methods for intracellular compound extraction with the advantages and limitations of each technique.

3. Physical Assisted Methods

Combining physical techniques with chemical and biological methods enhances extraction efficiency by reducing energy consumption, improving selectivity, and minimizing damage to sensitive compounds. The use of enzymes or mild chemical solvents alongside physical techniques allows physical forces to more easily complete the disruption, thus reducing the energy required for physical techniques. Each method brings unique advantages, and when combined, they create a synergistic effect that improves overall extraction yields (Table 5).

3.1. Combination of Physical with Chemical Methods

The combination of physical and chemical methods to extract intracellular compounds offers a promising avenue for enhancing the efficiency and yield of biologically active substances from various biological matrices. By integrating physical methods like ultrasonication or homogenization with chemical treatments such as solvent extraction, this hybrid approach can effectively disrupt cell walls and membranes, facilitating deeper penetration of chemicals that solubilize target compounds.

Zhang et al. investigated the efficacy of combining different physical treatments—pulsed electric fields, high-voltage electrical discharge, and ultrasonication—with green solvent extraction to extract water-soluble molecules (carbohydrates and proteins) and water-insoluble molecules (chlorophyll a) from three different microalgal species [83]. The research revealed that high-voltage electrical discharge-assisted solvent extraction was most effective for extracting carbohydrates, while ultrasonication-assisted solvent extraction was more efficient for extracting proteins and chlorophyll a from microalgal species (*Nannochloropsis* sp., *P. tricornutum*, and *P. kessleri*). Combining ultrasound with solvent extraction has proven effective in enhancing the release of intracellular compounds. For instance, a study led by Monks et al. explored methods of cell disruption to optimize the extraction of carotenoids from fungi [84]. Their results demonstrated that ultrasound alone showed relatively low carotenoids recovered while combining ultrasound with sodium bicarbonate doubled the number of recovered carotenoids. Another study led by Zheng et al. examined the use of ultrasonic-assisted deep eutectic solvent extraction to extract phenolic compounds from foxtail millet bran [85]. They optimized a green extraction method to maximize phenolic content. The optimized conditions involved a deep eutectic solvent composed of betaine and glycerol in a 1:2 molar ratio and ultrasonic power at 247 W. Under the optimal condition, a total phenolic content of 7.80 mg ferulic acid equivalent per gram was achieved, yielding higher total phenolics, flavonoids, antioxidant activity, and acetylcholinesterase inhibitory activity compared to conventional solvent extraction methods. Scanning electron microscopy revealed significant microstructural disruption in the millet bran, with more pores and cracks, after ultrasonic-assisted deep eutectic solvent extraction. To evaluate the effects of ultrasound-assisted lipid extraction using solvents from wet microalgal cells, a study by Keris-Sen et al. demonstrated that sonication at 0.4 kWh/L significantly enhanced cell disruption [17]. This process nearly doubled lipid extraction efficiency compared to using solvents alone. However, more than 30% lipid remained in the biomass. The effects of different types of ultrasound apparatuses (cup horn, immersion horn, and cavitating tube) on the ultrasound-assisted solvent extraction of soybean-germ oil were evaluated [86]. The study found that the highest oil yield was achieved using a cavitating tube at 19 kHz, combined with double sonication using an additional immersion horn at 25 kHz. This approach improved oil yields by up to 500% compared to conventional methods and significantly enhanced extraction efficiency. The maximum extraction rate of 25.9% was achieved with a power of 65 W at 45 °C for 30 min, compared to a 4.8% extraction rate using conventional solvent extraction over 4 h. The study conducted by Martinez-Guerra et al. showed that ultrasound and microwave-assisted extraction enhanced extractive transesterification of algal lipids from *Chlorella* sp. using ethanol, improving yields over the conventional bench-top Blich and Dyer method, which involves chloroform and methanol for isolating lipids [87]. They optimized the process conditions, finding that microwaves operating at 350 W for 5–6 min with a 1:12 algae to ethanol ratio achieved an 18.8% lipid yield and 96.2% fatty acid ethyl ester conversion. Ultrasonication at 490 W for 6 min with a 1:6 algae to ethanol ratio achieved a lipid extraction rate of 18.5% and fatty acid ethyl ester conversion rate of 95%, compared to the Blich and Dyer method, which had a 13.9% yield and 78.1% conversion. In addition, ultrasound offered not only lipids extraction from algal *Chlorella* sp. but also transesterification in a short reaction time period. Both methods surpassed the Blich and Dyer method in yield and conversion efficiency, indicating their potential for more efficient biodiesel production. Parniakov et al. examined ultrasound-assisted green solvent extraction of bioactive compounds from the

microalgae *Nannochloropsis* spp. The study evaluated different solvents (water, ethanol, and dimethyl sulfoxide) for extracting phenolic compounds and chlorophylls [88]. When using individual solvents, the efficiency of recovery was highest with dimethyl sulfoxide, followed by ethanol and water. The yield of total phenolic compounds increased over time and reached saturation after 5 min, irrespective of the solvent employed. However, the extraction kinetics of total chlorophylls varied depending on the solvent used. In ethanol and water, the extraction yield plateaued after 7.5 min of ultrasound-assisted extraction. In contrast, in dimethyl sulfoxide, the yield peaked at 5 min and subsequently declined after 7.5 min. The decline in yield could be attributed to the increase in sample temperature due to prolonged ultrasound energy, leading to heat degradation of the chlorophyll.

Besides ultrasonication, pulsed electric field technology has also been integrated with solvent extraction to enhance intracellular compound extraction. A study demonstrated pulsed electric field pretreatment to enhance lipid recovery from the microalga *Scenedesmus* [89]. The study found that combining pulsed electric field with solvent extraction markedly increased the yield of crude lipids and fatty acid methyl esters compared to direct solvent extraction of untreated samples. Pulsed electric field pretreated biomass, when extracted with solvents, yielded up to 3.1 times more fatty acid methyl esters than untreated biomass and required fewer solvents than using solvent extraction from untreated biomass. Under the optimal combination of pulsed electric field pretreatment and solvent extraction, a 12-fold reduction in solvent use while maintaining high lipid recovery efficiency was achieved. This suggests that pulsed electric field pretreatment is an effective method for enhancing lipid extraction from microalgae and reducing solvent consumption. Parniakov et al. investigated the pulsed electric field-assisted solvent extraction of valuable compounds from *Nannochloropsis* sp. using binary mixtures of organic solvents (dimethyl sulfoxide and ethanol) and water [90]. They compared a one-stage solvent extraction to a two-stage process involving initial pulsed electric field treatment followed by solvent extraction. The study found that pulsed electric field pretreatment significantly improved extraction efficiency, particularly for chlorophylls and carotenoids, and reduced the required solvent concentration. The two-stage process was more effective at extracting pigments and non-degraded proteins while minimizing solvent use. This approach demonstrated the potential of pulsed electric field to enhance extraction processes in a more sustainable manner by reducing solvent consumption and improving yield. Pulsed electric field technology has been proven effective as a pretreatment for enhancing lipid extraction from the green microalga *Ankistrodesmus falcatus* using the green solvent ethyl acetate [91]. The study showed that pulsed electric field pretreatment improved lipid recovery efficiency significantly compared to untreated samples. Pulsed electric field disrupted up to 90% of the cells, thereby reducing the required solvent contact time and accelerating lipid recovery. As a result, lipid yield increased to 6100 µg/L with pulsed electric field pretreatment, compared to 2600 µg/L without pretreatment. Pulsed electric fields were also used as pretreatment to assist solid–liquid extraction of aromatic and bioactive compounds from various plant sources including orange peels, vanilla pods, and cocoa bean shells [92]. The results demonstrated that pulsed electric field pretreatment with intensity of 3–5 kV cm⁻¹ and energy input as low as 15–40 kJ/kg enhanced the extraction yields significantly, demonstrating that pulsed electric field enhanced tissue permeabilization for extraction ability without degrading phenolic compounds.

Microwave-assisted extraction is an emerging technique for extracting lipids from wet microalgae, providing several advantages over traditional methods. Operating at a frequency of about 2.45 GHz, the microwave utilizes dielectric heating by absorbing energy in polar compounds present in the wet sample. This process causes polar molecules within the wet biomass to vibrate, increasing the temperature of the intracellular liquid. The resulting evaporation generates pressure on the cell walls, leading to their rupture and the release of lipids [93].

A number of studies have shown that microwave-assisted solvent extraction can enhance lipid yield and reduce extraction time from microalgae [94–109]. Cheng et al. devel-

oped a chloroform-free process for lipid extraction from wet microalgae *Chlorella pyrenoidosa*, employing microwave technology followed by hexane extraction [110]. The study identified 90 °C as the optimal temperature for this microwave-assisted solvent extraction process. This method efficiently converts triglycerides in wet microalgae into methyl esters, which are lower in molecular weight and, thus, dissolve more readily in hexane. As a result, the process enhanced the fatty acid methyl ester content in crude biodiesel to 86.7%. In addition, undesired polar pigments present in microalgae are not extracted during this process. Furthermore, pulsed microwave technology is considered an energy-saving pretreatment for microalgae. In a study by Zhang et al. using fresh *Auxenochlorella protothecoides*, the effects of pulse duration, repetition rate, and pulse power on cell permeabilization and lipid yield were assessed [111]. The results showed that pulsed microwaves at 2.8 kW peak power with 200 μ s pulses significantly enhanced lipid yield up to 90% of the total lipid content through solvent extraction. Efficiency was primarily influenced by the total energy input rather than specific pulse properties, demonstrating a positive correlation between energy input and lipid yield. Additionally, pulsed microwaves consumed less energy (2.53 MJ/kg dry weight) compared to traditional hexane extraction methods, highlighting their potential for energy-efficient and scalable microalgae processing.

3.2. Combination of Physical and Biological Methods

Combining physical and biological extraction methods using enzymes to extract intracellular compounds provides an efficient technique to increase the yield and purity of targeted compounds. Physical methods like ultrasonication physically disrupt cell structures, enhancing the accessibility of enzymes to the intracellular components. Subsequently, specific enzymes can be employed to selectively break down complex molecules.

Integrating a physical method with enzyme digestion has shown effective extraction of protein from *Chlorella* species with a 72.4% extraction efficiency [41]. The study combined ethanol soaking, enzymatic digestion, ultrasonication, and homogenization techniques. This multifaceted approach significantly improved protein yield compared to traditional solvent extraction methods, providing a reference for efficient bioactive compound extraction from microalgal cells. Ultrasonic assisted enzymatic hydrolysis was also employed on the extraction of protein from excess sludge. Ultrasonic pretreatment combined with enzymatic hydrolysis significantly enhances protein extraction rates and improves sludge dewatering performance [112]. By optimizing conditions such as ultrasonic power density, hydrolysis time, enzyme dose, and pH, protein extraction rates of 55.9% and 52.3% for two types of sludge were achieved. Ultrasound-assisted enzyme extraction was also applied to extract carotenoids from yeast from a fermentation broth [113]. Another study demonstrated that ultrasound-assisted aqueous enzymatic extraction could be used to extract oil from gardenia fruits [114]. Two enzymes, Cellic CTec3 and Alcalase 2.4 L, were used with ultrasonic pretreatment. The optimal conditions achieved up to 18.7% extraction efficiency. The research discussed ultrasonic pretreatment led to more efficient cell wall disruption and higher oil yields. The physicochemical properties of the extracted oil were better using ultrasound-assisted aqueous enzymatic extraction, indicated by the lowest acid value and peroxide value. Further expanding on techniques, a study by Hu et al. investigated the extraction of oil from cherry seeds using an ultrasonic microwave-assisted aqueous enzymatic extraction process, achieving an oil recovery of 83.9%. The oil extracted under these conditions showed no significant difference in fatty acid compositions when compared to traditional methods but displayed better physicochemical properties and a higher content of bioactive constituents [115].

Table 5. Summary of studies on physical assisting techniques extracting intracellular compound.

Microorganism	Target Compounds	Key Finding	Source
<i>Nannochloropsis</i> sp., <i>P. tricornutum</i> and <i>P. kessleri</i>	Proteins and chlorophyll a	High-voltage electrical discharge-assisted solvent extraction was most effective for extracting carbohydrates, while ultrasonication-assisted solvent extraction was more efficient for extracting proteins and chlorophyll a from microalgae.	[83]
Fungi	Carotenoids	Ultrasound with sodium bicarbonate doubled the number of recovered carotenoids.	[84]
Foxtail millet bran	Phenolic compounds	Ultrasonic-assisted deep eutectic solvent extraction method produced higher total phenolics, total flavonoids, in vitro antioxidant activity, and acetylcholinesterase inhibitory activity than the conventional solvent extraction.	[85]
Wet microalgae	Lipid	Coupling sonication significantly enhanced cell disruption and doubled lipid extraction efficiency compared to using solvents alone.	[17]
Soybean germ	Lipids	The highest oil yield was achieved by ultrasound-assisted extraction using a cavitating tube at 19 kHz, combined with double sonication using an additional immersion horn at 25 kHz.	[86]
<i>Chlorella</i> sp.	Lipids	Ultrasound not only improved yields over conventional bench-top Bligh and Dyer method but also shortened the transesterification of algal lipids.	[87]
<i>Nannochloropsis</i> sp.	Phenolic compounds	Ultrasound extraction doubled the yield of total phenolic compounds compared to extraction without ultrasonication.	[88]
<i>Scenedesmus</i>	Lipids	Under the optimal combination of pulsed electric field pretreatment and solvent extraction, solvent use was reduced 12-fold while maintaining high lipid recovery efficiency.	[89]
<i>Nannochloropsis</i> sp.	Chlorophylls and carotenoids	Pulsed electric field pretreatment significantly improved extraction efficiency, particularly for chlorophylls and carotenoids, and reduced the required solvent concentration.	[90]
<i>Ankistrodesmus falcatus</i>	Lipids	Pulsed electric field pretreatment improved lipid recovery efficiency significantly compared to untreated samples extracted with green solvent ethyl acetate.	[91]
Plant	Aromatic and bioactive compounds	Pulsed electric field pretreatment with intensity of 3–5 kV cm ⁻¹ and energy input as low as 15–40 kJ/kg enhanced the solid–liquid extraction yields significantly.	[92]
<i>Chlorella pyrenoidosa</i>	Lipids	Microwave-assisted hexane extraction can replace the traditional chloroform method.	[110]
<i>Auxenochlorella protothecoides</i>	Lipids	Pulsed microwaves consume less energy compared to traditional extraction methods.	[111]
microalgae <i>Chlorella</i>	Protein	A multifaceted approach combining ethanol soaking, enzymatic digestion, ultrasonication, and homogenization techniques significantly improved protein yield compared to traditional methods.	[41]
Excess sludge	Protein	Ultrasonic pretreatment combined with enzymatic hydrolysis significantly enhances protein extraction rates and improves sludge dewatering performance.	[112]
Gardenia fruits	Oil	Physicochemical properties of the extracted oil were better using ultrasound-assisted aqueous enzymatic extraction, indicated by the lowest acid value and peroxide value.	[114]
Cherry seeds	Oil	An ultrasonic microwave-assisted aqueous enzymatic extraction process displayed better physicochemical properties and a higher content of bioactive constituents.	[115]

4. Challenges and Future Perspectives

While physical disruption techniques have shown considerable promise, they come with their own set of limitations of challenges. One of the key limitations of physical methods is their lack of selectivity compared to the well-established chemical methods. Chemical methods, particularly solvent-based extractions, offer great selectivity by using tailored solvent to selectively extract targeted compounds without dissolving unwanted cellular contents, resulting in high-purity final products, and simplifying the downstream purification process. In contrast, physical methods, like HPH and mechanical milling, rely on mechanical forces to indiscriminately disrupt the cells, leading to the non-specific release of all intracellular components, including cell debris and other unwanted intracellular organelles. Thus, the extracted compounds by using physical methods usually have a lower purity compared to those extracted by using solvent extraction, thereby complexing the downstream process as additional filtration or clarification are often needed to remove those unwanted byproducts. Although advanced techniques, such as ultrasound and pulsed electric field, offer relatively higher selectivity to HPH and mechanical milling, they still fall short in product purity and selectivity compared to chemical methods.

Second, while physical methods avoid the use of toxic and environmentally unsustainable organic solvents, they often come at the expense of higher energy consumption, particularly of electrical energy [116]. Mechanical milling, for instance, consumes intensive electricity to constantly agitation beads and rotate large drums, and both HPH and ultrasounds also need significant electricity to maintain the high pressure or ultrasonic waves in liquid medium for cell disruption. When developing these technologies at a lab-scale, the energy consumption is often overlooked due to the small-scale operation; however, the energy requirement is enormous in continuous industrial processes and can significantly increase operating costs. Therefore, the economics and environmental aspects of the commercialization of these methods should be considered at the early stages.

Third, some physical methods, such as mechanical milling and HPH, can generate large amounts of heat as a byproduct of the mechanical forces applied to break the cells walls. The heat can increase the liquid-medium temperature and potentially cause thermal damage to heat-sensitive bioactive compounds, such as therapeutic proteins, enzymes, and certain bioactive compounds [117]. Although some cooling systems, such as water cooling and air cooling, can be integrated into these physical disruption methods, it increases the equipment cost and operating complexity of the system.

To address these challenges, further research and development are needed to improve the efficiency, selectivity, and sustainability of physical cell disruption methods for intracellular compound recovery. Although most physical methods, like HPH and high-pressure homogenization, experience low-selectivity challenges, techniques such as pulsed electric field and ultrasound offer comparatively better selectivity among physical methods, making them promising candidates for further development. Currently, while these two techniques still do not match the precision level of organic solvent extraction, we can precisely optimize the key processing parameters, such as ultrasound frequency, duration, electric field strength, medium conductivity, to specific cell types and intracellular compounds for increasing the selectivity and purity of targeted compounds. In addition, beyond individual physical methods, combining physical and chemical approaches could significantly improve selectivity. For instance, the integration of membrane filtration systems with physical methods could facilitate the simultaneous removal of cell debris and impurities during the disruption process.

Reducing energy consumption of the physical methods is critical for improving the technology adoption and economics. In addition to the traditional ways to reduce energy through the improvements of equipment design (e.g., bead size in mechanical milling) and optimization of operating conditions (e.g., HPH pressure, electric field strength), the latest machine learning techniques, especially the new concept of the digital twin system, offer grand opportunities to control the entire processes and optimize energy use. A digital twin is a virtual model of a physical system that can be used to simulate the entire

bioprocess, allowing real-time data to be analyzed and used for predictive process control. By integrating digital twins with machine learning algorithms, engineers can dynamically optimize parameters like pressure, pulse frequency, and power consumption, ensuring that energy use is minimized while enhancing the product quality and process efficiency.

Lastly, it is important to incorporate techno-economic analysis (TEA) and life cycle assessment (LCA) into the early stage of the development of the methods, to ensure that newly developed physical disruption methods are both economically viable and environmentally sustainable. By integrating TEA and LCA, engineers can not only assess the overall economic and environmental metrics of a process, but also identify the bottlenecks regarding the cost and energy consumption before the technology reaches the pilot or commercial stage. This allows for more informed decision making to select appropriate technical routes, such as whether to increase the HPH pressure to enhance product recovery or maintain the pressure to reduce the capital and operating (energy) cost to make the whole process economically feasible and environmentally sustainable.

5. Conclusions

In summary, the use of physical disruption techniques marks a crucial step forward in extracting intracellular compounds, potentially offering a more environmentally sustainable and effective option compared to traditional chemical and biological methods. Through the application of high-pressure homogenization, ultrasonication, milling, and pulsed electric fields, high yields of intracellular compounds can be achieved with fewer negative impacts on the environment. These methods not only address the environmental concerns associated with conventional chemical extraction but also simplify the processing steps. Physical disruption technology has great potential in intracellular compound extraction. As bioprocessing continues to be focused on sustainability, these physical methods will gain more applications. Continued improvements in the equipment and processing parameters, as well as developments of novel physical destruction techniques, are expected to unlock possibilities for physical extracting valuable compounds independently from a variety of biological sources. Looking forward, the significance of physical disruption techniques in extracting intracellular compounds is expected to increase, driven by the need for cleaner, more efficient, and more environmentally friendly processes. Continued research and innovation in this field are likely to broaden our understanding and enhance our bioprocessing capabilities.

Author Contributions: Conceptualization, F.Z. and H.H.; writing—original draft preparation, F.Z.; writing—review and editing, F.Z., Z.W. and H.H.; visualization, F.Z.; project administration, H.H.; funding acquisition, H.H. and Z.W. All authors have read and agreed to the published version of the manuscript.

Funding: This project is supported by USDA AFRI (Grant Number 2023-79000-39973), USDA. This project is also partially funded by Virginia Agricultural Experiment Station and the Water INTERface-Interdisciplinary Graduate Education Program.

Conflicts of Interest: The authors declare no conflicts of interest.

References

- Dong, T.; Knoshaug, E.P.; Pienkos, P.T.; Laurens, L.M.L. Lipid recovery from wet oleaginous microbial biomass for biofuel production: A critical review. *Appl. Energy* **2016**, *177*, 879–895. [CrossRef]
- Becker, E.W. Micro-algae as a source of protein. *Biotechnol. Adv.* **2007**, *25*, 207–210. [CrossRef] [PubMed]
- Obruca, S.; Sedlacek, P.; Slaninova, E.; Fritz, I.; Daffert, C.; Meixner, K.; Sedrlova, Z.; Koller, M. Novel unexpected functions of PHA granules. *Appl. Microbiol. Biotechnol.* **2020**, *104*, 4795–4810. [CrossRef] [PubMed]
- Kirti, K.; Amita, S.; Priti, S.; Mukesh Kumar, A.; Jyoti, S. Colorful World of Microbes: Carotenoids and Their Applications. *Adv. Biol.* **2014**, *2014*, 837891. [CrossRef]
- Bleakley, S.; Hayes, M. Algal Proteins: Extraction, Application, and Challenges Concerning Production. *Foods* **2017**, *6*, 33. [CrossRef]
- Ijaola, A.O.; Akamo, D.O.; George, T.T.; Sengul, A.; Adediji, M.Y.; Asmatulu, E. Algae as a potential source of protein: A review on cultivation, harvesting, extraction, and applications. *Algal Res.* **2024**, *77*, 103329. [CrossRef]

7. Di Salvo, E.; Lo Vecchio, G.A.-O.; De Pasquale, R.; De Maria, L.; Tardugno, R.A.-O.; Vadalà, R.; Cicero, N.A.-O. Natural Pigments Production and Their Application in Food, Health and Other Industries. *Nutrients* **2023**, *15*, 1923. [CrossRef]
8. Nfor, B.K.; Ahamed, T.; van Dedem, G.W.; van der Wielen, L.A.; van de Sandt, E.J.; Eppink, M.H.; Ottens, M. Design strategies for integrated protein purification processes: Challenges, progress and outlook. *J. Chem. Technol. Biotechnol.* **2008**, *83*, 124–132. [CrossRef]
9. Garcia-Vaquero, M.; Rajauria, G.; Tiwari, B. Chapter 7—Conventional extraction techniques: Solvent extraction. In *Sustainable Seaweed Technologies*; Torres, M.D., Kraan, S., Dominguez, H., Eds.; Elsevier: Amsterdam, The Netherlands, 2020; pp. 171–189.
10. Belwal, T.; Chemat, F.; Venskutonis, P.R.; Cravotto, G.; Jaiswal, D.K.; Bhatt, I.D.; Devkota, H.P.; Luo, Z. Recent advances in scaling-up of non-conventional extraction techniques: Learning from successes and failures. *TrAC Trends Anal. Chem.* **2020**, *127*, 115895. [CrossRef]
11. Gertenbach, D.; Cooper, B. Scale-Up Issues from Bench to Pilot. In Proceedings of the 2009 AIChE Annual Meeting, Nashville, TN, USA, 8–13 November 2009.
12. Saini, R.A.-O.; Prasad, P.A.-O.; Shang, X.; Keum, Y.S. Advances in Lipid Extraction Methods—A Review. *Int. J. Mol. Sci.* **2021**, *22*, 13643. [CrossRef]
13. Jin, G.; Yang, F.; Hu, C.; Shen, H.; Zhao, Z.K. Enzyme-assisted extraction of lipids directly from the culture of the oleaginous yeast *Rhodospiridium toruloides*. *Bioresour. Technol.* **2012**, *111*, 378–382. [CrossRef] [PubMed]
14. Liu, D.; Zeng, X.-A.; Sun, D.-W.; Han, Z. Disruption and protein release by ultrasonication of yeast cells. *Innov. Food Sci. Emerg. Technol.* **2013**, *18*, 132–137. [CrossRef]
15. Carullo, D.; Abera, B.D.; Casazza, A.A.; Donsi, F.; Perego, P.; Ferrari, G.; Pataro, G. Effect of pulsed electric fields and high pressure homogenization on the aqueous extraction of intracellular compounds from the microalgae *Chlorella vulgaris*. *Algal Res.* **2018**, *31*, 60–69. [CrossRef]
16. Diels, A.M.J.; Michiels, C.W. High-Pressure Homogenization as a Non-Thermal Technique for the Inactivation of Microorganisms. *Crit. Rev. Microbiol.* **2006**, *32*, 201–216. [CrossRef] [PubMed]
17. Keris-Sen, U.D.; Sen, U.; Soydemir, G.; Gurol, M.D. An investigation of ultrasound effect on microalgal cell integrity and lipid extraction efficiency. *Bioresour. Technol.* **2014**, *152*, 407–413. [CrossRef] [PubMed]
18. Tamer, I.M.; Moo-Young, M.; Chisti, Y. Disruption of *Alcaligenes latus* for Recovery of Poly(β -hydroxybutyric acid): Comparison of High-Pressure Homogenization, Bead Milling, and Chemically Induced Lysis. *Ind. Eng. Chem. Res.* **1998**, *37*, 1807–1814. [CrossRef]
19. Lam, G.P.t.; Postma, P.R.; Fernandes, D.A.; Timmermans, R.A.H.; Vermuë, M.H.; Barbosa, M.J.; Eppink, M.H.M.; Wijffels, R.H.; Olivieri, G. Pulsed Electric Field for protein release of the microalgae *Chlorella vulgaris* and *Neochloris oleoabundans*. *Algal Res.* **2017**, *24*, 181–187. [CrossRef]
20. Martins, R.; Barbosa, A.; Advinha, B.; Sales, H.; Pontes, R.; Nunes, J. Green Extraction Techniques of Bioactive Compounds: A State-of-the-Art Review. *Processes* **2023**, *11*, 2255. [CrossRef]
21. Brookman, J.S.G. Mechanism of cell disintegration in a high pressure homogenizer. *Biotechnol. Bioeng.* **1974**, *16*, 371–383. [CrossRef]
22. Fellows, P.J. Size reduction. In *Food Processing Technology*; Woodhead Publishing Limited: Cambridge, UK, 2009; pp. 125–156.
23. Martínez-Monteagudo, S.I.; Yan, B.; Balasubramaniam, V.M. Engineering Process Characterization of High-Pressure Homogenization—From Laboratory to Industrial Scale. *Food Eng. Rev.* **2017**, *9*, 143–169. [CrossRef]
24. Doran, P.M. Chapter 11—Unit Operations. In *Bioprocess Engineering Principles*, 2nd ed.; Doran, P.M., Ed.; Academic Press: London, UK, 2013; pp. 445–595.
25. Jubeau, S.; Marchal, L.; Pruvost, J.; Jaouen, P.; Legrand, J.; Fleurence, J.; Jubeau, S.; Marchal, L.; Pruvost, J.; Jaouen, P.; et al. High pressure disruption: A two-step treatment for selective extraction of intracellular components from the microalga *Porphyridium cruentum*. *J. Appl. Phycol.* **2012**, *25*, 983–989. [CrossRef]
26. Zhang, R.; Grimi, N.; Marchal, L.; Vorobiev, E. Application of high-voltage electrical discharges and high-pressure homogenization for recovery of intracellular compounds from microalgae *Parachlorella kessleri*. *Bioprocess Biosyst. Eng.* **2018**, *42*, 29–36. [CrossRef] [PubMed]
27. Shene, C.; Monsalve, M.T.; Vergara, D.; Lienqueo, M.E.; Rubilar, M. High pressure homogenization of *Nannochloropsis oculata* for the extraction of intracellular components: Effect of process conditions and culture age. *Eur. J. Lipid Sci. Technol.* **2015**, *118*, 631–639. [CrossRef]
28. Domozych, D.S. Algal Cell Walls. In *eLS*; 2011.
29. Liu, D.; Lebovka, N.I.; Vorobiev, E.; Liu, D.; Lebovka, N.I.; Vorobiev, E. Impact of Electric Pulse Treatment on Selective Extraction of Intracellular Compounds from *Saccharomyces cerevisiae* Yeasts. *Food Bioprocess Technol.* **2011**, *6*, 576–584. [CrossRef]
30. Shynkaryk, M.V.; Lebovka, N.I.; Lanoisellé, J.L.; Nonus, M.; Bedel-Clotour, C.; Vorobiev, E. Electrically-assisted extraction of bio-products using high pressure disruption of yeast cells (*Saccharomyces cerevisiae*). *J. Food Eng.* **2009**, *92*, 189–195. [CrossRef]
31. Ling, Y.; Wong, H.H.; Thomas, C.J.; Williams, D.R.G.; Middelberg, A.P.J.; Ling, Y.; Wong, H.H.; Thomas, C.J.; Williams, D.R.G.; Middelberg, A.P.J. Pilot-scale extraction of PHB from recombinant *E. coli* by homogenization and centrifugation. *Bioseparation* **1998**, *7*, 9–15. [CrossRef]
32. Lipke, P.N.; Ovalle, R. Cell wall architecture in yeast: New structure and new challenges. *J. Bacteriol.* **1998**, *180*, 3735–3740. [CrossRef]

33. Donsi, F.; Ferrari, G.; Lenza, E.; Maresca, P. Main factors regulating microbial inactivation by high-pressure homogenization: Operating parameters and scale of operation. *Chem. Eng. Sci.* **2009**, *64*, 520–532. [CrossRef]
34. Pereda, J.; Ferragut, V.; Quevedo, J.M.; Guamis, B.; Trujillo, A.J. Effects of ultra-high pressure homogenization on microbial and physicochemical shelf life of milk. *J. Dairy Sci.* **2007**, *90*, 1081–1093. [CrossRef]
35. Comuzzo, P.; Calligaris, S. Potential Applications of High Pressure Homogenization in Winemaking: A Review. *Beverages* **2019**, *5*, 56. [CrossRef]
36. Pekarsky, A.; Spadiut, O.; Rajamanickam, V.; Wurm, D.J. A fast and simple approach to optimize the unit operation high pressure homogenization—A case study for a soluble therapeutic protein in *E. coli*. *Prep. Biochem. Biotechnol.* **2019**, *49*, 74–81. [CrossRef] [PubMed]
37. Tribst, A.A.; Cota, J.; Murakami, M.T.; Cristianini, M. Effects of high pressure homogenization on the activity, stability, kinetics and three-dimensional conformation of a glucose oxidase produced by *Aspergillus niger*. *PLoS ONE* **2014**, *9*, e103410. [CrossRef] [PubMed]
38. Eggenreich, B.; Wurm, D.J.; Rajamanickam, V.; Klausser, R.; Slouka, C.; Spadiut, O. High pressure homogenization is a key unit operation in inclusion body processing. *J. Biotechnol.* **2020**, *324*, 100022. [CrossRef] [PubMed]
39. Choi, W.Y.; Lee, H.Y. Effective production of bioenergy from marine *Chlorella* sp. by high-pressure homogenization. *Biotechnol. Biotechnol. Equip.* **2016**, *30*, 81–89. [CrossRef]
40. Yap, B.H.J.; Dumsday, G.J.; Scales, P.J.; Martin, G.J.O. Energy evaluation of algal cell disruption by high pressure homogenisation. *Bioresour. Technol.* **2015**, *184*, 280–285. [CrossRef]
41. Zhang, R.; Chen, J.; Zhang, X. Extraction of intracellular protein from *Chlorella pyrenoidosa* using a combination of ethanol soaking, enzyme digest, ultrasonication and homogenization techniques. *Bioresour. Technol.* **2018**, *247*, 267–272. [CrossRef]
42. Li, Y.; Kiani, H.; Tiwari, B.K.; Halim, R. 11-Unit operations applied to cell disruption of microalgae. In *3rd Generation Biofuels*; Jacob-Lopes, E., Zepka, L.Q., Severo, I.A., Maroneze, M.M., Eds.; Woodhead Publishing: Cambridge, UK, 2022; pp. 225–248.
43. Lentacker, I.; De Cock, I.; Deckers, R.; De Smedt, S.C.; Moonen, C.T. Understanding ultrasound induced sonoporation: Definitions and underlying mechanisms. *Adv. Drug Deliv. Rev.* **2014**, *72*, 49–64. [CrossRef]
44. Majid, I.; Nayik, G.A.; Nanda, V. Ultrasonication and food technology: A review. *Cogent Food Agric.* **2015**, *1*, 1071022. [CrossRef]
45. Yusaf, T.; Al-Juboori, R.A. Alternative methods of microorganism disruption for agricultural applications. *Appl. Energy* **2014**, *114*, 909–923. [CrossRef]
46. Soria, A.C.; Villamiel, M. Effect of ultrasound on the technological properties and bioactivity of food: A review. *Trends Food Sci. Technol.* **2010**, *21*, 323–331. [CrossRef]
47. Wu, T.; Yu, X.; Hu, A.; Zhang, L.; Jin, Y.; Abid, M. Ultrasonic disruption of yeast cells: Underlying mechanism and effects of processing parameters. *Innov. Food Sci. Emerg. Technol.* **2015**, *28*, 59–65. [CrossRef]
48. Shi, Y.; Sheng, J.; Yang, F.; Hu, Q. Purification and identification of polysaccharide derived from *Chlorella pyrenoidosa*. *Food Chem.* **2007**, *103*, 101–105. [CrossRef]
49. Aouir, A.; Amiali, M.; Kirilova-Gachovska, T.; Benchabane, A.; Bitam, A. The effect of pulsed electric field (PEF) and ultrasound (US) technologies on the extraction of phycopiliproteins from *Arthrospira platensis*. In Proceedings of the 2015 IEEE Canada International Humanitarian Technology Conference (IHTC2015), Ottawa, ON, Canada, 31 May–4 June 2015; pp. 1–4.
50. Natarajan, R.; Ang, W.M.; Chen, X.; Voigtman, M.; Lau, R. Lipid releasing characteristics of microalgae species through continuous ultrasonication. *Bioresour. Technol.* **2014**, *158*, 7–11. [CrossRef] [PubMed]
51. Halim, R.; Rupasinghe, T.W.; Tull, D.L.; Webley, P.A. Mechanical cell disruption for lipid extraction from microalgal biomass. *Bioresour. Technol.* **2013**, *140*, 53–63. [CrossRef]
52. Ranjha, M.M.A.N.; Irfan, S.; Lorenzo, J.M.; Shafique, B.; Kanwal, R.; Pateiro, M.; Arshad, R.N.; Wang, L.; Nayik, G.A.; Roobab, U.; et al. Sonication, a Potential Technique for Extraction of Phytoconstituents: A Systematic Review. *Processes* **2021**, *9*, 1406. [CrossRef]
53. Saranya, N.; Devi, P.; Nithiyantham, S.; Jeyalaxmi, R. Cells Disruption by Ultrasonication. *BioNanoScience* **2014**, *4*, 335–337. [CrossRef]
54. Peng, K.; Tian, S.; Zhang, Y.; Qu, W.; Wang, Q. Kinetic analysis of free radical scavenging in sonochemistry. *Chem. Eng. Process.-Process Intensif.* **2023**, *193*, 109571. [CrossRef]
55. Miljevic, B.; Hedayat, F.; Stevanovic, S.; Fairfull-Smith, K.E.; Bottle, S.E.; Ristovski, Z.D. To Sonicate or Not to Sonicate PM Filters: Reactive Oxygen Species Generation Upon Ultrasonic Irradiation. *Aerosol Sci. Technol.* **2014**, *48*, 1276–1284. [CrossRef]
56. Middelberg, A.P.J. Process-scale disruption of microorganisms. *Biotechnol. Adv.* **1995**, *13*, 491–551. [CrossRef]
57. Goldberg, S. Mechanical/Physical Methods of Cell Disruption and Tissue Homogenization. In *2D PAGE: Sample Preparation and Fractionation*; Posch, A., Ed.; Humana Press: Totowa, NJ, USA, 2008; pp. 3–22.
58. Varinot, C.; Hiltgun, S.; Pons, M.-N.; Dodds, J. Identification of the fragmentation mechanisms in wet-phase fine grinding in a stirred bead mill. *Chem. Eng. Sci.* **1997**, *52*, 3605–3612. [CrossRef]
59. Matsanga, N.; Nheta, W.; Chimwani, N. A Review of the Grinding Media in Ball Mills for Mineral Processing. *Minerals* **2023**, *13*, 1373. [CrossRef]
60. Bunge, F.; Pietzsch, M.; Müller, R.; Syltatk, C. Mechanical disruption of *Arthrobacter* sp. DSM 3747 in stirred ball mills for the release of hydantoin-cleaving enzymes. *Chem. Eng. Sci.* **1992**, *47*, 225–232. [CrossRef]

61. Zhang, J.; Bai, Y.; Dong, H.; Wu, Q.; Ye, X. Influence of ball size distribution on grinding effect in horizontal planetary ball mill. *Adv. Powder Technol.* **2014**, *25*, 983–990. [CrossRef]
62. Postma, P.R.; Miron, T.L.; Olivieri, G.; Barbosa, M.J.; Wijffels, R.H.; Eppink, M.H.M. Mild disintegration of the green microalgae *Chlorella vulgaris* using bead milling. *Bioresour. Technol.* **2015**, *184*, 297–304. [CrossRef]
63. Tamer, I.M.; Moo-Young, M.; Tamer, I.M.; Moo-Young, M. Optimization of poly(β -hydroxybutyric acid) recovery from *Alcaligenes latus*: Combined mechanical and chemical treatments. *Bioprocess Eng.* **1998**, *19*, 459–468. [CrossRef]
64. Postma, P.R.; Suarez-Garcia, E.; Safi, C.; Yonathan, K.; Olivieri, G.; Barbosa, M.J.; Wijffels, R.H.; Eppink, M.H.M. Energy efficient bead milling of microalgae: Effect of bead size on disintegration and release of proteins and carbohydrates. *Bioresour. Technol.* **2017**, *224*, 670–679. [CrossRef]
65. Schwenzfeier, A.; Wierenga, P.A.; Gruppen, H. Isolation and characterization of soluble protein from the green microalgae *Tetraselmis* sp. *Bioresour. Technol.* **2011**, *102*, 9121–9127. [CrossRef]
66. Loureiro, L.; Machado, L.; Geadá, P.; Vasconcelos, V.; Vicente, A.A. Evaluation of efficiency of disruption methods for *Coelastrella* sp. in order to obtain high yields of biochemical compounds release. *Algal Res.* **2023**, *73*, 103158. [CrossRef]
67. Günerkin, E.; D’Hondt, E.; Eppink, M.; Elst, K.; Wijffels, R. Influence of nitrogen depletion in the growth of *N. oleoabundans* on the release of cellular components after beadmilling. *Bioresour. Technol.* **2016**, *214*, 89–95. [CrossRef]
68. Ricci-Silva, M.E.; Vitolo, M.; Abrahão-Neto, J. Protein and glucose 6-phosphate dehydrogenase releasing from baker’s yeast cells disrupted by a vertical bead mill. *Process Biochem.* **2000**, *35*, 831–835. [CrossRef]
69. Mei, C.Y.; Ti, T.B.; Ibrahim, M.N.; Ariff, A.; Chuan, L.T. The disruption of *Saccharomyces cerevisiae* cells and release of glucose 6-phosphate dehydrogenase (G6PDH) in a horizontal dyno bead mill operated in continuous recycling mode. *Biotechnol. Bioprocess Eng.* **2005**, *10*, 284–288. [CrossRef]
70. Balasundaram, B.; Skill, S.C.; Llewellyn, C.A. A low energy process for the recovery of bioproducts from cyanobacteria using a ball mill. *Biochem. Eng. J.* **2012**, *69*, 48–56. [CrossRef]
71. Haque, S.; Khan, S.; Wahid, M.; Mandal, R.K.; Tiwari, D.; Dar, S.A.; Paul, D.; Areeshi, M.Y.; Jawed, A. Modeling and optimization of a continuous bead milling process for bacterial cell lysis using response surface methodology. *RSC Adv.* **2016**, *6*, 16348–16357. [CrossRef]
72. Mariño-Salguero, J.; Jorge, J.; Menéndez-Aguado, J.M.; Álvarez-Rodríguez, B.; de Felipe, J.J. Heat generation model in the ball-milling process of a tantalum ore. *Miner. Metall. Process.* **2017**, *34*, 10–19. [CrossRef]
73. Stolle, A.; Szuppa, T.; Leonhardt, S.E.S.; Ondruschka, B. Ball milling in organic synthesis: Solutions and challenges. *Chem. Soc. Rev.* **2011**, *40*, 2317–2329. [CrossRef] [PubMed]
74. Tylewicz, U. 1-How does pulsed electric field work? In *Pulsed Electric Fields to Obtain Healthier and Sustainable Food for Tomorrow*; Barba, F.J., Parniakov, O., Wiktor, A., Eds.; Academic Press: Cambridge, MA, USA, 2020; pp. 3–21.
75. Weaver, J.C.; Chizmadzhev, Y.A. Theory of electroporation: A review. *Bioelectrochemistry Bioenerg.* **1996**, *41*, 135–160. [CrossRef]
76. Goettel, M.; Eing, C.; Gusbeth, C.; Straessner, R.; Frey, W. Pulsed electric field assisted extraction of intracellular valuables from microalgae. *Algal Res.* **2013**, *2*, 401–408. [CrossRef]
77. Luengo, E.; Condon-Abanto, S.; Alvarez, I.; Raso, J. Effect of pulsed electric field treatments on permeabilization and extraction of pigments from *Chlorella vulgaris*. *J. Membr. Biol.* **2014**, *247*, 1269–1277. [CrossRef]
78. Coustets, M.; Joubert-Durigneux, V.; Héroult, J.; Schoefs, B.; Blanckaert, V.; Garnier, J.-P.; Teissié, J. Optimization of protein electroextraction from microalgae by a flow process. *Bioelectrochemistry* **2015**, *103*, 74–81. [CrossRef]
79. Postma, P.R.; Pataro, G.; Capitoli, M.; Barbosa, M.J.; Wijffels, R.H.; Eppink, M.H.M.; Olivieri, G.; Ferrari, G. Selective extraction of intracellular components from the microalga *Chlorella vulgaris* by combined pulsed electric field–temperature treatment. *Bioresour. Technol.* **2016**, *203*, 80–88. [CrossRef]
80. Luengo, E.; Martínez, J.M.; Coustets, M.; Álvarez, I.; Teissié, J.; Rols, M.-P.; Raso, J. A Comparative Study on the Effects of Millisecond- and Microsecond-Pulsed Electric Field Treatments on the Permeabilization and Extraction of Pigments from *Chlorella vulgaris*. *J. Membr. Biol.* **2015**, *248*, 883–891. [CrossRef] [PubMed]
81. Ganeva, V.; Angelova, B.; Galutzov, B.; Goltsev, V.; Zhiponova, M. Extraction of Proteins and Other Intracellular Bioactive Compounds From Baker’s Yeasts by Pulsed Electric Field Treatment. *Front. Bioeng. Biotechnol.* **2020**, *8*, 552335. [CrossRef] [PubMed]
82. Fincan, M.; DeVito, F.; Dejmeck, P. Pulsed electric field treatment for solid–liquid extraction of red beetroot pigment. *J. Food Eng.* **2004**, *64*, 381–388. [CrossRef]
83. Zhang, R.; Lebovka, N.; Marchal, L.; Vorobiev, E.; Grimi, N. Pulsed electric energy and ultrasonication assisted green solvent extraction of bio-molecules from different microalgal species. *Innov. Food Sci. Emerg. Technol.* **2020**, *62*, 102358. [CrossRef]
84. Monks, L.M.; Rigo, A.; Mazutti, M.A.; Vladimir Oliveira, J.; Valduga, E. Use of chemical, enzymatic and ultrasound-assisted methods for cell disruption to obtain carotenoids. *Biocatal. Agric. Biotechnol.* **2013**, *2*, 165–169. [CrossRef]
85. Zheng, B.; Yuan, Y.; Xiang, J.; Jin, W.; Johnson, J.B.; Li, Z.; Wang, C.; Luo, D. Green extraction of phenolic compounds from foxtail millet bran by ultrasonic-assisted deep eutectic solvent extraction: Optimization, comparison and bioactivities. *LWT* **2022**, *154*, 112740. [CrossRef]
86. Cravotto, G.; Boffa, L.; Mantegna, S.; Perego, P.; Avogadro, M.; Cintas, P. Improved extraction of vegetable oils under high-intensity ultrasound and/or microwaves. *Ultrason. Sonochemistry* **2008**, *15*, 898–902. [CrossRef]

87. Martinez-Guerra, E.; Gude, V.G.; Mondala, A.; Holmes, W.; Hernandez, R. Microwave and ultrasound enhanced extractive-transesterification of algal lipids. *Appl. Energy* **2014**, *129*, 354–363. [CrossRef]
88. Parniakov, O.; Apicella, E.; Koubaa, M.; Barba, F.J.; Grimi, N.; Lebovka, N.; Pataro, G.; Ferrari, G.; Vorobiev, E. Ultrasound-assisted green solvent extraction of high-added value compounds from microalgae *Nannochloropsis* spp. *Bioresour. Technol.* **2015**, *198*, 262–267. [CrossRef]
89. Lai, Y.S.; Parameswaran, P.; Li, A.; Baez, M.; Rittmann, B.E. Effects of pulsed electric field treatment on enhancing lipid recovery from the microalga, *Scenedesmus*. *Bioresour. Technol.* **2014**, *173*, 457–461. [CrossRef]
90. Parniakov, O.; Barba, F.J.; Grimi, N.; Marchal, L.; Jubeau, S.; Lebovka, N.; Vorobiev, E. Pulsed electric field assisted extraction of nutritionally valuable compounds from microalgae *Nannochloropsis* spp. using the binary mixture of organic solvents and water. *Innov. Food Sci. Emerg. Technol.* **2015**, *27*, 79–85. [CrossRef]
91. Zbinden, M.D.A.; Sturm, B.S.M.; Nord, R.D.; Carey, W.J.; Moore, D.; Shinogle, H.; Stagg-Williams, S.M. Pulsed electric field (PEF) as an intensification pretreatment for greener solvent lipid extraction from microalgae. *Biotechnol. Bioeng.* **2013**, *110*, 1605–1615. [CrossRef] [PubMed]
92. Carpentieri, S.; Režek Jambak, A.; Ferrari, G.; Pataro, G. Pulsed Electric Field-Assisted Extraction of Aroma and Bioactive Compounds From Aromatic Plants and Food By-Products. *Front. Nutr.* **2022**, *8*, 792203. [CrossRef] [PubMed]
93. Kapoore, R.A.-O.; Butler, T.A.-O.; Pandhal, J.; Vaidyanathan, S.A.-O. Microwave-Assisted Extraction for Microalgae: From Biofuels to Biorefinery. *Biology* **2018**, *7*, 18. [CrossRef] [PubMed]
94. Balasubramanian, S.; Allen, J.D.; Kanitkar, A.; Boldor, D. Oil extraction from *Scenedesmus obliquus* using a continuous microwave system—Design, optimization, and quality characterization. *Bioresour. Technol.* **2011**, *102*, 3396–3403. [CrossRef]
95. Ali, M.; Watson, I.A. Microwave treatment of wet algal paste for enhanced solvent extraction of lipids for biodiesel production. *Renew. Energy* **2015**, *76*, 470–477. [CrossRef]
96. Ansari, F.A.; Shriwastav, A.; Gupta, S.K.; Rawat, I.; Guldhe, A.; Bux, F. Lipid extracted algae as a source for protein and reduced sugar: A step closer to the biorefinery. *Bioresour. Technol.* **2015**, *179*, 559–564. [CrossRef]
97. Iqbal, J.; Theegala, C. Microwave assisted lipid extraction from microalgae using biodiesel as co-solvent. *Algal Res.* **2013**, *2*, 34–42. [CrossRef]
98. Zheng, H.; Yin, J.; Gao, Z.; Huang, H.; Ji, X.; Dou, C. Disruption of *Chlorella vulgaris* Cells for the Release of Biodiesel-Producing Lipids: A Comparison of Grinding, Ultrasonication, Bead Milling, Enzymatic Lysis, and Microwaves. *Appl. Biochem. Biotechnol.* **2011**, *164*, 1215–1224. [CrossRef]
99. Chen, C.-L.; Huang, C.-C.; Ho, K.-C.; Hsiao, P.-X.; Wu, M.-S.; Chang, J.-S. Biodiesel production from wet microalgae feedstock using sequential wet extraction/transesterification and direct transesterification processes. *Bioresour. Technol.* **2015**, *194*, 179–186. [CrossRef]
100. Gim, G.H.; Kim, S.W. Optimization of Cell Disruption and Transesterification of Lipids from *Botryococcus braunii* LB572. *Biotechnol. Bioprocess Eng.* **2018**, *23*, 550–556. [CrossRef]
101. Nogueira, D.A.; da Silveira, J.M.; Vidal, É.M.; Ribeiro, N.T.; Veiga Burkert, C.A. Cell Disruption of *Chaetoceros calcitrans* by Microwave and Ultrasound in Lipid Extraction. *Int. J. Chem. Eng.* **2018**, *2018*, 9508723. [CrossRef]
102. Pohndorf, R.S.; Camara, Á.S.; Larrosa, A.P.Q.; Pinheiro, C.P.; Strieder, M.M.; Pinto, L.A.A. Production of lipids from microalgae *Spirulina* sp.: Influence of drying, cell disruption and extraction methods. *Biomass Bioenergy* **2016**, *93*, 25–32. [CrossRef]
103. Viguera, M.; Marti, A.; Masca, F.; Prieto, C.; Calvo, L. The process parameters and solid conditions that affect the supercritical CO₂ extraction of the lipids produced by microalgae. *J. Supercrit. Fluids* **2016**, *113*, 16–22. [CrossRef]
104. Wahidin, S.; Idris, A.; Yusof, N.M.; Kamis, N.H.H.; Shaleh, S.R.M. Optimization of the ionic liquid-microwave assisted one-step biodiesel production process from wet microalgal biomass. *Energy Convers. Manag.* **2018**, *171*, 1397–1404. [CrossRef]
105. Krishnan, S.; Ghani, N.A.; Aminuddin, N.F.; Quraishi, K.S.; Azman, N.S.; Cravotto, G.; Leveque, J.-M. Microwave-assisted lipid extraction from *Chlorella vulgaris* in water with 0.5%–2.5% of imidazolium based ionic liquid as additive. *Renew. Energy* **2020**, *149*, 244–252. [CrossRef]
106. Zhou, X.; Jin, W.; Tu, R.; Guo, Q.; Han, S.-f.; Chen, C.; Wang, Q.; Liu, W.; Jensen, P.D.; Wang, Q. Optimization of microwave assisted lipid extraction from microalga *Scenedesmus obliquus* grown on municipal wastewater. *J. Clean. Prod.* **2019**, *221*, 502–508. [CrossRef]
107. Onumaegbu, C.; Alaswad, A.; Rodriguez, C.; Olabi, A. Modelling and optimization of wet microalgae *Scenedesmus quadricauda* lipid extraction using microwave pre-treatment method and response surface methodology. *Renew. Energy* **2019**, *132*, 1323–1331. [CrossRef]
108. Xu, J.; Zhao, F.; Su, X. Direct extraction of lipids from wet microalgae slurries by super-high hydrostatic pressure. *Algal Res.* **2021**, *58*, 102412. [CrossRef]
109. Mat Aron, N.S.; Chew, K.W.; Ang, W.L.; Ratchahat, S.; Rinklebe, J.; Show, P.L. Recovery of microalgae biodiesel using liquid biphasic flotation system. *Fuel* **2022**, *317*, 123368. [CrossRef]
110. Cheng, J.; Huang, R.; Li, T.; Zhou, J.; Cen, K. Biodiesel from wet microalgae: Extraction with hexane after the microwave-assisted transesterification of lipids. *Bioresour. Technol.* **2014**, *170*, 69–75. [CrossRef] [PubMed]
111. Zhang, Y.; Soldatov, S.; Papachristou, I.; Nazarova, N.; Link, G.; Frey, W.; Silve, A. Pulsed microwave pretreatment of fresh microalgae for enhanced lipid extraction. *Energy* **2022**, *248*, 123555. [CrossRef]

112. Yan, Y.; Qin, L.; Gao, J.; Nan, R.; Gao, J. Protein extraction and sludge dewatering performance of ultrasound-assisted enzymatic hydrolysis of excess sludge. *Environ. Sci. Pollut. Res.* **2020**, *27*, 18317–18328. [CrossRef]
113. Cheng, Y.-T.; Yang, C.-F. Using strain *Rhodotorula mucilaginosa* to produce carotenoids using food wastes. *J. Taiwan Inst. Chem. Eng.* **2016**, *61*, 270–275. [CrossRef]
114. Wang, D.; Yuan, Y.; Xie, T.; Tang, G.; Song, G.; Li, L.; Yuan, T.; Zheng, F.; Gong, J. Ultrasound-assisted aqueous enzymatic extraction of gardenia fruits (*Gardenia jasminoides* Ellis) oil: Optimization and quality evaluation. *Ind. Crops Prod.* **2023**, *191*, 116021. [CrossRef]
115. Hu, B.; Wang, H.; He, L.; Li, Y.; Li, C.; Zhang, Z.; Liu, Y.; Zhou, K.; Zhang, Q.; Liu, A.; et al. A method for extracting oil from cherry seed by ultrasonic-microwave assisted aqueous enzymatic process and evaluation of its quality. *J. Chromatogr. A* **2019**, *1587*, 50–60. [CrossRef]
116. Kobus, Z.; Krzywicka, M.; Pecyna, A.; Buczaj, A. Process Efficiency and Energy Consumption during the Ultrasound-Assisted Extraction of Bioactive Substances from Hawthorn Berries. *Energies* **2021**, *14*, 7638. [CrossRef]
117. Pingret, D.; Fabiano-Tixier, A.-S.; Chemat, F. Degradation during application of ultrasound in food processing: A review. *Food Control* **2013**, *31*, 593–606. [CrossRef]

Disclaimer/Publisher’s Note: The statements, opinions and data contained in all publications are solely those of the individual author(s) and contributor(s) and not of MDPI and/or the editor(s). MDPI and/or the editor(s) disclaim responsibility for any injury to people or property resulting from any ideas, methods, instructions or products referred to in the content.

Review

Hybrid Modeling for On-Line Fermentation Optimization and Scale-Up: A Review

Mariana Albino ¹, Carina L. Gargalo ¹, Gisela Nadal-Rey ², Mads O. Albæk ², Ulrich Krühne ¹
and Krist V. Gernaey ^{1,*}

¹ Process and Systems Engineering Center (PROSYS), Department of Chemical and Biochemical Engineering, Technical University of Denmark, Building 228A, 2800 Kongens Lyngby, Denmark; marial@kt.dtu.dk (M.A.); carlour@kt.dtu.dk (C.L.G.); ulkr@kt.dtu.dk (U.K.)

² Novonesis A/S, Fermentation Pilot Plant, Krogshoejvej 36, 2880 Bagsvaerd, Denmark; gsnr@novonesis.com (G.N.-R.); maoa@novonesis.com (M.O.A.)

* Correspondence: kvg@kt.dtu.dk

Abstract: Modeling is a crucial tool in the biomanufacturing industry, namely in fermentation processes. This work discusses both mechanistic and data-driven models, each with unique benefits and application potential. It discusses semi-parametric hybrid modeling, a growing field that combines these two types of models for more accurate and easy result extrapolation. The characteristics and structure of such hybrid models will be examined. Moreover, its versatility will be highlighted, showing its usefulness in various stages of process development, including real-time monitoring and optimization. Scale-up remains one of the most relevant topics in fermentation processes, as it is important to have reproducible critical quality attributes, such as titer and yield, on larger scales. Furthermore, the process still relies on empirical correlations and iterative optimization. For these reasons, it is important to improve scale-up predictions, through e.g., the use of digital tools. Perspectives will be presented on the potential that hybrid modeling has by predicting performance across different process scales. This could provide more efficient and reliable biomanufacturing processes that require less resource consumption through experimentation.

Keywords: scale-up; hybrid modeling; industrial fermentation; mechanistic modeling; data-driven modeling

Citation: Albino, M.; Gargalo, C.L.; Nadal-Rey, G.; Albæk, M.O.; Krühne, U.; Gernaey, K.V. Hybrid Modeling for On-Line Fermentation Optimization and Scale-Up: A Review. *Processes* **2024**, *12*, 1635. <https://doi.org/10.3390/pr12081635>

Academic Editors: Ali Demirci, Irfan Turhan and Ehsan Mahdinia

Received: 14 June 2024

Revised: 10 July 2024

Accepted: 19 July 2024

Published: 3 August 2024



Copyright: © 2024 by the authors. Licensee MDPI, Basel, Switzerland. This article is an open access article distributed under the terms and conditions of the Creative Commons Attribution (CC BY) license (<https://creativecommons.org/licenses/by/4.0/>).

1. Introduction

Industrial fermentation processes for producing different compounds, such as pharmaceuticals and food ingredients, have long been used in the biotechnology industry. Various microorganisms can be used for these processes, from different species of bacteria to yeast and fungi [1]. Furthermore, cell culture processes with mammalian cells are relevant in the biopharmaceutical context, particularly for the production of monoclonal antibodies. Working with each organism has advantages and challenges, but some challenges are common to all upstream bioprocesses. Essentially, these organisms are extremely complex biologically, as different metabolic networks are present in each cell, which are differentially activated under different circumstances. Furthermore, the interaction with the external environment affects the biological phenomena at the cellular level [2]. For example, one of the major challenges when implementing/deploying a new fermentation process is its scale-up, since changes in geometry and physical conditions on a large scale can affect process performance through the formation of gradients (e.g., of substrate concentration) [3,4].

Models are essential tools in the field of bioprocesses [5]. They can be used to transform process knowledge and data into relevant predicted variables. Ultimately, they can be used in real-time for monitoring and process optimization [6,7]. Regarding the topic of this review article, fermentation processes, models can also be useful tools to predict differences in performance once the scale changes [8]. In this way, the scaling process can be made more

seamlessly, thus reducing the time spent deploying a new process to full-scale production. These models can essentially be divided into two categories: mechanistic and data-driven.

Mechanistic models, also commonly referred to as “white-box” models, are mathematical representations of the knowledge of the process. They are described by first-principles equations, whose parameters have physical meaning [9,10]. On the other hand, data-driven models (“black box”) do not require any previous knowledge of the process but rather predict process outputs solely based on available process data [11,12].

Both of these modeling approaches have their strengths and weaknesses, and because of that, their application also differs. This will be further discussed in specific sections in this article, Sections 2 and 3, for mechanistic and data-driven modeling, respectively. Combining both approaches is a strategy to overcome their limitations [11]. This is broadly defined as hybrid or gray-box modeling [12]; this is the terminology adopted in this work. Hybrid modeling creates the possibility of taking advantage of the process knowledge available to build a model that can be easily adapted to different cases (within a specific range) [13,14] and simultaneously use data-driven approaches to explain parts of the process for which there is no mechanistic knowledge available [15,16].

This review aims to describe each of the above-mentioned types of models, their advantages and disadvantages, how they have been applied in the context of fermentation processes in the past, as well as up-to-date examples. Furthermore, we will discuss how their combination—hybrid modeling—has been used and the opportunities it opens in topics that can be aided by modeling. Finally, we will present perspectives on how such models can enhance scale-up, a topic of broad interest in this research area.

The article is divided into six sections, the first being the Introduction section. Sections 2 and 3 refer to mechanistic and data-driven models, respectively. The following Section 4 focuses on hybrid modeling, its structure, and potential applications in fermentation processes. Section 5 highlights some of the issues concerning scale-up and the role that models can play in solving them. Finally, Section 6 presents the conclusion of the review, summarizing the main take-home messages and future perspectives.

2. Mechanistic Modeling

Mechanistic models are based on the fundamental laws of natural science and aim to describe systems and their mechanisms using mathematical equations derived from process knowledge. Equation parameters can have a biological, chemical, or physical meaning. They can be based on mass, heat, and momentum balances as well as kinetic rate equations. Figure 1 illustrates the process of developing such models. In fermentation processes, the most critical aspects to predict are biomass growth, substrate consumption, and product formation [10]. These models can have different levels of complexity regarding the assumptions made about cell heterogeneity (segregated vs. unsegregated models) and the detail considered when calculating cell growth (structured vs. unstructured models) [10]. Segregated models focus on studying heterogeneity in cell populations. For the purpose of bioprocess optimization, their high complexity makes them challenging and time-consuming, and therefore, an average description of the cell is more commonly applied [17]. Thus, the focus is on unsegregated models, and so there is no further discussion on the differences between segregated and unsegregated models. A review of the methods utilized for cell population modeling and its applications can be found in the publication of Waldherr [18]. Table 1 highlights the differences between structured and unstructured mechanistic models and their advantages and disadvantages.

Unstructured kinetic models are widespread because they usually do not contain many parameters, and as a consequence, they are not computationally expensive. They consider biomass as a black box that converts a substrate into the product of interest and do not detail the chemical reactions occurring inside the cells. Therefore, this type of model focuses on studying the impact that external parameters, such as temperature and pH, have on the biological component of the process or others, such as agitation power and aeration, have on the physical component of the system. The lower resolution of the biological

component allows for more detail on the physical characterization of the process [10]. Some successful applications of these types of models are (a) modeling of overflow metabolism in *Escherichia coli* [19]; (b) modeling of enzyme production in *Aspergillus oryzae* under different aeration and agitation conditions [20]; and, (c) kinetic modeling of glucose and xylose co-fermentation for the production of lignocellulosic ethanol [21].

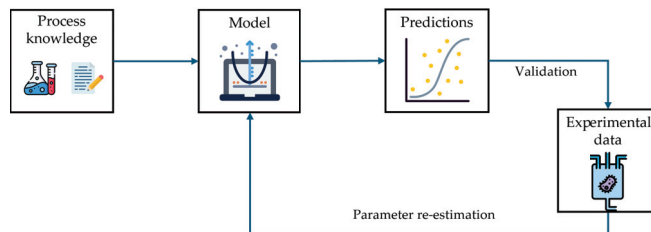


Figure 1. Schematic of mechanistic model development.

Table 1. Summary of mechanistic model characteristics.

Type of Model	Characteristics	Advantages	Disadvantages
Unstructured	Biomass as black-box Balanced growth approximation Mass balances and kinetic equations	Description of the physical aspects of the process	Potential over-simplification of biomass-product dynamics
Structured	Biomass as a multi-component organism Cell growth calculated based on interaction of intracellular components Metabolic flux equations	Suitable to model complex systems (e.g., metabolic networks)	Extensive parameter identification (e.g. metabolomics analysis)

On the other hand, structured models consider biomass as multi-component organisms with internal structure [22]. They can be useful, for example, for improving the metabolic efficiency (yield) of a target product. For example, Tang et al. [23] used a pooled metabolic model to predict the metabolic impact in *P. chrysogenum* of a feast–famine cycle, both on the hour and minute time scales, making it relevant for studying the influence of large-scale mixing. Jahan et al. [24] developed a model to estimate specific growth rates based on reaction kinetics for wild-type and genetic mutants of *Escherichia coli*. In another study, Çelik et al. [25] developed a structured kinetic model for *Pichia pastoris* growth and recombinant protein production for optimizing feeding strategy.

Unstructured models are simpler but can still provide a useful description of the process and, therefore, can be easily used for design purposes [10]. Special attention must be paid since they cannot be easily extrapolated. On the other hand, dynamic metabolic modeling provides a more accurate description of growth metabolism, increasing extrapolating capabilities [26]. However, it requires many equations, and a significant number of parameters must be experimentally identified. Ultimately, what defines a good model depends on the desired application context, and thus, model complexity should be decided according to the question to be answered.

In Table 2, more examples are summarized, both for structured and unstructured approaches. Most applications concern the prediction of growth or product formation under different process conditions. Nevertheless, these models have also been used to determine optimal process parameters or to understand the cell’s metabolic responses. In summary, mechanistic models are based on process understanding, which means that they can be extrapolated, to some extent, outside the specific context in which they are developed by tuning some of the model parameters [10]. On the downside, they require

intensive study/knowledge of the process and thus are time- and resource-consuming to develop and maintain [9].

Table 2. Examples of applications of mechanistic models of fermentation processes.

Microorganism	Type of Model	Studied Parameter	Main Findings	Reference
<i>Aspergillus oryzae</i>	Unstructured	Different agitation and aeration conditions	Prediction of several fermentation parameters, e.g., rheological behavior at different process conditions	[20]
<i>Bacillus subtilis</i>	Unstructured	Oxygen supply	Optimize aeration rate for higher protein production, using low-cost substrates	[27]
CHO cell	Unstructured	Temperature shift	Optimization of temperature profiles for optimal cell growth and productivity	[28]
<i>Escherichia coli</i>	Unstructured	Overflow metabolism	Prediction of growth and acetate-induced dynamics	[19]
	Structured kinetic	Specific growth rate	Prediction of growth rate based on reaction kinetics for wild-type and genetic mutants	[24]
<i>Penicillium chrysogenum</i>	Pooled metabolic model	Dynamic feeding conditions	Prediction of metabolic response induced by feast-famine feeding cycles	[23]
	Structured kinetic	On- and off-line process measurements	Prediction of process measurements including e.g., off-gas analysis	[29]
<i>Pichia pastoris</i>	Unstructured	Protein production	Strategy to improve product formation based on growth kinetics	[30]
	Structured kinetic	Growth and recombinant protein production	Prediction of optimal feed strategy	[25]
<i>Saccharomyces cerevisiae</i>	Unstructured	Ethanol production	Prediction of ethanol production under non-sterile conditions in biofilm reactor	[31]
<i>Zymomonas mobilis</i>	Unstructured	Glucose and xylose co-fermentation	Prediction of ethanol yield across a wide range of initial process conditions	[21]
Not disclosed	Unstructured	On-line monitoring	On-line prediction of product concentration	[32]

3. Data-Driven Modeling

Unlike mechanistic models, data-driven approaches ignore relationships that originate from process knowledge, and the parameters of the mathematical equations will not have a physical meaning. Figure 2 illustrates how historical process data are used to develop these models. In a fermentation context, these models aim to predict critical quality attributes (CQA), such as titer, productivity, and carbon efficiency, based on critical process parameters, without accounting for the mechanistic causalities that describe the relationships [11].

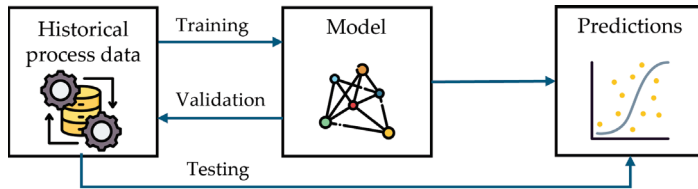


Figure 2. Schematic of data-driven model development.

Machine learning is a widely used data-driven modeling method and can be divided into two categories: supervised and unsupervised learning. Some authors also introduce the classification of reinforcement learning, though others defend that it should not be considered a specific class of learning methods but rather as a paradigm where an agent learns how to behave in an environment based on a reward signal [33,34]. Nonetheless, the three types (supervised, unsupervised, and reinforcement) of learning will be discussed and examples will be given on their application in the modeling of fermentation processes (Table 3).

In supervised learning, the data are labeled, which means that in addition to inputs, there are also predetermined output attributes that are considered in the modeling process [33]. In the case of fermentation processes, the output attributes would be, e.g., biomass and product concentration, and the input attributes, online process data. Therefore, the algorithm will identify the relationship between input and output variables and use it to predict the target values based on new input values. Supervised learning includes the use of artificial neural networks (ANN). These have been successfully implemented for fermentation processes. For example, Tavasoli et al. [35] used neural networks to develop a μ -stat approach to control methanol feeding in an *E. coli* fermentation for recombinant protein production. The results showed significant improvements compared to previously used approaches for methanol feeding. Furthermore, Nagy [36] has used dynamic neural networks to develop a model predictive controller of temperature for continuous yeast fermentation.

On the other hand, unsupervised learning focuses on identifying hidden patterns in the data without considering a target attribute. All variables in the dataset are used as inputs. Thus, these methods are suitable for clustering and association techniques [33]. Some examples are PCA (principal component analysis) and PLS (partial least squares) regressions. Andersen et al. [37] applied a partitioned PLS model to predict the yield of a batch fermentation based on selected process variables. Another example is the use of a data-driven Gaussian process regression model by Barton et al. [38] on a batch fermentation model. The model was used to increase productivity from batch to batch by manipulating process variables, e.g., batch cycle time. Nucci et al. [39] used a PCA algorithm to detect when the process is not progressing as planned, providing decision-making support. A sub-category for unsupervised learning methods recurs to maximum-likelihood properties. These methods take into account the measurement error variance information, making them suitable for processes with limited and noisy data, such as fermentation or cell culture. In the works of Dewasme et al. [40] and Pimentel et al. [41], they are applied to PCA and nonnegative matrix decomposition (NMD), respectively, to reduce data dimensionality and identify relevant process models in hybridoma cell culture for the production of monoclonal antibodies.

Classified between supervised and unsupervised learning, reinforcement learning is a type of algorithm in which the agent (in this case, the model) learns how to behave in a dynamic environment through trial and error interactions, and the only feedback is a scalar reward signal [34,42]. Two main strategies are used for solving this type of problem: (a) search the space of behaviors for one that performs well in the environment; this is achieved, for example, using genetic algorithms; (b) use statistical and dynamic programming methods for estimating the effect that taking different actions has on the different states of the system [42]. These types of models find applications in fermentation processes, particularly in the development of feed control strategies. Treloar et al. [43]

applied a deep reinforcement learning method to control substrate feeding rates to maintain the desired population levels (in a co-culture) to optimize product formation. In another example, Kim et al. [44] used model-based reinforcement learning to develop a feed rate control that led to an increase in yield and productivity in an in silico penicillin production plant.

Table 3 summarizes the examples given in the text above, in addition to more relevant examples of the application of data-driven models. It highlights the capabilities of these approaches. To conclude, the main advantage of data-driven models is the automatic assembly of the models and the low computational burden, which makes them suitable for real-time monitoring and control [11]. However, unlike mechanistic modeling, its predictive capabilities are limited to the space where they were validated, restricting its use for bioprocess control and optimization to very specific cases [12].

Table 3. Examples of applications of data-driven modeling of fermentation processes.

Microorganism	Type of Model	Studied Parameter	Main Findings	Reference
<i>Bacillus megaterium</i>	PCA	Fault detection	On-line fault detection providing decision-making support	[39]
<i>Escherichia coli</i>	Neural networks	μ -stat feeding control	Increased cell growth and target protein production	[35]
	Reinforcement learning	Feed rate control	Product formation optimization in a simulated chemostat with co-cultures	[43]
Hybridoma cells	Maximum-likelihood PCA	Macroscopic reactions	Determine minimum number of reactions and parameters for process model	[40]
	Maximum-likelihood NMD	Prediction of relevant parameters	Identified model with good prediction results	[41]
<i>Penicillium chrysogenum</i>	Reinforcement learning	Feed rate control	Optimized yield and productivity of in silico penicillin production plant	[44]
	Reinforcement learning	Feed rate control	Overperformed other feed control strategies for a digital industrial penicillin plant	[45]
<i>Saccharomyces cerevisiae</i>	Neural networks	Temperature model predictive controller	More robust temperature control, compared to linear model predictive controller	[36]
	Neural networks	Monitoring of relevant parameters	Prediction results with on-line fluorescence spectroscopy and a process model were equivalent to those of the model where offline calibration data were used	[46]
	Gaussian process regression	Manipulation of cycle time	Increased productivity from each batch to the following one	[38]
<i>Streptomyces</i> sp.	PLS	API production	Identification of process variables responsible for variation in API production	[47]
Not disclosed	PLS	Yield prediction	Similar performance to more complex genetic algorithm	[37]

4. Hybrid Modeling

As stated in the preceding sections, despite their advantages, both mechanistic and data-driven models have their shortcomings, as summarized in Table 4. Semi-parametric hybrid modeling, here named hybrid modeling, has the possibility of combining these approaches. It results in a more accurate mechanistic model by incorporating historical process data or a data-driven model that can be extrapolated outside the specific context in

which it has been trained [48]. This is particularly relevant for modeling complex systems where only partial process understanding exists. An example would be a fermentation process in which the mass and energy balances are well defined, but the parameters of the kinetic rate equations are complicated to determine [49]. Process data are used by data-driven models to fill in knowledge gaps. An advantage of this type of model is that it integrates existing knowledge into a structured data-driven framework, allowing predictions to be improved as more experimental data on the process are collected and added to the model [50]. For monitoring purposes, the models should predict the relevant parameters, based on online measurements. When it comes to fermentation processes, this can be achieved, e.g., for biomass concentration (from oxygen and carbon evolution rates, for example) [51], straightforwardly through data-driven techniques; however, this is more challenging for product concentration, due to, for example, relatively low product titers [52]. By integrating the two types of knowledge, mechanistic and data-driven, the limitations presented in Table 4 can be reduced [52]. Hybrid modeling is a relevant approach for model predictive control since the model needs to remain robust in untested regions of the process [50]. Hybrid models are characterized by their extrapolation capabilities, making them suitable for process control outside the tested process conditions [53]. For this application, the extrapolation capabilities of mechanistic models are an important complement to data-driven approaches. Furthermore, the underlying mechanistic structure of these models makes them more transparent and easier to scrutinize than their purely data-driven counterparts [53].

Table 4. Advantages and limitations of mechanistic and data-driven models.

Type of Model	Advantages	Limitations
Mechanistic	Increased process understanding	Time-consuming development
	Process control and optimization	Extensive experimental work for validation
	Model-based DOE	Intensive process knowledge required
Data-driven	Automatic model assembly	Poor extrapolation capabilities
	Real-time monitoring and fault detection	Requires representative and reliable data
	Low computational burden	Limited for control and optimization

The work of Narayanan et al. [13] highlights the benefits of hybrid modeling by comparing the performance metrics of a process model with varying degrees of hybridization. This study evaluates seven process models in which 0% (equal to a fully data-driven model) to 100% (a fully mechanistic model) of process knowledge is included. The fully data-driven model utilized was PLS since it was the best performing among other tested structures (e.g., NN); when incorporating process knowledge, NN were chosen as the data-driven components. As for the mechanistic component, the added knowledge to each of the five hybrid models was (1) the rate of accumulation, (2) mass balances, (3) specific rate, (4) specific growth and death rate, and (5) kinetic terms. The fully mechanistic model further included Monod equations for the metabolites.

Table 5 summarizes the results obtained. Essentially, the models were tested in two contexts: interpolation and extrapolation, i.e., within process conditions present in the training dataset and conditions not observed in the training data, namely the feed profiles. For both cases, hybrid approaches showed superior performance. Most interestingly, the data requirements for each level of knowledge incorporation differed. In the interpolation scenario, it is possible to observe that, by adding an equation for the accumulation rates, the same performance as the data-driven model was achieved with 20 fewer training runs. Hybrid Model 3, which contained a variable for the specific formation/consumption rate of each variable, was the best performer, having the lowest MSE (mean squared error) and the least training data. As more knowledge was added to the model, more training data were necessary to achieve equal performance. In these cases, the additional knowl-

edge of the process means that a larger number of outputs need to be predicted using the NN, thus having more parameters and requiring a larger quantity of data. As for the mechanistic model, the MSE obtained is the highest observed; however, only 10 runs are necessary. With the same number of runs, the data-driven model exhibits significantly worse performance (MSE of 0.15).

Table 5. Model performance across hybridization levels [13].

Degree of Hybridization	Interpolation		Extrapolation	
	Optimal Run Number ¹	Best MSE ²	Optimal Run Number	Best RMSE
Data-driven	50	0.039	50	0.32
Hybrid 1-rAcc ³	30	0.039	50	0.20
Hybrid 2-MB ⁴	30	0.030	50	0.10
Hybrid 3-rSp ⁵	30	0.025	30	0.05
Hybrid 4-rXv ⁶	50	0.025	50	0.05
Hybrid 5-kin ⁷	50	0.025	50	0.05
Mechanistic	10	0.060	30	0.10

¹ Number of training runs necessary to achieve the lowest MSE. ² Lowest mean squared error. ³ Rate of accumulation. ⁴ Mass balance. ⁵ Specific rates. ⁶ Specific growth and death rates. ⁷ Kinetic terms.

The differences became more striking in the extrapolation test scenario. The data-driven model performed poorly even with 50 training runs. By adding some knowledge, the performance of hybrid model 1 improved significantly, although its performance was still not satisfactory. Similarly to the interpolation case, hybrid model 3 was the best performer. It exhibited the lowest MSE while also requiring the least training data. The models with a larger mechanistic component once again required more training data and had an equally low MSE. Finally, the fully mechanistic model presented an MSE higher than that of the best hybrid models, although it needed the least amount of data. Considering only 30 training runs, it was only outperformed by hybrid model 3. Furthermore, when comparing the two extremes, data-driven and mechanistic, it is clear that the latter is superior when extrapolation is necessary. Overall, with an adequate selection of the mechanistic component, hybrid models present several advantages, resulting in more accurate models with good extrapolation properties and with lower data requirements than data-driven counterparts.

Depending on how the different types of models are combined, two hybrid model structures can be defined, parallel and serial (Figure 3). The parallel structure (Figure 3a) is suitable when the parametric (mechanistic) model exists independently, but its prediction capabilities are limited due to, e.g., unmodeled effects and nonlinearities [12]. As such, the parametric model can be used by itself, and the non-parametric component only improves the quality of the predictions [48]. The downside of this approach is that the model's prediction will remain poor for the input space in which the data-driven model has not been trained. As for the serial structure (Figure 3b,c), the "white-box" model will be composed of first-principles equations, such as mass and energy balances, for example, and the "black-box" model component will be used to represent, for example, kinetic terms, since these are harder to validate [12]. The serial structure is particularly suitable when there is insufficient knowledge of the underlying process mechanisms to build a fully mechanistic model, but sufficient process data are available to calibrate the data-driven component. On the other hand, a serial structure can also be applied in the case where the predictions of the mechanistic model are used as input to the data-driven model, establishing relationships between the process parameters or the inputs [12].

The main determinant of the best structure to adopt is the structure of the mechanistic model, as the assumptions made in that model constrain the solution space [54]. As such, when the mechanistic model cannot correctly represent some aspects of the process, e.g., complex nonlinear kinetics, a parallel structure is preferred. It can perform better than the serial arrangement since the data-driven model can partially compensate for the structural weakness in the mechanistic model. When the structure of the mechanistic

model is accurate, the serial model gives better predictions compared to the parallel model. In addition, the extrapolation properties will be significantly better.

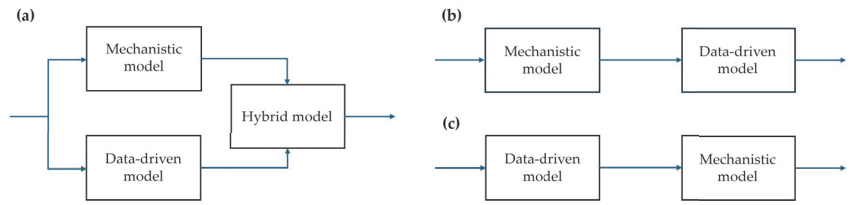


Figure 3. Schematic of the three ways to combine the two types of models. (a) Parallel configuration. (b,c) Serial configurations.

Hybrid modeling is a relatively recent field. Despite significant efforts in this area, as evidenced by applications in fermentation processes (refer to Table 6), there are still challenges to overcome. These challenges should be addressed to allow their widespread application in the field of biochemical engineering. A detailed discussion of current challenges can be found in the review of Schweidtmann et al. [48]. Some examples that are found particularly relevant for fermentation processes are: (a) the complexity in parameter estimation in dynamic hybrid models since this could lead to an increase in computational demand [55,56]; (b) the lack of well-documented methods for incremental learning, i.e., being able to train the model on new data without requiring access to the original data, which could be essential to improve the model's predictions as more experimental data are collected. This is relevant since the most common approach at the moment is batch incremental learning, which requires the model to be re-trained using the whole dataset (original data and new data) and that can become computationally expensive for increasing quantities of data [57]; and (c) the use in adaptive and evolving systems, since this can be the case in fermentation processes, such as processes with distinct phases for growth and product synthesis [58]. This results in a metabolic shift, which can be represented by keeping the same structure (e.g., the equation used to describe the growth rate) and changing the value of certain parameters—adaptive—or by constructing a different model for each phase (e.g., choosing a new equation that better describes the growth rate in the new conditions)—evolving.

Table 6. Applications of hybrid models of fermentation processes.

Microorganism	Type of Model	Application	Studied Parameter	Main Findings	Reference
<i>Aspergillus niger</i>	Unstructured mechanistic model + LBGM	Prediction	Glucose, glycerol and biomass concentration	Soft-sensor for glucose concentration coupled with a kinetic model for glycerol and biomass prediction	[59]
<i>Bordetella pertussis</i>	Unstructured mechanistic model + PLS	Monitoring	Biomass, glutamate, and lactate concentration	Real-time monitoring of the fermentation with improved prediction compared to the PLS model on its own	[60]
<i>Candida rugosa</i>	Unstructured mechanistic model + NN	Monitoring	Lypolitic activity	Decreased prediction error of lipase activity with on-line implementation	[61]
<i>Cunninghamella echinulata</i>	Unstructured mechanistic model + NN	Prediction	Kinetic parameter estimation	The data-driven model is directly built as the kinetic parameters are estimated	[58]
<i>Escherichia coli</i>	Unstructured mechanistic model + NN	Optimization	Induction conditions	Significant reduction in required DOE to determine optimal parameters	[49]
	Unstructured mechanistic model + NN	Control	Feed rate	Improved batch-to-batch reproducibility by introducing a model-based feed rate control	[62]

Table 6. Cont.

Microorganism	Type of Model	Application	Studied Parameter	Main Findings	Reference
<i>Mammalian cell culture</i>	Unstructured mechanistic model + NN	Control	Harvesting point	Real-time monitoring of the fermentation and model predictive feed control	[63]
	Unstructured mechanistic model + NN	Prediction	Degree of hybridization	Determination of the ideal level of mechanistic knowledge to be included for optimal performance	[13]
<i>Pichia pastoris</i>	Unstructured mechanistic model + NN	Prediction	Prediction of dynamic variables	Increased depth of the neural network led to a decrease in prediction errors	[64]
	Carbon balance + Multiple linear regression	Monitoring	Biomass concentration	Prediction of biomass concentration, based on online data of three different fermentation phases	[51]
<i>Saccharomyces cerevisiae</i>	Unstructured mechanistic model + Neural ODEs	Prediction	Unknown kinetic dynamics	Improved model accuracy from the incorporation of neural ODEs	[16]
	Unstructured mechanistic model + PLS	Monitoring	Substrate uptake and ethanol production	Real-time monitoring of the fermentation using advanced spectroscopy data	[65]
<i>Xanthophyllomyces dendrorhous</i>	Unstructured mechanistic model + Gaussian process model	Prediction	Kinetic parameter estimation in mixed-sugar conditions	Embedding of the Gaussian process model reduces model uncertainty and prediction error	[56]
Non disclosed	Unstructured mechanistic model + NN	Prediction	Uncertain parameters, e.g., biomass, product and substrate	Superior performance versus the kinetic model	[15]

Applications in Fermentation Processes

This section will focus on applications of hybrid modeling in the field of fermentation. Hybrid modeling can be used as a prediction tool in the process development stage [16,49], and its applications extend to monitoring, control, and optimization. Table 6 summarizes some examples of the application of this type of model.

As an early development stage example, von Stosch et al. [49] applied a hybrid model for a reduced DOE for an *E. coli* fermentation process. The selected structure for the model was a serial structure (Figure 3c), where the data-driven component (ANN) is used to predict the rates and correlation parameters included in the mechanistic component (material balances). Essentially, the mechanistic model uses ODEs to describe the variation over time of volume, biomass, and product concentrations, by establishing the relationships between these variables and rates (biomass and product formation) and the added base and feed solution. The data-driven model is an artificial neural network with three layers. The inputs for this model are the process parameters X (biomass concentration), P/X (specific productivity), T (temperature), pH , and the carbon feed rate. The structure of the neural network (number of nodes and hidden layers) as well as the most relevant process parameters to include were decided on the basis of the performance of the model on the validation set. The hybrid model could predict the impact of different induction conditions (e.g., temperature and pH) on biomass growth and recombinant protein formation, allowing for better process understanding without added experiments.

For monitoring purposes, the models can be used as a soft sensor where online measurements are taken by the model and turned into relevant predictions. For example, Brunner et al. [51] use the online data of CO_2 , measured in the off-gas for real-time prediction of biomass concentration throughout the different stages of a fermentation process (batch, transition phase, and fed-batch), recurring to a simple carbon balance model coupled with multiple linear regression. In this case, a serial structure is adopted as well; however, unlike the previous example, the mechanistic model's predictions are fed into the data-driven component (Figure 3b). The rate of carbon production is calculated mechanistically based on mass balances. This value, along with the volume of the base solution that has

been fed into the reactor, is input into the multiple linear regression model. This model will calculate the biomass concentration. Furthermore, a phase detection algorithm is used to determine the current process stage, and automatically adapt the values of the model's parameters, based on the concentration of CO₂ measured online in the off-gas.

In another approach, Boareto et al. [61] used NNs to improve a previously developed mechanistic model of the produced lipolytic enzyme titer. The model utilized CO₂ and substrate feed rate measurements to predict, in real-time, the enzyme titer, as well as substrate and biomass concentrations. In this approach, a parallel structure is adopted to combat the structural mismatch in the original mechanistic model. The mechanistic component of the model was adapted from the literature and reduced so that it would include ODEs only for the biomass and substrate concentration, using the well-known Monod equation to predict the growth rate. The equations describing the evolution in enzyme activity were removed due to their inaccurate predictions. The data-driven component of the model (ANN) is used to calculate the enzyme's titer based on the carbon evolution rate, substrate feed rate (online measurements), and biomass concentration (calculated by the mechanistic component). The selected neural network model had three layers and its structure was determined by cross-validation. The final model significantly improved the accuracy of the enzyme titer predictions while maintaining the same performance for the prediction of biomass concentration.

Cabaneros Lopez et al. [65] uses mid-infrared spectroscopy data to feed a PLS model. Combined with a kinetic model, they can predict glucose, biomass, and ethanol concentration in a lignocellulosic fermentation. The model presents a parallel structure, and the predictions of both components are fused by a continuous-discrete extended Kalman filter (CD-EKF). The mechanistic component is a kinetic model composed of eight ODEs describing all the variables of interest, and the parameter estimation was performed by the non-linear least-squares method. For the data-driven component, PLS models were used to predict glucose, xylose, and ethanol concentrations from the spectral data. The predictions of the hybrid model were compared to the predictions of the mechanistic and data-driven models on their own. In all but one case, the hybrid model presented lower RMSE values than the other models. In one of the test fermentations, the RMSE for the prediction of ethanol concentration was lower for the mechanistic model than for the hybrid model.

For control purposes, robust models with high extrapolation possibilities are required [52]—characteristic of hybrid models—however, not many applications are reported. However, there are some examples such as the work of Dors et al. [63] and Jenzsch et al. [62], in which the predictions of the hybrid model are used as input to control the fermentation feed profile, leading to a more stable process and improved batch-to-batch reproducibility, respectively. In the first case, a parallel structure is adopted. The mechanistic component consists of ODEs that describe the mass balances for all relevant process variables and uses Monod relationships to describe the kinetics of the process. The data-driven component (ANN) is used to partially calculate the consumption and production rates. The predictions of both components are weighted according to the process data available to train the neural network in the region corresponding to the current process state; i.e., if sufficient historical data for the current state exist, the prediction of the neural network will have a superior weight to the one of the mechanistic components. Finally, the hybrid model is used to calculate an optimal feed rate. The use of hybrid modeling for online applications, namely monitoring, is already significant. Real-time predictions of key process variables open the possibility of detecting if the process is running as expected and can aid the decision-making of operators. This would push the industry towards a more digital operation, being less dependent on variations influenced by human interaction.

5. Model Aided Scale-Up

The topic of scale-up has been central in the research activities concerning fermentation for years. This entails taking a newly developed process from lab to full production scale. The aim is to produce large product quantities while maintaining the CQAs observed at the

small scale. The challenge is that as the reactor size increases, the conditions for favorable growth may be harder to attain, e.g., due to less efficient mixing. This, in turn, can lead to lower process reproducibility, yields, and product quality [66]. Process scale-up is still, to this day, a major challenge in the fermentation industry, as it is usually not based on mathematical process models but on empirical correlations.

The ideal way to tackle the challenges found on large scales would be to perform experiments on the actual production site. However, this is not economically feasible, not only due to the large amount of resources consumed but also due to the loss of production capacity [67]. The alternative is the use of scale-down approaches, in which a laboratory or pilot scale reactor is used to replicate the conditions experienced at an industrial scale, so the results are relevant for production process optimization. Achieving a successful scale-down is also a challenge since some conditions might be difficult to replicate at smaller scales, such as oxygen transfer, shear rate, and flow patterns. Several platforms can be used for it, including pilot scale reactors, microtiter plates [68], shake flasks, microbioreactors or milliliter scale stirred reactors [69]. Another interesting approach is the use of two connected STRs or a STR and a PFR [70]. This approach allows a potential study of gradients by having each small-scale reactor represent a specific zone of the large-scale reactor, for example, of substrate or oxygen depletion.

5.1. Use of CFD-Coupled Kinetic Models

A relevant problem in industrial-scale reactors that should be taken into account when planning a scale-up is the formation of gradients. There are significant gradients that may impact fermentation process performance of, e.g., substrate or dissolved oxygen concentration. These gradients will occur when the local rate of consumption is higher than the rate of transport [3]. The consequence will be the occurrence of different zones inside the bioreactor with a surplus or a deficiency of nutrients or oxygen. For example, if the substrate is dosed at the top, then the cells located there will experience high nutrient concentrations which can lead to, for example, overflow metabolism in *E. coli* with the production of inhibitory by-products like acetate as a consequence.

A useful tool to study gradients is the combination of computational fluid dynamics (CFD) simulations and biological models. By combining the fluid flow information gained from the CFD model, with the cell metabolism information from the biological model, it is possible to predict the cell response to environmental factors and ultimately the impact this has on CQAs [71].

Several studies have been conducted, with the biological model's complexity ranging from simpler unstructured approaches to complex structured metabolic models. Although unstructured approaches are useful for a better understanding of gradients, they cannot capture the response of the organisms to the different conditions, as metabolic models can. Table 7 summarizes examples of models developed. To highlight a few, Pigou and Morchain [4] were able to predict the areas of the bioreactor where acetate would be consumed or produced by *E. coli* due to the formation of a glucose gradient. They used a population balance model in combination with a compartment model, reducing the computational burden compared to a CFD simulation. In the work of Sibling et al. [72], they could predict the impact of the CO gradient on the cell population. Through their work, the scale-up of this syngas fermentation can be performed by taking into account the need to improve CO mass transfer or engineering strains that better cope with this limitation.

Table 7. Applications of CFD-coupled kinetic models of fermentation processes.

Microorganism	Approach	Main Findings	Reference
<i>Clostridium ljungdahlii</i>	Unstructured kinetic model	Need to improve CO mass transfer and/or to engineer strains that cope with the conditions	[72]
<i>Escherichia coli</i>	Metabolic model	Glucose gradients induce production/consumption of acetate in different parts of the reactor	[4]

Table 7. Cont.

Microorganism	Approach	Main Findings	Reference
<i>Penicillium chrysogenum</i>	Dynamic gene regulation model	Statistical assessment of the substrate fluctuations experienced by organisms in industrial-scale fermentation	[73]
	Pooled metabolic model	Identified targets for metabolic and reactor optimization of large-scale fermentation	[26]
<i>Pseudomonas putida</i>	Cell cycle model	Insights into the intracellular mechanisms that determine growth phenotypes	[74]
<i>Saccharomyces cerevisiae</i>	Unstructured kinetic model	The approach provides a simulation strategy for the design and operation of bioreactors, particularly when single cell behavior is relevant	[75]

5.2. Use of Hybrid Modelling in Scale-Up

So far, this section has illustrated how modeling can be used to predict a challenge that can be encountered when scaling up the formation of gradients. However, models that can predict the fermentation performance to some extent on a large scale, namely what the CQAs would look like under different conditions, would be extremely beneficial when planning the scale transition. Although there are numerous instances of hybrid models being applied to fermentation processes, their utilization for scale-up is not commonly mentioned. We believe that this modeling approach offers a significant opportunity to accelerate the scale-up stage of fermentation process development.

As mentioned in Section 4, hybrid models can have good extrapolation properties (which are determined by the mechanistic component of the model) while being less time-consuming to develop than purely mechanistic models. This highlights their suitability as an approach for scale-up since the model could be developed and calibrated at a smaller scale and then extrapolated to a larger scale. One strategy is to develop a mechanistic model on a small scale and complement it with data-driven approaches to represent scale-specific parts of the model. The data-driven component will account for scale-up factors and other assumptions made in the mechanistic model that are not valid on larger scales [12,76]. Another option is to use mainly small-scale experimental data to develop the model but include a few validation experiments at a larger scale. This will be sufficient to significantly improve the model's prediction capabilities on a large scale, while at the same time not requiring a big increase in resource consumption [50].

Here, two examples are described where a hybrid model is used to predict larger-scale performance. In the work of Bayer et al. [50], a hybrid model was developed from a DOE with 300 mL shake flasks and re-calibrated with only three batches at the 15 L lab-scale reactor. These few experimental runs on a larger scale were sufficient for the model to accurately describe cell behavior and product formation on the 15 L scale under different process conditions. These included shifts in temperature and substrate concentration in the feed, throughout the fermentation time, while the model had only been trained in static conditions. Regarding the work of Rogers et al. [14], three hybrid models are developed on the 1 L scale, where each model has a different quantity of kinetic knowledge incorporated, i.e., number of parameters. The models are then used to predict the performance of fermentations in 5 L reactors under a temperature change that was not present in the training data. They found that the model with intermediate knowledge incorporation performed the best in this case and is suitable for model-based bioreactor optimization and scale-up. Although the model with the largest kinetic information had more confident predictions, it showed lower accuracy. This highlights that incorporating information that is not fully understood can lead to incorrect bias and poorer model performance, i.e., overfitting the model.

No examples of applications of similar strategies to industrial scales have been found in the literature. However, an adaptation of the described strategies to larger scales could be of interest.

6. Conclusions

The development and application of process models continue to be crucial research areas in biotechnology. These models can be utilized at various stages of process development, from initial design to optimization, for scale-up, and ultimately as a more detailed way of monitoring and controlling processes. The main takeaways of this review are:

- Both mechanistic and data-driven models continue to be relevant strategies in the development of fermentation processes, both with different specific use cases. Data-driven models are particularly relevant for online process models and are frequently used in the development of soft-sensors. On the other hand, the interpretability and extrapolation capabilities of mechanistic models make them suitable for process optimization and understanding the impact of different parameters on the cell's metabolic responses.
- Hybrid modeling is a rapidly evolving field and offers substantial benefits in the context of fermentation processes. It enables the exploitation of the strengths of both types of aforementioned models while combatting their weaknesses, ideally leading to a more agile development process.
- The level of mechanistic knowledge included in hybrid models must be carefully selected to avoid overparametrizing or biasing the model. If performed adequately, the result will be a more accurate and extrapolative model, with lower data requirements than a data-driven counterpart.
- Most use cases still focus on the prediction and monitoring of relevant process variables, but they present great potential for model predictive control applications. Furthermore, it appears to be an interesting tool for aiding in process upscaling due to good extrapolation capabilities across scales.
- The technology readiness level of hybrid modeling is still considered low. Some challenges, like the expansion of models as more data becomes available or the complexity in parameter estimation, need to be overcome for their successful implementation as relevant tools for industrial bioprocesses.

Author Contributions: Conceptualization, M.A. and C.L.G. writing—original draft preparation, M.A. and C.L.G.; writing—review and editing, G.N.-R., K.V.G., M.O.A. and U.K. All authors have read and agreed to the published version of the manuscript.

Funding: This research was funded by Novo Nordisk Foundation: Sustain4.0: Real-time sustainability analysis for Industry 4.0 (NNF0080136).

Acknowledgments: This project received support from the Technical University of Denmark and Novonesis A/S.

Conflicts of Interest: The authors Gisela Nadal-Rey and Mads O. Albæk were employed by the company Novonesis A/S. The remaining authors declare that the research was conducted in the absence of any commercial or financial relationships that could be construed as a potential conflict of interest. The authors declare that this study received funding from the Novo Nordisk Foundation. The funder was not involved in the study design, collection, analysis, interpretation of data, the writing of this article or the decision to submit it for publication".

Abbreviations

The following abbreviations are used in this manuscript:

ANN	artificial neural networks
API	active pharmaceutical ingredient
CFD	computational fluid dynamics
CHO	Chinese hamster ovary

CQA	critical quality attribute
DOE	design of experiments
NN	neural networks
ODE	ordinary differential equation
PCA	principal component analysis
PFR	plug flow reactor
PLS	partial least squares
STR	stirred tank reactor

References

1. Behera, S.S.; Ray, R.C.; Das, U.; Panda, S.K.; Saranraj, P. Microorganisms in Fermentation. In *Essentials in Fermentation Technology*; Berenjian, A., Ed.; Springer International Publishing: Cham, Switzerland, 2019; pp. 1–39. [CrossRef]
2. González-Figueroa, C.; Flores-Estrella, R.A.; Rojas-Rejón, O.A. Fermentation: Metabolism, kinetic models, and bioprocessing. In *Current Topics in Biochemical Engineering*; IntechOpen: Rijeka, Croatia, 2018; Volume 1.
3. Nadal-Rey, G.; McClure, D.D.; Kavanagh, J.M.; Cornelissen, S.; Fletcher, D.F.; Gernaey, K.V. Understanding gradients in industrial bioreactors. *Biotechnol. Adv.* **2021**, *46*, 107660. [CrossRef] [PubMed]
4. Pigou, M.; Morchain, J. Investigating the interactions between physical and biological heterogeneities in bioreactors using compartment, population balance and metabolic models. *Chem. Eng. Sci.* **2015**, *126*, 267–282. [CrossRef]
5. Gargalo, C.L.; de las Heras, S.C.; Jones, M.N.; Udugama, I.; Mansouri, S.S.; Krühne, U.; Gernaey, K.V. Towards the Development of Digital Twins for the Bio-manufacturing Industry. In *Digital Twins: Tools and Concepts for Smart Biomanufacturing*; Herwig, C., Pörtner, R., Möller, J., Eds.; Springer International Publishing: Cham, Switzerland, 2021; pp. 1–34. [CrossRef]
6. Becker, T.; Enders, T.; Delgado, A. Dynamic neural networks as a tool for the online optimization of industrial fermentation. *Bioprocess Biosyst. Eng.* **2002**, *24*, 347–354. [CrossRef]
7. Lourenço, N.D.; Lopes, J.A.; Almeida, C.F.; Sarraguça, M.C.; Pinheiro, H.M. Bioreactor monitoring with spectroscopy and Chemometrics: A Review. *Anal. Bioanal. Chem.* **2012**, *404*, 1211–1237. [CrossRef] [PubMed]
8. Janoska, A.; Buijs, J.; van Gulik, W.M. Predicting the influence of combined oxygen and glucose gradients based on scale-down and modelling approaches for the scale-up of penicillin fermentations. *Process Biochem.* **2023**, *124*, 100–112. [CrossRef]
9. Mears, L.; Stocks, S.M.; Albaek, M.O.; Sin, G.; Gernaey, K.V. Mechanistic fermentation models for process design, monitoring, and Control. *Trends Biotechnol.* **2017**, *35*, 914–924. [CrossRef] [PubMed]
10. Gernaey, K.V.; Lantz, A.E.; Tufvesson, P.; Woodley, J.M.; Sin, G. Application of mechanistic models to fermentation and biocatalysis for next-generation processes. *Trends Biotechnol.* **2010**, *28*, 346–354. [CrossRef] [PubMed]
11. Tsopanoglou, A.; Jiménez del Val, I. Moving towards an era of hybrid modelling: Advantages and challenges of coupling mechanistic and data-driven models for upstream pharmaceutical bioprocesses. *Curr. Opin. Chem. Eng.* **2021**, *32*, 100691. [CrossRef]
12. von Stosch, M.; Oliveira, R.; Peres, J.; Feyo de Azevedo, S. Hybrid semi-parametric modeling in process systems engineering: Past, present and future. *Comput. Chem. Eng.* **2014**, *60*, 86–101. [CrossRef]
13. Narayanan, H.; Luna, M.; Sokolov, M.; Butté, A.; Morbidelli, M. Hybrid Models Based on Machine Learning and an Increasing Degree of Process Knowledge: Application to Cell Culture Processes. *Ind. Eng. Chem. Res.* **2022**, *61*, 8658–8672. [CrossRef]
14. Rogers, A.W.; Song, Z.; Ramon, F.V.; Jing, K.; Zhang, D. Investigating ‘greyness’ of hybrid model for bioprocess predictive modelling. *Biochem. Eng. J.* **2023**, *190*, 108761. [CrossRef]
15. Shah, P.; Sherif, M.Z.; Bangi, M.S.F.; Kravaris, C.; Kwon, J.S.I.; Botre, C.; Hirota, J. Deep neural network-based hybrid modeling and experimental validation for an industry-scale fermentation process: Identification of time-varying dependencies among parameters. *Chem. Eng. J.* **2022**, *441*, 135643. [CrossRef]
16. Bangi, M.S.F.; Kao, K.; Kwon, J.S.I. Physics-informed neural networks for hybrid modeling of lab-scale batch fermentation for β -carotene production using *Saccharomyces cerevisiae*. *Chem. Eng. Res. Des.* **2022**, *179*, 415–423. [CrossRef]
17. Moser, A.; Appl, C.; Brüning, S.; Hass, V.C. Mechanistic Mathematical Models as a Basis for Digital Twins. In *Digital Twins: Tools and Concepts for Smart Biomanufacturing*; Springer: Berlin/Heidelberg, Germany, 2021. [CrossRef]
18. Waldherr, S. Estimation methods for heterogeneous cell population models in systems biology. *J. R. Soc. Interface* **2018**, *15*, 20180530 [CrossRef]
19. Anane, E.; López C, D.C.; Neubauer, P.; Cruz Bournazou, M.N. Modelling overflow metabolism in *Escherichia coli* by acetate cycling. *Biochem. Eng. J.* **2017**, *125*, 23–30. [CrossRef]
20. Albaek, M.O.; Gernaey, K.V.; Hansen, M.S.; Stocks, S.M. Modeling enzyme production with *Aspergillus oryzae* in pilot scale vessels with different agitation, aeration, and agitator types. *Biotechnol. Bioeng.* **2011**, *108*, 1828–1840. [CrossRef] [PubMed]
21. Grisales Díaz, V.H.; Willis, M.J. Ethanol production using *Zymomonas mobilis*: Development of a kinetic model describing glucose and xylose co-fermentation. *Biomass Bioenergy* **2019**, *123*, 41–50. [CrossRef]
22. Du, Y.H.; Wang, M.Y.; Yang, L.H.; Tong, L.L.; Guo, D.S.; Ji, X.J. Optimization and Scale-Up of Fermentation Processes Driven by Models. *Bioengineering* **2022**, *9*, 473. [CrossRef] [PubMed]

23. Tang, W.; Deshmukh, A.T.; Haringa, C.; Wang, G.; van Gulik, W.; van Winden, W.; Reuss, M.; Heijnen, J.J.; Xia, J.; Chu, J.; et al. A 9-pool metabolic structured kinetic model describing days to seconds dynamics of growth and product formation by *Penicillium chrysogenum*. *Biotechnol. Bioeng.* **2017**, *114*, 1733–1743. [CrossRef] [PubMed]
24. Jahan, N.; Maeda, K.; Matsuoka, Y.; Sugimoto, Y.; Kurata, H. Development of an accurate kinetic model for the central carbon metabolism of *Escherichia coli*. *Microb. Cell Factories* **2016**, *15*, 112. [CrossRef] [PubMed]
25. Çelik, E.; Çalık, P.; Oliver, S.G. A structured kinetic model for recombinant protein production by Mut⁺ strain of *Pichia pastoris*. *Chem. Eng. Sci.* **2009**, *64*, 5028–5035. [CrossRef]
26. Haringa, C.; Tang, W.; Wang, G.; Deshmukh, A.T.; van Winden, W.A.; Chu, J.; van Gulik, W.M.; Heijnen, J.J.; Mudde, R.F.; Noorman, H.J. Computational fluid dynamics simulation of an industrial *P. chrysogenum* fermentation with a coupled 9-pool metabolic model: Towards rational scale-down and design optimization. *Chem. Eng. Sci.* **2018**, *175*, 12–24. [CrossRef]
27. Pan, S.; Chen, G.; Zeng, J.; Cao, X.; Zheng, X.; Zeng, W.; Liang, Z. Fibrinolytic enzyme production from low-cost substrates by marine *Bacillus subtilis*: Process optimization and kinetic modeling. *Biochem. Eng. J.* **2019**, *141*, 268–277. [CrossRef]
28. Xu, J.; Tang, P.; Yongky, A.; Drew, B.; Borys, M.C.; Liu, S.; Li, Z.J. Systematic development of temperature shift strategies for Chinese hamster ovary cells based on short duration cultures and kinetic modeling. *mAbs* **2019**, *11*, 191–204. [CrossRef] [PubMed]
29. Goldrick, S.; Ştefan, A.; Lovett, D.; Montague, G.; Lennox, B. The development of an industrial-scale fed-batch fermentation simulation. *J. Biotechnol.* **2015**, *193*, 70–82. [CrossRef] [PubMed]
30. Barrigon, J.M.; Valero, F.; Montesinos, J.L. A macrokinetic model-based comparative meta-analysis of recombinant protein production by *Pichia pastoris* under AOX1 promoter. *Biotechnol. Bioeng.* **2015**, *112*, 1132–1145. [CrossRef] [PubMed]
31. Germeç, M.; Karhan, M.; Demirci, A.; Turhan, I. Kinetic modeling, sensitivity analysis, and techno-economic feasibility of ethanol fermentation from non-sterile carob extract-based media in *Saccharomyces cerevisiae* biofilm reactor under a repeated-batch fermentation process. *Fuel* **2022**, *324*, 124729. [CrossRef]
32. Mears, L.; Stocks, S.M.; Albaek, M.O.; Sin, G.; Gernaey, K.V. Application of a mechanistic model as a tool for on-line monitoring of pilot scale filamentous fungal fermentation processes—The importance of evaporation effects. *Biotechnol. Bioeng.* **2017**, *114*, 589–599. [CrossRef] [PubMed]
33. Alloghani, M.; Al-Jumeily, D.; Mustafina, J.; Hussain, A.; Aljaaf, A.J. A Systematic Review on Supervised and Unsupervised Machine Learning Algorithms for Data Science. In *Supervised and Unsupervised Learning for Data Science*; Springer: Berlin/Heidelberg, Germany, 2020. [CrossRef]
34. Wiering, M.A.; Van Otterlo, M. Reinforcement learning. *Adapt. Learn. Optim.* **2012**, *12*, 739.
35. Tavasoli, T.; Arjmand, S.; Ranaei Siadat, S.O.; Shojaosadati, S.A.; Sahebghadam Lotfi, A. A robust feeding control strategy adjusted and optimized by a neural network for enhancing of alpha 1-antitrypsin production in *Pichia pastoris*. *Biochem. Eng. J.* **2019**, *144*, 18–27. [CrossRef]
36. Nagy, Z.K. Model based control of a yeast fermentation bioreactor using optimally designed artificial neural networks. *Chem. Eng. J.* **2007**, *127*, 95–109. [CrossRef]
37. Andersen, S.W.; Runger, G.C. Partitioned partial least squares regression with application to a batch fermentation process. *J. Chemom.* **2011**, *25*, 159–168. [CrossRef]
38. Barton, M.; Duran-Villalobos, C.A.; Lennox, B. Multivariate batch to batch optimisation of fermentation processes to improve productivity. *J. Process. Control* **2021**, *108*, 148–156. [CrossRef]
39. Nucci, E.R.; Cruz, A.J.; Giordano, R.C. Monitoring bioreactors using Principal Component Analysis: Production of penicillin G acylase as a case study. *Bioprocess Biosyst. Eng.* **2009**, *33*, 557–564. [CrossRef] [PubMed]
40. Dewasme, L.; Cote, F.; Filee, P.; Hantson, A.L.; Vande Wouwer, A. Dynamic modeling of hybridoma cell cultures using maximum likelihood principal component analysis. *IFAC-PapersOnLine* **2017**, *50*, 12143–12148. [CrossRef]
41. Pimentel, G.A.; Dewasme, L.; Wouwer, A.V. Data-driven Linear Predictor based on Maximum Likelihood Nonnegative Matrix Decomposition for Batch Cultures of Hybridoma Cells. *IFAC-PapersOnLine* **2022**, *55*, 903–908. [CrossRef]
42. Kaelbling, L.P.; Littman, M.L.; Moore, A.W. Reinforcement learning: A survey. *J. Artif. Intell. Res.* **1996**, *4*, 237–285. [CrossRef]
43. Treloar, N.J.; Fedorec, A.J.H.; Ingalls, B.; Barnes, C.P. Deep reinforcement learning for the control of microbial co-cultures in bioreactors. *PLoS Comput. Biol.* **2020**, *16*, e1007783. [CrossRef] [PubMed]
44. Kim, J.W.; Park, B.J.; Oh, T.H.; Lee, J.M. Model-based reinforcement learning and predictive control for two-stage optimal control of fed-batch bioreactor. *Comput. Chem. Eng.* **2021**, *154*, 107465. [CrossRef]
45. Oh, T.H.; Park, H.M.; Kim, J.W.; Lee, J.M. Integration of reinforcement learning and model predictive control to optimize semi-batch bioreactor. *AIChE J.* **2022**, *68*, e17658. [CrossRef]
46. Paquet-Durand, O.; Assawarajuwan, S.; Hitzmann, B. Artificial neural network for bioprocess monitoring based on fluorescence measurements: Training without offline measurements. *Eng. Life Sci.* **2017**, *17*, 874–880. [CrossRef] [PubMed]
47. Lopes, J.; Menezes, J.; Westerhuis, J.; Smilde, A. Multiblock PLS analysis of an industrial pharmaceutical process. *Biotechnol. Bioeng.* **2002**, *80*, 419–427. [CrossRef] [PubMed]
48. Schweidtmann, A.M.; Zhang, D.; von Stosch, M. A review and perspective on hybrid modeling methodologies. *Digit. Chem. Eng.* **2024**, *10*, 100136. [CrossRef]
49. von Stosch, M.; Hamelink, J.M.; Oliveira, R. Hybrid modeling as a QBD/PAT tool in process development: An industrial *E. coli* case study. *Bioprocess Biosyst. Eng.* **2016**, *39*, 773–784. [CrossRef] [PubMed]

50. Bayer, B.; Duerkop, M.; Striedner, G.; Sissolak, B. Model Transferability and Reduced Experimental Burden in Cell Culture Process Development Facilitated by Hybrid Modeling and Intensified Design of Experiments. *Front. Bioeng. Biotechnol.* **2021**, *9*, 740215. [CrossRef] [PubMed]
51. Brunner, V.; Siegl, M.; Geier, D.; Becker, T. Biomass soft sensor for a *Pichia pastoris* fed-batch process based on phase detection and hybrid modeling. *Biotechnol. Bioeng.* **2020**, *117*, 2749–2759. [CrossRef] [PubMed]
52. von Stosch, M.; Davy, S.; Francois, K.; Galvanuskas, V.; Hamelink, J.M.; Luebbert, A.; Mayer, M.; Oliveira, R.; O’Kennedy, R.; Rice, P.; et al. Hybrid modeling for quality by design and PAT-benefits and challenges of applications in biopharmaceutical industry. *Biotechnol. J.* **2014**, *9*, 719–726. [CrossRef] [PubMed]
53. von Stosch, M.; Oliveira, R.; Peres, J.; Feyer de Azevedo, S. A general hybrid semi-parametric process control framework. *J. Process. Control.* **2012**, *22*, 1171–1181. [CrossRef]
54. Psychogios, D.C.; Ungar, L.H. A hybrid neural network-first principles approach to process modeling. *AIChE J.* **1992**, *38*, 1499–1511. [CrossRef]
55. Cruz-Bournazou, M.N.; Narayanan, H.; Fagnani, A.; Butté, A. Hybrid Gaussian Process Models for continuous time series in bolus fed-batch cultures. *IFAC-PapersOnLine* **2022**, *55*, 204–209. [CrossRef]
56. Vega-Ramon, F.; Zhu, X.; Savage, T.R.; Petsagkourakis, P.; Jing, K.; Zhang, D. Kinetic and hybrid modeling for yeast astaxanthin production under uncertainty. *Biotechnol. Bioeng.* **2021**, *118*, 4854–4866. [CrossRef] [PubMed]
57. Read, J.; Bifet, A.; Pfahringer, B.; Holmes, G. Batch-Incremental versus Instance-Incremental Learning in Dynamic and Evolving Data. In Proceedings of the Advances in Intelligent Data Analysis XI, Helsinki, Finland, 25–27 October 2012; Springer: Berlin/Heidelberg, Germany, 2012; pp. 313–323.
58. Rogers, A.W.; Cardenas, I.O.S.; Del Rio-Chanona, E.A.; Zhang, D. Investigating physics-informed neural networks for bioprocess hybrid model construction. *Comput. Aided Chem. Eng.* **2023**, *52*, 83–88. [CrossRef]
59. Rydal, T.; Frandsen, J.; Nadal-Rey, G.; Albæk, M.O.; Ramin, P. Bringing a scalable adaptive hybrid modeling framework closer to industrial use: Application on a multiscale fungal fermentation. *Biotechnol. Bioeng.* **2024**, *121*, 1609–1625. [CrossRef] [PubMed]
60. von Stosch, M.; Oliveria, R.; Peres, J.; de Azevedo, S.F. Hybrid modeling framework for process analytical technology: Application to *Bordetella pertussis* cultures. *Biotechnol. Prog.* **2012**, *28*, 284–291. [CrossRef] [PubMed]
61. Boareto, Á.J.M.; De Souza, M.B., Jr.; Valero, F.; Valdman, B. A hybrid neural model (HNM) for the on-line monitoring of lipase production by *Candida rugosa*. *J. Chem. Technol. Biotechnol.* **2007**, *82*, 319–327. [CrossRef]
62. Jenzsch, M.; Gnath, S.; Kleinschmidt, M.; Simutis, R.; Lübbert, A. Improving the batch-to-batch reproducibility of microbial cultures during recombinant protein production by regulation of the total carbon dioxide production. *J. Biotechnol.* **2007**, *128*, 858–867. [CrossRef] [PubMed]
63. Dors, M.; Simutis, R.; Lübbert, A. Hybrid Process Modeling for Advanced Process State Estimation, Prediction, and Control Exemplified in a Production-Scale Mammalian Cell Culture. In *Biosensor and Chemical Sensor Technology*; American Chemical Society: Washington, DC, USA, 1996. [CrossRef]
64. Pinto, J.; Mestre, M.; Ramos, J.; Costa, R.S.; Striedner, G.; Oliveira, R. A general deep hybrid model for bioreactor systems: Combining first principles with deep neural networks. *Comput. Chem. Eng.* **2022**, *165*, 107952. [CrossRef]
65. Cabaneros Lopez, P.; Udugama, I.A.; Thomsen, S.T.; Roslander, C.; Junicke, H.; Iglesias, M.M.; Gernaey, K.V. Transforming data to information: A parallel hybrid model for real-time state estimation in lignocellulosic ethanol fermentation. *Biotechnol. Bioeng.* **2021**, *118*, 579–591. [CrossRef] [PubMed]
66. Schmidt, F.R. Optimization and scale up of industrial fermentation processes. *Appl. Microbiol. Biotechnol.* **2005**, *68*, 425–435. [CrossRef] [PubMed]
67. Formenti, L.R.; Nørregaard, A.; Bolic, A.; Hernandez, D.Q.; Hagemann, T.; Heins, A.L.; Larsson, H.; Mears, L.; Mauricio-Iglesias, M.; Krühne, U.; et al. Challenges in industrial fermentation technology research. *Biotechnol. J.* **2014**, *9*, 727–738. [CrossRef] [PubMed]
68. Funke, M.; Buchenauer, A.; Schnakenberg, U.; Mokwa, W.; Diederichs, S.; Mertens, A.; Müller, C.; Kensity, F.; Büchs, J. Microfluidic biolector—microfluidic bioprocess control in microtiter plates. *Biotechnol. Bioeng.* **2010**, *107*, 497–505. [CrossRef]
69. Tajssoleiman, T.; Mears, L.; Krühne, U.; Gernaey, K.V.; Cornelissen, S. An industrial perspective on scale-down challenges using miniaturized bioreactors. *Trends Biotechnol.* **2019**, *37*, 697–706. [CrossRef] [PubMed]
70. Junne, S.; Klingner, A.; Kabisch, J.; Schweder, T.; Neubauer, P. A two-compartment bioreactor system made of commercial parts for bioprocess scale-down studies: Impact of oscillations on *Bacillus subtilis* fed-batch cultivations. *Biotechnol. J.* **2011**, *6*, 1009–1017. [CrossRef] [PubMed]
71. Wang, G.; Haringa, C.; Noorman, H.; Chu, J.; Zhuang, Y. Developing a Computational Framework To Advance Bioprocess Scale-Up. *Trends Biotechnol.* **2020**, *38*, 846–856. [CrossRef] [PubMed]
72. Siebler, F.; Lapin, A.; Hermann, M.; Takors, R. The impact of CO gradients on *C. ljungdahlii* in a 125 m³ bubble column: Mass transfer, circulation time and lifeline analysis. *Chem. Eng. Sci.* **2019**, *207*, 410–423. [CrossRef]
73. Haringa, C.; Tang, W.; Deshmukh, A.T.; Xia, J.; Reuss, M.; Heijnen, J.J.; Mudde, R.F.; Noorman, H.J. Euler-Lagrange computational fluid dynamics for (bio)reactor scale down: An analysis of organism lifelines. *Eng. Life Sci.* **2016**, *16*, 652–663. [CrossRef] [PubMed]
74. Kuschel, M.; Siebler, F.; Takors, R. Lagrangian Trajectories to Predict the Formation of Population Heterogeneity in Large-Scale Bioreactors. *Bioengineering* **2017**, *4*, 27. [CrossRef] [PubMed]

75. Lapin, A.; Müller, D.; Reuss, M. Dynamic behavior of microbial populations in stirred bioreactors simulated with Euler-Lagrange methods: Traveling along the lifelines of single cells. *Ind. Eng. Chem. Res.* **2004**, *43*, 4647–4656. [CrossRef]
76. Simon, L.L.; Fischer, U.; Hungerbühler, K. Modeling of a Three-Phase Industrial Batch Reactor Using a Hybrid First-Principles Neural-Network Model. *Ind. Eng. Chem. Res.* **2006**, *45*, 7336–7343. [CrossRef]

Disclaimer/Publisher’s Note: The statements, opinions and data contained in all publications are solely those of the individual author(s) and contributor(s) and not of MDPI and/or the editor(s). MDPI and/or the editor(s) disclaim responsibility for any injury to people or property resulting from any ideas, methods, instructions or products referred to in the content.

Article

Characterizing Novel Acetogens for Production of C2–C6 Alcohols from Syngas

Rahul Thunuguntla ¹, Hasan K. Atiyeh ^{1,*}, Raymond L. Huhnke ¹ and Ralph S. Tanner ²

¹ Department of Biosystems and Agricultural Engineering, Oklahoma State University, Stillwater, OK 74078, USA

² Department of Microbiology and Plant Biology, University of Oklahoma, Norman, OK 73019, USA

* Correspondence: hasan.atiyeh@okstate.edu; Tel.: +1-405-744-8397

Abstract: Utilizing syngas components CO, CO₂, and H₂ to produce fatty acids and alcohols offers a sustainable approach for biofuels and chemicals, reducing the global carbon footprint. The development of robust strains, especially for higher alcohol titers in C₄ and C₆ compounds, and the creation of cost-effective media are crucial. This study compared syngas fermentation capabilities of three novel strains (*Clostridium carboxidivorans* P20, *C. ljungdahlii* P14, and *C. muellerianum* P21) with existing strains (*C. ragsdalei* P11 and *C. carboxidivorans* P7) in three medium formulations. Fermentations in 250-mL bottles were conducted at 37 °C using H₂:CO₂:CO (30:30:40) using P11, P7, and corn steep liquor (CSL) media. Results showed that P11 and CSL media facilitated higher cell mass, alcohol titer, and gas conversion compared to the P7 medium. Strains P7, P14, and P20 formed 1.4- to 4-fold more total alcohols in the CSL medium in comparison with the P7 medium. Further, strain P21 produced more butanol (0.9 g/L) and hexanol (0.7 g/L) in the medium with CSL, offering cost advantages over P7 and P11 media containing yeast extract. Enhancing strain activity and selectivity in converting syngas into C₄ and C₆ alcohols requires further development, medium formulation improvements, and characterization, particularly for the new strain P21.

Keywords: syngas; novel acetogens; ethanol; butanol; hexanol

Citation: Thunuguntla, R.; Atiyeh, H.K.; Huhnke, R.L.; Tanner, R.S. Characterizing Novel Acetogens for Production of C₂–C₆ Alcohols from Syngas. *Processes* **2024**, *12*, 142. <https://doi.org/10.3390/pr12010142>

Academic Editor: Francesca Raganati

Received: 3 December 2023

Revised: 26 December 2023

Accepted: 26 December 2023

Published: 6 January 2024



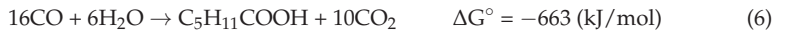
Copyright: © 2024 by the authors. Licensee MDPI, Basel, Switzerland. This article is an open access article distributed under the terms and conditions of the Creative Commons Attribution (CC BY) license (<https://creativecommons.org/licenses/by/4.0/>).

1. Introduction

Biofuel production gained significant attention due to its advantages in reducing dependence on fossil fuels and greenhouse gas emissions (GHG) [1–3]. The United States is the leading biofuel producer in the world, producing 17 billion gallons per year from corn ethanol in 275 biorefineries [4]. Second-generation biofuel production from lignocellulosic biomass is estimated to range from 30 to 60 billion gallons per year in the U.S.A. by 2050 [5]. In addition to ethanol, there has been a growing interest in making renewable butanol and hexanol [6,7]. Butanol is more compatible with the existing infrastructure and well-suited for the production of jet fuels [7–10]. Similarly, hexanol was used as a co-solvent in making biodiesel to improve the cold flow properties, making it more effective in cold temperatures [2].

The production of biofuels derived from crops like corn and sugarcane has raised concerns about potential impacts on food availability [11,12]. As an alternative, syngas fermentation is gaining attention for producing biofuels and biobased products. Syngas fermentation converts CO, CO₂, and H₂, which can be generated from non-edible feedstocks such as industrial waste gases and the gasification of agricultural residues and municipal solid wastes into biofuels [1,3,13]. Syngas fermentation can be integrated into existing industries like gasification, carbon capture, steel mills, and biogas production, which can help reduce GHG and generate revenues from waste streams [9,14–17]. Syngas fermentation has been used to produce two- to six-carbon (C₂–C₆) alcohols and acids, 2,3 butanediol,

and other products [7,13,18]. The balanced equations for making C2–C6 alcohols and acids from CO are listed below [3,13].



Researchers investigated syngas fermentation, including the effect of minerals and trace metals [15,19], the use of defined and complex media [20–22], supplementation of media with biochar [8,9], genetic modification of strains [18,23], and the use of single or multistage bioreactors [24–26]. Furthermore, *C. ragsdalei*, *C. carboxidivorans*, *C. ljungdahlii* and *C. autoethanogenum* have been studied for syngas fermentation. *C. ljungdahlii*, *C. carboxidivorans*, and *C. autoethanogenum* have been genetically modified to produce higher alcohol titers or specific alcohol from syngas [2,13,18]. *C. ragsdalei* and *C. autoethanogenum* have already been studied at pilot and industrial scale to produce ethanol [27–29]. In addition, *C. carboxidivorans*, *C. ljungdahlii*, and *C. autoethanogenum* were reported to make butanol and hexanol from CO and CO₂ [2,8,18].

However, there are limiting factors to produce higher alcohols, especially its toxicity, which can negatively impact the strain's growth and fermentation abilities. Research findings have shown that hexanol, at around 1 g/L, reduced *C. ljungdahlii* activity, and a further increase to 5 g/L completely inhibited *C. ljungdahlii* while also inhibiting *C. carboxidivorans* at 1.2 g/L hexanol [30,31]. To tackle the toxicity issue, studies have employed extractive fermentation to increase hexanol production with *C. carboxidivorans*, achieving 1 g/L [32] and 5 g/L [2]. However, economic feasibility challenges remain to be addressed in syngas fermentation technology, including the need for more robust strains for higher alcohol titers, especially C₄ and C₆ compounds, and the development of low-cost media.

This study explores the potential of three new acetogens, namely *C. ljungdahlii* P14, *C. muellerianum* P21, and *C. carboxidivorans* P20, to make C4–C6 alcohols and fatty acids from syngas. It compares these new strains with two previously studied strains, *C. ragsdalei* P11 and *C. carboxidivorans* P7, for gas fermentation. Additionally, the study evaluates the activity of these acetogens in three syngas fermentation media. The characterization of new acetogens, particularly for C4–C6 products, makes this investigation important in advancing syngas fermentation.

2. Material and Methods

2.1. Microorganisms

The strains used in this study (*C. carboxidivorans* P7 and P20, *C. ragsdalei* P11, *C. ljungdahlii* P14, and *C. muellerianum* P21) were isolated and enriched by R.S. Tanner as previously described [33–36]. These microorganisms were preserved in the P11 medium, as previously reported [8].

2.2. Inoculum Preparation

The inoculum of the five *Clostridium* strains was prepared using P11 medium [8]. P11 medium contains (per L) yeast extract (0.5 g), mineral solution (25 mL), 4-morpholineethane sulfonic acid (MES, 10 g), trace metal solution (10 mL), cysteine sulfide reducing agent (10 mL), vitamin solution (10 mL), and 0.1% resazurin (1 mL) [37]. The medium's initial pH was modified to 6.0 with KOH (5N), falling within the optimum pH range for the growth of the five strains [33–35]. Table 1 provides the composition details of all stock solutions.

Table 1. Compositions of solutions for media (P7, P11, and CSL).

Components	P7 (g/L)	P11 and CSL (g/L)
<i>Minerals solution</i>		
NH ₄ Cl	100	100
KH ₂ PO ₄	10	10
KCl	10	10
CaCl ₂ ·2H ₂ O	4	4
MgSO ₄ ·7H ₂ O	20	20
<i>Vitamin solution</i>		
Pyridoxine	-	0.010
Riboflavin	-	0.005
Thiamine	-	0.005
Thioctic acid	-	0.005
Nicotinic acid	-	0.005
Vitamin B ₁₂	-	0.005
2-Mercaptoethanesulfonic acid sodium salt (MESNA)	-	0.010
Calcium pantothenate	0.005	0.005
p-(4)-Aminobenzoic Acid	0.005	0.005
Biotin	0.002	0.002
<i>Trace Metal Solution</i>		
Nitrilotriacetic acid	2.00	2.00
Fe(NH ₄) ₂ (SO ₄) ₂ ·6H ₂ O	0.80	0.80
ZnSO ₄ ·7H ₂ O	0.20	1.00
MnSO ₄ ·H ₂ O	1.00	1.00
NiCl ₂ ·6H ₂ O	0.02	0.20
Na ₂ SeO ₄	0.02	0.10
Na ₂ WO ₄ ·2H ₂ O	0.02	0.20
CoCl ₂ ·6H ₂ O	0.20	0.20
Na ₂ MoO ₄ ·2H ₂ O	0.20	0.02

The inoculum of each strain (50 mL) was prepared in 250 mL bottles. P11 medium (40 mL) was transferred into 250 mL bottles and sterilized for 30 min at 121 °C. After sterilization, the P11 medium was cooled and then reduced with cysteine sulfide. Active cells (10 mL) of each strain were inoculated into the 40 mL of P11 medium. Then, the bottles were pressurized with H₂:CO₂:CO:N₂ (5:15:20:60) to 142.6 kPa and horizontally incubated at 37 °C for 68 h. The headspace in each bottle was replenished with H₂:CO₂:CO (30:30:40) to 101.3 kPa. Then, the same syngas was fed at 90 h to 142.6 kPa and at 114 h and 138 h to 170.2 kPa. The optical density (OD) of the inoculum was determined at 138 h. The OD for the P7, P14, P20, and P21 strains was measured at 600 nm, and for the P11 strain, it was measured at 660 nm. The culture pH was monitored, and if it dropped below 5, it was adjusted to 5.1 using 10% NH₄OH to minimize acid stress. Each strain inoculum was ready for syngas fermentation after 162 h with an OD of 0.6–0.7.

2.3. Syngas Fermentation Medium Preparation

For testing the five *Clostridium* strains, three fermentation media were used: corn steep liquor (CSL, Sigma-Aldrich, MO, USA), P7, and P11 media. Table 2 summarizes the composition of each medium used in the study. The P7 medium was previously formulated for alcohol production from syngas by strain P7 [7], while the CSL and P11 media were developed for the conversion of syngas to alcohol using strain P11 [9,20]. MES was added to the inoculum and fermentation media to prevent a rapid pH drop caused by acid production, which stresses cell activity. This choice was made due to the use of three new strains (P14, P20, and P21) and their performance in different medium formulations being unknown. In addition, CSL was selected as a cost-effective medium component, which

costs 2% of the industrial price of yeast extract [20]. For the CSL medium, the CSL was initially centrifuged at 13,000 rpm for 10 min to remove the solids, which was about 50% of CSL stock. The liquid portion was prepared to an initial concentration of 20 g/L CSL, which resulted in the best performance as previously reported [20,22]. After the addition of all components to deionized water (DI), the initial pH of the medium was modified to 6 using 5N KOH. The medium was then boiled for 2 min to remove dissolved O₂. Afterward, N₂ was purged through the medium to eliminate dissolved O₂. Further, 40 mL of the purged medium was placed into 250 mL bottles and autoclaved for 30 min at 121 °C. Following sterilization, each bottle containing medium was purged with H₂:CO₂:CO (30:30:40) for 2 min and reduced with cysteine sulfide. Syngas fermentation in triplicate was initiated with an inoculum of 20% (*v/v*). Bottles were fed with H₂:CO₂:CO (30:30:40) to 170.2 kPa and incubated at 125 rpm and 37 °C, with syngas replenished every 24 h for 360 h to ensure substrate gases were not limiting. During fermentation, the culture pH was monitored and adjusted to 5.1 if it fell below 5, using 10% NH₄OH to lessen acid stress on cells.

Table 2. Media composition.

Media	P7	P11	CSL
Concentration	mL/L		
Mineral solution ^a	20	25	25
Trace metal solution ^a	10	10	10
Vitamin solution ^a	10	10	10
Resazurin	1	1	1
Cysteine-sulfide	5	10	10
Others	g/L		
Yeast extract	0.5	0.5	0.0
MES monohydrate ^b	10	10	10
CSL ^b	0	0	20

^a Composition of solutions in Table 1. ^b CSL: corn steep liquor; MES: 4-morpholineethanesulfonic acid.

2.4. Analytical Procedures

2.4.1. Cell Mass

A 1.5 mL of culture sample was taken daily to determine the pH and cell mass concentration. The OD was measured at 660 nm and 600 nm, optimal for *Clostridium* bacteria due to clear cell visibility and compatibility with the redox indicator, oxidized resazurin, which doesn't absorb in this wavelength range. Although there's little practical difference between 600 and 660 nm, measuring at the reported literature wavelengths for strains P7 and P11 would facilitate comparison. To ensure accurate OD measurement, each sample was diluted with DI water so that the OD was below 0.4 (i.e., within the calibration curve linear range) [21]. Calibration equations were developed to estimate the cell mass (X_{cell}) in g/L: P7 ($X_{\text{cell}} = 0.337 \times \text{OD}_{600} - 0.004$), P11 ($X_{\text{cell}} = 0.377 \times \text{OD}_{600} - 0.003$), P14 ($X_{\text{cell}} = 0.359 \times \text{OD}_{600} - 0.001$), P20 ($X_{\text{cell}} = 0.364 \times \text{OD}_{600} - 0.002$) and P21 ($X_{\text{cell}} = 0.343 \times \text{OD}_{600} - 0.002$).

2.4.2. Solvent and Gas Analysis

After measuring the OD of the culture, the liquid samples were centrifuged (Microfuge 20R, Beckman Coulter, Brea, CA, USA) for 10 min at 13,000 rpm to remove the cells before product analysis. A gas-chromatograph (Agilent 6890N, Agilent Technologies, Wilmington, DE, USA) with an FID and DB-FFAP capillary column was used to determine C2 to C6 product titers, following the method described previously [7]. In addition, 100 µL gas samples every 24 h were analyzed on a Supelco PLOT 1010 column (Supelco, Bellefonte, PA, USA) using an Agilent 6890N GC with a TCD as described previously [38].

2.4.3. Statistical Analysis and Product Yields

Tukey's multiple comparisons of means with a 95% confidence were conducted with JMP Pro 16.0 (SAS Institute Inc., Cary, NC, USA). The aim was to identify pairwise statistical variances in various parameters, such as cell mass concentration and yield (g/L and g/mol CO), utilization of H₂, CO, and CO₂ (%), total alcohol and total acid concentrations, and alcohol-to-acid ratios. These comparisons were made between each strain in the same medium and for the same strain among the three different media. The following equations were used to estimate the yields of cell mass, ethanol, butanol, and hexanol from CO and utilization of H₂ and CO. The yield of the specific C2–C6 alcohol was estimated based on the total experimentally measured CO consumed minus the estimated CO consumed to make other C2–C6 alcohols and acids measured in the culture over 360 h, divided by the theoretical yield according to equations 1 to 3. These equations evaluate the efficiency and selectivity of the production of a desired alcohol.

$$\text{Cell mass yield} \left(\frac{\text{g}}{\text{mol}} \right) = \frac{\text{Maximum cell mass} - \text{initial cell mass}}{\text{moles of CO consumed}} \quad (7)$$

$$\% \text{ EtOH yield} = \frac{\frac{\text{Total moles of ethanol produced}}{\text{total moles of CO consumed} - \text{moles of CO consumed for other C2-C6 products}}}{\frac{1 \text{ mol of ethanol produced}}{6 \text{ mol of CO consumed}}} \times 100\% \quad (8)$$

$$\% \text{ BuOH yield} = \frac{\frac{\text{Total moles of butanol produced}}{\text{total moles of CO consumed} - \text{moles of CO consumed for other C2-C6 products}}}{\frac{1 \text{ mol of butanol produced}}{12 \text{ mol of CO consumed}}} \times 100\% \quad (9)$$

$$\% \text{ HeOH yield} = \frac{\frac{\text{Total moles of hexanol produced}}{\text{total moles of CO consumed} - \text{moles of CO consumed for other C2-C6 products}}}{\frac{1 \text{ mol of hexanol produced}}{18 \text{ mol of CO consumed}}} \times 100\% \quad (10)$$

$$\% \text{ H}_2 \text{ utilization} = \frac{\text{Total moles of H}_2 \text{ consumed}}{\text{Total moles of H}_2 \text{ supplied}} \times 100\% \quad (11)$$

$$\% \text{ CO utilization} = \frac{\text{Total moles of CO consumed}}{\text{Total moles of CO supplied}} \times 100\% \quad (12)$$

3. Results and Discussion

3.1. Syngas Fermentation in P7 Medium

Syngas fermentation profiles for the five *Clostridium* strains in the P7 medium are displayed in Figure 1. The culture's initial pH was about 5.7 for all strains (Figure 1A). Strains P7, P11, P14, and P20 exhibited similar pH drop trends, reaching a pH of 4.6 after 72 and 96 h. The pH remained above 5 after 120 h. However, the pH was adjusted to 5.1 using NH₄OH (10%) whenever it dropped below 5. All strains grew on syngas in the P7 medium, with similar growth patterns observed for the P7, P11, and P20 strains. However, strain P21 showed the highest cell mass production (0.5 g/L), while the lowest cell mass concentration was observed for strain P14 (Figure 1B).

All strains exhibited growth-associated acetic acid production. Strain P11 had the highest acetic acid production of 4.7 g/L at 120 h, while strain P21 produced only 2.7 g/L at 196 h (Figure 1C). Ethanol production began after 48 h in P7 medium, with strain P21 showing significantly higher ($p < 0.05$) ethanol titers (8.9 g/L) compared to other strains: 2.6 g/L for strain P11, 3.5 g/L for strain P7, 1.4 g/L for strain P14 and 4.4 g/L for strain P20 (Figure 1D). Strain P7 produced the highest quantity of butyric acid of 0.24 g/L, while strain P11 did not produce C4 products (Figure 1E,F). The highest butanol titer (0.2 g/L) was produced by strain P21, while strains P11 and P14 did not produce butanol in the P7 medium. In comparison with the other strains, strain P21 also exhibited a significantly higher ($p < 0.05$) ethanol yield (91.6%), butanol yield (16.6%), ethanol to the acetic acid ratio (9.4 mmol/mmol), and butanol to butyric acid ratio (1.0 mmol/mmol) in P7 medium (Table 3). In addition, strain P21 produced 9.1 g/L total alcohol in the P7 medium, which

was 2- to 6-fold higher compared to other strains. On the other hand, total acid production in the P7 medium was highest with strain P7, at 3.5 g/L, which was 3 to 39% higher than for the other strains. The cumulative uptake of H₂ and CO for all strains in the P7 medium is illustrated in Figure 1G,H. Strain P21 in the P7 medium demonstrated the highest gas uptake (22 mmol H₂ and 34.5 mmol CO) of all strains. Moreover, strain P21 in the P7 medium converted significantly more ($p < 0.05$) H₂ (42%) and CO (44%) compared to the other strains (Table 3). However, none of the strains formed C₆ products in the P7 medium, possibly due to nutrient limitation in this medium.

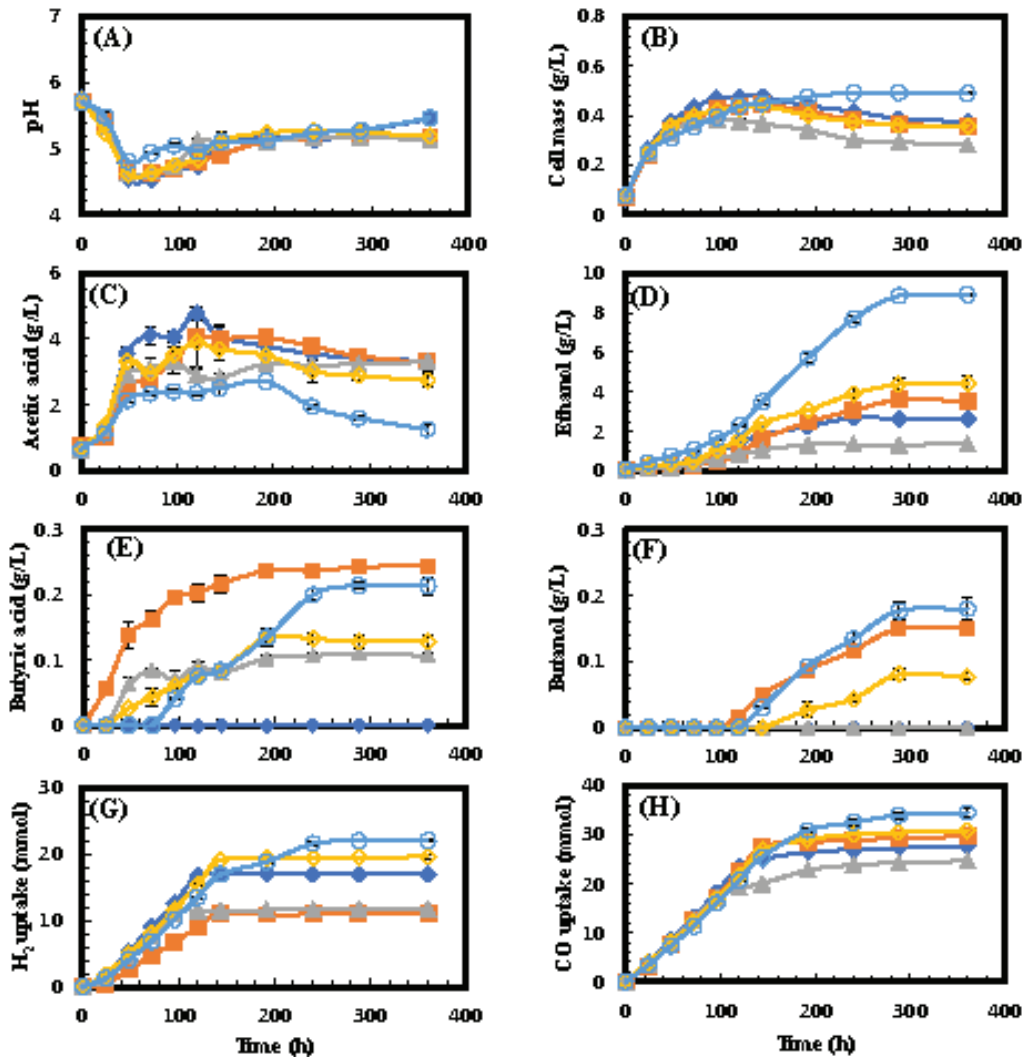


Figure 1. Profiles of syngas fermentation in P7 medium by strains P7 (■), P11 (◆), P14 (▲), P20 (◇), and P21 (○). (A) pH; (B) cell mass; (C) acetic acid; (D) ethanol; (E) butyric acid; (F) butanol; (G) cumulative H₂ uptake; (H) cumulative CO uptake.

Table 3. Syngas fermentation parameters in P7, P11, and CSL media (n = 3).

Fermentation Parameters/Strains	P7	P11	P14	P20	P21
P7 Medium					
Cell mass yield (g/mol) ⁱ	0.9 ± 0.1 A,b	0.8 ± 0.0 B,c	0.7 ± 0.0 E,c	0.7 ± 0.1 C,c	0.7 ± 0.1 D,c
Ethanol yield (%) ⁱⁱ	54.8 ± 2.3 C,c	43.6 ± 0.8 D,c	25.6 ± 0.8 E,c	61.2 ± 6.4 B,c	91.6 ± 7.2 A,b
Butanol yield (%) ⁱⁱ	16.7 ± 2.6 A,c	0.0 ± 0.0 D,b	0.0 ± 0.0 D,c	14.5 ± 3.1 B,c	10.5 ± 1.2 C,c
Hexanol yield (%) ⁱⁱ	0.0 ± 0.0 A,c	0.0 ± 0.0 A,b	0.0 ± 0.0 A,c	0.0 ± 0.0 A,c	0.0 ± 0.0 A,c
EtOH/HAc (mol/mol) ⁱⁱⁱ	1.4 ± 0.1 C,c	1.0 ± 0.0 D,c	0.6 ± 0.0 E,c	2.1 ± 0.3 B,a	9.4 ± 1.5 A,a
BuOH/HBua (mol/mol) ⁱⁱⁱ	0.7 ± 0.1 B,c	0.0 ± 0.0 D,b	0.0 ± 0.0 D,c	0.7 ± 0.1 C,c	1.0 ± 0.1 A,b
HeOH/Hhex (mol/mol) ⁱⁱⁱ	0.0 ± 0.0 A,b	0.0 ± 0.0 A,b	0.0 ± 0.0 A,c	0.0 ± 0.0 A,c	0.0 ± 0.0 A,c
Total alcohols (g/L)	3.7 ± 0.0 C,c	2.7 ± 0.1 D,c	1.4 ± 0.0 E,c	4.5 ± 0.4 B,b	9.1 ± 0.1 A,a
Total acids (g/L)	3.5 ± 0.3 A,c	3.3 ± 0.0 C,c	3.4 ± 0.1 B,b	2.9 ± 0.2 D,c	1.5 ± 0.2 E,c
Sp. alcohol yield (g _{alcol} /g _x)	10.4 ± 0.4 C,c	7.0 ± 0.1 D,c	4.9 ± 0.1 E,c	12.5 ± 1.3 B,a	18.6 ± 0.1 A,a
Sp. acid yield (g _{acid} /g _x)	9.9 ± 0.5 B,c	8.9 ± 0.1 C,b	12.1 ± 0.3 A,b	8.0 ± 0.4 D,c	3.0 ± 0.4 E,c
CO consumption (%)	37.6 ± 1.3 C,c	35.1 ± 0.9 D,c	31.3 ± 0.7 E,c	39.0 ± 0.7 B,c	44.2 ± 1.0 A,b
H ₂ consumption (%)	19.4 ± 1.3 E,c	30.0 ± 1.0 C,c	20.1 ± 0.7 D,c	34.6 ± 1.2 B,a	42.4 ± 0.8 A,a
P11 Medium					
Cell mass yield (g/mol) ⁱ	0.9 ± 0.0 A,b	0.9 ± 0.0 B,b	0.8 ± 0.0 C,b	0.9 ± 0.0 A,B,b	0.9 ± 0.1 A,b
Ethanol yield (%) ⁱⁱ	92.2 ± 1.8 C,b	97.4 ± 0.8 A,a	90.5 ± 1.8 D,a	63.4 ± 1.7 E,b	93.7 ± 1.6 B,a
Butanol yield (%) ⁱⁱ	23.1 ± 0.6 A,b	0.0 ± 0.0 E,b	16.5 ± 0.2 C,a	15.1 ± 1.4 D,b	17.2 ± 0.5 B,b
Hexanol yield (%) ⁱⁱ	8.7 ± 1.0 B,b	0.0 ± 0.0 E,b	5.8 ± 0.1 C,b	2.8 ± 0.2 D,b	11.6 ± 0.4 A,b
EtOH/HAc (mol/mol) ⁱⁱⁱ	1.6 ± 0.0 D,a	3.0 ± 0.1 B,a	3.5 ± 0.1 A,a	1.3 ± 0.0 E,b	2.5 ± 0.0 C,b
BuOH/HBua (mol/mol) ⁱⁱⁱ	2.3 ± 0.0 B,a	0.0 ± 0.0 E,b	2.4 ± 0.1 A,a	1.9 ± 0.2 C,a	0.9 ± 0.0 D,c
HeOH/Hhex (mol/mol) ⁱⁱⁱ	1.1 ± 0.1 B,a	0.0 ± 0.0 D,b	1.7 ± 0.1 A,a	1.1 ± 0.1 B,a	0.8 ± 0.0 C,b
Total alcohols (g/L)	6.1 ± 0.0 C,b	8.1 ± 0.0 A,b	6.8 ± 0.1 B,a	4.4 ± 0.1 D,c	8.1 ± 0.1 A,b
Total acids (g/L)	4.7 ± 0.0 B,b	3.5 ± 0.2 D,b	2.7 ± 0.1 E,c	4.5 ± 0.1 C,b	5.0 ± 0.1 A,b
Sp. alcohol yield (g _{alcol} /g _x)	17.0 ± 0.6 C,a	21.4 ± 0.1 B,a	24.3 ± 0.5 A,a	12.3 ± 0.3 E,a	16.5 ± 0.1 D,b
Sp. acid yield (g _{acid} /g _x)	13.1 ± 0.4 A,a	9.4 ± 0.4 D,b	9.6 ± 0.3 D,c	12.6 ± 0.3 B,a	10.3 ± 0.0 C,b
CO consumption (%)	42.5 ± 0.9 B,a	47.6 ± 0.9 A,b	41.8 ± 0.6 C,a	40.6 ± 0.9 D,b	47.4 ± 0.8 A,a
H ₂ consumption (%)	23.1 ± 1.4 E,b	47.2 ± 1.0 A,a	28.4 ± 0.8 C,a	25.6 ± 1.2 D,b	40.8 ± 1.2 B,b
CSL Medium					
Cell mass yield (g/mol) ⁱ	1.3 ± 0.0 C,a	1.5 ± 0.1 A,a	1.2 ± 0.0 D,a	1.4 ± 0.1 B,a	1.1 ± 0.1 E,a
Ethanol yield (%) ⁱⁱ	98.1 ± 0.9 A,a	96.8 ± 0.7 B,b	85.8 ± 0.8 E,b	89.7 ± 1.4 C,a	86.5 ± 1.0 D,c
Butanol yield (%) ⁱⁱ	25.7 ± 1.1 B,a	17.1 ± 0.9 D,a	15.8 ± 0.3 E,b	18.4 ± 0.3 C,a	30.7 ± 1.4 A,a
Hexanol yield (%) ⁱⁱ	12.3 ± 1.7 B,a	3.7 ± 0.2 E,a	8.2 ± 0.4 C,a	3.9 ± 0.2 D,a	25.6 ± 0.9 A,a
EtOH/HAc (mol/mol) ⁱⁱⁱ	1.5 ± 0.0 A,b	1.3 ± 0.0 C,b	1.0 ± 0.0 E,b	1.3 ± 0.0 B,b	1.20 ± 0.0 D,c
BuOH/HBua (mol/mol) ⁱⁱⁱ	1.5 ± 0.0 B,b	1.2 ± 0.0 C,a	0.6 ± 0.0 E,b	1.6 ± 0.1 A,b	1.1 ± 0.1 D,a
HeOH/Hhex (mol/mol) ⁱⁱⁱ	1.2 ± 0.1 A,a	0.8 ± 0.0 C,a	0.5 ± 0.0 D,b	0.5 ± 0.0 D,b	1.1 ± 0.0 B,a
Total alcohols (g/L)	7.9 ± 0.0 B,a	8.7 ± 0.1 A,a	5.0 ± 0.0 E,b	6.5 ± 0.0 C,a	6.2 ± 0.1 D,c
Total acids (g/L)	7.0 ± 0.1 B,a	9.0 ± 0.2 A,a	6.8 ± 0.0 D,a	6.7 ± 0.1 E,a	6.8 ± 0.1 C,a
Sp. alcohol yield (g _{alcol} /g _x)	14.0 ± 0.3 B,b	14.4 ± 0.2 B,b	13.2 ± 0.1 C,b	11.0 ± 0.1 D,b	16.3 ± 0.8 A,b
Sp. acid yield (g _{acid} /g _x)	12.3 ± 0.4 C,b	14.9 ± 0.4 B,a	17.7 ± 0.2 A,a	11.3 ± 0.2 D,b	17.8 ± 0.9 A,a
CO consumption (%)	41.2 ± 1.0 B,b	48.0 ± 0.9 A,a	36.3 ± 0.6 C,b	42.8 ± 0.8 B,a	35.2 ± 0.8 D,c
H ₂ consumption (%)	32.9 ± 1.0 C,a	45.6 ± 0.9 A,b	22.0 ± 1.0 E,b	34.8 ± 0.8 B,a	25.3 ± 1.1 D,c

No significant differences ($p > 0.05$) between strains in the same medium share the same capital letter in each row, while no significant differences ($p > 0.05$) for the same strain between three media are indicated by the same small letter in each row. ⁱ Estimated at highest cell mass concentration. For P7 medium → strains P11 and P7 at 120 h, strains P14, P20 at 144 h, strain P21 at 196 h. For P11 medium → all strains at 120 h. For CSL medium → strains P11, P7, P20 and P21 at 96 h, strain P14 at 120 h. ⁱⁱ CO consumed and calculated over 360 h. ⁱⁱⁱ EtOH/HAc (ethanol/acetic acid); BuOH/HBua (butanol/butyric acid); HeOH/Hhex (hexanol/hexanoic acid).

3.2. Syngas Fermentation in P11 Medium

All strains grew on syngas in the P11 medium and produced C2–C6 products except strain P11, which produced only C2 products (Figure 2). P11 medium contains higher levels of vitamins, Zn, Ni, Se, and W in comparison with P7 medium (Table 1). The initial pH of the cultures was 5.8 (Figure 2A). The pH changes in the P11 medium for all strains

were nearly identical. When the pH in the P11 medium with all strains was below 5, it was adjusted back to 5.1 using NH_4OH (10%). The growth patterns observed in the P7 medium (Figure 1B) and the P11 medium (Figure 2B) were similar, with more growth observed in the P11 medium (Table 3). The highest cell mass in the P11 medium was achieved by strains P11 and P21.

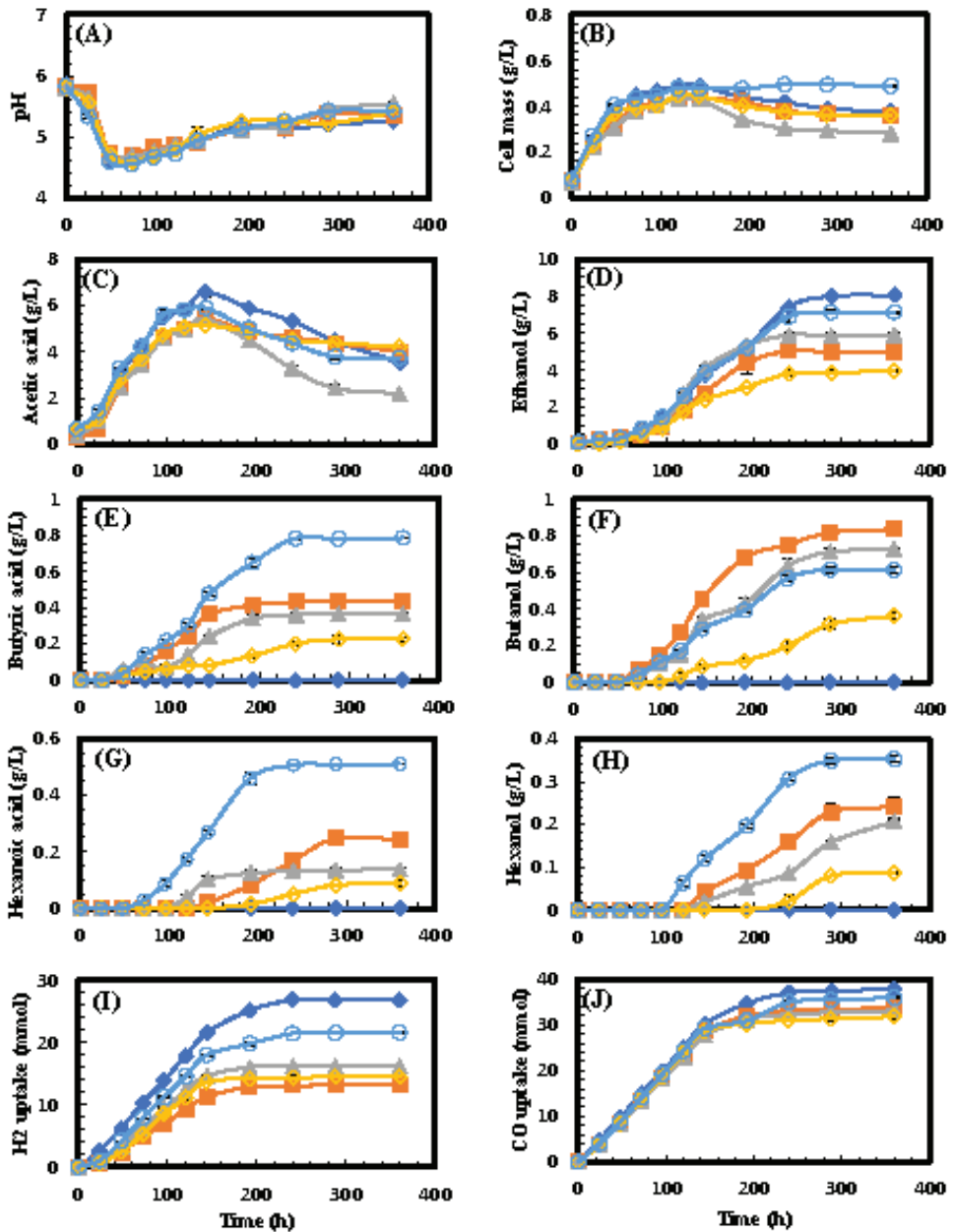


Figure 2. Profiles of syngas fermentation in P11 medium by strains P7 [■], P11 [◆], P14 [▲], P20 [◇], and P21 [○]. (A) pH; (B) cell mass; (C) acetic acid; (D) ethanol; (E) butyric acid; (F) butanol; (G) hexanoic acid; (H) hexanol; (I) cumulative H_2 uptake; (J) cumulative CO uptake.

Strain P11 demonstrated a peak acetic acid concentration (6.6 g/L) at 144 h in the P11 medium, significantly ($p < 0.05$) more than with other strains (Figure 2C). After 144 h, all strains exhibited a gradual decrease in acetic acid concentration, likely due to its conversion into ethanol. Strain P11 also exhibited the highest ethanol production (8.0 g/L) in the P11 medium, which was 1.2- to 2-fold more ($p < 0.05$) than that of the other strains (Figure 2D). Table 3 further shows that strain P11 had a higher ($p < 0.05$) ethanol yield at about 97%, with an ethanol to acetic acid ratio of 3.0 mmol/mmol compared to the other strains. Strain P11 only produced C2 compounds in the P11 medium, whereas the other four strains produced C2–C6 products. Among these strains, strain P7 exhibited the highest butanol production (Figure 2F). However, strain P21 had the highest concentrations of butyric acid (0.8 g/L), hexanoic acid (0.5 g/L), and hexanol (0.4 g/L) in the P11 medium. Strain P20 produced the lowest amounts of C4 and C6 compounds (Figure 2E–H).

Strains P11 and P21 produced similar amounts of total alcohol ($p > 0.05$) in P11 medium (Table 3). However, strain P11 produced only ethanol, while strain P21 produced ethanol, butanol and hexanol. Furthermore, strain P21 in the P11 medium exhibited significantly more ($p < 0.05$) total acid formation than with other strains. In terms of gas uptake, strain P11 had higher ($p < 0.05$) cumulative H₂ uptake (26.7 mmol) than other strains in the P11 medium, while strain P7 had the lowest H₂ uptake (13.1 mmol), as shown in Figure 2I. Similarly, strain P11 had the highest CO uptake (37.7 mmol), while strain P20 had the lowest CO uptake (31.7 mmol) (Figure 2J). Additionally, strain P11 in the P11 medium showed higher ($p < 0.05$) CO and H₂ conversion efficiencies in comparison to other strains (Table 3).

3.3. Syngas Fermentation in CSL Medium

Figure 3 shows the fermentation profiles during syngas consumption in a CSL medium. The initial pH in the CSL medium for all strains was 5.8 (Figure 3A). The pH remained relatively stable until 24 h, after which strains P11, P20, and P7 exhibited a rapid decrease in pH from 5.7 to 4.6 between 48 and 96 h. Except for strain P21, the pH of the cultures with the other strains dropped below pH 5 between 48 and 144 h and was subsequently adjusted to 5.1 using 10% NH₄OH. The profiles of cell mass concentration for strains P11, P7, and P20 in the CSL medium were similar (Figure 3B), with higher cell mass measured compared to strains P14 and P21 (Table 3).

Unlike P7 or P11 media (Figures 1 and 2), all strains formed C2–C6 acids and alcohols in the CSL medium (Figure 3C–H). Strain P11 in the CSL medium produced more ($p < 0.05$) acetic acid (8.6 g/L) than other strains (Figure 3C). Furthermore, strain P11 produced significantly more ($p < 0.05$) ethanol (8.1 g/L) than strain P7 (7.0 g/L), strain P14, P21 (4.6 g/L), and strain P20 (6.1 g/L). Ethanol yields (>95%) were the highest for strains P7 and P11 in the CSL medium (Table 3).

Among the tested strains, P21 produced more ($p < 0.05$) butanol (0.9 g/L), butyric acid (1.0 g/L), hexanol (0.7 g/L), and hexanoic acid (0.7 g/L), indicating its superior production ability of C4–C6 products. Conversely, strain P11, known for its ethanol production, produced butanol (0.5 g/L) and hexanol (0.1 g/L) in the CSL medium. Previous reports have highlighted strain P11's potential to produce C4 and C6 alcohols using CSL as a medium [20]. Additionally, strain P11 exhibited higher H₂ and CO uptakes (25.8 mmol and 38.15 mmol, respectively) ($p < 0.05$) in the CSL medium (Figure 3I,J), along with H₂ and CO conversion efficiencies of 46% and 48%, respectively, surpassing the other strains (Table 3). The 20 g/L CSL medium initially contained 4.3 g/L of sugar. In the first 72 h, 85% of the sugars were consumed by all strains, with minimal consumption observed in subsequent measurements (data not presented). Assuming 85% sugar utilization for ethanol production, the strains can yield a maximum of 1.8 g/L, representing about 12% of the total products generated. This emphasizes that syngas resulted in most product formation. Furthermore, distinguishing the extent to which growth and products originate from the consumption of sugars or syngas is challenging. The availability of amino acids

and other essential nutrients in CSL, including some sugars, further enhanced *Clostridium* strains' ability to form higher alcohols [19,20,24].

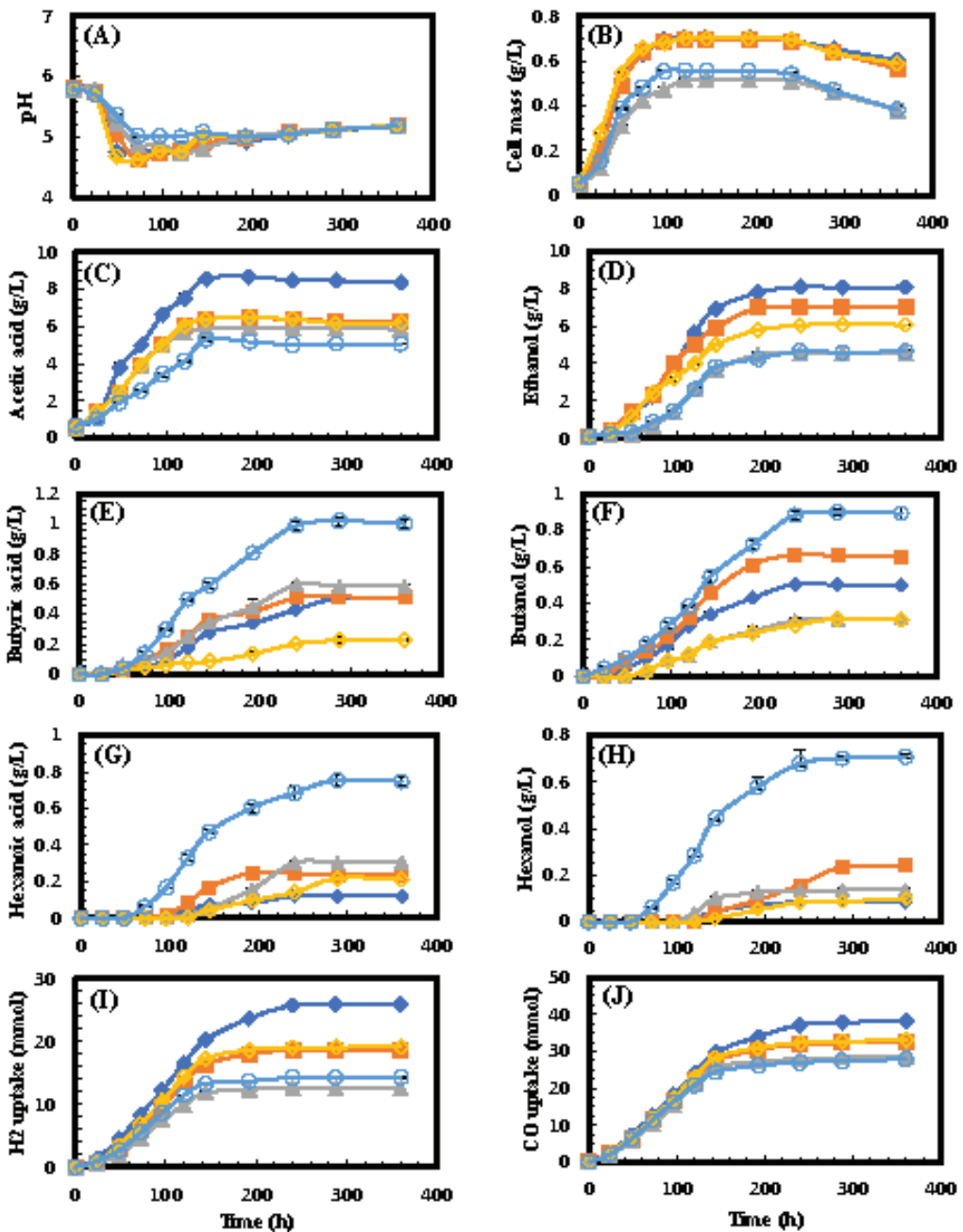


Figure 3. Profiles of syngas fermentation in CSL medium by strains P7 [■], P11 [◆], P14 [▲], P20 [◇], and P21 [○]. (A) pH; (B) cell mass; (C) acetic acid; (D) ethanol; (E) butyric acid; (F) butanol; (G) hexanoic acid; (H) hexanol; (I) cumulative H₂ uptake; (J) cumulative CO uptake.

All strains successfully converted syngas into C2, C4, and C6 alcohols and acids using mainly P11 and CSL media. However, the concentrations of these compounds varied among the strains and type of medium. CSL medium provided the highest growth potential for all strains (Table 3). P11 medium exhibited the second highest growth, while P7 medium supported the least growth among the tested strains. Strain P11 exhibited robust ethanol production, especially in P11 and CSL media, with ethanol yield above 95% (Table 3). However, ethanol concentration with strain P11 in the P7 medium was significantly lower ($p < 0.05$), about 3-fold lower than in P11 or CSL media, likely due to the lack of certain vitamins and other nutrients.

P7 medium contained lower concentrations of Se (5X), W (10X), Ni (10X), and Zn (5X) compared to P11 medium [19]. For example, the increase in Se, W, Ni, and Zn concentration in the P11 medium was reported to increase ethanol production by strain P11 by 2- to 5-fold compared to a base medium [19]. Details on the effect of these elements on the growth and solvent production of acetogens, like strains P7 and P11, were reported previously [7,20]. As shown in Table 3, all strains except strain P21 exhibited higher total alcohol formation in the CSL medium than in either the P7 or P11 medium. However, ethanol remained the dominant alcohol produced by all strains in all three media. P11 and CSL media, with more nutrients, facilitated higher butanol and hexanol production compared to the P7 medium [19,20]. Strain P21 demonstrated specific total alcohol yields from 16 to 19 g/g dry cell weight, surpassing other strains, especially in P7 and CSL media (Table 3). Strain P21 demonstrated the highest specific total acid yield (17.8 g/g dry cell) in the CSL medium. Strain P14 in the P11 medium showed the highest specific total alcohol yield (24.3 g/g dry cells), followed by strain P11. Strain P20 exhibited a specific total alcohol yield of 11–13 g/g dry cells, performing similarly in all media. All strains except P14 and P21 produced total alcohols in the CSL medium, with generally lower alcohol production in the P7 medium. In both CSL and P11 media, all strains achieved 2- to 4.5-fold greater specific total alcohol production than previously reported for strain P11 [20]. Additionally, the specific total alcohol yields of the five strains in the present study were 1- to 4-fold higher than reported previously in the P7 medium [8]. Total acids made by all strains were consistently higher in the CSL medium (Table 3). While strain P11 in the CSL medium yielded the highest total acid concentration, the maximum specific total acid production (17.8 g acid/g dry mass) was measured in the CSL medium with strains P14 and P21 (Table 3).

There was a net CO₂ production during syngas fermentation by all strains in the three media (Figure 4). CO₂ was formed from CO and H₂ utilization, where CO is used as a carbon and energy source. Acetogens prefer utilizing CO and H₂ over CO₂ and H₂ due to thermodynamic favorability [3]. Their gas preference is influenced by their metabolic capabilities, environmental conditions such as gas partial pressure and pH, and the presence of specific enzymes for gas utilization [3,39]. The lower H₂ consumption compared to CO (Figure 1G,H, Figure 2I,J and Figure 3I,J) can be due to hydrogenase inhibition by CO and the thermodynamic disadvantage of H₂ utilization with the presence of CO [39]. The CO₂ production profiles in Figure 4 align with the observed CO uptake profiles for all strains in the three media.

Figure 5 shows the maximum product titers and cumulative gas uptake. Strain P11 in P11 and CSL media demonstrated the highest ethanol production, which was 3-fold more than in the P7 medium. The top butanol producers were strains P7 and P21, each producing about 0.9 g/L butanol. In the P11 medium, strain P7 produced 6-fold more butanol than in the P7 medium and 1.3-fold more than in the CSL medium. The highest butanol titers were formed by strain P21 in the CSL medium. Moreover, strain P21 produced the highest amounts of butyric acid, hexanol, and hexanoic acid in the CSL medium (Figure 5). None of the strains produced C6 products in the P7 medium. Strains P14 and P20 produced C2–C6 alcohols in P11 and CSL media. Strain P14 produced 1.3-fold more ethanol, 2-fold more butanol, and 1.5-fold more hexanol in the P11 medium than in the CSL medium (Figure 5). Strain P20 in the CSL medium produced 1.4-fold more ethanol than in the P11 medium. However, butanol and hexanol production by strain P20 were almost identical in P11 and

CSL media. Strain P11 uptake of CO and H₂ was higher ($p < 0.05$) in P11 and CSL media than in P7 medium (Figure 5). Strain P21 demonstrated similar gas uptake in P7 and P11 media, which were slightly higher than in the CSL medium.

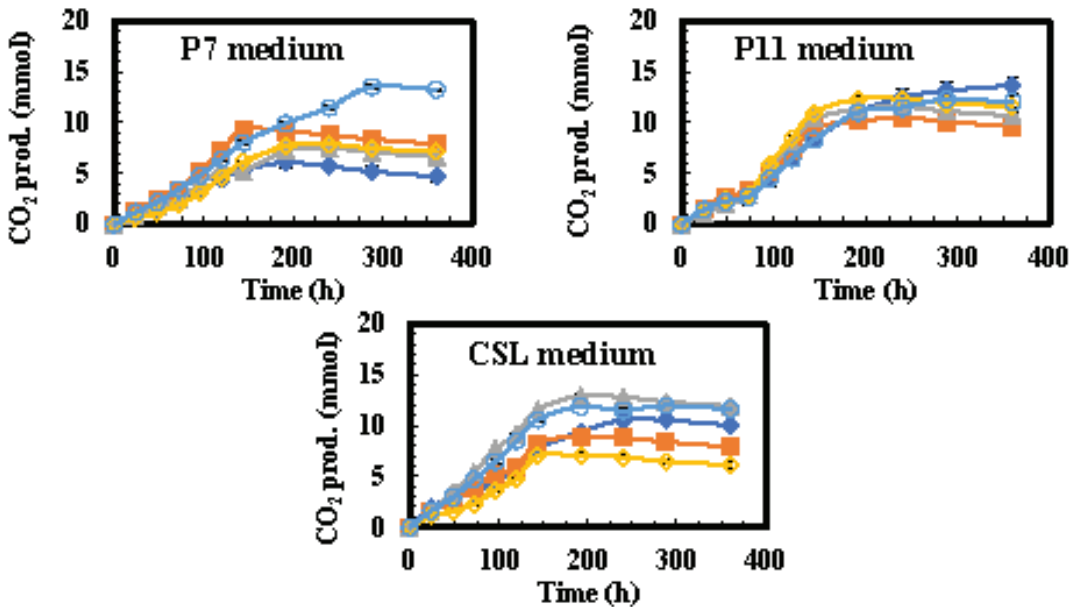


Figure 4. Profiles of cumulative CO₂ formation during syngas fermentation in P7, P11, and CSL media by strains P7 [■], P11 [◆], P14 [▲], P20 [◇], and P21 [○].

Strain P11 is known as one of the best ethanol producers in gas fermentations, achieving high yield in various media: 9.6 g/L ethanol in CSL medium in a 3-L CSTR [20], 13 g/L ethanol in P11 medium with biochar [26] and 20 g/L ethanol in P11 medium supplemented with activated carbon [6]. Ethanol production in the bottles by strain P11 (8.1 g/L) in the present study was 1.7- to 4-fold higher than previously reported [9,20]. In addition, ethanol production by strain P11 in the bottles in the present study was 6-fold and 3.5-fold higher than produced by *Alkalibaculum bacchi* strain CP15 in yeast extract and CSL media [40] and 1.5-fold higher than by strain P11 in a trickle bed reactor with yeast extract medium [41]. Similar to the findings in the present study, the CSL medium enabled strain P11 to produce 0.5 g/L butanol and 0.1 g/L hexanol from syngas [20].

Similarly, strain P7 is known for its ability to produce butanol from syngas, in addition to ethanol. In P11 and CSL media, strain P7 achieved higher ethanol titers (5 g/L and 7 g/L, respectively) than in P7 medium. In this study, ethanol formed by strain P7 in P11 and CSL media was 1.5- to 2-fold higher than the previous reports in the P7 medium [7] and in the P7 medium supplemented with biochar [8,9]. Additionally, strain P7 showed a remarkable 9-fold increase in butanol production compared to *A. bacchi* CP15 in CSL medium [40] and a 1.4-fold increase compared to P7 medium supplemented with biochar [9]. The butanol titer (0.9 g/L) formed by strain P7 in the P7 medium in the present study was consistent with a previous report [7].

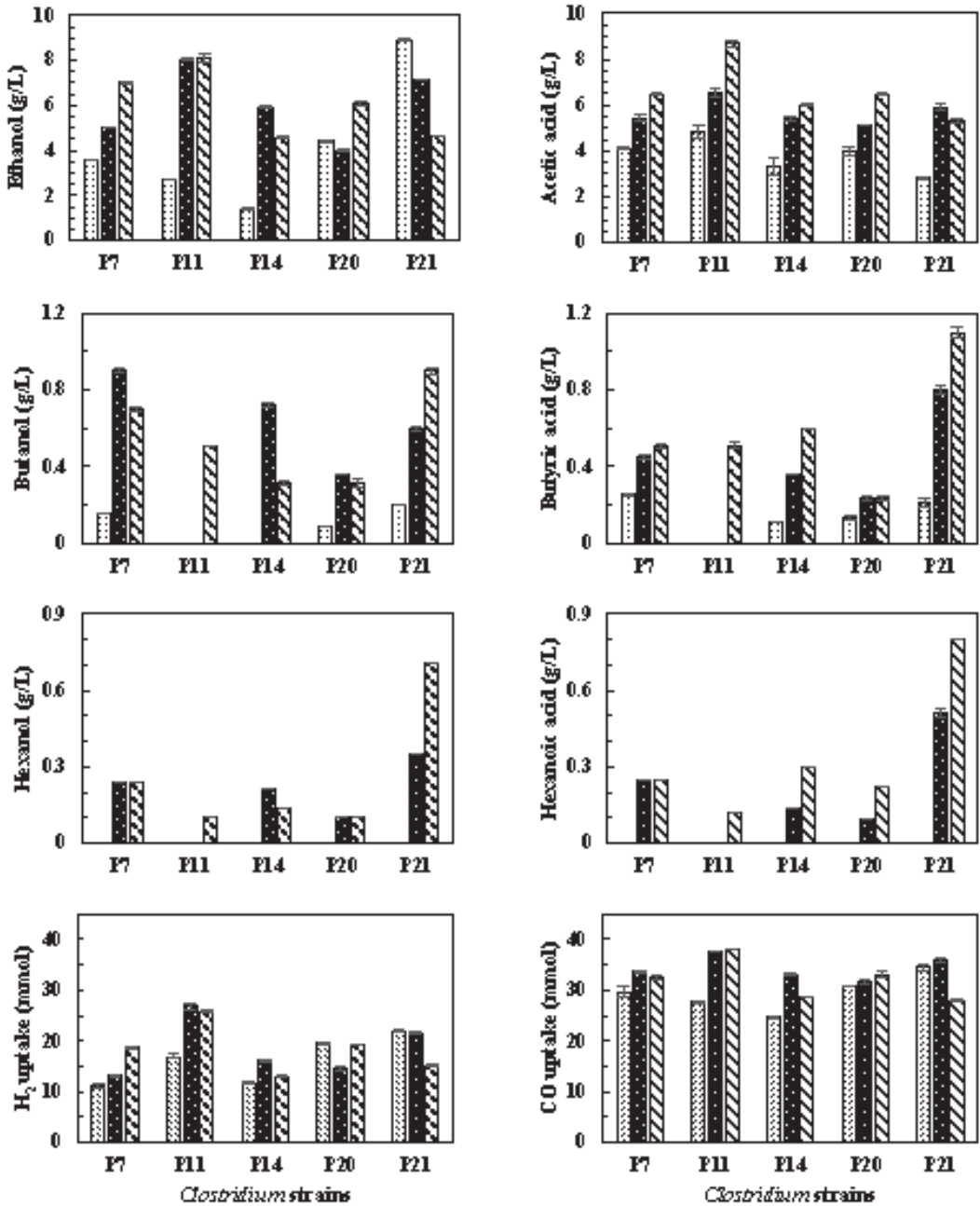


Figure 5. Maximum product concentrations and cumulative gas uptake during syngas fermentation in P7 medium (▨), P11 medium (■), and CSL medium (▧).

The new *C. ljungdahlii* P14 and *C. carboxidivorans* P20 strains showed abilities to make C2–C6 products (Figure 5). While both strains produced similar amounts of C2 products in each medium, strain P14 produced more C4 and C6 products than strain P20. The maximum ethanol synthesized by strain P14 (6 g/L) in the P11 medium in this study was

comparable to strain P11 reported by [41], 3-fold more than strain P7 in the P7 medium [23] and 6-fold higher than *C. autoethanogenum* in the modified mineral medium reported by [42]. Further, strain P14's highest butanol titer (0.7 g/L) in the P11 medium was 1.1-fold more than strain P7 in a P7 medium supplemented by biochar [9], 1.4-fold higher than genetically modified strain P7 [23] and 4- to 6-fold higher than genetically modified *C. ljungdahlii* in complex yeast extract, tryptone, fructose medium [43]. With further development, the new *C. ljungdahlii* strain P14 can potentially compete with strains P7, P11, and genetically modified *C. ljungdahlii* strains in producing C2 and C4 products from syngas. This is achieved through medium modification, biochar supplementation, and genetic engineering to increase selectivity for specific alcohols and improve titer.

C. carboxidivorans P20 produced 2- to 3-fold more ethanol from syngas than previous studies with strain P11 in CSL medium [20] and cotton seed extract medium [44]. However, strain P20 butanol and hexanol production abilities were 2- to 3-fold and 2.4- to 7-fold lower, respectively, compared to strains P7, P14 and P21 (Figure 5). Additional improvements, such as adding sugars and biochar to the medium or increasing headspace pressure, could enhance strain P20's ability to produce C4 and C6 alcohols. *C. muellerianum* P21 showed great promise for the production of C4 and C6 alcohols. In the CSL medium, it achieved the highest butanol (0.9 g/L) and hexanol (0.7 g/L) titers from syngas. Moreover, strain P21 produced 1.4-fold more butanol from syngas than strain P7 in a P7 medium supplemented with biochar [9]. Strain P21 also produced similar amounts of hexanol from syngas reported in a previous study using strain P7 with temperature variance [45]. However, strain P21 showed slightly lower hexanol production from syngas compared to strain P7 in previous studies, particularly those utilizing extractive syngas fermentation [32,46–48].

In contrast to CO₂ fermentation in P7, P11, and CSL media using a gas mixture (H₂:CO₂:N₂ 60:20:20) [36], the five strains in the present study produced 2-fold more ethanol and comparable amounts of butanol and hexanol from syngas. Furthermore, the CSL medium yielded the highest total alcohol and acid titers with syngas in the current study and previously reported CO₂ fermentation [36].

The results highlighted the influence of medium composition on *Clostridium* strains' growth and syngas fermentation capabilities, especially for making higher-chain fatty acids and alcohols via the acetyl-CoA pathway. The new P14, P20, and P21 strains demonstrated the potential to produce C4 and C6 alcohols. Differences in vitamin and nutrient content in the P7 medium might have limited C6 product formation (Table 1). P11 medium, with more vitamins and specific trace metals, enhanced C₂, C₄, and C₆ product titers, particularly with the new strains. Utilizing CSL as a nutrient-rich source instead of yeast extract improved cell mass and alcohol titers while reducing cost. Further development, medium formulation improvements, and characterization of the new strains, especially P21, are needed to enhance the strain's activity and selectivity in converting syngas into C4 and C6 alcohols.

4. Conclusions

Clostridium muellerianum P21 was the best butanol and hexanol producer from syngas, particularly in CSL medium, while *C. ragsdalei* P11 showed the highest ethanol production. *C. carboxidivorans* P7, *C. ljungdahlii* P14, *C. carboxidivorans* P20, and *C. muellerianum* P21 demonstrated potential in generating C4 and C6 products in P11 and CSL media. CSL medium supported higher cell mass, alcohol titers, and gas conversion compared to the P7 medium. The highest ethanol (8.0 g/L) was produced by strain P11 in P11 and CSL media, which was 3-fold more than in P7 medium. Strain P21 achieved ethanol, butanol, and hexanol yields of 87%, 31%, and 26%, respectively, in the CSL medium. These results confirm the viability of the novel strains, particularly strain P21, and the efficacy of CSL medium for C4 and C6 alcohol synthesis from syngas.

Author Contributions: R.T.: Formal analysis, Investigation, Conceptualization, Writing—original draft preparation, Methodology, Writing—review and editing, Data curation. R.L.H.: Resources, Writing—review and editing. R.S.T.: Resources, Methodology, Writing—review and editing. H.K.A.: Funding acquisition, Project administration, Resources, Conceptualization, Supervision, Methodology, Writing—review and editing, Data curation, Formal analysis. All authors have read and agreed to the published version of the manuscript.

Funding: This study received support from the National Institute of Food and Agriculture, U.S. Department of Agriculture, under award number 2019-38502-30120 through the South Central Sun Grant Program and USDA–NIFA Project No. OKL03163 and Oklahoma Agricultural Experiment Station.

Data Availability Statement: Data are contained within the article.

Conflicts of Interest: The authors declare no conflict of interest.

References

1. Fernández-Naveira, Á.; Veiga, M.C.; Kennes, C. Selective anaerobic fermentation of syngas into either C2–C6 organic acids or ethanol and higher alcohols. *Bioresour. Technol.* **2019**, *280*, 387–395. [CrossRef] [PubMed]
2. Oh, H.J.; Gong, G.; Ahn, J.H.; Ko, J.K.; Lee, S.M.; Um, Y. Effective hexanol production from carbon monoxide using extractive fermentation with *Clostridium carboxidivorans* P7. *Bioresour. Technol.* **2023**, *367*, 128201. [CrossRef] [PubMed]
3. Phillips, J.; Huhnke, R.; Atiyeh, H. Syngas fermentation: A microbial conversion process of gaseous substrates to various products. *Fermentation* **2017**, *3*, 28. [CrossRef]
4. EIA. Available online: <https://www.eia.gov/todayinenergy/detail.php?id=53539> (accessed on 5 May 2023).
5. Brandt, C.C.; Davis, M.R.; Davison, B.; Eaton, L.M.; Efroymson, R.A.; Hilliard, M.R.; Kline, K.; Langholtz, M.H.; Myers, A.; Sokhansanj, S.; et al. *Billion-Ton Report: Advancing Domestic Resources for a Thriving Bioeconomy, Volume 1: Economic Availability of Feedstocks*; Oak Ridge National Lab.: Oak Ridge, TN, USA, 2016.
6. Atiyeh, H.K.; Lewis, R.S.; Phillips, J.R.; Huhnke, R.L. Method Improving Producer Gas Fermentation. U.S. Patents 10053711, 21 August 2018.
7. Phillips, J.R.; Atiyeh, H.K.; Tanner, R.S.; Torres, J.R.; Saxena, J.; Wilkins, M.R.; Huhnke, R.L. Butanol and hexanol production in *Clostridium carboxidivorans* syngas fermentation: Medium development and culture techniques. *Bioresour. Technol.* **2015**, *190*, 114–121. [CrossRef] [PubMed]
8. Sun, X.; Atiyeh, H.K.; Kumar, A.; Zhang, H.; Tanner, R.S. Biochar enhanced ethanol and butanol production by *Clostridium carboxidivorans* from syngas. *Bioresour. Technol.* **2018**, *265*, 128–138. [CrossRef] [PubMed]
9. Sun, X.; Thunuguntla, R.; Zhang, H.; Atiyeh, H. Biochar amended microbial conversion of C1 gases to ethanol and butanol: Effects of biochar feedstock type and processing temperature. *Bioresour. Technol.* **2022**, *360*, 127573. [CrossRef]
10. De Jong, S.; Antonissen, K.; Hoefnagels, R.; Lonza, L.; Wang, M.; Faaij, A.; Junginger, M. Life-cycle analysis of greenhouse gas emissions from renewable jet fuel production. *Biotechnol. Biofuel.* **2017**, *10*, 64. [CrossRef]
11. Pimentel, D. Ethanol fuels: Energy balance, economics, and environmental impacts are negative. *Nat. Resour. Res.* **2003**, *12*, 127–134. [CrossRef]
12. Subramaniam, Y.; Masron, T.A.; Azman, N.H.N. The impact of biofuels on food security. *Int. Econ.* **2019**, *160*, 72–83. [CrossRef]
13. Sun, X.; Atiyeh, H.K.; Huhnke, R.L.; Tanner, R.S. Syngas fermentation process development for production of biofuels and chemicals: A review. *Bioresour. Technol. Rep.* **2019**, *7*, 100279. [CrossRef]
14. Wu, C.; Lo, J.; Urban, C.; Gao, X.; Yang, B.; Humphreys, J.; Shinde, S.; Wang, X.; Chou, K.J.; Maness, P.; et al. Acetyl-CoA synthesis through a bicyclic carbon-fixing pathway in gas-fermenting bacteria. *Nat. Synth.* **2022**, *1*, 615–625. [CrossRef]
15. Han, Y.-F.; Xie, B.T.; Wu, G.X.; Guo, Y.Q.; Li, D.M.; Huang, Z.Y. Combination of trace metal to improve solventogenesis of *Clostridium carboxidivorans* P7 in syngas fermentation. *Front Microbiol.* **2020**, *11*, 577266. [CrossRef] [PubMed]
16. Zhu, C.; Fang, B. Application of a two-stage temperature control strategy to enhance 1, 3-propanediol productivity by *Clostridium butyricum*. *J. Chem. Technol. Biotechnol.* **2013**, *88*, 853–857. [CrossRef]
17. Bengelsdorf, F.R.; Beck, M.H.; Erz, C.; Hoffmeister, S.; Karl, M.M.; Riegler, P.; Wirth, S.; Poehlein, A.; Weuster-Botz, D.; Dürre, P. Bacterial anaerobic synthesis gas (syngas) and CO₂+ H₂ fermentation. *Adv. Appl. Microbiol.* **2018**, *103*, 143–221. [PubMed]
18. Köpke, M.; Mihalcea, C.; Liew, F.; Tizard, J.H.; Ali, M.S.; Conolly, J.J.; Al-Sinawi, B.; Simpson, S.D. 2,3-Butanediol production by acetogenic bacteria, an alternative route to chemical synthesis, using industrial waste gas. *Appl. Environ. Microbiol.* **2011**, *77*, 5467–5475. [CrossRef] [PubMed]
19. Saxena, J.; Tanner, R.S. Effect of trace metals on ethanol production from synthesis gas by the ethanologenic acetogen, *Clostridium ragsdalei*. *J. Ind. Microbiol. Biotechnol.* **2011**, *38*, 513–521. [CrossRef] [PubMed]
20. Maddipati, P.; Atiyeh, H.K.; Bellmer, D.D.; Huhnke, R.L. Ethanol production from syngas by *Clostridium* strain P11 using corn steep liquor as a nutrient replacement to yeast extract. *Bioresour. Technol.* **2011**, *102*, 6494–6501. [CrossRef]

21. Panneerselvam, A. Effect of Glucose and Reducing Agents on Syngas Fermentation by Clostridia Species P11. Master's Thesis, Department of Biosystems and Agricultural Engineering, Oklahoma State University, Stillwater, OK, USA, 2009; p. 82.
22. Ramachandriya, K.D.; Kundiyana, D.K.; Wilkins, M.R.; Terrill, J.B.; Atiyeh, H.K.; Huhnke, R.L. Carbon dioxide conversion to fuels and chemicals using a hybrid green process. *Appl. Energy*. **2013**, *112*, 289–299. [CrossRef]
23. Ukpong, M.N.; Atiyeh, H.K.; De Lorme, M.J.; Liu, K.; Zhu, X.; Tanner, R.S.; Wilkins, M.R.; Stevenson, B.S. Physiological response of *Clostridium carboxidivorans* during conversion of synthesis gas to solvents in a gas-fed bioreactor. *Biotechnol. Bioeng.* **2012**, *109*, 2720–2728. [CrossRef]
24. Kundiyana, D.K.; Huhnke, R.L.; Wilkins, M.R. Effect of nutrient limitation and two-stage continuous fermentor design on productivities during “*Clostridium ragsdalei*” syngas fermentation. *Bioresour. Technol.* **2011**, *102*, 6058–6064. [CrossRef]
25. Orgill, J.J.; Atiyeh, H.K.; Devarapalli, M.; Phillips, J.R.; Lewis, R.S.; Huhnke, R.L. A comparison of mass transfer coefficients between trickle-bed, hollow fiber membrane and stirred tank reactors. *Bioresour. Technol.* **2013**, *133*, 340–346. [CrossRef] [PubMed]
26. Sun, X.; Atiyeh, H.K.; Zhang, H.; Tanner, R.S.; Huhnke, R.L. Enhanced ethanol production from syngas by *Clostridium ragsdalei* in continuous stirred tank reactor using medium with poultry litter biochar. *Appl. Energy* **2019**, *236*, 1269–1279. [CrossRef]
27. Karlson, B.; Bellavitis, C.; France, N. Commercializing LanzaTech, from waste to fuel: An effectuation case. *J. Manag. Organ.* **2021**, *27*, 175–196. [CrossRef]
28. Köpke, M.; Mihalcea, C.; Bromley, J.C.; Simpson, S.D. Fermentative production of ethanol from carbon monoxide. *Curr. Opin. Biotechnol.* **2011**, *22*, 320–325. [CrossRef] [PubMed]
29. LanzaTech. The LanzaTech Process. 2015. Available online: <https://www.lanzajet.com/what-we-do> (accessed on 3 March 2023).
30. Kottenhahn, P.; Philipps, G.; Jennewein, S. Hexanol biosynthesis from syngas by *Clostridium carboxidivorans* P7—product toxicity, temperature dependence and in situ extraction. *Heliyon* **2021**, *7*, e07732. [CrossRef] [PubMed]
31. Lauer, I.; Philipps, G.; Jennewein, S. *Syngas Fermentation: Toxicity Analysis of Potential Products on Clostridium ljungdahlii*; Clostridium XV: 18-19.09; TU Munich: Freising, Germany, 2018.
32. Shen, S.; Gu, Y.; Chai, C.; Jiang, W.; Zhuang, Y.; Wang, Y. Enhanced alcohol titre and ratio in carbon monoxide-rich off-gas fermentation of *Clostridium carboxidivorans* through combination of trace metals optimization with variable-temperature cultivation. *Bioresour. Technol.* **2017**, *239*, 236–243. [CrossRef] [PubMed]
33. Huhnke, R.L.; Lewis, R.S.; Tanner, R.S. Isolation and Characterization of Novel Clostridial Species. U.S. Patent 7,704,723, 27 April 2010.
34. Liou, J.S.; Balkwill, D.L.; Drake, G.R.; Tanner, R.S. *Clostridium carboxidivorans* sp. nov., a solvent-producing clostridium isolated from an agricultural settling lagoon, and reclassification of the acetogen *Clostridium scatologenes* strain SL1 as *Clostridium drakei* sp. nov. *Int. J. Syst. Evol. Microbiol.* **2005**, *55*, 2085–2091. [CrossRef]
35. Doyle, D.A.; Smith, P.R.; Lawson, P.A.; Tanner, R.S. *Clostridium muellerianum* sp. nov., a carbon monoxide-oxidizing acetogen isolated from old hay. *Int. J. Syst. Evol. Microbiol.* **2022**, *72*, 005297. [CrossRef]
36. Thunuguntla, R.; Atiyeh, H.K.; Huhnke, R.L.; Tanner, R.S. CO₂-based production of C2-C6 acids and alcohols: The potential of novel Clostridia. *Bioresour. Technol. Rep.* **2023**, *25*, 101713. [CrossRef]
37. Tanner, R.S. Cultivation of bacteria and fungi. In *Manual of Environmental Microbiology*, 3rd ed.; Hurst, C.J., Crawford, R.L., Mills, A.L., Garland, J.L., Stetzenbach, L.D., Lipson, D.A., Eds.; ASM Press: Washington, DC, USA, 2007; pp. 69–78.
38. Liu, K.; Atiyeh, H.K.; Stevenson, B.S.; Tanner, R.S.; Wilkins, M.R.; Huhnke, R.L. Continuous syngas fermentation for the production of ethanol, n-propanol and n-butanol. *Bioresour. Technol.* **2014**, *151*, 69–77. [CrossRef]
39. Hu, P.; Bowen, S.H.; Lewis, R.S. A thermodynamic analysis of electron production during syngas fermentation. *Bioresour. Technol.* **2011**, *102*, 8071–8076. [CrossRef] [PubMed]
40. Liu, K.; Atiyeh, H.K.; Stevenson, B.S.; Tanner, R.S.; Wilkins, M.R.; Huhnke, R.L. Mixed culture syngas fermentation and conversion of carboxylic acids into alcohols. *Bioresour. Technol.* **2014**, *152*, 337–346. [CrossRef]
41. Devarapalli, M.; Atiyeh, H.K.; Phillips, J.R.; Lewis, R.S.; Huhnke, R.L. Ethanol production during semi-continuous syngas fermentation in a trickle bed reactor using *Clostridium ragsdalei*. *Bioresour. Technol.* **2016**, *209*, 56–65. [CrossRef] [PubMed]
42. Abubackar, H.N.; Veiga, M.C.; Kennes, C. Carbon monoxide fermentation to ethanol by *Clostridium autoethanogenum* in a bioreactor with no accumulation of acetic acid. *Bioresour. Technol.* **2015**, *186*, 122–127. [CrossRef] [PubMed]
43. Lauer, I.; Philipps, G.; Jennewein, S. Metabolic engineering of *Clostridium ljungdahlii* for the production of hexanol and butanol from CO₂ and H₂. *Microb. Cell Factories* **2022**, *21*, 85. [CrossRef]
44. Kundiyana, D.K.; Huhnke, R.L.; Maddipati, P.; Atiyeh, H.K.; Wilkins, M.R. Feasibility of incorporating cotton seed extract in *Clostridium ragsdalei* fermentation medium during synthesis gas fermentation. *Bioresour. Technol.* **2010**, *101*, 9673–9680. [CrossRef]
45. Shen, S.; Wang, G.; Zhang, M.; Tang, Y.; Gu, Y.; Jiang, W.; Wang, Y.; Zhuang, Y. Effect of temperature and surfactant on biomass growth and higher-alcohol production during syngas fermentation by *Clostridium carboxidivorans* P7. *Bioresour. Bioprocess.* **2020**, *7*, 56. [CrossRef]
46. Ramío-Pujol, S.; Ganigué, R.; Bañeras, L.; Colprim, J. Incubation at 25 C prevents acid crash and enhances alcohol production in *Clostridium carboxidivorans* P7. *Bioresour. Technol.* **2015**, *192*, 296–303. [CrossRef]

47. Oh, H.J.; Ko, J.K.; Gong, G.; Lee, S.M.; Um, Y. Production of hexanol as the main product through syngas fermentation by *Clostridium carboxidivorans* P7. *Front. Bioeng. Biotechnol.* **2022**, *10*, 850370. [CrossRef]
48. Kim, J.; Kim, K.Y.; Ko, J.K.; Lee, S.M.; Gong, G.; Kim, K.H.; Um, Y. Characterization of a Novel Acetogen *Clostridium* sp. JS66 for Production of Acids and Alcohols: Focusing on Hexanoic Acid Production from Syngas. *Biotechnol. Bioprocess. Eng.* **2022**, *27*, 89–98. [CrossRef]

Disclaimer/Publisher’s Note: The statements, opinions and data contained in all publications are solely those of the individual author(s) and contributor(s) and not of MDPI and/or the editor(s). MDPI and/or the editor(s) disclaim responsibility for any injury to people or property resulting from any ideas, methods, instructions or products referred to in the content.

Article

Yeast Lipids from Crude Glycerol Media and Utilization of Lipid Fermentation Wastewater as Maceration Water in Cultures of Edible and Medicinal Mushrooms

Ilias Diamantis ^{1,2}, Seraphim Papanikolaou ^{1,*}, Savvoula Michou ¹, Vassilios Anastasopoulos ¹ and Panagiota Diamantopoulou ^{2,*}

¹ Laboratory of Food Microbiology and Biotechnology, Department of Food Science and Human Nutrition, Agricultural University of Athens, 75 Iera Odos Str., 11855 Athens, Greece; idiamantis@aua.gr (I.D.); chemsevvy@gmail.com (S.M.); vasianas1@aua.gr (V.A.)

² Laboratory of Edible Fungi, Institute of Technology of Agricultural Products, Hellenic Agricultural Organization-Dimitra, 1 Sofokli Venizelou Str., 14123 Lycovryssi, Greece

* Correspondence: spapanik@aua.gr (S.P.); pdiamantopoulou@elgo.gr (P.D.)

Abstract: Four wild “red” yeast strains (*Rhodospiridium kratochvilovae* FMCC Y70, *R. toruloides* NRRL Y-27013, *R. toruloides* NRRL Y-17902 and *R. toruloides* NRRL Y-6985) were cultured in shake flasks on industrial glycerol at an initial substrate (Gly_0) concentration ≈ 50 g/L under nitrogen limitation. Strains NRRL Y-27013, NRRL Y-17902 and NRRL Y-6985 presented appreciable dry cell weight (DCW) and lipid synthesis (DCW up to 18–19 g/L containing lipids in quantities $\approx 47\%$, w/w). Strains NRRL Y-27013 and NRRL Y-6985 were further tested in higher Gly_0 concentrations (≈ 90 g/L and ≈ 110 g/L) with the same initial nitrogen quantity as in the first (“screening”) experiment. Both strains, despite the high Gly_0 concentrations and C/N ratios (up to 120 moles/moles) imposed, presented significant DCW production (up to c. 29.0–29.5 g/L). Yeast biomass contained significant lipid (42–43%, w/w) and endopolysaccharide (up to 42%, w/w) quantities. Both lipids and endopolysaccharide quantities (in % w/w) noticeably increased as a response to the imposed nitrogen limitation. Lipids containing mainly oleic and palmitic acids constituted ideal candidates for biodiesel synthesis. Thereafter, the wastewaters derived from the lipid production process (lipid fermentation wastewaters—LFWs) were used as maceration waters in cultivations of edible and medicinal fungi, where novel (non-conventional) substrates were used in the performed cultures. CW (coffee residue + wheat straw), CB (coffee residue + beech wood shavings), OW (olive crop + wheat straw), OB (olive crop + beech wood shavings), RW (rice husk + wheat straw) and RB (rice husk + beech wood shavings) were soaked/sprayed with LFWs or tap water and utilized in the cultivation of *Pleurotus*, *Ganoderma* and *Lentinula* mushrooms. The impact of LFWs on the mycelial growth rate (mm/d) and biomass production was evaluated. The results show that regardless of the wetting method, the highest growth rates (6.2–6.6 mm/d) were noticed on RW and RB for *Pleurotus eryngii* and *Ganoderma resinaceum*, on OW, OB and RW for *Ganoderma applanatum* and on RW, OW and OB for *Lentinula edodes*. Nevertheless, high biomass production was obtained on substrates soaked with LFWs for *Pleurotus ostreatus* (RW: 443 mg/g d.w.), *L. edodes* (RB: 238 mg/g d.w.) and *Ganoderma lucidum* (RW: 450 mg/g d.w.). Overall, this study demonstrates the possibility of the industrial conversion of low-value agro-waste to mycelial mass and eventually to important food products.

Citation: Diamantis, I.; Papanikolaou, S.; Michou, S.; Anastasopoulos, V.; Diamantopoulou, P. Yeast Lipids from Crude Glycerol Media and Utilization of Lipid Fermentation Wastewater as Maceration Water in Cultures of Edible and Medicinal Mushrooms. *Processes* **2023**, *11*, 3178. <https://doi.org/10.3390/pr11113178>

Academic Editors: Irfan Turhan, Ehsan Mahdinia and Ali Demirci

Received: 12 October 2023

Revised: 28 October 2023

Accepted: 30 October 2023

Published: 7 November 2023



Copyright: © 2023 by the authors. Licensee MDPI, Basel, Switzerland. This article is an open access article distributed under the terms and conditions of the Creative Commons Attribution (CC BY) license (<https://creativecommons.org/licenses/by/4.0/>).

Keywords: glycerol; intra-cellular lipids; intra-cellular polysaccharides; glucosamine; biomass; oleaginous yeasts; *Rhodospiridium toruloides*; *Pleurotus*; *Ganoderma*; *Lentinula*

1. Introduction

One of the most important priorities in the utilization of microorganisms as sources of lipids is focused upon their ability to convert several by-products into microbial lipids (“single-cell oils” (SCOs), viz. oils produced by microorganisms) [1–3]. Although the

cost of these lipids was higher than that of traditional animal fats or vegetable oils, SCOs were initially used to replace expensive fatty materials; however, currently, due to the global increase in food cost, SCOs (mainly yeast lipids) can be used as substitutes for common plant oils for the fabrication of biodiesel [1–7]. Furthermore, the huge expansion of biodiesel (viz. FA alkyl-esters) has resulted in a significant rise in the production of glycerol, which is the main side-product of the trans-esterification reaction process. As a result, an important decrease in the price of glycerol occurred last year, and the topic of its valorization has become crucial for biotechnological industries [2,5,7,8]. The utilization of oleaginous yeasts in the conversion of crude glycerol closes the loop of biodiesel production since the principal residue of this industrial activity (viz. crude glycerol) is transformed into triacylglycerols that subsequently will be converted into “second-generation” biodiesel, a process with obvious economic and ecological interest [2,5–8].

In the current study, biodiesel-derived glycerol was utilized as a substrate in “red” non-conventional and non-extensively studied yeast strains (belonging to the genus *Rhodospiridium*), in culture conditions enabling the production of SCOs (viz. fermentations carried out under conditions of limited nitrogen). Under the biorefinery concept, the zero-waste release approach and the water-saving optic recently adopted by various authorities and funding bodies, the wastewaters deriving from the lipid production process (viz. lipid fermentation wastewaters-LFWs) were utilized as maceration waters in innovative solid-state fermentation (SSF) processes performed using edible and pharmaceutical mushrooms. The treatment of LFWs may increase the whole SCO bioprocess cost given that in several cases, these waters can potentially contain non-assimilated and non-used fixed carbon sources (specifically if increased initial sugar quantities are used for the SCO synthesis to be performed). Moreover, LFWs certainly contain (potentially important) quantities of salts [2,4]. These salt-containing wastewaters can be used as maceration waters for the cultivation of edible and pharmaceutical fungi since several of them can present significant growth with or without salts in the culture media [9–13].

Mushrooms may produce several non-specific lignocellulosic enzymes that affect their growth and development [9,14,15]. *Pleurotus*, *Lentinula* and *Ganoderma* species, widely cultivated worldwide, are effective lignocellulosic residue bio-converters, resulting in mushrooms with unique biological and pharmacological properties [9,16–22]. During fermentation and substrate colonization, mushrooms obtain the nutrients required for their growth, mainly carbon and nitrogen sources, minerals and vitamins (these are possibly contained in LFW) [23–25] that along with substrate composition (amount of cellulose, lignin, etc.) may affect both the mycelial growth and mushroom production, and therefore, their evaluation is needed prior to cultivation [26–28].

Additionally, the process of mushroom cultivation has many advantages, as through the recycling or degradation of several agro-industrial wastes (e.g., olive mill waste, coffee residues, rice husk), an alternative way to reduce these impacts is generated and by turning these wastes into valuable products and food, environmental balance and economic prosperity are provided in the frame of a zero-waste economy [26,29–31]. On the other hand, very often, new methods and techniques in mushroom cultivation are proposed, including innovations in substrate preparation and cultivation conditions, to improve their productivity and quality [9,11,32,33]. For example, Dedousi et al. [11], with the addition of oils, nitrogen and calcium salts, achieved a shorter incubation period, higher biological efficiency and high-quality mushrooms. Moreover, the ability of various wastes to serve as substrates is often examined by utilizing large glass tubes and measuring the fungal growth rate (mm/day, Kr), as cultivating mushrooms in “bag-logs” is time-consuming. This technique has been successfully used by many researchers to determine the mycelial growth and fructification in a variety of fungal species, including *Agrocybe aegerita*, *Volvariella volvacea*, *Pleurotus* spp. and *L. edodes* [26,34]. Also, the mycelial mass can be estimated indirectly at the end of the colonization period using the glucosamine content of the fungal cell wall [11,27,35,36]. Chitin is a structural polysaccharide of the fungal cell wall and is composed of $\beta(1,4)$ -linked units of N-acetyl-D-glucosamine. Because of their

antibacterial and antioxidant qualities, chitin and chitosan are useful compounds with diverse uses, for food and medicinal purposes [37]. Chitin synthesized through fungal SSFs has been proposed, therefore, as an alternate source, as glucosamine may be obtained under controlled conditions utilizing a simple extraction process [38,39]. Apart from that, the determination of both Kr and biomass is necessary for the evaluation of various residues and wastes as potential substrates for high-yield mushroom cultivation.

Therefore, in the present study, four “red” not previously extensively studied yeast strains were used as cell factories amenable to turning biodiesel-derived glycerol into SCOs. The synthesis of other intra-cellular metabolites (i.e., polysaccharides) was also evaluated. Then, LFWs constituted the wetting agents in the SSF of several strains of edible and pharmaceutical fungi with agricultural residues, non-conventional in mushroom cultivation. The purpose of this study was first to estimate the possibility of using the lipid fermentation wastewater from *Rhodospiridium toruloides* instead of tap water during the SSFs of mushrooms. Then, to simplify the procedure and gain time, spraying was used as a wetting technique for residues prior to substrate preparation. For this purpose, three agro-industrial residues not extensively studied (e.g., olive crop residues, rice husk and coffee residue) along with various species of the higher fungi with dietary and/or medicinal properties, such as *Pleurotus*, *Ganoderma* and *Lentinula*, were evaluated for their bioconversion efficacy during small scale SSF (in glass tubes). In this work, the main growth parameters (*viz.* colonization rates, mycelial mass production) were noted, and the effect of substrate components and cultivation handling on them was considered. Finally, further investigation of the impact of LFW on selected substrates and mushroom strains regarding carposome production and metabolic compound synthesis (e.g., polysaccharides, proteins, antioxidants and lipids) is currently taking place.

2. Materials and Methods

2.1. Submerged Cultures of Yeasts for Lipid Production

In the present study, the “red” yeast strains *Rhodospiridium kratochvilovae* FMCC Y-70, *R. toruloides* NRRL Y-27013, *R. toruloides* NRRL Y-17902 and *R. toruloides* NRRL Y-6985 were used. The strain coded FMCC was a new strain deriving from the Laboratory of Food Microbiology and Biotechnology (Agricultural University of Athens, Athens, Greece), isolated from gilt-head sea bream (*Sparus aurata*) and characterized [40]. Strains coded NRRL Y were purchased by the ARS Culture Collection (Peoria, IL, USA). All four mentioned strains have been scarcely employed in works related to their growth opportunity on substrates containing glycerol and their potential for producing microbial lipids. According to Abeln and Chuck [2], the most frequently studied strains of the species *R. toruloides* in relation to their lipid production properties are the strains DSM 4444 (14% of the published papers on the topic of SCO production by *R. toruloides* strains), AS 2.1389 (12% of the published papers) and ATCC 10788 (7% of the published papers), while concerning the strains deriving from the ARS Culture Collection, only the strain NRRL Y-1091 has been studied in some cases in relation to its SCO potential (7% of the published papers) [2]. Therefore, the present study is indeed one of the first in the literature demonstrating the potential of lipid production by the mentioned wild-type yeast strains.

All strains were maintained on yeast peptone dextrose agar (YPDA) supplemented with malt extract, at $T = 4.0 \pm 0.5$ °C, and were sub-cultured every 2 months to maintain their viability. Experiments regarding the production of SCOs were carried out in submerged cultures in media with the following salt composition (in g/L) [41]: KH_2PO_4 , 7.0; Na_2HPO_4 , 2.5; $\text{MgSO}_4 \cdot 7\text{H}_2\text{O}$, 1.5; $\text{CaCl}_2 \cdot 2\text{H}_2\text{O}$ 0.15; $\text{FeCl}_3 \cdot 6\text{H}_2\text{O}$, 0.15; $\text{ZnSO}_4 \cdot 7\text{H}_2\text{O}$, 0.02; $\text{MnSO}_4 \cdot \text{H}_2\text{O}$, 0.06. Peptone and yeast extract were used as nitrogen sources in concentrations of 2.0 and 1.0 g/L, respectively. Peptone contained *c.* 18%, *w/w* nitrogen and *c.* 30%, *w/w* carbon, whereas yeast extract contained *c.* 7%, *w/w* nitrogen and *c.* 12%, *w/w* carbon. The initial pH for all media before and after sterilization (performed at $T = 115$ °C, 20 min) was 6.0 ± 0.1 . In all performed trials, crude glycerol was employed as a microbial substrate. The feedstock was provided by the Hellenic biodiesel-producing

industry “ELIN VERD SA” (Velesino, Magnissia Prefecture, Greece). The purity of crude glycerol was as follows: glycerol content $\approx 88\%$, w/w , salts of potassium and sodium $\approx 6\%$, w/w , non-glycerol organic compounds (mostly free fatty acids) $\approx 1\%$, w/w and water (5%, w/w). In the first part (“screening” experiment), all strains were cultivated in shake-flask fermentations in media in which initial glycerol (Gly_0) concentration was adjusted to ≈ 50 g/L. The culture was performed under the limitation of nitrogen (initial C/N molar ratio ≈ 55 moles/moles) to direct the metabolic activity in favor of SCO production [2,5,6]. Two of the strains that presented better performances (namely the strains NRRL Y-27013 and NRRL Y-6985) were cultured at higher Gly_0 amounts (≈ 90 and ≈ 110 g/L), while the initial nitrogen quantity remained as before (therefore, peptone and yeast extract concentrations were 2.0 and 1.0 g/L, respectively); thus, in the second set of experiments, besides the increasing Gly_0 concentrations, the initial molar ratio C/N also increased (at $Gly_0 \approx 90$ g/L, the initial molar ratio C/N was ≈ 100 moles/moles, while at $Gly_0 \approx 110$ g/L, the initial molar ratio C/N was ≈ 120 moles/moles). The calculations took into consideration the purity of the industrial feedstock to yield the above-mentioned Gly_0 concentrations of the media.

Most of the submerged fermentations were conducted in non-baffled Erlenmeyer flasks of 250 mL filled at 20%, v/v of previously sterilized culture medium. The pre-cultures were prepared in similar 250 mL Erlenmeyer flasks, equally filled at 20%, v/v with previously sterilized YPD medium (glucose, peptone and yeast extract at 10 g/L of each), which were aseptically inoculated from a fresh slant that contained the strain. Pre-cultures were incubated in an orbital shaker (Zhicheng ZHWY 211C; PR of China) for 48 ± 4 h at 180 ± 5 rpm, $T = 28 \pm 1$ °C. The concentration of yeast dry biomass of the pre-culture at 48 ± 4 h was 5.0 ± 0.5 g/L. Flasks of the principal cultures were inoculated with 1.0 mL of pre-culture and were incubated in the same shaker at the same conditions as the pre-cultures.

To assess the kinetics of the “red” yeasts on glycerol-based media, the contents of flask samples were periodically subjected to centrifugation ($9000 \times g/15$ min at $T = 10$ °C) in a Hettich Universal 320R (Vlotho, Germany) centrifuge. Recovered wet cells were extensively washed with distilled water and were re-centrifuged. Yeast dry biomass (X , g/L) was determined by means of its DCW wet biomass, which was put in a pre-weighed McCartney glass bottle and placed at $T = 85 \pm 2$ °C until constant weight (in most cases for c. 30 ± 4 h). The pH of the culture medium was measured off-line using a Jenway 3020 (Cole-Parmer, Eaton Socon, UK) pH meter. In all the fermentations and irrespective of the strain or the Gly_0 concentrations, pH in the medium ranged between 5.1 and 5.9 and there was no need to perform correction. The dissolved oxygen tension (DOT) was measured off-line using a selective electrode (Bante Instruments Inc., Shanghai, China) according to Filippousi et al. [42]. The DOT was always $\geq 10\%$ v/v during all growth phases for all shake-flask fermentations, providing evidence that all trials were performed under fully aerobic conditions [42].

Residual glycerol in the growth medium was quantitatively determined through HPLC analysis [40]. The free amino nitrogen (FAN) concentration in the liquid samples was determined according to Kachrimanidou et al. [43]. Total cellular lipids (L , g/L) were extracted from the microbial DCW with the modified protocol of Folch (placement of mixture of chloroform/methanol 2:1 v/v into the McCartney bottle containing the yeast DCW for at least 5 days, cell debris removal through filtration and solvent mixture evaporation), as presented in detail in the work of Sarantou et al. [44]. Cellular lipids were converted to their respective fatty acid (FA) methyl-esters that were subsequently analyzed in a gas chromatograph (GC-FID) apparatus (Fisons 8060, Markham, ON, Canada), equipped with a Chrompack (São Paulo, Brazil) column (60 m \times 0.32 mm) and a flame ionization detector using helium as a carrier gas (2.0 mL/min), according to Giannakis et al. [45]. Finally, intra-cellular polysaccharides (IPS , g/L) were quantitatively determined according to the modified protocol adapted by Argyropoulos et al. [46].

To collect LFWs obtained from the microbial lipid fermentation processes, trials on glycerol ($Gly_0 \approx 50$ g/L) were conducted in shake flasks of a total volume of 2.5 L, filled with 450 mL of previously sterilized culture medium and inoculated with 50 mL of exponential pre-culture. These 2.5 L flasks were incubated in the same orbital shaker as before for 320 ± 10 h at 250 ± 10 rpm and $T = 28 \pm 1$ °C. LFWs were collected through centrifugation (see above) of the cultures and stored in a freezer ($T = 4 \pm 1$ °C). These fermentation wastewaters contained glycerol at a final concentration of 2.5 ± 0.5 g/L and a FAN concentration of 15 ± 5 mg/L. Phosphate and sulfate ions were also found in these LFWs.

2.2. Fungi

In this work, seven higher fungi (mushrooms) were used: *Pleurotus ostreatus* (AMRL 135), *P. eryngii* (AMRL 161), *P. pulmonarius* (AMRL 177), *Ganoderma applanatum* (AMRL 341), *G. resinaceum* (AMRL 325), *G. lucidum* (AMRL 330) and *Lentinula edodes* (AMRL 121), deriving from the Laboratory of Edible Fungi of Institute of Technology of Agricultural Products/Hellenic Agricultural Organization—Dimitra. The strains were maintained on potato dextrose agar (PDA, Merck, Germany) at $T = 4 \pm 1$ °C and regularly sub-cultured. Prior to experiments, fresh mycelia were produced on PDA Petri dishes by incubation at $T = 26 \pm 1$ °C and relative humidity of 75%.

2.3. Substrates for Fungal Growth

Agro-residues, i.e., olive crop residues (leaves and branches) (OC), rice husk (RH), beech wood shavings (BW), wheat straw (WS), wheat bran and poplar sawdust, originated from Greek farms and industries and coffee residue (CR) was obtained from local coffee shops. They were dried in a $T = 60 \pm 1$ °C oven, until constant weight (Elvem, Athens, Greece) and milled to size <0.2 mm in a Janke & Kunkel, IKA-WERK, analytical mill (Staufen im Breisgau, Germany). Several physicochemical analyses were performed on the raw residues and the final substrates before their inoculation with the mushroom strains. Total nitrogen and organic matter were determined according to the Kjeldahl (Total Kjeldahl, Nitrogen, TKN) method (APHA) [47] and Sparks et al. [48], respectively. Protein content was determined through nitrogen concentration, with the use of the factor 6.25. The FAN concentration of LFW was assayed by the ninhydrin colorimetric method according to Lie [49]. Regarding the pH and electrical conductivity (EC) calculation, residue aliquots of 10 g were suspended in 100 mL distilled water for 2 h and the above parameters were measured using a Crison pH meter GLR 21 (Barcelona, Spain) and a Hanna Instruments HI 8733 (Padova, Italy) electrical conductivity instrument, respectively.

Prior to substrate preparation, dry WS, BW and OC residues were cut to ~2 cm using a cutting machine (Novital, mod. Magnum-4V, Lonate Pozzolo VA, Italy) and then they were (a) soaked in LFW from *R. toruloides* fungal culture or tap water for 5–8 h, with the excess water being drained off after 2 h, and (b) sprayed with 20%, w/w LFW. Different substrates were prepared by combining residues (dry substrate weight) as follows: (1) CR:80, WS:18 (named CW); (2) CR:80, CB:18 (CB); (3) OC:70, WS:12 (OW); (4) OC:70, BW:12 (OB); (5) RH:70, WS:12 (RW); and (6) RH:70, BW:12 (RB). Wheat bran and soybean flour were used as supplements to obtain a final C/N ratio of 20–30, CW and CB at 1%, w/w each and the other four substrates (OW, OB, RW and RB) at 13% and 5%, w/w, respectively. Calcium carbonate was also added to the substrates (1% w/w, in terms of dry weight) to obtain a pH = 6.0–7.5. Glass tubes (200 × 28 mm, five/substrate/strain) were uniformly filled with 80 mL of substrates and autoclaved at $T = 121 \pm 1$ °C (1.1 atm) for 2 h. The water content of the sterilized substrates was 60–75%. When room temperature was reached, tubes were inoculated with one agar plug (of 6 mm diameter cut from the periphery of a fresh fungal colony grown on PDA) and finally, they were incubated at $T = 26 \pm 1$ °C (in an ENTERLAB, mod. GROW-1300 HR, Terrassa, Spain) in the dark, until full colonization of the substrate.

2.4. Growth Rate Measurement and Glucosamine Content Determination

During substrate colonization by the fungi, the measurements of colony diameter were taken in two perpendicular directions of the tubes every two to three days and the mycelial growth rate (Kr , expressed in mm/d) was determined in five tubes [50]. At 100% of colonization, duplicate tube samples were used for biomass estimation. They were frozen at $T = -20 \pm 1$ °C for 48 h and then dried using a Heto LyoLab 3000 freeze-dryer (Heto-Holten Als, Denmark), milled and sieved. The measurement of N-acetylglucosamine, as derived from fungal chitin hydrolysis, was used for the indirect determination of biomass production [51]. Specifically, 2 g of dry sample (substrate and biomass) was mixed with 5 mL of 72% H_2SO_4 (Merck, Darmstadt, Germany) and agitated for 30 min at 130 ± 2 rpm in a rotary shaker (ZHWHY-211C, Shanghai, China). Following dilution with 54 mL deionized water, the mixture was autoclaved for two hours at $T = 121 \pm 1$ °C to initiate hydrolysis. Using NaOH solution, the hydrolysate was neutralized. Equal volumes of (3 mL) of 5% (w/v) $NaNO_2$ and 5% $KHSO_4$ were added to a 3 mL sample from the previous step. The mixture was shaken for 15 min and then centrifuged at $1500 \times g$ (Micro 22R, Hettich, Germany), for 2 min at $T = 2 \pm 0.1$ °C. Following that, a 3 mL sample of the supernatant was mixed with 1 mL of 12.5% $NH_4SO_3NH_2$ and shaken for 5 min. Next, 1 mL of 0.5% 3-methyl-2-benzothiazolonehydrazone hydrochloride (MBTH) solution was added and heated for 3 min in a boiling water bath and then cooled, and 1 mL of 0.5% $FeCl_3$ was added. After 30 min, the absorbance was measured. The glucosamine was quantified spectrophotometrically at 650 nm using a Jasco V-530 UV/VIS spectrophotometer (Tokyo, Japan) and the results were expressed as mg of fungal biomass/g of dry substrate. Glucosamine standard curves were obtained using several concentrations of N-acetylglucosamine (Sigma-Aldrich, Taufkirchen, Germany). The glucosamine content of each fungus was determined through the mycelia produced in liquid cultures for 25 days, in 100 mL Erlenmeyer flasks with glucose (Alpha Aesar, Karlsruhe, Germany) 30 g/L, yeast extract (Fluka, Steinheim, Germany) 3 g/L, peptone (Merck, Darmstadt, Germany) 3 g/L and $CaCO_3$ 0.1 g/L, as growth medium, at $T = 26 \pm 1$ °C under static conditions [26]. The equations correlating mycelial mass with glucosamine content, for each strain, were obtained after fitting the linear model to the experimental data.

2.5. Data Analysis

For all submerged fermentation cultures performed, each experimental point of all the kinetics presented in the tables and figures is the mean value of two independent determinations, in which two lots of independent cultures were conducted using different inocula. The standard error (SE) for most of the experimental points was $\leq 15\%$. Kinetics concerning the submerged lipid-production cultures were plotted using Kaleidagraph 4.0 Version 2005 showing the mean values with the standard error mean.

2.6. Abbreviations and Units

X : biomass (dry cell weight (DCW)) (g/L); L : lipids (g/L); Gly : glycerol (g/L); IPS : intra-cellular polysaccharides (g/L); r_{Gly} : glycerol consumption rate (g/L/h); $Y_{X/Gly}$: yield of total biomass produced on glycerol consumed (g/g); $Y_{L/Gly}$: yield of lipids produced on glycerol consumed (g/g); L/X : lipids in DCW (% w/w); IPS/X : intra-cellular polysaccharides in DCW (% w/w); Kr : mycelial growth rate (mm/d).

3. Results and Discussion

3.1. Screening of "Red" Yeasts for Lipid Production

The four "red" yeast strains used in the present study (*R. kratochvilovae* FMCC Y-70, *R. toruloides* NRRL Y-27013, *R. toruloides* NRRL Y-17902 and *R. toruloides* NRRL Y-6985) were cultured in shake-flask experiments under nitrogen limitation (glycerol excess) with Gly_0 concentration ≈ 50 g/L (initial C/N molar ratio ≈ 55 moles/moles) and the obtained results are presented in Table 1. All the tested strains presented important quantities of consumed glycerol and varying concentrations of total yeast biomass, cellular lipids and

cellular polysaccharide production. In all fermentations performed, after a given point (i.e., at $t \approx 50$ h), media were under limited nitrogen conditions (initial FAN = 80 ± 10 mg/L, FAN after $t \approx 50$ h = 15 ± 5 mg/L). Three out of the four screened strains (namely NRRL Y-27013, NRRL Y-17902 and NRRL Y-6985) presented almost equivalent kinetic and physiological profiles; for these strains, the consumption rate of glycerol (r_{Gly}) as calculated by the formula $r_{Gly} = -\frac{\Delta Gly}{\Delta t}$ for the period, where glycerol was virtually found in non-negligible concentrations in the growth medium (i.e., $Gly \geq 5.0$ g/L), was unaffected by the nitrogen-limited conditions in the medium and was almost similar for all these trials ($r_{Gly} = 0.20 \pm 0.2$ g/L/h), while at $t = 240$ – 270 h after inoculation, glycerol consumption was almost complete (at that time, the consumed glycerol represented $c. 94$ – 99% , w/w of the total initial substrate concentration). Moreover, for these strains, the values of total yeast DCW, L , IPS , L/X and IPS/X constantly increased, reaching their maximum values at the end of fermentation (viz. when almost all available glycerol quantity had been assimilated). On the other hand, a different profile in which L/X and IPS/X values presented a peak at the middle of fermentation and thereafter decreased, although the quantity of non-assimilated glycerol was high, was demonstrated for strain FMCC Y-70. The kinetics of the culture in one characteristic case (viz. the strain *R. toruloides* NRRL Y-6985) are illustrated in Figure 1. It is interesting to indicate that, as previously mentioned, the values of L/X and IPS/X increased simultaneously, suggesting that the microorganism accumulated reserve lipid and reserve non-lipid compounds at the same time. This agrees with the results presented for *R. toruloides* CBS 14 growing on glucose under nitrogen-limited conditions [52,53]. On the contrary, for other strains (i.e., strains NRRL Y-27012 and DSM 4444), the IPS/X values were high in the first culture phases, and in the presence of assimilable nitrogen in the medium, they decreased as the fermentation proceeded, with a simultaneous increase in the L/X values [13,54].

Table 1. Quantitative data of *R. kratochvilovae* FMCC Y-70, *R. toruloides* Y-17902, *R. toruloides* NRRL Y-27013 and *R. toruloides* NRRL Y-6985 strains deriving from kinetics on crude glycerol, in nitrogen-limited shake-flask cultures, with initial glycerol (Gly_0) concentration ≈ 50 g/L and initial nitrogenous compounds peptone and yeast extract added at 2.0 and 1.0 g/L (initial molar ratio C/N ≈ 55 moles/moles). Four different points in the fermentations are represented: (1) when the maximum quantity of total dry yeast biomass (X , g/L) was observed; (2) when the maximum quantity of lipids per DCW (L/X , % w/w) was observed; (3) when the maximum quantity of intra-cellular polysaccharides per DCW (IPS/X , % w/w) was observed; (4) when the maximum quantity of absolute lipid value (L , g/L) was observed. Culture condition: initial glycerol concentration ($Gly_0 \approx 50$ g/L), growth on 250 mL conical flasks at 180 ± 5 rpm, initial pH = 6.0 ± 0.1 , culture pH ranging between 5.1 and 5.9, incubation temperature $T = 28 \pm 1$ °C. Each experimental point is the mean value of two measurements (SE for most experimental points is $\leq 17\%$).

Strains		Time (h)	Gly_{cons} (g/L)	X (g/L)	$Y_{X/Gly}$ (g/g)	L (g/L)	L/X (% w/w)	IPS/X (% w/w)
NRRL Y-27013	1, 2, 3, 4	240	47.7 ± 1.9	19.0 ± 2.0	0.40	8.8 ± 0.9	46.3	31.2
NRRL Y-6985	1, 2, 3, 4	270	49.4 ± 1.7	18.5 ± 1.6	0.37	8.8 ± 0.8	47.6	33.9
NRRL Y-17902	1, 2, 3, 4	250	46.7 ± 1.9	19.0 ± 2.2	0.41	8.6 ± 1.0	45.2	33.1
FMCC Y-70	2, 3, 4	82	21.2 ± 2.2	9.1 ± 1.5	0.43	2.3 ± 0.5	25.4	39.9
	1	245	43.7 ± 2.7	15.1 ± 1.3	0.35	1.8 ± 0.4	12.2	32.1

Fermentation time (h); yield of total yeast biomass produced on glycerol consumed ($Y_{X/Gly}$, g/g); and quantities of total dry yeast biomass (X , g/L), total lipids (L , g/L) and glycerol consumed (Gly_{cons} , g/L) are also depicted for all the above-mentioned fermentation points.

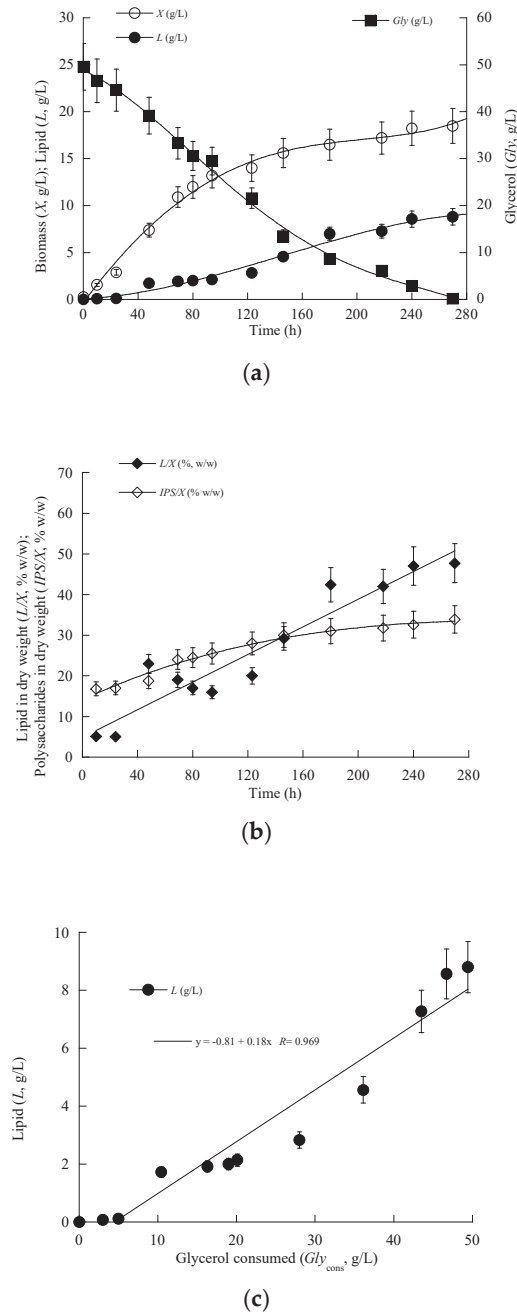


Figure 1. Changes in total biomass (X , g/L), glycerol (Gly , g/L) and cellular lipids (L , g/L) (a) and cellular lipid per DCW (L/X , % w/w) and cellular polysaccharides per DCW (IPS/X , % w/w) (b) as a function of fermentation time for *R. toruloides* NRRL Y-6985 grown on glycerol in shake-flask trials. Representation of global conversion yield of lipids produced per unit of glucose consumed as shown by linear regression of produced lipids as a function of consumed glycerol (c) for the same set of data. Each point is the mean value of two independent measurements. $SE \leq 15\%$.

The fatty acid (FA) composition of the cellular lipids synthesized in this set of cultures is presented in Table 2 (concerning t from 120 to 160 h after inoculation). The principal cellular FAs detected were mostly oleic acid ($\Delta^9\text{C18:1}$) and palmitic acid (C16:0). Cellular lipids of the yeast *R. toruloides* NRRL Y-27013 contained increased concentrations of saturated FAs (i.e., C16:0 = 39.9%, w/w and C18:0 = 13.5%, w/w, meaning that the concentration of saturated FAs was = 53.4%, w/w of total cellular lipids produced). In fact, when the concentration of saturated cellular FAs is $\geq 40\%$, w/w of total cellular lipids, as was the case of the mentioned strain NRRL Y-27013, the yeast produces lipids of a similar composition to palm oil [55–57]. Palm oil has an important number of applications, including food and biodiesel production, and its enormous utilization, specifically during the last decade, is a leading contributor to tropical deforestation, the major result of which is the constantly increasing CO₂ emissions that have been noted [55]. Nevertheless, all yeast lipids synthesized (see Table 2) contained high concentrations of oleic acid; therefore, these yeast SCOs can be used for the synthesis of second-generation biodiesel [2,5,6,56]. Finally, poly-unsaturated cellular FAs (specifically the ones with ≥ 3 double bonds) were detected in low or negligible quantities in the cellular lipids of the tested yeasts, in accordance with the literature [2,3,6,58,59].

Table 2. Fatty acid composition of the cellular lipids produced by yeast strains cultivated on crude glycerol in shake-flask experiments ($\text{Gly}_0 \approx 50 \text{ g/L}$, C/N ≈ 55 moles/moles). Time of fermentation for the determination of the fatty acid composition was between 120 and 160 h after inoculation. Culture conditions were as in Table 1.

Strain/Fatty Acid	C16:0 (% w/w)	C18:0 (% w/w)	C18:1 (% w/w)	C18:2 (% w/w)	C18:3 (% w/w)
NRRL Y-27013	39.9	13.5	42.8	1.6	n.d.
NRRL Y-6985	30.1	2.6	54.2	2.0	0.8
NRRL Y-17902	31.2	2.7	54.0	1.3	0.7
FMCC Y-70	25.9	9.5	39.5	15.5	7.9

n.d.: <0.5%, w/w.

3.2. Trials in Higher Initial Glycerol Concentrations and C/N Molar Ratios

Two of the four previously tested “red” yeast strains (*R. toruloides* NRRL Y-27013 and *R. toruloides* NRRL Y-6985) were cultured in shake-flask experiments under higher Gly_0 concentrations ($\approx 90 \text{ g/L}$ and $\approx 110 \text{ g/L}$), while the initial nitrogen amount remained the same as before (*viz.* peptone and yeast extract at 2.0 and 1.0 g/L, respectively). Therefore, in the second set of experiments, besides the increasing Gly_0 concentrations, the initial molar ratio C/N significantly increased (at $\text{Gly}_0 \approx 90 \text{ g/L}$, the initial C/N molar ratio was ≈ 100 moles/moles, while at $\text{Gly}_0 \approx 110 \text{ g/L}$, it was ≈ 120 moles/moles). The obtained results as regards *R. toruloides* NRRL Y-27013 and *R. toruloides* NRRL Y-6985 are shown in Table 3. From the obtained results, it can be indicated that for both strains and despite both the elevated Gly_0 concentrations and initial molar ratios C/N imposed, high quantities of glycerol had been assimilated. For all trials, as previously indicated, the r_{Gly} calculated by the formula $r_{\text{Gly}} = -\frac{\Delta\text{Gly}}{\Delta t}$ was $\approx 0.26\text{--}0.27 \text{ g/L/h}$, which was higher than that of the previous experiment with the lower Gly_0 concentration and initial molar ratio C/N imposed. It is also interesting to indicate that the fermentation was stopped, however, the trend of the kinetics for all experiments was that the available glycerol quantity would be finally grosso modo consumed; therefore, even higher quantities of DCW and intra-cellular metabolites could have been synthesized. For both studied strains (*viz.* NRRL Y-27013 and NRRL Y-6985), lipid and polysaccharide quantities (in terms of L/X and IPS/X , in %, w/w) globally increased. In absolute values, the significant lipid quantity of 12.6 g/L was recorded for both strains in the cultures with the increased Gly_0 concentration and initial molar ratio C/N imposed. However, by comparing the L/X values for all the performed trials and

for both the strains NRRL Y-27013 and NRRL Y-6985, it can be seen that the more the Gly_0 concentration and the initial C/N molar ratio increased, the lower the recorded L/X values were (see Tables 1 and 3). Therefore, although lipid quantities increased in absolute values, lipids in DCW values decreased, presumably in favor of the biosynthesis and accumulation of intra-cellular polysaccharides, the IPS/X values of which drastically increased (see Tables 1 and 3). Once more, therefore, it can be suggested that the studied strains (NRRL Y-27013 and NRRL Y-6985) presented a biochemical similarity with the strain CBS 14 growing on glucose, where the values of IPS/X and L/X constantly increased in response to the nitrogen-limited conditions imposed [52,53]. It is known that after nitrogen depletion in the medium, a fast reduction of the concentration of cellular AMP occurs [1,2]. As a response, there will subsequently be either a decrease in the activity of the Krebs cycle (decrease in the activity of NAD^+ or $NADP^+$ isocitrate dehydrogenase, leading to the enhanced synthesis of cellular fatty acids and triacylglycerols) or a decrease in the glycolysis rate due to decreased activity of phospho-fructokinase (for reviews, see [1,2,53,59]). Apparently, for the case of both strains NRRL Y-27013 and NRRL Y-6985 (and potentially for the strain NRRL Y-17902), the response to the imposed nitrogen limitation seems to be the accumulation of both lipids and storage polysaccharides. On the other hand, some substrate inhibition was observed against both NRRL Y-27013 and NRRL Y-6985 strains, due to the increased Gly_0 concentration imposed, as calculated through the biomass conversion yield $Y_{X/Gly}$ obtained in all fermentations. Therefore, the yield $Y_{X/Gly}$ calculated by the formula $Y_{X/Gly} = \frac{X_{max} - X_0}{Gly_{cons}}$ was ≈ 0.40 g/g for the strain NRRL Y-27013 at $Gly_0 \approx 50$ g/L and decreased to ≈ 0.32 – 0.33 g/g at the highest initial glycerol concentrations. Concerning the strain NRRL Y-6985, at $Gly_0 \approx 50$ g/L, the yield value was ≈ 0.38 g/g, decreasing to ≈ 0.32 g/g at the highest Gly_0 concentration. Representative results of DCW production and lipids in DCW values for yeasts cultivated on glycerol and the comparisons with the current study are demonstrated in Table 4.

Table 3. Quantitative data of *R. toruloides* NRRL Y-27013 and *R. toruloides* NRRL Y-6985 strains deriving from kinetics on crude glycerol, in nitrogen-limited shake-flask cultures, with increasing initial glycerol (Gly_0) concentration (≈ 90 g/L, C/N ≈ 100 moles/moles; ≈ 110 g/L, C/N ≈ 120 moles/moles) at constant initial nitrogen concentration in the medium (initial nitrogenous compounds were peptone and yeast extract added at 2.0 and 1.0 g/L, respectively). Four different points in the fermentations are represented: (1) when the maximum quantity of total dry yeast biomass (X , g/L) was observed; (2) when the maximum quantity of lipids per DCW (L/X , % w/w) was observed; (3) when the maximum quantity of intra-cellular polysaccharides per DCW (IPS/X , % w/w) was observed; (4) when the maximum quantity of absolute lipid value (Ls , g/L) was observed. Fermentation time (h); quantities of yeast biomass (X , g/L), total lipids (Ls , g/L) and glycerol consumed (Gly_{cons} , g/L); and yield of total biomass produced per glycerol consumed ($Y_{X/Gly}$, g/g) are also depicted for all the above-mentioned fermentation points. Culture conditions as in Table 1.

$Glyc_0$ (g/L)		Time (h)	$Glyc_{cons}$ (g/L)	X (g/L)	$Y_{X/S}$ (g/g)	L (g/L)	L/X (%, w/w)	IPS/X (%, w/w)
<i>R. toruloides</i> NRRL Y-27013								
≈ 90	1, 2, 3, 4	264	70.4 ± 3.1	23.4 ± 2.7	0.33	11.1 ± 1.6	47.4	34.9
≈ 110	1, 2, 3, 4	336	89.0 ± 2.9	29.3 ± 3.3	0.33	12.6 ± 1.9	43.0	41.3
<i>R. toruloides</i> NRRL Y-6985								
$Glyc_0$ (g/L)		Time (h)	$Glyc_{cons}$ (g/L)	X (g/L)	$Y_{X/S}$ (g/g)	L (g/L)	L/X (%, w/w)	IPS/X (%, w/w)
≈ 90	1, 2, 3, 4	288	77.1 ± 2.1	24.4 ± 2.9	0.32	11.0 ± 1.9	45.1	36.2
≈ 110	1, 2, 3, 4	336	90.9 ± 3.3	29.1 ± 2.6	0.32	12.6 ± 2.7	43.2	42.1

Table 4. Representative results concerning the production of total dry biomass and lipids in DCW values by yeast species cultivated on glycerol under various fermentation modes.

Strain	Cultivation Type	X (g/L)	L/X (% w/w)	Reference
<i>Cryptococcus curvatus</i> ATCC 20509	Fed-batch reactor	118.0	25.0	Meesters et al. [60]
<i>C. curvatus</i> ATCC 20509	Fed-batch reactor	32.9	52.9	Liang et al. [61]
<i>C. curvatus</i> ATCC 20509	Fed-batch reactor	22.0	49.0	Cui et al. [62]
<i>Yarrowia lipolytica</i> MUCL 28849	Fed-batch reactor	42.2	38.2	Fontanille et al. [63]
<i>Rodosporidium torulooides</i> AS2.1389	Batch reactor	26.7	69.5	Xu et al. [64]
<i>R. torulooides</i> Y4	Batch reactor	35.3	46.0	Uçkun Kiran et al. [65]
<i>R. torulooides</i> Y4	Batch flasks	24.9	48.9	Yang et al. [66]
<i>Lipomyces starkeyi</i> DSM 70296	Batch flasks	34.4	35.9	Tchakouteu et al. [67]
<i>R. torulooides</i> DSM 4444	Fed-batch reactor	37.4	51.3	Leiva-Candia et al. [68]
<i>R. torulooides</i> DSM 4444	Fed-batch reactor	41.0	60.0	Signori et al. [69]
<i>R. torulooides</i> DSM 4444	Batch flasks	37.0	37.0	Papanikolaou et al. [70]
<i>R. torulooides</i> ATCC 10788	Batch flasks	10.3	34.0	Uprety et al. [71]
<i>R. torulooides</i> AS 2.1389	Batch flasks	18.9	64.5	Kamal et al. [72]
<i>R. torulooides</i> DSM 4444	Batch flasks	28.9	43.3	Diamantopoulou et al. [13]
<i>R. torulooides</i> DSM 4444	Batch flasks	27.3	54.6	Sarantou et al. [44]
<i>C. curvatus</i> ATCC 20509	Batch flasks	12.6	48.4	Karayannis et al. [7]
<i>R. torulooides</i> NRRL Y-27013	Batch flasks	29.3	43.0	Present study
<i>R. torulooides</i> NRRL Y-6985	Batch flasks	29.1	43.2	Present study

The FA composition of the cellular lipids synthesized in this set of cultures is presented in Table 5 (analysis performed at t ranging between 120 and 160 h after inoculation). As in the previous set of experiments, the principal cellular FAs were mostly the C18:1 and the C16:0. As compared to the trial performed at $Gly_0 \approx 50$ g/L, the cellular lipids of the strain NRRL Y-27013 in the trials with higher FA Gly_0 concentrations imposed seemed less saturated (see Tables 2 and 5). In contrast, for the strain NRRL Y-6985, no significant differences were recorded in the trials with the various Gly_0 concentrations imposed. In all cases, cellular C18:1 was the principal cellular FA, rendering the lipids of *R. torulooides* as precursors for the production of second-generation biodiesel [2,5,6,56].

Table 5. Fatty acid composition of the cellular lipids produced by the selected yeast strains NRRL Y-27013 and NRRL Y-6985 cultivated on crude glycerol in shake-flask experiments ($Gly_0 \approx 90$ g/L and $Gly_0 \approx 110$ g/L). Time of fermentation for the determination of the fatty acid composition was between 120 and 160 h after inoculation. Culture conditions were as in Table 1.

Gly_0 (g/L)	Strain	C14:0 (% w/w)	C16:0 (% w/w)	C16:1 (% w/w)	C18:0 (% w/w)	C18:1 (% w/w)	C18:2 (% w/w)	C18:3 (% w/w)
≈ 90	NRRL Y-27013	2.1	25.3	n.d. *	11.1	51.5	6.7	3.3
	NRRL Y-6985	n.d.	28.8	11.9	2.1	54.8	2.1	0.3
≈ 110	NRRL Y-27013	2.1	26.3	n.d.	11.0	49.8	5.4	5.4
	NRRL Y-6985	n.d.	27.0	10.9	3.1	55.2	3.1	0.7

* n.d.: <0.5%, w/w.

3.3. Substrate Analysis for Mushroom Cultivation

Primary analysis conducted on the residues used in the present study concerning their pH, EC and N and C contents provided the basic information needed before their mixture and final substrate synthesis (Table 6). The six substrate formulations prepared contained different amounts of residues so that the appropriate conditions (e.g., C/N = 20–30) and the necessary ingredients in adequate quantities for fungal growth were provided [9]. Parame-

ters such as total C, N, C/N ratio, pH and EC of the final substrates (before inoculation) are important for mycelium growth and mushroom fructification.

Table 6. Physicochemical profile of agro-industrial residues used in the study.

Residue	Moisture Content (%)	pH	EC	Nitrogen	Protein	Carbon
			($\mu\text{S}/\text{cm}$)	(% d.w.)	(% d.w.)	(% d.w.)
WS *	7.15	7.35	840	0.65	4.06	31.44
BW	7.89	5.57	285	0.23	1.44	33.07
CR	7.20	5.36	228	1.90	11.88	32.83
OC	6.15	5.24	516	1.24	7.75	39.00
RH	7.92	6.84	465	0.35	2.19	28.52
WB	10.86	6.21	894	3.37	21.06	31.79
SF	10.58	6.06	752	5.88	36.75	67.59

Data are presented as mean values from duplicated measurements. * WS: wheat straw, BW: beech wood shavings, CR: coffee residue, OC: olive crop, RH: rice husk, WB: wheat bran, SF: soybean flour.

The results show (Table 7) that the C (%) concentration among the different substrates presented no great differences, as values ranged from 31.25 to 38.70% (*w/w*). The C/N ratio varied from 19.03 (CW) to 31.46 (RB), the desirable values for mushroom production [26,27]. The pH values ranged from 6.28 to 6.94, making *Pleurotus* cultivation feasible, as the fungal mycelium obtains nutrients from the substrate at a particular range of pH, whereas rapid mycelial growth occurs at pH 6.4–7.8 [73,74]. The EC values presented great variations among substrates. The highest value was recorded in RB substrate treated with tap water (987 $\mu\text{S}/\text{cm}$, 0.987 mS/cm), and the lowest values were recorded in CW (229 $\mu\text{S}/\text{cm}$, 0.229 mS/cm). In general, the optimal EC for mushroom cultivation is usually in the range of 0.5 to 2.5 mS/cm. However, each species of mushrooms may have different requirements, as the optimal EC for the cultivation of the oyster mushroom (*P. ostreatus*) has been recorded at around 1.0 to 2.0 mS/cm, while for shiitake mushrooms (*L. edodes*), an EC of 1.5 to 2.5 mS/cm has been recommended [16].

Table 7. Composition and physicochemical profile of substrates used in solid-state fermentation experiments (final mixtures before inoculation).

	Substrate	C/N	Moisture Content (%)	pH	EC ($\mu\text{S}/\text{cm}$)	Protein (% d.w.)	C (% d.w.)	N (% d.w.)
H ₂ O	CW *	19.03	66.10	6.62	229	10.81	32.92	1.73
	CB	20.08	60.88	6.75	714	10.31	33.21	1.65
	OW	23.00	71.38	6.61	698	10.50	38.50	1.68
	OB	23.96	69.45	6.48	795	10.19	38.70	1.63
	RW	29.54	66.34	6.45	957	6.63	31.25	1.06
	RB	31.46	68.14	6.81	987	6.25	31.44	1.00
LFW (so) **	CW	19.03	62.73	6.28	266	10.81	32.92	1.73
	CB	20.08	58.97	6.87	721	10.31	33.21	1.65
	OW	23.00	68.58	6.66	741	10.50	38.50	1.68
	OB	23.96	70.12	6.48	658	10.19	38.70	1.63
	RW	29.54	72.90	6.94	495	6.63	31.25	1.06
	RB	31.46	74.45	6.57	321	6.25	31.44	1.00
LFW (sp)	CW	19.03	64.71	6.52	248	10.81	32.92	1.73
	CB	20.08	57.74	6.41	787	10.31	33.21	1.65
	OW	23.00	70.84	6.71	753	10.50	38.50	1.68
	OB	23.96	69.84	6.47	823	10.19	38.70	1.63
	RW	29.54	74.45	6.53	776	6.63	31.25	1.06
	RB	31.46	71.14	6.54	793	6.25	31.44	1.00

* CW: coffee residue + wheat straw, CB: coffee residue + beech wood shavings, OW: olive crop + wheat straw, OB: olive crop + beech wood shavings, RW: rice husk + wheat straw, RB: rice husk + beech wood shavings. ** LFW (so): soaked in lipid fermentation wastewater, LFW (sp): sprayed with lipid fermentation wastewater.

3.4. Mycelial Growth Rate

It is well known that mycelial growth and biomass production require the utilization of competent species and effective substrates [34,35]. Also, the combination of different residues leads to substrates with a more balanced chemical composition than the homogeneous ones, boosting quick development and high yields [75,76]. Thus, in our experiments, CR, OC, RH, BS and WS residues were used in several quantities for each substrate to achieve a C/N ratio of 20–30 and enhance their production [9] (see Table 7). In this study, *P. ostreatus*, *P. eryngii*, *P. pulmonarius*, *G. applanatum*, *G. resinaceum*, *G. lucidum* and *L. edodes* species were subjected to trials in which their ability to grow on the above wastes was evaluated, and in the view of water economy, two wetting methods were used: soaking and spraying substrates with LFWs.

The results of the mycelium linear growth (K_r , mm/d) for each substrate are shown in Figure 2. The colonization rates were higher in most substrates treated with LFWs compared to the control (tap water) (Figure 3), and they were affected by the substrate and the mushroom genus, as has been already demonstrated by previous studies [11,26,27,77]. The novel (non-conventional) substrates consisting of RH, OC and CR successfully supported mycelial growth, and K_r values varied among mushroom strains. Several of the highest growth rates ($K_r > 6$ mm/d) were recorded in RW (for *P. eryngii*, *G. resinaceum* and *L. edodes*) and RB (for *P. eryngii*, *G. resinaceum*) and in some cases, OW and OB gave better results (e.g., *P. pulmonarius* $K_r = 5.46$ mm/d in OW, *G. lucidum* $K_r = 5.07$ mm/d in OW and *G. applanatum* $K_r = 6.36$ mm/d in OB). Furthermore, *Ganoderma* species demonstrated fast colonization on OW and OB substrates, as well as high growth rates on RW and RB, probably due to the higher C/N ratio of these substrates and the relatively lower nitrogen content that acts beneficially. It seems, therefore, that the C/N ratio of the substrates was positively correlated with the growth rate. This positive correlation has been also previously reported by D'Agostini et al. [78] for *P. ostreatus* and *L. edodes*. Melanouri et al. [27] and Philippoussis et al. [9] observed higher growth rates (mean $K_r = 9.58$ – 6.92 mm/d) for *Pleurotus* spp. in a variety of substrates with C/N = 20–30, whereas in the study of Economou et al. [51], spent mushroom substrate of *P. ostreatus* (C/N = 30) favored the mycelial growth rate of *P. ostreatus* and *P. pulmonarius* (7–8 mm/day). However, in this study, OW and OB were unsuitable substrates for *P. eryngii* growth ($K_r = 1.65$ mm/d). Overall, as K_r data revealed that the addition of LFW had a slightly positive effect or no effect on the colonization of the various substrates tested by the several mushroom strains, it seems feasible to further use this waste in mushroom cultivation.

3.5. Mycelial Mass Production

As stated before, the parameter K_r expresses the hyphal progression on a substrate [79], but not the fungal ability to produce mycelial mass, so in the present study, the concentration of the biomass produced at the end of the colonization stage was estimated by glucosamine content measurement. The equations correlating mycelial mass with glucosamine content for each strain are presented in Table 8. The results showed that the highest biomass production was produced on substrates with the addition of LFW (soaked or sprayed) (Figure 3), probably because excess nitrogen, lipids and several minerals in the medium enhanced biomass production and RW and CR were the substrates where the production of biomass showed a significant increase; e.g., among the coffee substrates, these sprayed with LFW had a notable effect on *P. eryngii*. Particularly, LFW was beneficial to the growth of *Pleurotus* species, as *P. ostreatus* produced a biomass of more than 240 mg/g d.w. of substrate in all the treatments (maximum at RW: 443 mg/g d.w.; CW: 374 mg/g d.w.), while biomass production of *P. eryngii* and *P. pulmonarius* ranged from 186 to 292 mg/g d.w., with the highest values being recorded on OW and OB substrates. The addition of WS to the main substrate was more beneficial for biomass production than the addition of BW, as shown in *P. ostreatus* on CR and RH (soaked with LFW). Also, there was a significant positive effect of spraying LFW in the case of *L. edodes* (maximum at RB: 238 mg/g d.w.). In the current study, *Ganoderma* species presented lower biomass production in CW, CB,

OW and OB than in RW and RB substrates. The data also showed that the spraying method produced a higher biomass amount for *G. resinaceum* (182–292 mg/g, d.w.) compared to *G. lucidum* and *G. applanatum* in these substrates. It is worth noting that the addition of BW in CR resulted in higher values of biomass for *G. lucidum*. Contrariwise, in RW and RB, *G. resinaceum* and *G. lucidum* achieved twofold biomass production values (443–636 mg/g d.w.). Several studies in the past included data on mycelium mass concentration produced on SSFs. For example, Melanouri et al. [27] demonstrated a higher biomass production for *P. eryngii* and *P. ostreatus* grown in substrates containing CR (over 250 mg/g d.w.), but in RH, the biomass production was lower. Dedousi et al. [11] also recorded lower values of *P. ostreatus* biomass in RH substrate, in contrast with this study. However, the high mycelial mass production on grape pomace residue by *P. ostreatus* AMRL 135 (420 mg/g d.w.) shown by Papadaki et al. [35] was like the biomass produced by the same strain on RW in this study. Economou et al. [51] found that with an increase in the C/N ratio, biomass production decreased during SSF of waste mushroom substrate (spent WS), but in our case, with an increase in the C/N ratio, biomass production was enhanced. Regarding biomass production and mycelial growth rate, no correlation between these parameters could be established by examining the present data, although in other studies it has been reported that they are negatively related [27,51,80,81]. Finally, the addition of LFW was shown to have a positive effect on the biomass production of the examined fungi and CR and RH are better than OC in supporting the growth of *Pleurotus* spp., *Ganoderma* spp. and *L. edodes* mushrooms.

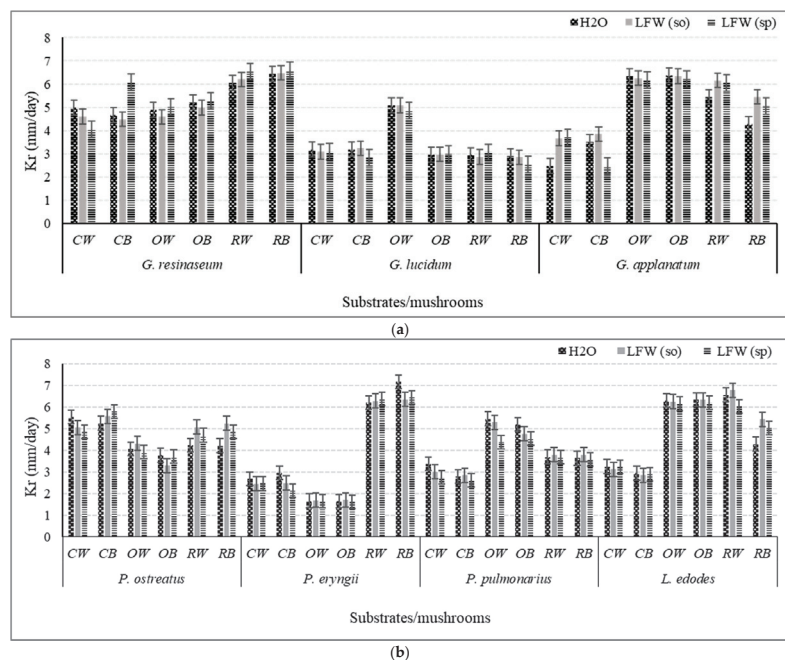


Figure 2. Mycelial growth rates (Kr, mm/d) of *P. ostreatus*, *P. eryngii*, *P. pulmonarius*, *G. applanatum*, *G. resinaceum*, *G. lucidum* and *L. edodes* mushrooms during solid-state fermentation (incubation—colonization stage) in substrates CW (coffee residue + wheat straw), CB (coffee residue + beech wood shavings), OW (olive crop + wheat straw), OB (olive crop + beech wood shavings), RW (rice husk + wheat straw) and RB (rice husk + beech wood shavings) prepared after soaking in lipid fermentation wastewater from *R. toruloides* (LFW) fungal culture or tap water or being sprayed with 20% w/w of LFW at 26 ± 1 °C. Mean values with error bars indicate the standard deviations from duplicate experiments of four replicates.

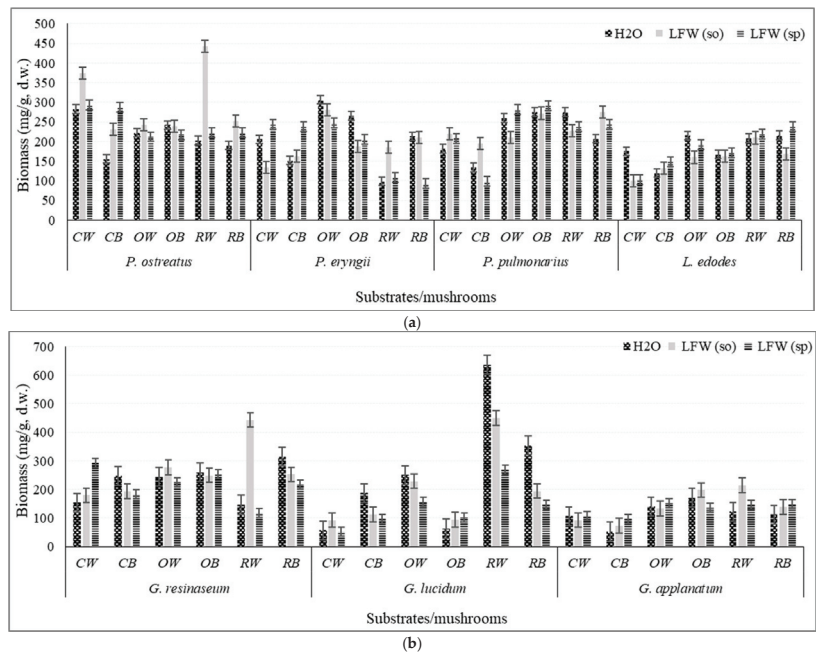


Figure 3. Biomass production (mg/g d.w. substrate) of *P. ostreatus*, *P. eryngii*, *P. pulmonarius*, *G. applanatum*, *G. resinaceum*, *G. lucidum* and *L. edodes* at the final stage of solid-state fermentation (incubation—colonization stage) in substrates CW, CB, OW, OB, RW and RB prepared after soaking in or being sprayed with LFW or tap water at 26 ± 1 °C. Mean values with error bars indicate the standard deviations from duplicate experiments of four replicates.

Table 8. Linear regression equations of glucosamine (mg) and biomass (g) of *Pleurotus*, *Ganoderma* and *Lentinula* species grown on liquid cultures with glucose as main carbon source under static conditions.

Fungi	Equation of Glucosamine mg (x)/Biomass g (y)	R ²
<i>P. ostreatus</i>	$y = 0.0338x - 0.004$	0.975
<i>P. eryngii</i>	$y = 0.0324x - 0.038$	0.993
<i>P. pulmonarius</i>	$y = 0.0509x - 0.022$	0.999
<i>G. applanatum</i>	$y = 0.0168x - 0.009$	0.947
<i>G. lucidum</i>	$y = 0.0467x - 0.031$	0.992
<i>G. resinaceum</i>	$y = 0.0338x - 0.004$	0.994
<i>L. edodes</i>	$y = 0.0594x - 0.049$	0.987

4. Conclusions

Crude glycerol, a by-product of the biodiesel production process, was revealed as a competitive substrate used in the lipid production process by novel *R. toruloides* strains. Cultures at high initial glycerol concentrations and C/N ratios were accompanied by significant biomass and lipid production. Due to the imposed nitrogen limitation, values of lipids and IPS (in DCW) increased with the fermentation time. Cellular lipids contained high concentrations of oleic acid and constituted ideal precursors for the synthesis of second-generation biodiesel. The use of LFWs, as replacements for tap water, in solid-state mushroom cultures where non-conventional substrates were used, proved to be suitable and beneficial for mushroom growth, especially when using the alternative spraying method. These results are in line with the circular economy principles of waste and water reuse, offering new options for environmental protection. Nevertheless, to complete the

investigation, further experiments concerning the impact of these new substrates on the quantity and quality of harvested mushrooms are taking place.

Author Contributions: I.D.: Investigation, Methodology, Formal Analysis, Validation, Data Curation; S.P.: Conceptualization, Project Administration, Writing—Original Draft, Review and Editing; S.M.: Investigation, Methodology, Validation, Data Curation; V.A.: Investigation, Methodology, Validation, Data Curation; P.D.: Conceptualization, Methodology, Data Curation, Writing—Original Draft, Review and Editing. All authors have read and agreed to the published version of the manuscript.

Funding: This current investigation has been co-financed by the European Regional Development Fund of the European Union and Greek national funds (European Social Fund—ESF) through the Operational Program Competitiveness, Entrepreneurship and Innovation, under the call RESEARCH—CREATE-INNOVATE (acronym Addvalue2glycerol, project code: T1EΔK-03002).

Data Availability Statement: Available after request to the cor. authors.

Conflicts of Interest: The authors declare no conflict of interest.

References

1. Valdés, G.; Mendonça, R.T.; Aggelis, G. Lignocellulosic biomass as a substrate for oleaginous microorganisms: A review. *Appl. Sci.* **2020**, *10*, 7698. [CrossRef]
2. Abeln, F.; Chuck, C.J. The history, state of the art and future prospects for oleaginous yeast research. *Microb. Cell Factories* **2021**, *20*, 221. [CrossRef] [PubMed]
3. Bellou, S.; Baeshen, M.N.; Elazzazy, A.M.; Aggeli, D.; Sayegh, F.; Aggelis, G. Microalgal lipids biochemistry and biotechnological perspectives. *Biotechnol. Adv.* **2014**, *32*, 1476–1493. [CrossRef] [PubMed]
4. Ratledge, C.; Cohen, Z. Microbial and algal oils: Do they have a future for biodiesel or as commodity oils. *Lipid Technol.* **2008**, *20*, 155–160. [CrossRef]
5. Qin, L.; Liu, L.; Zeng, A.-P.; Wei, D. From low-cost substrates to single cell oils synthesized by oleaginous yeasts. *Bioresour. Technol.* **2017**, *245*, 1507–1519. [CrossRef]
6. Kothri, M.; Mavrommati, M.; Elazzazy, A.M.; Baeshen, M.N.; Moussa, T.A.; Aggelis, G. Microbial sources of polyunsaturated fatty acids (PUFAs) and the prospect of organic residues and wastes as growth media for PUFA-producing microorganisms. *FEMS Microbiol. Lett.* **2020**, *367*, fnaa028. [CrossRef] [PubMed]
7. Karayannis, D.; Papanikolaou, S.; Vatistas, C.; Paris, C.; Chevalot, I. Yeast lipid produced through glycerol conversions and its use for enzymatic synthesis of amino acid-based biosurfactants. *Int. J. Mol. Sci.* **2022**, *24*, 714. [CrossRef]
8. Bellou, S.; Moustogianni, A.; Makri, A.; Aggelis, G. Lipids containing polyunsaturated fatty acids synthesized by Zygomycetes grown on glycerol. *Appl. Biochem. Biotechnol.* **2012**, *166*, 146–158. [CrossRef]
9. Philippoussis, A.N. Production of mushrooms using agro-industrial residues as substrates. In *Biotechnology for Agro-Industrial Residues Utilisation: Utilisation of Agro-Residues*; Nigam, P.S., Pandey, A., Eds.; Springer: Dordrecht, The Netherlands, 2009; pp. 163–196.
10. Diamantopoulou, P.; Papanikolaou, S.; Kapoti, M.; Komaitis, M.; Aggelis, G.; Philippoussis, A. Mushroom polysaccharides and lipids synthesized in liquid agitated and static cultures. Part I: Screening various mushroom species. *Appl. Biochem. Biotechnol.* **2012**, *167*, 536–551. [CrossRef]
11. Dedousi, M.; Melanouri, E.-M.; Diamantopoulou, P. Carposome Productivity of *Pleurotus ostreatus* and *Pleurotus eryngii* growing on agro-industrial residues enriched with nitrogen, calcium salts and oils. *Carbon. Resour. Convers.* **2023**, *6*, 150–165. [CrossRef]
12. Dedousi, M.; Fourtaka, K.; Melanouri, E.-M.; Argyropoulos, D.; Psallida, C.; Diamantis, I.; Papanikolaou, S.; Diamantopoulou, P. Detoxification of molasses and production of mycelial mass and valuable metabolites by *Morchella* species. *Appl. Sci.* **2021**, *11*, 9481. [CrossRef]
13. Diamantopoulou, P.; Filippousi, R.; Antoniou, D.; Varfi, E.; Xenopoulos, E.; Sarris, D.; Papanikolaou, S. Production of added-value microbial metabolites during growth of yeast strains on media composed of biodiesel-derived crude glycerol and glycerol/xylose blends. *FEMS Microbiol. Lett.* **2020**, *367*, fnaa063. [CrossRef]
14. Kuforiji, O.O.; Fasidi, I.O. Enzyme activities of *Pleurotus tuber-regium* (fries) singer, cultivated on selected agricultural wastes. *Bioresour. Technol.* **2008**, *99*, 4275–4278. [CrossRef]
15. Zhang, R.; Li, X.; Fadel, J.G. Oyster mushroom cultivation with rice and wheat straw. *Bioresour. Technol.* **2002**, *82*, 277–284. [CrossRef] [PubMed]
16. Miles, P.G.; Chang, S.-T. *Mushrooms: Cultivation, Nutritional Value, Medicinal Effect, and Environmental Impact*; CRC Press: Boca Raton, FL, USA, 2004.
17. Wasser, S. Medicinal mushrooms as a source of antitumor and immunomodulating polysaccharides. *Appl. Microbiol. Biotechnol.* **2002**, *60*, 258–274.
18. Wasser, S. Medicinal mushroom science: Current perspectives, advances, evidences, and challenges. *Biomed. J.* **2014**, *37*, 345–356. [CrossRef]

19. Elisashvili, V.I.; Kachlishvili, E.; Asatiani, M.D. Shiitake medicinal mushroom, *Lentinus edodes* (higher basidiomycetes) productivity and lignocellulolytic enzyme profiles during wheat straw and tree leaf bioconversion. *Int. J. Med. Mushrooms* **2015**, *17*, 77–86. [CrossRef] [PubMed]
20. Wasser, S.P. Medicinal mushroom science: History, current status, future trends, and unsolved problems. *Int. J. Med. Mushrooms* **2010**, *12*, 1–16. [CrossRef]
21. Wasser, S.P. Current findings, future trends, and unsolved problems in studies of medicinal mushrooms. *Appl. Microbiol. Biotechnol.* **2011**, *89*, 1323–1332. [CrossRef]
22. Cheung, P.C. Nutritional value and health benefits of mushrooms. *Mushrooms Funct. Foods* **2008**, *2*, 71–109.
23. Oyetayo, O.V.; Ariyo, O.O. Micro and macronutrient properties of *Pleurotus ostreatus* (jacq: Fries) cultivated on different wood substrates. *Jordan J. Biol. Sci.* **2013**, *147*, 1–4. [CrossRef]
24. Baldrian, P.; Valášková, V. Degradation of cellulose by Basidiomycetous fungi. *FEMS Microbiol. Rev.* **2008**, *32*, 501–521. [CrossRef]
25. Kües, U.; Liu, Y. Fruiting body production in basidiomycetes. *Appl. Microbiol. Biotechnol.* **2000**, *54*, 141–152. [CrossRef]
26. Philippoussis, A.; Zervakis, G.; Diamantopoulou, P. Bioconversion of agricultural lignocellulosic wastes through the cultivation of the edible mushrooms *Agrocybe aegerita*, *Volvariella volvacea* and *Pleurotus* spp. *World J. Microbiol. Biotechnol.* **2001**, *17*, 191–200. [CrossRef]
27. Melanouri, E.-M.; Dedousi, M.; Diamantopoulou, P. Cultivating *Pleurotus ostreatus* and *Pleurotus eryngii* mushroom strains on agro-industrial residues in solid-state fermentation. Part I: Screening for growth, endoglucanase, laccase and biomass production in the colonization phase. *Carbon. Resour. Convers.* **2022**, *5*, 61–70. [CrossRef]
28. Ogundele, G.F.; Abdulazeez, R.O.; Bamidele, O.P. Effect of pure and mixed substrate on oyster mushroom (*Pleurotus ostreatus*) cultivation. *J. Exp. Biol. Agric. Sci.* **2014**, *2*, 215–219.
29. Hannon, J.; Zaman, A.U. Exploring the phenomenon of zero waste and future cities. *Urban Sci.* **2018**, *2*, 90. [CrossRef]
30. Coma, M.; Chatzifragkou, A. Chemicals from food supply chain by-products and waste streams. *Molecules* **2019**, *24*, 978. [CrossRef]
31. Pilafidis, S.; Diamantopoulou, P.; Gkatzionis, K.; Sarris, D. Valorization of agro-industrial wastes and residues through the production of bioactive compounds by macrofungi in liquid state cultures: Growing circular economy. *Appl. Sci.* **2022**, *12*, 11426. [CrossRef]
32. Bellettini, M.B.; Fiorda, F.A.; Maieves, H.A.; Teixeira, G.L.; Ávila, S.; Hornung, P.S.; Júnior, A.M.; Ribani, R.H. Factors affecting mushroom *Pleurotus* spp. *Saudi J. Biol. Sci.* **2019**, *26*, 633–646. [CrossRef] [PubMed]
33. Sath, P.K.; Kumar, S.; Chawla, P.; Duhan, J.S. Fermentation: A boon for production of bioactive compounds by processing of food industries wastes (by-products). *Molecules* **2018**, *23*, 2560. [CrossRef]
34. Philippoussis, A.; Diamantopoulou, P.; Israilides, C. Productivity of agricultural residues used for the cultivation of the medicinal fungus *Lentinula edodes*. *Int. Biodeterior. Biodegrad.* **2007**, *59*, 216–219. [CrossRef]
35. Papadaki, A.; Kachrimanidou, V.; Papanikolaou, S.; Philippoussis, A.; Diamantopoulou, P. Upgrading grape pomace through *Pleurotus* spp. cultivation for the production of enzymes and fruiting bodies. *Microorganisms* **2019**, *7*, 207. [CrossRef] [PubMed]
36. Economou, C.; Philippoussis, A.; Diamantopoulou, P. Spent mushroom substrate for a second cultivation cycle of *Pleurotus* mushrooms and dephenolization of agro-industrial wastewaters. *FEMS Microbiol. Lett.* **2020**, *367*, fnaa060. [CrossRef]
37. Hamed, I.; Özogul, F.; Regensteiner, J.M. Industrial applications of crustacean by-products (chitin, chitosan, and chitooligosaccharides): A Review. *Trends Food Sci. Technol.* **2016**, *48*, 40–50. [CrossRef]
38. Sitanggang, A.B.; Sophia, L.; Wu, H.S. Aspects of glucosamine production using microorganisms. *Int. Food Res. J.* **2012**, *19*, 393.
39. Wu, G.; Fang, Y.-Z.; Yang, S.; Lupton, J.R.; Turner, N.D. Glutathione metabolism and its implications for health. *J. Nutr.* **2004**, *134*, 489–492. [CrossRef]
40. Tryfinopoulou, P.; Tsakalidou, E.; Vancanneyt, M.; Hoste, B.; Swings, J.; Nychas, G.J.E. Identification of *Shewanella* spp. strains isolated from Mediterranean fish. *J. Appl. Microbiol.* **2006**, *103*, 711–721.
41. Papanikolaou, S.; Muniglia, L.; Chevalot, I.; Aggelis, G.; Marc, I. *Yarrowia lipolytica* as a potential producer of citric acid from raw glycerol. *J. Appl. Microbiol.* **2002**, *92*, 737–744. [CrossRef]
42. Filippousi, R.; Tsouko, E.; Mordini, K.; Ladakis, D.; Koutinas, A.A.; Aggelis, G.; Papanikolaou, S. Sustainable arabitol production by a newly isolated *Debaryomyces prosopidis* strain cultivated on biodiesel-derived glycerol. *Carbon Resour. Convers.* **2022**, *5*, 92–99. [CrossRef]
43. Kachrimanidou, V.; Kopsahelis, N.; Chatzifragkou, A.; Papanikolaou, S.; Yanniotis, S.; Kookos, I.; Koutinas, A.A. Utilisation of by-products from sunflower-based biodiesel production processes for the production of fermentation feedstock. *J. Waste Manag.* **2013**, *4*, 529–537. [CrossRef]
44. Makri, A.; Fakas, S.; Aggelis, G. Metabolic activities of biotechnological interest in *Yarrowia lipolytica* grown on glycerol in repeated batch cultures. *Bioresour. Technol.* **2010**, *101*, 2351–2358. [CrossRef]
45. Giannakis, N.; Carmona-Cabello, M.; Makri, A.; Leiva-Candia, D.E.; Filippi, K.; Argeiti, C.; Pateraki, C.; Dorado, M.P.; Koutinas, A.A.; Stylianou, E. Spent coffee grounds and orange peel residues based biorefinery for microbial oil and biodiesel conversion estimation. *Renew. Energy.* **2023**, *209*, 382–392. [CrossRef]
46. Argyropoulos, D.; Psallida, C.; Sitareniou, P.; Fletmetakis, E.; Diamantopoulou, P. Biochemical evaluation of *Agaricus* and *Pleurotus* strains in batch cultures for production optimization of valuable metabolites. *Microorganisms* **2022**, *10*, 964. [CrossRef] [PubMed]

47. Apha, A. *Standard Methods for the Examination of Water and Wastewater: Apha Washington*; American Public Health Association: Washington, DC, USA, 1985.
48. Sparks, D.L.; Fendorf, S.E.; Toner IV, C.V.; Carski, T.H. Kinetic methods and measurements. *Methods Soil. Anal. Part 3 Chem. Methods* **1996**, *5*, 1275–1307.
49. Lie, S. The ebc-ninhydrin method for determination of free alpha amino nitrogen. *J. Inst. Brew.* **1973**, *79*, 37–41. [CrossRef]
50. Philippoussis, A.; Diamantopoulou, P.; Zervakis, G. Correlation of the properties of several lignocellulosic substrates to the crop performance of the shiitake mushroom *Lentinula edodes*. *World J. Microbiol. Biotechnol.* **2003**, *19*, 551–557. [CrossRef]
51. Economou, C.; Diamantopoulou, P.; Philippoussis, A. Valorization of spent oyster mushroom substrate and laccase recovery through successive solid state cultivation of *Pleurotus*, *Ganoderma*, and *Lentinula* strains. *Appl. Microbiol. Biotechnol.* **2017**, *101*, 5213–5222. [CrossRef] [PubMed]
52. Evans, C.T.; Ratledge, C. Phosphofructokinase and the regulation of the flux of carbon from glucose to lipid in the oleaginous yeast *Rhodospiridium toruloides*. *Microbiology* **1984**, *130*, 3251–3264. [CrossRef]
53. Evans, C.T.; Ratledge, C. The physiological significance of citric acid in the control of metabolism in lipid-accumulating yeasts. *Biotechnol. Genet. Eng. Rev.* **1985**, *3*, 349–376. [CrossRef]
54. Filippousi, R.; Diamantopoulou, P.; Stavropoulou, M.; Makris, D.P.; Papanikolaou, S. Lipid production by *Rhodospiridium toruloides* from biodiesel-derived glycerol in shake flasks and bioreactor: Impact of initial C/N molar ratio and added onion-peel extract. *Proc. Biochem.* **2022**, *123*, 52–62. [CrossRef]
55. Whiffin, F.; Santomauro, F.; Chuck, C.J. Toward a microbial palm oil substitute: Oleaginous yeasts cultured on lignocellulose. *Biofuel. Bioprod. Biorefin.* **2016**, *10*, 316–334. [CrossRef]
56. Bharathiraja, B.; Sridharana, S.; Sowmya, V.; Yuvaraj, D.; Praveenkumar, R. Microbial oil—A plausible alternate resource for food and fuel application. *Bioresour. Technol.* **2017**, *233*, 423–432. [CrossRef]
57. Diamantopoulou, P.; Sarris, D.; Tchakouteu, S.S.; Xenopoulos, E.; Papanikolaou, S. Growth response of non-conventional yeasts on sugar-rich media: Part 1: High production of lipid by *Lipomyces starkeyi* and citric acid by *Yarrowia lipolytica*. *Microorganisms* **2023**, *11*, 1863. [CrossRef] [PubMed]
58. Bellou, S.; Triantaphyllidou, I.E.; Mizerakis, P.; Aggelis, G. High lipid accumulation in *Yarrowia lipolytica* cultivated under double limitation of nitrogen and magnesium. *J. Biotechnol.* **2016**, *234*, 116–126. [CrossRef]
59. Bellou, S.; Triantaphyllidou, I.-E.; Aggeli, D.; Elazzazy, A.M.; Baeshen, M.N.; Aggelis, G. Microbial oils as food additives: Recent approaches for improving microbial oil production and its polyunsaturated fatty acid content. *Curr. Opin. Biotechnol.* **2016**, *37*, 24–35. [CrossRef]
60. Meesters, P.; Huijberts, G.N.M.; Eggink, G. High-cell-density cultivation of the lipid accumulating yeast *Cryptococcus curvatus* using glycerol as a carbon source. *Appl. Microbiol. Biotechnol.* **1996**, *45*, 575–579. [CrossRef]
61. Liang, Y.; Cui, Y.; Trushenski, J.; Blackburn, J.W. Converting crude glycerol derived from yellow grease to lipids through yeast fermentation. *Bioresour. Technol.* **2010**, *101*, 7581–7586. [CrossRef]
62. Cui, Y.; Blackburn, J.W.; Liang, Y. Fermentation optimization for the production of lipid by *Cryptococcus curvatus*: Use of response surface methodology. *Biomass Bioenergy* **2012**, *47*, 410–417. [CrossRef]
63. Fontanille, P.; Kumar, V.; Christophe, G.; Nouaille, R.; Larroche, C. Bioconversion of volatile fatty acids into lipids by the oleaginous yeast *Yarrowia lipolytica*. *Bioresour. Technol.* **2012**, *114*, 443–449. [CrossRef]
64. Xu, J.; Zhao, X.; Wang, W.; Du, W.; Liu, D. Microbial conversion of biodiesel by-product glycerol to triacylglycerols by oleaginous yeast *Rhodospiridium toruloides* and the individual effect of some impurities on lipid production. *Biochem. Eng. J.* **2012**, *65*, 30–36. [CrossRef]
65. Kiran, E.U.; Trzcinski, A.; Webb, C. Microbial oil produced from biodiesel by-products could enhance overall production. *Bioresour. Technol.* **2013**, *129*, 650–654. [CrossRef]
66. Yang, X.; Jin, G.; Gong, Z.; Shen, H.; Bai, F.; Zhao, Z.K. Recycling biodiesel-derived glycerol by the oleaginous yeast *Rhodospiridium toruloides* Y4 through the two-stage lipid production process. *Biochem. Eng. J.* **2014**, *91*, 86–91. [CrossRef]
67. Tchakouteu, S.S.; Kalantzi, O.; Gardeli, C.; Koutinas, A.A.; Aggelis, G.; Papanikolaou, S. Lipid production by yeasts growing on biodiesel-derived crude glycerol: Strain selection and impact of substrate concentration on the fermentation efficiency. *J. Appl. Microbiol.* **2015**, *118*, 911–927. [CrossRef] [PubMed]
68. Leiva-Candia, D.E.; Tsakona, S.; Kopsahelis, N.; Garcia, I.L.; Papanikolaou, S.; Dorado, M.P.; Koutinas, A.A. Biorefining of by-product streams from sunflower-based biodiesel production plants for integrated synthesis of microbial oil and value-added co-products. *Bioresour. Technol.* **2015**, *190*, 57–65. [CrossRef] [PubMed]
69. Signori, L.; Ami, D.; Posteri, R.; Giuzzi, A.; Mereghetti, P.; Porro, D.; Branduardi, P. Assessing an effective feeding strategy to optimize crude glycerol utilization as sustainable carbon source for lipid accumulation in oleaginous yeasts. *Microb. Cell Factories* **2016**, *15*, 75. [CrossRef] [PubMed]
70. Papanikolaou, S.; Kampsisopoulou, E.; Blanchard, F.; Rondags, E.; Gardeli, C.; Koutinas, A.A.; Chevalot, I.; Aggelis, G. Production of secondary metabolites through glycerol fermentation under carbon-excess conditions by the yeasts *Yarrowia lipolytica* and *Rhodospiridium toruloides*. *Eur. J. Lipid Sci. Technol.* **2017**, *119*, 1600507. [CrossRef]
71. Uprety, B.K.; Samavi, M.; Rakshit, S.K. Contribution of specific impurities in crude glycerol towards improved lipid production by *Rhodospiridium toruloides* ATCC 10788. *Bioresour. Technol. Rep.* **2018**, *3*, 27–34. [CrossRef]

72. Kamal, R.; Liu, Y.; Li, Q.; Huang, Q.; Wang, Q.; Yu, X.; Zhao, Z.K. Exogenous L-proline improved *Rhodospiridium toruloides* lipid production on crude glycerol. *Biotechnol. Biofuels* **2020**, *13*, 159. [CrossRef]
73. Iqbal, M.; Shah, A.A. Effect of CaCO₃ on substrate of *Pleurotus Sajor-Caju*. *Sarhad J. Agric.* **1989**, *5*, 359–361.
74. Sarker, N.C.; Hossain, M.M.; Sultana, N.; Mian, I.H.; Karim, A.; Amin, S.M.R. Effect of different levels of pH on the growth and yield of *Pleurotus ostreatus* (Jacquin Ex. Fr.) kummer. *Bangladesh J. Mush* **2007**, *1*, 57–62.
75. Hoa, H.T.; Wang, C.-L.; Wang, C.-H. The Effects of different substrates on the growth, yield, and nutritional composition of two oyster mushrooms (*Pleurotus ostreatus* and *Pleurotus cystidiosus*). *Mycobiology* **2015**, *43*, 423–434. [CrossRef] [PubMed]
76. Liang, C.-H.; Wu, C.-Y.; Lu, P.-L.; Kuo, Y.-C.; Liang, Z.-C. Biological efficiency and nutritional value of the culinary-medicinal mushroom *Auricularia* cultivated on a sawdust basal substrate supplement with different proportions of grass plants. *Saudi J. Biol. Sci.* **2019**, *26*, 263–269. [CrossRef]
77. Dedousi, M.; Melanouri, E.-M.; Karayannis, D.; Kaminarides, E.-I.; Diamantopoulou, P. Utilization of spent substrates and waste products of mushroom cultivation to produce new crops of *Pleurotus ostreatus*, *Pleurotus eryngii* and *Agaricus bisporus*. *Carbon. Resour. Convers.* **2023**, *in press*. [CrossRef]
78. D'Agostini, É.C.; Mantovani, T.R.D.; do Valle, J.S.; Paccola-Meirelles, L.D.; Colauto, N.B.; Linde, G.A. Low Carbon/Nitrogen ratio increases laccase production from basidiomycetes in solid substrate cultivation. *Sci. Agric.* **2011**, *68*, 295–300. [CrossRef]
79. Zervakis, G.; Philippoussis, A.; Ioannidou, S.; Diamantopoulou, P. Mycelium growth kinetics and optimal temperature conditions for the cultivation of edible mushroom species on lignocellulosic substrates. *Folia Microbiol.* **2001**, *46*, 231–234. [CrossRef]
80. Philippoussis, A.; Diamantopoulou, P.; Papadopoulou, K.; Lakhtar, H.; Roussos, S.; Parissopoulos, G.; Papanikolaou, S. Biomass, laccase and endoglucanase production by *Lentinula edodes* during solid state fermentation of reed grass, bean stalks and wheat straw residues. *World J. Microbiol. Biotechnol.* **2011**, *27*, 285–297. [CrossRef]
81. Philippoussis, A.; Diamantopoulou, P. Exploitation of the biotechnological potential of agro-industrial by-products through mushroom cultivation. In *Mushroom Biotechnology and Bioengineering*; Petre, M., Berovic, M., Eds.; University of Pitesti, CD Publishing House: Bucuresti, Romania, 2012; pp. 161–184. ISBN 978-606-528-146-2.

Disclaimer/Publisher's Note: The statements, opinions and data contained in all publications are solely those of the individual author(s) and contributor(s) and not of MDPI and/or the editor(s). MDPI and/or the editor(s) disclaim responsibility for any injury to people or property resulting from any ideas, methods, instructions or products referred to in the content.

Article

Screening of Microbial Strains Used to Ferment *Dendrobium officinale* to Produce Polysaccharides, and Investigation of These Polysaccharides' Skin Care Effects

Xin Tang^{1,2}, Bulei Wang^{1,2}, Bingyong Mao^{1,2}, Jianxin Zhao^{1,2}, Guangrong Liu³, Kaiye Yang^{3,*} and Shumao Cui^{1,2,*}

- ¹ State Key Laboratory of Food Science and Resources, Jiangnan University, Wuxi 214122, China; 7210112101@stu.jiangnan.edu.cn (B.W.); zhaojianxin@jiangnan.edu.cn (J.Z.)
² School of Food Science and Technology, Jiangnan University, Wuxi 214122, China
³ Infinitus (China) Co., Ltd., Guangzhou 510423, China; jim.liu@infinitus-int.com
* Correspondence: kyle.yang@infinitus-int.com (K.Y.); cuishumao@jiangnan.edu.cn (S.C.)

Abstract: The microbial fermentation of plants is a promising approach for enhancing the yield of polysaccharides with increased activity. In this study, ten microbial strains, *Lactiplantibacillus plantarum* CCFM8661, *Limosilactobacillus reuteri* CCFM8631, *Lactobacillus helveticus* M10, *Lactocaseibacillus rhamnosus* CCFM237, *Lactilactobacillus sakei* GD17-9, *Lactocaseibacillus casei* CCFM1073, *Bacillus subtilis* CCFM1162, *Bacteroides cellulosilyticus* FTJSI-E-2, *Bacteroides stercoris* FNMHLBEIK-4, and *Saccharomyces cerevisiae* HN7-A5, were used to ferment *Dendrobium officinale*. The skin care activity of the resulting polysaccharides (F-DOP) was evaluated in cultured HaCaT and RAW 264.7 cells, and a mouse model. The results indicated that *D. officinale* medium promoted strain proliferation, and fermentation significantly enhanced polysaccharide yield (up to 1.42 g/L) compared to that without fermentation (0.76 g/L). Moreover, F-DOPs, especially after CCFM8631 fermentation, exhibited an excellent ability to attenuate sodium dodecyl sulfate-induced HaCaT cell injury (from 69.04 to 94.86%) and decrease nitric oxide secretion (from 42.86 to 22.56 μ M) in lipopolysaccharide-stimulated RAW 264.7 cells. In vivo, CCFM8631-FDOP reduced the transdermal water loss rate, skin epidermal thickness, and interleukin 6, and enhanced the expression of filaggrin, improving 2,4-dinitrofluorobenzene-induced skin damage. Therefore, considering viable cell counts, polysaccharide yields, and skin care efficacy in vitro and in vivo, CCFM8631 is the most suitable strain to enhance the skin care activity of DOPs and possesses promising potential for applications in the cosmetics industry.

Keywords: *Dendrobium officinale*; fermentation; *Limosilactobacillus reuteri* CCFM8631; polysaccharides

Citation: Tang, X.; Wang, B.; Mao, B.; Zhao, J.; Liu, G.; Yang, K.; Cui, S. Screening of Microbial Strains Used to Ferment *Dendrobium officinale* to Produce Polysaccharides, and Investigation of These Polysaccharides' Skin Care Effects. *Processes* **2023**, *11*, 2563. <https://doi.org/10.3390/pr11092563>

Academic Editors: Ali Demirci, Irfan Turhan and Ehsan Mahdinia

Received: 24 July 2023
Revised: 17 August 2023
Accepted: 24 August 2023
Published: 27 August 2023



Copyright: © 2023 by the authors. Licensee MDPI, Basel, Switzerland. This article is an open access article distributed under the terms and conditions of the Creative Commons Attribution (CC BY) license (<https://creativecommons.org/licenses/by/4.0/>).

1. Introduction

Dendrobium officinale, belonging to the family Orchidaceae, is widely distributed in several countries worldwide, including China, Japan, and Australia [1]. In China, *D. officinale* has been recognized as one of the most valuable traditional Chinese medicines (TCMs) for thousands of years. TCM practitioners believe that *D. officinale* offers a wide range of health benefits, such as fever reduction, stomach nourishment, and lifespan extension [2]. Modern pharmaceutical studies have revealed multiple bioactivities associated with *D. officinale*, such as immune-regulatory, antitumor, cardioprotective, and anti-aging bioactivities [3]. Owing to its exceptional nutritional value, *D. officinale* is considered a life-saving herb [4].

As a complex botanical matrix, *D. officinale* is rich in polysaccharides, flavonoids, alkaloids, pigments, and other small-molecule components [3,5,6]. Among these constituents, *D. officinale* polysaccharides (DOPs), such as glucomannan with 1,4- β -D-Manp and 1,4- β -D-Glcp, the main active component with antioxidant, moisturizing, and hair growth-promoting effects, have a great potential in functional foods and cosmetics [7]. However, studies investigating the structure–bioactivity relationship of polysaccharides

have suggested that the original polysaccharide structures present in plants may not exhibit optimal bioactivities [8]. Therefore, it is crucial to develop a suitable method to improve the yield and biological activity of DOPs.

Microbial fermentation has emerged as a promising biomodification technology for natural products and has garnered increasing attention. During fermentation, microorganisms produce a large number of extracellular enzymes, such as proteases, cellulases, glycosidases, and pectinases. These enzymes rupture plant cells and accelerate the dissolution of active ingredients, resulting in improved polysaccharide yield. Additionally, during fermentation, microorganisms can transform the original polysaccharides into novel fermented polysaccharides with enhanced bioactivity [9]. A previous study where *Panax ginseng* was fermented with *Saccharomyces cerevisiae* GIW-1 reported that fermentation increased the yield of polysaccharides while also enhancing their in vitro antioxidant capacity (by scavenging hydroxyl and superoxide anion free radicals) and in vivo anti-inflammatory effects (by reducing tumor necrosis factor (TNF)- α , interleukin (IL)-1 β , and IL-6 content) [10]. *Bacillus* sp. DU-106 fermentation altered the Mw and monosaccharide composition of DOPs, which enhanced the immunoregulatory ability of DOPs [11].

The skin, the largest organ in the body, plays a critical role in protecting the internal environment and maintaining homeostasis [12]. However, prolonged exposure to UV radiation, air pollution, and harmful organisms can damage the skin structure, leading to abnormalities in the skin barrier. Unfortunately, a compromised function of the skin barrier is often accompanied by dysregulated dermal immune responses, which in turn exacerbate damage to the skin barrier, creating a vicious cycle [13]. DOPs, which help maintain the integrity of the skin barrier and normalize immune responses, have the potential to promote skin health [14]. However, reports on the yields and bioactivities of polysaccharides derived from strains fermenting *D. officinale* are limited and fragmented. Therefore, the objective of this study was to obtain a strain that enhanced the skin care properties of DOPs. This study aimed to facilitate the application of microbial fermentation in herbal medicine and provide a theoretical foundation for the development of novel skin care products.

2. Materials and Methods

2.1. Chemicals and Reagents

The stems of *D. officinale*, provided by Nutri-Woods Bio-tech Co., Ltd. (Beijing, China), were crushed (60 mesh). Yeast extract FM528 was purchased from Angel Yeast Co., Ltd. (Yichang, China). Sodium dodecyl sulfate (SDS), methyl thiazolyl tetrazolium (MTT), and dimethyl sulfoxide (DMSO) were purchased from Beijing Solarbio Science & Technology Co., Ltd. (Beijing, China). Lipopolysaccharide (LPS) was obtained from Sigma-Aldrich Co., Ltd. (St. Louis, MO, USA). The enzyme-linked immunosorbent assay (ELISA) kits for nitric oxide (NO), filaggrin (FLG), and interleukin (IL)-6 were purchased from Jiangsu Meibiao Biotechnology Co., Ltd. (Yancheng, China). The other chemicals used in this study were of analytical grade and were purchased from Sinopharm Chemical Reagent Co., Ltd. (Shanghai, China).

2.2. Screening of Strains for Fermenting DOPs

2.2.1. Activation and Culture of Strains

The Lactobacillus (*L. plantarum* CCFM8661, *L. helveticus* M10, *L. rhamnosus* CCFM237, *L. reuteri* CCFM8631, *L. sakei* GD17-9, *L. casei* CCFM1073), Bacillus (*B. subtilis* CCFM1162), Bacteroides (*B. cellulosilyticus* FTJSI-E-2, *B. stercoris* FNMHLBEIK-4), and yeast (*S. cerevisiae* HN7-A5) strains were obtained from Culture Collection of Food Microorganisms of Jiangnan University and cultured in specific media. Lactobacillus strains were cultured in MRS medium containing 20 g/L glucose, 5 g/L yeast extract, 10 g/L tryptone, 10 g/L beef extract, 2 g/L sodium acetate, 0.58 g/L MgSO₄·7H₂O, 0.25 g/L MnSO₄·H₂O, 2 g/L ammonium citrate dibasic, 2.6 g/L K₂HPO₄·3H₂O, and 1 mL/L Tween 80. Bacillus strains were cultured in LB medium containing 10 g/L tryptone, 10 g/L yeast extract, and 10 g/L NaCl. Bacteroides strains were cultured in BHI medium containing 38.5 g/L brain heart

infusion, 1 g/L L-cysteine, 1 g/L hemin, and 1 g/L vitamin K. *Saccharomyces cerevisiae* was cultured in YPD medium containing 10 g/L yeast extract, 10 g/L tryptone, and 20 g/L glucose. Each strain was streaked onto its corresponding solid medium and incubated to obtain single colonies. After incubation, a single colony was picked and inoculated twice into liquid medium to obtain highly viable seed cultures for further experiments.

2.2.2. Fermentation of *D. officinale*

For the fermentation process, *D. officinale* (40 g/L) was used as the single carbon source (replacing glucose) to prepare *D. officinale*-based MRS, LB, BHI, and YPD media. The activated strains (10^7 CFU/mL) were inoculated into the corresponding *D. officinale*-based medium. The *Lactobacillus*, *Bacillus*, and *Bacteroides* strains were cultured at 37 °C and pH 6.0 for 16 h, and the yeast was cultured at 30 °C and pH 6.0 for 48 h. Sterile water was used instead of the microorganisms in the unfermented group. At the end of fermentation, the cell counts of the strains were determined using the plate dilution method [15], and the fermentation solutions were collected for polysaccharide extraction.

2.2.3. Extraction of DOPs and F-DOP

Polysaccharides' extraction was performed using an ultrasonic-assisted method, according to a previous report [16]. The *D. officinale* fermentation solution was sonicated at a power level of 500 W for 10 min. The resulting supernatant was collected by centrifugation ($8000\times g$ for 15 min), deproteinated using Sevag reagent, precipitated by adding four volumes of ethanol at 4 °C for 24 h, and lyophilized to obtain DOPs (polysaccharides from non-fermented *D. officinale*) and F-DOPs (polysaccharides from fermented *D. officinale* solution). The total carbohydrate content was determined using the anthrone–sulfuric acid method [17].

2.3. Evaluation of F-DOPs Skin Care Effects In Vitro

2.3.1. Cell Culture

Human-immortalized keratinocytes (HaCaT cells) and mouse mononuclear macrophages (RAW 264.7 cells) were purchased from China Center for Type Culture Collection (Wuhan, China). The cells were cultured in Dulbecco's Modified Eagle Medium (DMEM), containing 10% fetal bovine serum (FBS) (Gibco, Billings, MT, USA) and incubated at 37 °C in a 5% CO₂ atmosphere. Prior to use, the polysaccharide samples were dissolved in the culture medium and sterilized by passage through a 0.22 µm membrane filter.

2.3.2. Cytoprotection of SDS-Injured HaCaT Cell

SDS, the most-used anionic alkyl sulfate surfactant, was used to induce skin barrier damage [18]. Log-phase HaCaT cells (5×10^3 cells/well) were collected, seeded in a 96-well plate, and divided into three groups: (1) control group (medium), (2) model group (SDS), and (3) treated group (DOP/F-DOP + SDS). After incubating for 12 h, the cells were pretreated with various polysaccharide samples (1000 µg/mL) for 24 h. Subsequently, the cells were exposed to SDS (50 µg/mL) for 24 h. Cell survival was determined using the CCK-8 assay.

2.3.3. Anti-Inflammation in LPS-Induced RAW 264.7 Cell

The anti-inflammatory properties of the polysaccharide samples were characterized using an NO content assay in LPS-stimulated RAW 264.7 cells [19]. Logarithmic phase cells (5×10^3 cells/well) were collected, seeded in a 96-well plate, and divided into three groups: (1) control group (medium), (2) model group (LPS), and (3) treated group (DOP/F-DOP + LPS). After incubation for 12 h, the RAW 264.7 cells were pretreated with various polysaccharide samples (1000 µg/mL) for 24 h. The cells were then stimulated with LPS (5 g/mL) for 24 h. The culture supernatants were collected, and the NO content was measured using a commercial NO assay kit, according to the manufacturer's instructions.

2.4. Evaluation of F-DOPs Skin Care Effects In Vivo

2.4.1. Preparation of F-DOP-Based Ointment

The ingredients of the DOP/F-DOP ointments are listed in Table 1. Briefly, the oil phase (shark squalene and emulsifier), aqueous phase I (DOP/F-DOP, glycerin, and water), and aqueous phase II (nipagin ethyl ester and water at 90 °C) were prepared. Subsequently, aqueous phases I and II were slowly added to the oil phase and stirred continuously to obtain a DOP/F-DOP-based ointment [20].

Table 1. *Dendrobium officinale* polysaccharide (DOP)-based ointment composition and function of each ingredient in the formulation.

Added Material	Amount Added (g)	Function
Unfermented/Fermented DOP	1.50	The main drug
Shark squalene	3.90	Oil phase
Emulsifier (Montanov S)	2.10	Surfactant
Glycerin	2.40	Water phase, humectant
Nipagin ethyl ester	0.03	Preservative
Distilled water	Volume to 30.00	Solvent

2.4.2. Animals and Experimental Design

Specific pathogen-free BALB/c male mice (6–8 weeks old, 18–20 g) were purchased from the Guangdong Medical Laboratory Animal Center (Foshan, China). The mice were housed under standard conditions with ad libitum access to standard food and water. The housing environment maintained a constant temperature of 25 ± 2 °C, humidity of $50 \pm 10\%$, and a 12-h light/dark cycle. Following acclimation for one week, the mice were prepared for experimentation. The dorsal skin of each mouse, measuring 4 cm \times 2 cm, was shaved. The mice were then randomly divided into five groups, each containing five mice: (A) normal control group (NC), (B) model control group (MC), (3) unfermented DOP cream treatment group (DOP), (C) CCFM8631-FDOP cream treatment group (CCFM8631), and (D) prednisolone cream treatment group as a positive control (PC). The experimental animal use license was approved by SYXK (Guangdong) 2018-0186.

2.4.3. Induction of Skin Damage Model

The 2,4-dinitrofluorobenzene (DNFB)-induced skin damage in vivo model was established as previously described [21]. Briefly, 100 μ L of 0.25% DNFB (*w/v*) dissolved in a 3:1 mixture of acetone/olive oil was painted onto the dorsal skin of each mouse on days 1 and 4. Furthermore, the same skin area was exposed to 100 μ L of 0.2% DNFB on days 7 and 10 to induce skin injury (MC group). The NC group was treated with acetone/olive oil only. The DOP, CCFM8631, and PC groups were administered DOP/F-DOP-based ointment or prednisolone cream in DNFB-injured mice twice a day from day 7 to day 15, respectively.

2.4.4. Macroscopic Observation and Transepidermal Water Loss (TEWL) Test

On day 16, all mice were transferred to a room with controlled temperature (23 ± 1 °C) and humidity ($50 \pm 10\%$). The dorsal skin of each mouse was photographed to evaluate the morphological changes in tissue appearance. Moreover, TEWL, an important indicator reflecting the integrity of the skin barrier and tissue gas exchange with the environment, was measured by the Tewameter[®] TM 300 (Courage & Khazaka, Cologne, Germany).

2.4.5. Hematoxylin and Eosin (H&E) Staining

At the end of the experiment, all mice were euthanized by cervical dislocation. Dorsal skin samples were collected and divided into two sections. One portion was immediately immersed in 4% paraformaldehyde for histological observation, and the other was stored at -80 °C for further analysis. The fixed skin samples were embedded in paraffin, sliced into 6- μ m-thick sections, and stained with hematoxylin and eosin for histopathological assess-

ment, as described in a previous study [22]. The H&E-stained sections were observed under an optical microscope, and the epidermal thickness was measured using ImageJ software.

2.4.6. Biochemical Assays

Skin tissue samples were weighed (0.1 g), homogenized in normal saline (1 mL), and centrifuged at $12,000 \times g$ for 15 min at 4°C to obtain the tissue supernatant. Protein content was determined using the BCA method using bovine serum albumin (BSA) as a standard [23]. The levels of FLG and IL-6 were measured using ELISA kits.

2.5. Statistical Analysis

All results of this study are expressed as means \pm standard deviation (SD). Statistical significance was determined using SPSS software (version 23.0) with one-way analysis of variance followed by Tukey's test. Origin 2023 software was employed for the preparation of graphs. Different letters mean $p < 0.05$, which was considered statistically significant for all analyses.

3. Results and Discussion

3.1. Determination of Viable Cell Counts and Polysaccharide Yields

The ten strains were cultivated in *D. officinale*-based medium, and the viable cell counts after fermentation are shown in Table 2. Supplementation with *D. officinale* increased the proliferation of various strains. The viable cell counts of *B. cellulosilyticus* FTJJSI-E-2, *B. subtilis* CCFM1162, *L. casei* CCFM1073, *B. stercoris* FNMHLBEIK-4, *L. plantarum* CCFM8661, *L. reuteri* CCFM8631, and *L. sakei* GD17-9 were 130×10^7 , 100×10^7 , 45×10^7 , 35×10^7 , 19×10^7 , 16×10^7 , and 10×10^7 CFU/mL, respectively.

Table 2. Viable cell counts and polysaccharide yields from *D. officinale* fermented by different strains.

Strains	Viable Cell Counts ($\times 10^7$)/(CFU/mL)	Polysaccharides Yield (g/L)
<i>L. plantarum</i> CCFM8661	19.0 ± 1.41 cde	1.40 ± 0.04 a
<i>L. helveticus</i> M10	2.1 ± 0.42 e	1.41 ± 0.06 a
<i>L. rhamnosus</i> CCFM237	7.2 ± 0.14 e	1.36 ± 0.03 ab
<i>L. reuteri</i> CCFM8631	16.0 ± 1.41 de	1.30 ± 0.04 abc
<i>L. sakei</i> GD17-9	10.0 ± 1.41 de	1.36 ± 0.06 ab
<i>L. casei</i> CCFM1073	45.0 ± 5.66 c	1.23 ± 0.04 bc
<i>B. subtilis</i> CCFM1162	100.0 ± 14.14 b	0.32 ± 0.01 d
<i>B. cellulosilyticus</i> FTJJSI-E-2	130 ± 14.14 a	1.24 ± 0.01 bc
<i>B. stercoris</i> FNMHLBEIK-4	35.0 ± 2.83 cd	1.20 ± 0.01 c
<i>S. cerevisiae</i> HN7-A5	3.4 ± 0.14 e	1.42 ± 0.04 a

Statistical analysis with one-way analysis of variance (ANOVA) followed by post hoc multiple comparison analysis with the Tukey test. Different letters indicate significant differences among different groups ($p < 0.05$).

Moreover, the F-DOP yield after fermentation was determined and is illustrated in Table 2. Fermentation by the strains enhanced the F-DOP yield compared to that of DOPs. Strains in descending order of F-DOP yield were as follows: *S. cerevisiae* HN7-A5 (1.42 g/L), *L. helveticus* M10 (1.41 g/L), *L. plantarum* CCFM8661 (1.4 g/L), *L. rhamnosus* CCFM237 (1.36 g/L), *L. sakei* GD17-9 (1.36 g/L), and *L. reuteri* CCFM8631 (1.3 g/L). Based on the viable cell count and F-DOP yield, *L. plantarum* CCFM8661, *L. reuteri* CCFM8631, *L. casei* CCFM1073, *B. subtilis* CCFM1162, *B. cellulosilyticus* FTJJSI-E-2, and *S. cerevisiae* HN7-A5 were considered suitable strains for fermenting *D. officinale*. These F-DOPs were selected to evaluate their skin care effects in subsequent experiments. Our results indicated that the ten strains could grow in medium containing *D. officinale* as the sole carbon source, albeit with varying degrees of specificity among the strains. Additionally, the fermentation of *D. officinale* by these strains resulted in an increased polysaccharide yield. Similarly, it was reported that the polysaccharide yield from *Astragalus membranaceus* was 2.3-fold higher with *Lactobacillus plantarum* fermentation than without it [24].

3.2. Skin Care Effects of F-DOPs In Vitro

HaCaT cells maintain a normal keratinocyte shape and are commonly used to evaluate the skin protection of cosmetics, medicines, and food products [25]. Moreover, RAW 264.7 cells have a stable and mature adherent macrophage phenotype and are frequently employed to investigate the immune regulatory abilities and innate immune responses of samples [26].

SDS is an anionic surfactant widely used in household cleaning, cosmetics, and pharmaceutical products. However, prolonged exposure to SDS can disrupt cell membranes, leading to barrier disruption and skin irritation [27,28]. As presented in Figure 1, after treatment with 50 $\mu\text{g}/\text{mL}$ SDS for 24 h, the percent survival of HaCaT cells was significantly decreased (69.04%) compared to that of the control group, suggesting that the cell injury model was successfully established. Both DOP and F-DOP treatments attenuated SDS-induced cell injury and remarkably increased cell viability. F-DOPs exhibited superior cyto-protection compared with DOPs. In particular, F-DOPs produced from *L. reuteri* CCFM8631 fermentation resulted in the highest cell viability (94.86%) among all groups.

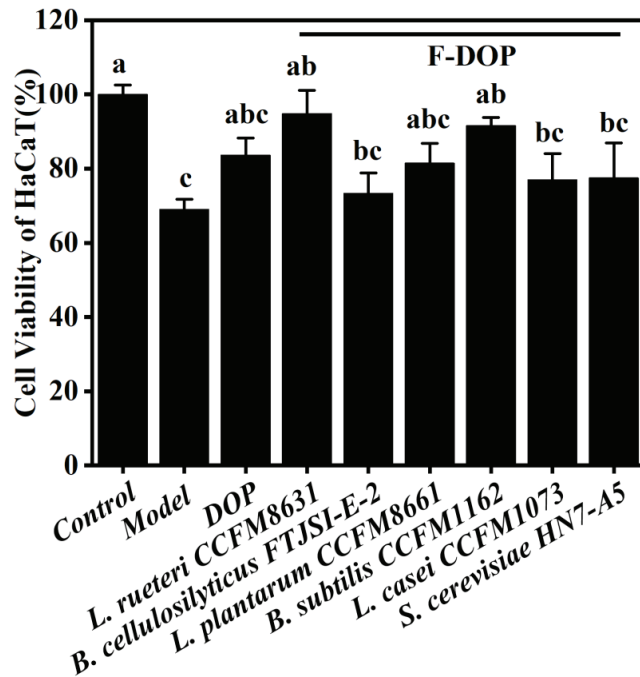


Figure 1. Effect of DOPs and fermented *Dendrobium officinale* polysaccharides (F-DOPs) on survival in sodium dodecyl sulfate (SDS)-injured HaCaT cells. Statistical analysis with one-way analysis of variance (ANOVA) followed by post hoc multiple comparison analysis with the Tukey test. Different letters indicate significant differences among different groups ($p < 0.05$).

LPS is known to bind to Toll-like receptors and activate NF- κ B through the MyD88-dependent signaling pathway, leading to the secretion of inflammatory mediators, such as TNF- α , IL-6, and NO [29]. As expected, after 24 h of LPS treatment in RAW264.7 cells, the NO content in the model group was 42.86 μM , which was significantly higher than that of the control group (13.42 μM) (Figure 2). However, this abnormal increase was inhibited by F-DOP supplementation. Specifically, F-DOPs after *L. reuteri* CCFM8631, *L. plantarum* CCFM8661, and *L. casei* CCFM1073 fermentation remarkably decreased the NO content to 22.56, 22.00, and 18.40 μM , respectively, indicating the outstanding anti-inflammatory activity of the F-DOPs. *L. reuteri* CCFM8631 was selected as the most suitable strain for the

fermentation of *D. officinale* based on the number of living bacteria, polysaccharide yield, and cell culture experiment results.

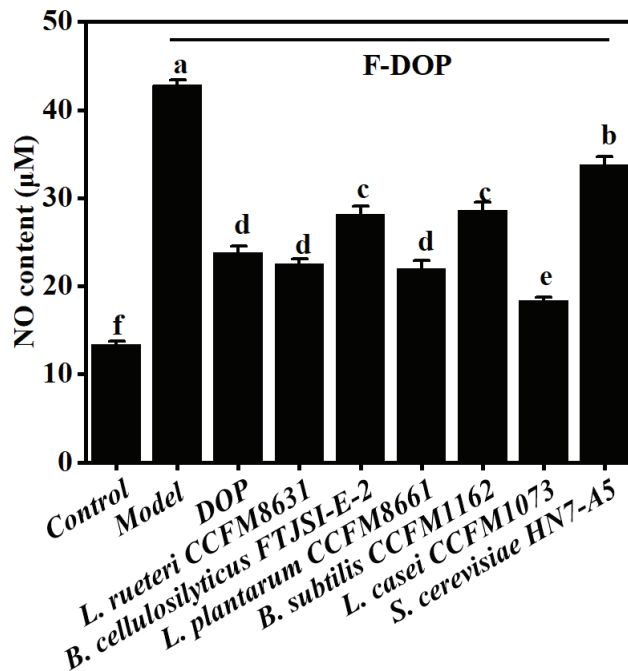


Figure 2. Effect of DOPs and F-DOPs on nitric oxide (NO) content in LPS-stimulated RAW 264.7 cells. Statistical analysis with one-way analysis of variance (ANOVA) followed by post hoc multiple comparison analysis with the Tukey test. Different letters indicate significant differences among different groups ($p < 0.05$).

Polysaccharides have attracted considerable attention owing to their low toxicity and diverse pharmacological activities [30]. A previous review summarized that DOPs decrease free radicals (2,2-diphenyl-1-picrylhydrazyl and hydroxyl), enhance antioxidant systems (superoxide dismutase, catalase, and glutathione peroxidase), inhibit the NF- κ B pathway, and downregulate inflammatory responses, having potential applications in the field of skin care and cosmetics [7]. Consistent with previous findings, our study also demonstrated that pretreatment with DOPs protected HaCaT cells from SDS-induced damage and decreased NO production in RAW 264.7 cells in LPS-induced inflammatory model. Interestingly, fermentation increased the polysaccharide yield of *D. officinale* and improved its antioxidant and anti-inflammatory activities. Yang et al. reported that *Polygonatum kingianum* polysaccharides fermented by *Lactobacillus casei* resulted in superior anti-aging effects on *Caenorhabditis elegans*, with a 10.09% increase in lifespan compared with that resulting from the original polysaccharides. This improvement could be attributed to a decrease in molecular weight distribution, a change in chemical and monosaccharide composition, and the smoothness of the microtopography [8]. The beneficial effects on skin health of DOPs and F-DOPs (fermented by *L. reuteri* CCFM8631) were investigated in a DNFB-induced injury model in vivo, which is described in Section 3.3.

3.3. Skin Care Effects of F-DOPs In Vivo

3.3.1. Apparent Skin Changes and H&E Staining

Representative skin images of the different groups are shown in Figure 3A. Repeated application of DNFB to the dorsal surface resulted in severe skin lesions characterized

by redness, swelling, crust formation, dryness, and incrustation, indicating the successful establishment of the skin damage model (MC group). However, these symptoms in the MC group were relieved by pretreatment with the DOP and F-DOP ointments. Notably, the CCFM8631 group showed better attenuation of skin damage than the DOP group, similar to that of the PC group.

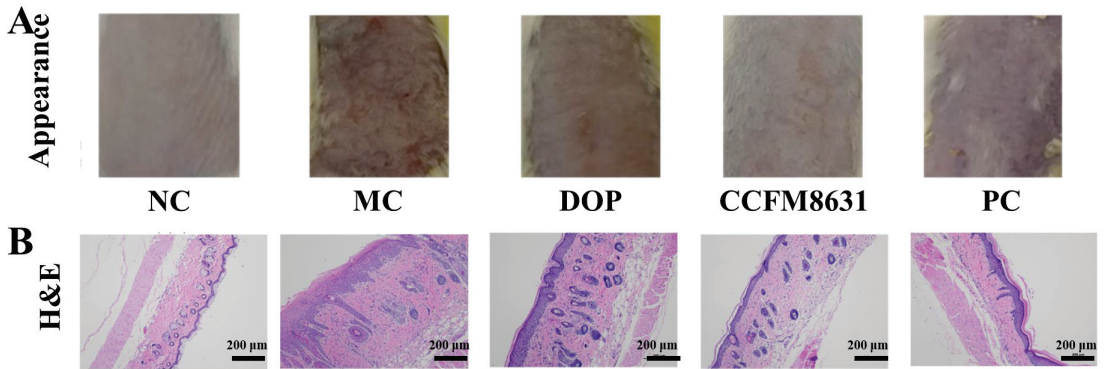


Figure 3. Effects of samples on (A) skin appearance and (B) hematoxylin and eosin staining in the DNFB-damaged model in vivo.

H&E staining was performed to examine structural changes in the skin tissue of each group. In the NC group, a distinct stratum corneum, thin stratified squamous epithelium, and well-organized and tightly arranged cells in the epidermis, with no apparent pathological alterations were observed (Figure 3B). After modeling with DNFB, the skin tissue structure was disrupted and was characterized by a thickened stratified squamous epithelium, disordered cell arrangement, and infiltration of inflammatory cells. Compared with the MC group, treatment with CCFM8631-FDOP, like the PC group, mitigated dorsal swelling and inflammatory infiltrating, which exhibited superior effects than the DOP group. Moreover, the epidermal thickness of the mouse skin was measured to further evaluate the skin protection of the samples. As shown in Figure 4, the epidermal thickness was significantly increased from 20 µm in the NC group to 199 µm in the MC group. Both DOP and CCFM8631-FDOP treatment decreased the epidermal thickness compared to that in the control group. In the CCFM8631 group, the epidermal thickness was 47 µm, which was better than that of the PC group (60 µm). These results indicate that the F-DOPs produced by CCFM8631 fermentation have the potential to alleviate DNFB-induced skin damage.

3.3.2. Change in TEWL

TEWL is an indirect measure of skin barrier integrity because it reflects the rate of water evaporation from the skin surface. Normally, the skin maintains a constant range of water loss. However, when its barrier function is compromised, water loss increases [31,32]. As shown in Figure 5, TEWL was significantly higher in the MC group (40.13%) than in the NC group (14.60%), indicating skin barrier damage. In the DOP, CCFM8631, and PC groups, TEWL values decreased to 28.63%, 27.68%, and 18.68%, respectively, suggesting that the samples could help restore skin barrier function.

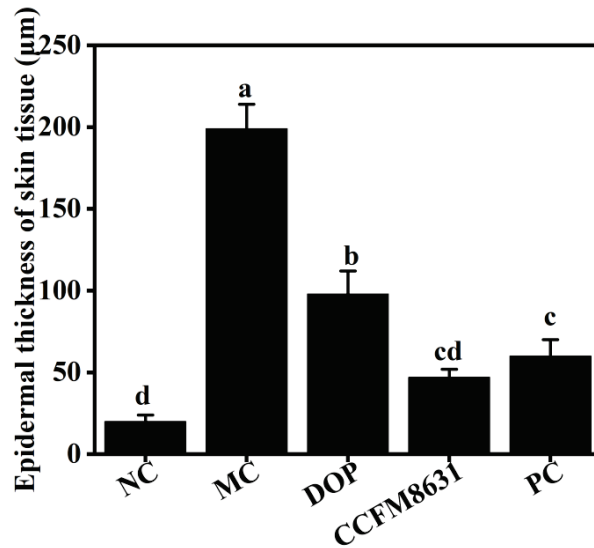


Figure 4. Changes in epidermal thickness of skin tissue. Statistical analysis with one-way analysis of variance (ANOVA) followed by post hoc multiple comparison analysis with the Tukey test. Different letters indicate significant differences among different groups ($p < 0.05$).

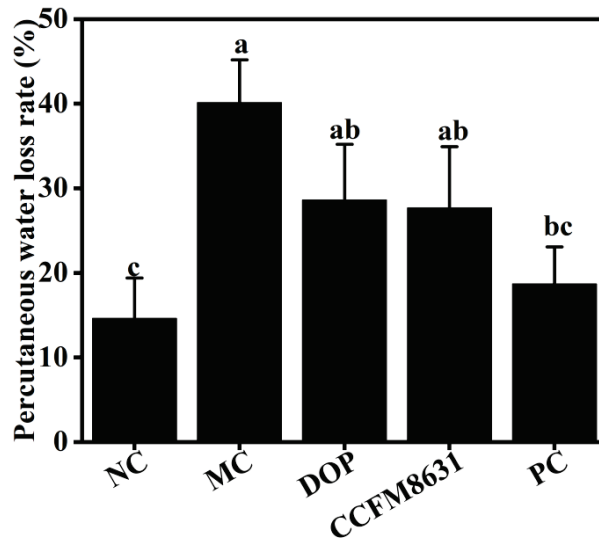


Figure 5. Effects of samples on TEWL values in DNFB-damaged model in vivo. Statistical analysis with one-way analysis of variance (ANOVA) followed by post hoc multiple comparison analysis with the Tukey test. Different letters indicate significant differences among different groups ($p < 0.05$).

3.3.3. FLG Content

FLG is a protein synthesized by keratinocytes that plays a crucial role in maintaining the integrity of the epidermal skin barrier. It aggregates keratin into filaments, which contribute to the structural stability of the skin barrier [33]. Moreover, the degradation products of FLG, known as natural moisturizing factors, regulate skin hydration [34]. As shown in Figure 6, the FLG content was significantly lower in the MC group (96.08 pg/mg)

than in the NC group (168.93 pg/mg), suggesting impairment of the skin barrier. However, this decrease in FLG content was ameliorated by treatment with DOPs or CCFM8631-FDOPs. The FLG level in the CCFM8631 group was 221.75 pg/mL, remarkably higher than that in the PC group (102.08 pg/mL). This result indicates that CCFM8631-FDOPs could improve the expression of FLG and repair DNFB-injured barrier function.

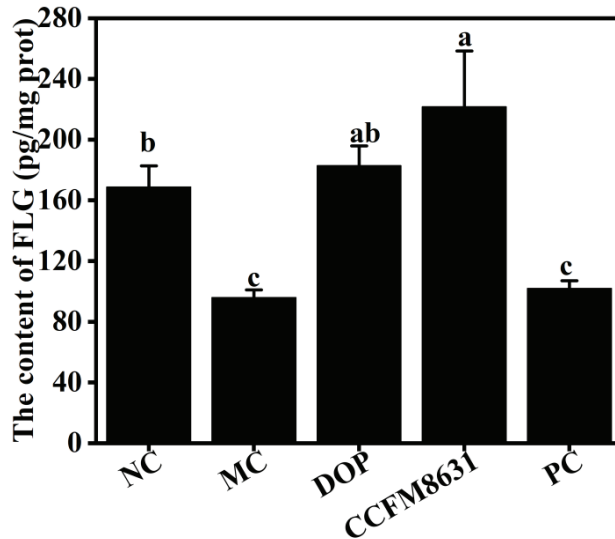


Figure 6. Effects of samples on FLG content in DNFB-damaged model in vivo. Statistical analysis with one-way analysis of variance (ANOVA) followed by post hoc multiple comparison analysis with the Tukey test. Different letters indicate significant differences among different groups ($p < 0.05$).

3.3.4. IL-6 Level

IL-6 is an important inflammatory cytokine produced by T cells and macrophages in response to infection and tissue damage. However, excessive IL-6 promotes the activation and aggregation of neutrophils, thereby amplifying injury [35]. Figure 7 shows the IL-6 levels in the skin tissue of the experimental mice. Compared to the NC group, DNFB treatment stimulated a strong inflammatory response, as evidenced by a significant increase in IL-6 levels. The administration of DOPs and CCFM8631-FDOP decreased the IL-6 content by 2.08% and 24.60%, respectively, compared to that in the MC group. Notably, the IL-6 level in the CCFM8631 group was 5.82 pg/mL, which was not significantly different from that in the PC group (5.59 pg/mL), suggesting an excellent anti-inflammatory effect.

DNFB is a hapten that interacts with various skin proteins to form covalent conjugates, resulting in an enhanced immune response. Multiple applications of DNFB disrupt the skin barrier and induce skin lesions [36]. Our results revealed that fermentation with *L. reuteri* CCFM8631 improved the ability of DOPs to alleviate DNFB-induced skin damage. This benefit is closely related to the combined effects of skin barrier repair and anti-inflammatory properties. In another study, *Punica granatum* L. polysaccharides suppressed the secretion of pro-inflammatory cytokines by inhibiting the NF- κ B and STAT3 signaling pathways and enhanced skin barrier protection by increasing aquaporin-3 and FLG expression, which then ameliorated imiquimod-elicited psoriasis [37]. Notably, the CCFM8631-FDOP was a mixture, containing fermented DOPs and microbial exopolysaccharides. It is not clear whether the increased activity of F-DOPs was caused by the structural change of DOPs during fermentation or the synergistic action of DOPs and CCFM8631 polysaccharides. Thus, in the future, our research will focus on the structure-activity relationship of CCFM8631-FDOP.

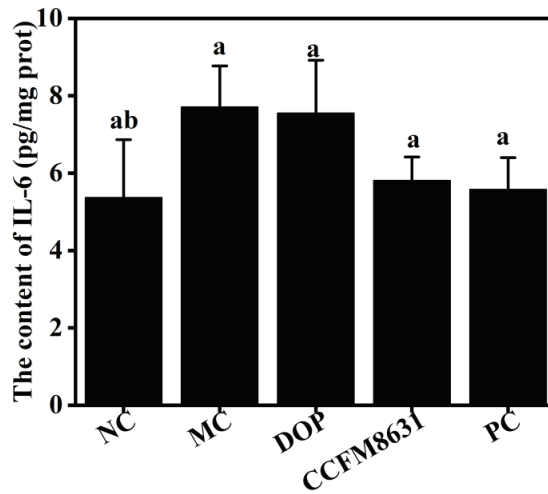


Figure 7. Effects of samples on IL-6 levels in DNFB-damaged model in vivo. Statistical analysis with one-way analysis of variance (ANOVA) followed by post hoc multiple comparison analysis with the Tukey test. Different letters indicate significant differences among different groups ($p < 0.05$).

4. Conclusions

This study aimed to screen suitable strains for fermenting *D. officinale* to produce polysaccharides with excellent skin care properties. Supplementation with *D. officinale* increased the proliferation of all ten microbial strains. Moreover, fermentation with *S. cerevisiae* HN7-A5, *L. helveticus* M10, *L. plantarum* CCFM8661, *L. rhamnosus* CCFM237, *L. sakei* GD17-9, and *L. reuteri* CCFM8631 resulted in significantly increased F-DOP yields compared with those of the unfermented group. Therefore, *L. plantarum* CCFM8661, *L. reuteri* CCFM8631, *L. casei* CCFM1073, *B. subtilis* CCFM1162, *B. cellulosilyticus* FTJSI-E-2, and *S. cerevisiae* HN7-A5 with high viable cell counts and polysaccharide yields were selected to evaluate skin care effects in vitro and in vivo. The results indicated that F-DOPs, especially after *L. reuteri* CCFM8631 fermentation, protected HaCaT cells from SDS-induced injury, decreased LPS-induced NO secretion in RAW 264.7 cells, and alleviated the DNFB-triggered skin damage in a mouse model with reduced inflammatory response and epidermal thickness and improved TEWL and skin barrier integrity. Summarily, in this study, CCFM8631 fermentation enhanced the yield of polysaccharides. More important, CCFM8631-FDOP exhibited better skin care ability than DOPs both of in cells and animal model in vitro and in vivo.

Author Contributions: X.T. and B.W., formal analysis and data curation and writing—original draft; B.M. and J.Z., writing—review and editing; J.Z. and G.L., supervision and project investigation; K.Y. and S.C., funding and supervision. All authors have read and agreed to the published version of the manuscript.

Funding: This work was supported by the National Natural Science Foundation of China (Grant No. 32172173), and Collaborative Innovation Center of Food Safety and Quality Control in Jiangsu Province.

Institutional Review Board Statement: License number of mice experiments was SYXK (Guangdong) 2018-0186.

Informed Consent Statement: Not applicable.

Data Availability Statement: All data are contained within the article.

Conflicts of Interest: The authors declare no conflict of interest.

References

- Chen, W.-H.; Wu, J.-J.; Li, X.-F.; Lu, J.-M.; Wu, W.; Sun, Y.-Q.; Zhu, B.; Qin, L.-P. Isolation, structural properties, bioactivities of polysaccharides from *Dendrobium officinale* Kimura et. Migo: A review. *Int. J. Biol. Macromol.* **2021**, *184*, 1000–1013. [CrossRef] [PubMed]
- Chen, X.; Li, L.; Yang, H.; Zhou, H. Effects of the Addition of *Dendrobium officinale* on Beer Yeast Fermentation. *Fermentation* **2022**, *8*, 595. [CrossRef]
- Chen, W.; Lu, J.; Zhang, J.; Wu, J.; Yu, L.; Qin, L.; Zhu, B. Traditional Uses, phytochemistry, pharmacology, and quality control of *dendrobium officinale kimura et. migo*. *Front. Pharmacol.* **2021**, *12*, 726528. [CrossRef]
- Yu, G.; Xie, Q.; Su, W.; Dai, S.; Deng, X.; Gu, Q.; Liu, S.; Yun, J.; Xiang, W.; Xiong, Y. Improvement of antioxidant activity and active ingredient of *Dendrobium officinale* via microbial fermentation. *Front. Microbiol.* **2023**, *14*, 1061970. [CrossRef] [PubMed]
- Tang, H.; Zhao, T.; Sheng, Y.; Zheng, T.; Fu, L.; Zhang, Y. *Dendrobium officinale* Kimura et Migo: A review on its ethnopharmacology, phytochemistry, pharmacology, and industrialization. *Evid.-Based Complement. Altern. Med.* **2017**, *2017*, 7436259. [CrossRef]
- Wang, Y.-H. Traditional uses and pharmacologically active constituents of *Dendrobium* plants for dermatological disorders: A review. *Nat. Prod. Bioprospect.* **2021**, *11*, 465–487. [CrossRef]
- Guo, L.; Qi, J.; Du, D.; Liu, Y.; Jiang, X. Current advances of *Dendrobium officinale* polysaccharides in dermatology: A literature review. *Pharm. Biol.* **2020**, *58*, 664–673. [CrossRef]
- Yang, J.-J.; Zhang, X.; Dai, J.-F.; Ma, Y.-G.; Jiang, J.-G. Effect of fermentation modification on the physicochemical characteristics and anti-aging related activities of *Polygonatum kingianum* polysaccharides. *Int. J. Biol. Macromol.* **2023**, *235*, 123661. [CrossRef]
- Li, L.; Wang, L.; Fan, W.; Jiang, Y.; Zhang, C.; Li, J.; Peng, W.; Wu, C. The application of fermentation technology in traditional Chinese medicine: A review. *Am. J. Chin. Med.* **2020**, *48*, 899–921. [CrossRef]
- Ai, Z.; You, Y.; Li, W.; Fan, J.; Wang, Y.; Huang, J.; Wang, Y.; Liu, J. Enhanced uronic acid content, antioxidant, and anti-inflammatory activities of polysaccharides from ginseng fermented by *Saccharomyces cerevisiae* GIW-1. *J. Food Process. Preserv.* **2020**, *44*, e14885. [CrossRef]
- Tian, W.; Dai, L.; Lu, S.; Luo, Z.; Qiu, Z.; Li, J.; Li, P.; Du, B. Effect of *Bacillus* sp. DU-106 fermentation on *Dendrobium officinale* polysaccharide: Structure and immunoregulatory activities. *Int. J. Biol. Macromol.* **2019**, *135*, 1034–1042. [CrossRef]
- Otsuka, A.; Moriguchi, C.; Shigematsu, Y.; Tanabe, K.; Haraguchi, N.; Iwashita, S.; Tokudome, Y.; Kitagaki, H. Fermented Cosmetics and Metabolites of Skin Microbiota—A New Approach to Skin Health. *Fermentation* **2022**, *8*, 703. [CrossRef]
- Maintz, L.; Bieber, T.; Simpson, H.D.; Demessant-Flavigny, A.-L. From skin barrier dysfunction to systemic impact of atopic dermatitis: Implications for a precision approach in dermocosmetics and medicine. *J. Pers. Med.* **2022**, *12*, 893. [CrossRef]
- Liang, Y.; Liu, G.; Xie, L.; Su, K.; Chang, X.; Xu, Y.; Chen, J.; Zhu, Z.; Yang, K.; Chen, H. *Dendrobium candidum* polysaccharide reduce atopic dermatitis symptoms and modulate gut microbiota in DNFB-induced AD-like mice. *Front. Physiol.* **2022**, *13*, 976421. [CrossRef] [PubMed]
- Cui, S.; Zhou, W.; Tang, X.; Zhang, Q.; Yang, B.; Zhao, J.; Mao, B.; Zhang, H. The Effect of Proline on the Freeze-Drying Survival Rate of *Bifidobacterium longum* CCFM 1029 and Its Inherent Mechanism. *Int. J. Mol. Sci.* **2022**, *23*, 13500. [CrossRef]
- Wang, Y.; Xiong, X.; Huang, G. Ultrasound-assisted extraction and analysis of maidenhairtree polysaccharides. *Ultrason. Sonochem.* **2023**, *95*, 106395. [CrossRef]
- Zhou, R.-R.; Huang, J.-H.; He, D.; Yi, Z.-Y.; Zhao, D.; Liu, Z.; Zhang, S.-H.; Huang, L.-Q. Green and Efficient Extraction of Polysaccharide and Ginsenoside from American Ginseng (*Panax quinquefolius* L.) by Deep Eutectic Solvent Extraction and Aqueous Two-Phase System. *Molecules* **2022**, *27*, 3132. [CrossRef] [PubMed]
- Ding, W.; Fan, L.; Tian, Y.; He, C. Study of the protective effects of cosmetic ingredients on the skin barrier, based on the expression of barrier-related genes and cytokines. *Mol. Biol. Rep.* **2022**, *49*, 989–995. [CrossRef]
- Tian, C.; Liu, X.; Chang, Y.; Wang, R.; Lv, T.; Cui, C.; Liu, M. Investigation of the anti-inflammatory and antioxidant activities of luteolin, kaempferol, apigenin and quercetin. *S. Afr. J. Bot.* **2021**, *137*, 257–264. [CrossRef]
- Baptista, S.; Pereira, J.R.; Guerreiro, B.M.; Baptista, F.; Silva, J.C.; Freitas, F. Cosmetic emulsion based on the fucose-rich polysaccharide FucoPol: Bioactive properties and sensorial evaluation. *Colloids Surf. B Biointerfaces* **2023**, *225*, 113252. [CrossRef]
- Tang, L.; Li, X.-L.; Deng, Z.-X.; Xiao, Y.; Cheng, Y.-H.; Li, J.; Ding, H. Conjugated linoleic acid attenuates 2, 4-dinitrofluorobenzene-induced atopic dermatitis in mice through dual inhibition of COX-2/5-LOX and TLR4/NF- κ B signaling. *J. Nutr. Biochem.* **2020**, *81*, 108379. [CrossRef] [PubMed]
- Yang, X.-G.; Jiang, B.-W.; Jing, Q.-Q.; Li, W.-J.; Tan, L.-P.; Bao, Y.-L.; Song, Z.-B.; Yu, C.-L.; Liu, L.; Liu, Y.-C. Nitidine chloride induces S phase cell cycle arrest and mitochondria-dependent apoptosis in HaCaT cells and ameliorates skin lesions in psoriasis-like mouse models. *Eur. J. Pharmacol.* **2019**, *863*, 172680. [CrossRef] [PubMed]
- Smith, P.E.; Krohn, R.I.; Hermanson, G.; Mallia, A.; Gartner, F.; Provenzano, M.; Fujimoto, E.; Goeke, N.; Olson, B.; Klenk, D. Measurement of protein using bicinchoninic acid. *Anal. Biochem.* **1985**, *150*, 76–85. [CrossRef] [PubMed]
- Qiao, H.; Zhang, X.; Shi, H.; Song, Y.; Bian, C.; Guo, A. Assessment of the physicochemical properties and bacterial composition of *Lactobacillus plantarum* and *Enterococcus faecium*-fermented *Astragalus membranaceus* using single molecule, real-time sequencing technology. *Sci. Rep.* **2018**, *8*, 11862. [CrossRef] [PubMed]
- Yang, C.-C.; Hung, Y.-L.; Ko, W.-C.; Tsai, Y.-J.; Chang, J.-F.; Liang, C.-W.; Chang, D.-C.; Hung, C.-F. Effect of neferine on DNCB-induced atopic dermatitis in HaCaT cells and BALB/c mice. *Int. J. Mol. Sci.* **2021**, *22*, 8237. [CrossRef] [PubMed]

26. Kim, M.; Lee, S.; Ki, C.S. Cellular behavior of RAW264. 7 cells in 3D poly (ethylene glycol) hydrogel niches. *ACS Biomater. Sci. Eng.* **2019**, *5*, 922–932. [CrossRef]
27. Li, F.; Nakanishi, Y.; Murata, K.; Shinguchi, K.; Fujita, N.; Chiba, S.; Takahashi, R. Coix Seed Extract Prevents Inflammation-mediated Skin Dryness Induced by Sodium Dodecyl Sulfate Exposure in HR-1 Hairless Mice. *Planta Medica Int. Open* **2022**, *9*, e108–e115. [CrossRef]
28. Proksch, E.; Soeberdt, M.; Neumann, C.; Kilic, A.; Abels, C. Modulators of the endocannabinoid system influence skin barrier repair, epidermal proliferation, differentiation and inflammation in a mouse model. *Exp. Dermatol.* **2019**, *28*, 1058–1065. [CrossRef]
29. Zhang, Y.; Luo, H.; Lv, X.; Liu, J.; Chen, X.; Li, Y.; Liu, A.; Jiang, Y. Axin-1 binds to Caveolin-1 to regulate the LPS-induced inflammatory response in AT-I cells. *Biochem. Biophys. Res. Commun.* **2019**, *513*, 261–268. [CrossRef]
30. Shi, C.; Han, W.; Zhang, M.; Zang, R.; Du, K.; Li, L.; Xu, X.; Li, C.; Wang, S.; Qiu, P. Sulfated polymannuroguronate TGC161 ameliorates leukopenia by inhibiting CD4+ T cell apoptosis. *Carbohydr. Polym.* **2020**, *247*, 116728. [CrossRef]
31. Nagase, S.; Ogai, K.; Urai, T.; Shibata, K.; Matsubara, E.; Mukai, K.; Matsue, M.; Mori, Y.; Aoki, M.; Arisandi, D. Distinct skin microbiome and skin physiological functions between bedridden older patients and healthy people: A single-center study in Japan. *Front. Med.* **2020**, *7*, 101. [CrossRef]
32. Berekéri, A.; Tiganescu, A.; Alase, A.A.; Vital, E.; Stacey, M.; Wittmann, M. Non-invasive approaches for the diagnosis of autoimmune/autoinflammatory skin diseases—A focus on psoriasis and lupus erythematosus. *Front. Immunol.* **2019**, *10*, 1931. [CrossRef] [PubMed]
33. Yoshida, T.; Beck, L.A.; De Benedetto, A. Skin barrier defects in atopic dermatitis: From old idea to new opportunity. *Allergol. Int.* **2022**, *71*, 3–13. [CrossRef] [PubMed]
34. Elias, P.M.; Schmuth, M. Abnormal skin barrier in the etiopathogenesis of atopic dermatitis. *Curr. Allergy Asthma Rep.* **2009**, *9*, 265–272. [CrossRef]
35. Zhang, X.; Ding, J.; Li, Y.; Song, Q.; Li, S.; Hayat, M.A.; Zhang, J.; Wang, H. The changes of inflammatory mediators and vasoactive substances in dairy cows' plasma with pasture-associated laminitis. *BMC Vet. Res.* **2020**, *16*, 119. [CrossRef] [PubMed]
36. Sanjel, B.; Shim, W.-S. The contribution of mouse models to understanding atopic dermatitis. *Biochem. Pharmacol.* **2022**, *203*, 115177. [CrossRef] [PubMed]
37. Chen, H.; Wang, C.; Tang, B.; Yu, J.; Lu, Y.; Zhang, J.; Yan, Y.; Deng, H.; Han, L.; Li, S.P. granatum Peel Polysaccharides Ameliorate Imiquimod-Induced Psoriasis-Like Dermatitis in Mice via Suppression of NF- κ B and STAT3 Pathways. *Front. Pharmacol.* **2022**, *12*, 3864. [CrossRef]

Disclaimer/Publisher's Note: The statements, opinions and data contained in all publications are solely those of the individual author(s) and contributor(s) and not of MDPI and/or the editor(s). MDPI and/or the editor(s) disclaim responsibility for any injury to people or property resulting from any ideas, methods, instructions or products referred to in the content.

Article

Production and Characterization of Kombucha Tea from Different Sources of Tea and Its Kinetic Modeling

Kubra Tarhan Kuzu^{1,2}, Gamze Aykut¹, Serap Tek¹, Ercan Yatmaz^{1,3}, Mustafa Germec¹, Ibrahim Yavuz¹ and Irfan Turhan^{1,*}

- ¹ Department of Food Engineering, Faculty of Engineering, Akdeniz University, 07058 Antalya, Turkey; kubratarhan@comu.edu.tr (K.T.K.); gamze_3507@hotmail.com (G.A.); seraptek91@hotmail.com (S.T.); ercanyatmaz@akdeniz.edu.tr (E.Y.); afatsumcemreg@gmail.com (M.G.); ibrahimyavuz07@gmail.com (I.Y.)
- ² Department of Food Processing, Vocational School of Technical Sciences, Çanakkale Onsekiz Mart University, Terzioğlu Campus, 17100 Çanakkale, Turkey
- ³ Göynük Culinary Arts Vocational School, Akdeniz University, 07980 Antalya, Turkey
- * Correspondence: iturhan@akdeniz.edu.tr; Tel.: +90-(242)-310-6573; Fax: +90-(242)-310-6306

Abstract: This study aimed to investigate the fermentation performance, sugar consumption, pH changes, total phenolic compounds, and antioxidant activity produced using different tea extracts and sugar concentrations and the kinetic characteristics of Kombucha fermentation. Three independent sugar concentrations (10 g/L, 40 g/L, and 70 g/L) were used in the fermentation process. The results showed that the Kombucha culture consumed all sugar in the fermentation medium when the sugar concentration was below a certain threshold, but when the sugar concentration was high, not all substrate was consumed. Sugar consumption values ranged from 48.39 to 55.40 g/L and affected biomass formation, with higher sugar consumption resulting in increased biomass production. The pH decreased during fermentation due to the production of organic acids and microbial by-products, while total acidity increased. Total phenolic compounds increased during fermentation, with the highest concentrations observed in herbal Kombucha teas. Antioxidant activity varied, with some samples showing a decrease in DPPH scavenging ability. Kinetic characterization revealed the relationship between substrate depletion, sugar consumption, total acidity, and phenolic compound production. The results showed that sugar concentration influenced the fermentation kinetics and end-product characteristics of Kombucha tea. Overall, this study provides valuable insights into the fermentation process of Kombucha tea and its impact on various parameters, contributing to the understanding of the factors affecting its quality and health benefits.

Keywords: Kombucha fermentation; bioactive component; proximate composition; kinetic parameters; kinetic modeling

Citation: Tarhan Kuzu, K.; Aykut, G.; Tek, S.; Yatmaz, E.; Germec, M.; Yavuz, I.; Turhan, I. Production and Characterization of Kombucha Tea from Different Sources of Tea and Its Kinetic Modeling. *Processes* **2023**, *11*, 2100. <https://doi.org/10.3390/pr11072100>

Academic Editor: Chi-Fai Chau

Received: 11 June 2023
Revised: 8 July 2023
Accepted: 11 July 2023
Published: 14 July 2023



Copyright: © 2023 by the authors. Licensee MDPI, Basel, Switzerland. This article is an open access article distributed under the terms and conditions of the Creative Commons Attribution (CC BY) license (<https://creativecommons.org/licenses/by/4.0/>).

1. Introduction

Kombucha has been consumed all over the world but historically in China, Russia, and Eastern European countries. Kombucha is a fermented sugared black tea by yeasts and *Acetobacter* species [1,2]. The various yeast species of Kombucha tea are *Brettanomyces bruxellensis* [3], *Candida stellata* [3], *Schizosaccharomyces pombe* [3], *Torulasporea delbrueckii* [3], *Zygosaccharomyces bailii* [3], *Saccharomyces ludwigii* [4], *Kloeckera apiculata* [5], *Saccharomyces cerevisiae* [4], *Brettanomyces lambicus* [6], *Brettanomyces custersii* [6], *Candida krusei* [5], and *Pichia* species [7]. This means that Kombucha culture differs from place to place and could easily be understood from different research about Kombucha cultures [2]. Namely, the kombucha culture is a symbiotic culture of bacteria and yeast (SCOBY) that is essential for the fermentation process of Kombucha [2]. The role of yeasts in the Kombucha fermentation is to hydrolyze sucrose from the cultivation medium to glucose and fructose and metabolize these monosaccharides to ethanol, which is further oxidized to acetic acid by acetic acid bacteria (AAB). AAB cannot uptake sucrose alone because of the lack of

enzymes for the extracellular hydrolysis of sucrose or its transport into the cell. AAB uses yeast-derived glucose to synthesize gluconic acid and bacterial cellulose in the form of a pellicle, which is commonly described as the “fungus” [8–10]. Microbial community type and composition play an important role in the biochemistry dynamics of Kombucha. These associations help to decrease pH and reduce microbial growth of other microorganisms with antimicrobial metabolites [11]. The time of Kombucha fermentation is between 7 and 60 days. During this time, biological activities increase. On the other hand, it was reported that the best results were yielded in an average of 10 days [12]. According to the Food and Drug Administration Model Food Code for Kombucha Brewing, more than 10 days of fermentation are not suggested if produced for human consumption [13]. Therefore, 8–10 days can be enough to obtain the best beverage specifications, and microorganisms use sugar to produce value-added acids and antimicrobial metabolites [14]. The kombucha tea yielded after fermentation consists of sugars (glucose, fructose), gluconic, glucuronic, L-lactic, acetic, malic, tartaric, malonic, citric, and oxalic acids, as well as ethanol, 14 amino acids, water-soluble vitamins, antibioticly active matters, and some hydrolytic enzymes [15].

Kombucha tea has beneficial features on human health, such as improving the immune system, detoxifying harmful substances, lowering blood pressure, treating gastritis and cholesterol, and exhibiting antioxidant, antibacterial, anticancer, and antidiabetic activities [2]. The research about the antimicrobial activity of Kombucha tea showed that the antimicrobial agent was acetic acid content, and it inhibited *Agrobacterium tumefaciens*, *Bacillus cereus*, *Salmonella choleraesuisserotypetypiphimurium*, *Staphylococcus aureus*, and *Escherichia coli*. However, due to the fermented samples including 33 g/L total acid (7 g/L acetic acid), these values indicated the yielded beverage samples were not suitable for drinkable levels, but Kombucha had antimicrobial activity against pathogenic bacteria [16]. The other research demonstrated that Kombucha tea had an antimicrobial effect against a range of pathogenic bacteria, several clinical *Candida* species, fermented *L. citriodora*, and *F. vulgare* [17]. Kombucha could also be used against enteropathogenic bacterial infections due to its polyphenolic content [18]. Various Kombucha cultures also showed different antioxidant activity under the same fermentation conditions (10% starter addition to the fresh medium prepared, 30 °C, and 15 days fermentation time), mostly indicating time-dependent properties [19]. The conformable research showed the difference between antioxidant activity values from different starter cultures and tea extracts [15]. The Kombucha fermentation with different initial sucrose concentrations (ISCs) (70 g/L, 50 g/L, and 35 g/L of sucrose) was studied, and the highest sugar concentration value was found to be an optimal concentration of carbon source, providing high pH, low acetic acid, and high L-lactic acid content and highest sucrose consumption [20].

In the literature, there are some similar studies regarding the production of Kombucha tea from different types of herbal and fruit teas. For instance, Zubaidah et al. [21] examined the physical, chemical, and microbiological features of Kombucha from different varieties of apples (Anna, Manalagi, Fuji, Granny Smith, Red Delicious, Rome Beauty, and Royal Gala). Based on the results, it was reported that the best treatment was yielded on Fuji varieties of Kombucha apple (total acid 1.33%, pH 2.95, total phenol 268.57 µg/mL GAE, total sugar 6.74%, antibacterial activity against *Staphylococcus aureus* 21.30 mm, antibacterial activity *Escherichia coli* 21.20 mm, antioxidant activity 35.62%, organoleptic aroma 3.55, taste 3.3, and color 3.4 (on a scale of 1–5)) [21]. In another study, where the different carbon sources (glucose, fructose, xylose, lactose, sucrose (70 g/L)), types of teas (black tea, green tea, sage tea, pomegranate (hibiscus) tea, blueberries tea, and rosehip tea), and coffee were used as resources to produce Kombucha [22], the pH, acidity, antioxidant activity, phenolic substance, biomass development, color change, organic acid profile, ethanol, and sensory analysis were examined. The results indicated that the value of pH decreased during fermentation, and the Kombucha from fruit teas were greater acidity than herbal teas and coffee extract. The phenolic substance content and antioxidant activity of the Kombucha produced have been found to have the potential to be an important product. Regarding biomass growth, it was determined most in glucose and sucrose (tea samples) and lactose

(coffee extract) and at the least in fructose (tea samples) and lactose (coffee extract). When color changes were examined, it was detected that the L, a, and b values of herbal tea changed in a fermentation medium supplemented with glucose, xylose, or fructose. During the fermentation, most of the organic acids, including oxalic acid, tartaric acid, malic acid, lactic acid, citric acid, succinic acid, and fumaric acid, were measured. On the other hand, it was reported that no ethanol production was observed at the end of the fermentation. Based on the sensory analysis, the most and least preferred Kombucha teas were produced from pomegranate and sage teas, respectively [22]. In a different study, Tamer et al. [23] evaluated the bio-accessibility and functional features of Kombucha teas fortified with different medicinal plant extracts (linden, lemon balm, sage, *Echinacea*, mint, and cinnamon). Based on the results, the antioxidant capacity (AC), ferric-reducing antioxidant power, and cupric-reducing AC were 13.96%, 48.90%, and 55.54%, respectively. It was also found that during 9-day storage, the bio-accessibility of total phenolic and AC dramatically increased after gastric and intestinal digestion [23]. Additionally, the changes in the content of organic acids and polyphenols during the Kombucha fermentation from green tea, black tea, and tea manufacturing waste [24] and the antibacterial and antifungal activities of black and green Kombucha teas [25] were also examined. Moreover, the kinetics of sucrose fermentation by Kombucha culture was also studied by using Boltzmann's functions [26]. The fermentation conditions were performed on 1.5 g/L of black tea, with 67 g/L of sucrose, and using 10% or 15% of Kombucha culture (*v/v*). The model was described as a sigmoid function at two different temperatures (22 °C and 30 °C). Based on the results, it was determined that the rate of fermentation was maximum on days 4–5, and after reaching the maximal rate, it dramatically decreased. It was reported that as the temperature and inoculum concentration increased, the rate of the fermentation increased, the optimal fermentation time was 3.5–5 days under the implemented circumstances, and the saturation curves indicated the sigmoid kinetics at the selected sucrose concentration [26]. When considering this information, this study has novelty in terms of the use of some different types of teas in the production of Kombucha teas, kinetic characterization of Kombucha fermentations performed at different substrate concentrations, and kinetic modeling of Kombucha fermentations in terms of substrate consumption and total acidity. Therefore, this study is filled the significant gap in the literature.

Kombucha tea is generally produced from black and green tea, but commercial firms' market started to produce new Kombucha teas with lemon, apples, peach, blackberries, and rosehip. Therefore, the objective of this study is to investigate the production of Kombucha teas with diverse chemical compositions by utilizing various substrates. Additionally, the study seeks to analyze the kinetic properties of Kombucha fermentation and develop a kinetic model for fermentations involving different tea sources.

2. Materials and Methods

2.1. Kombucha Culture and Media

Kombucha culture was obtained from the commercial firm "Comboutea" (Tema Pharmaceutical Vitamin Cosmetics Limited Company, Samsun, Turkey). The media components for stock and pre-culture were 10 g/L yeast extract, 20 g/L glucose, and 20 g/L peptone [27]. After the medium composition was prepared, the medium pH was adjusted to 4 using 10 N HCl. The prepared medium was sterilized at 121.1 °C for 15 min. Subsequently, the medium was cooled to room temperature. It was inoculated with 10% (*v/v*) of Kombucha culture. The stock and pre-cultures were incubated at 24 °C for 10 days, and the stock cultures were stored at 4 °C. Stock cultures were renewed for one month to have viability and productivity.

2.2. Experimental Design

In this study, different fruit (bilberry, rosehip, apple, and pomegranate tea) and herbal (green, sage, linden, and black tea) teas were used for tea extraction. On the other hand, the limited sugar value to produce Kombucha from different types of tea was determined

from a previous study [15]. After determining the maximum sugar limit, sucrose as the sole carbon source was added to the fermentation medium by decreasing it to 30 g/L to instigate the effect of the initial sucrose concentration. Thus, the ISCs were 10 g/L, 40 g/L, and 70 g/L in the present study. Each of the extracts was prepared with three different ISCs (10 g/L, 40 g/L, and 70 g/L), and a coded system for the samples is given in Table 1. All production and analyses were replicated two times. Kinetic parameters of Kombucha fermentation were also calculated. Fermentations were kinetically modeled using the logistic model (LM) and the Luedeking–Piret model (LPM) [28]. The LM was used to predict the experimental substrate consumption values, and LPM was employed to estimate the experimental total acidity values of fermentation.

Table 1. Sample code system.

Tea Origin	Tea	Initial Sugar Concentration (g/L)		
		10	40	70
Herbal tea	Sage tea (ST)	ST-10	ST-40	ST-70
	Linden tea (LT)	LT-10	LT-40	LT-70
	Green tea (GT)	GT-10	GT-40	GT-70
	Black tea (BT)	BT-10	BT-40	BT-70
Fruit tea	Apple tea (AT)	AT-10	AT-40	AT-70
	Rosehip tea (RT)	RT-10	RT-40	RT-70
	Pomegranate tea (PT)	PT-10	PT-40	PT-70
	Bilberry tea (BBT)	BBT-10	BBT-40	BBT-70

2.3. Preparation of Tea Extracts, Inoculation, and Fermentation

Four different herbal teas (green (GT), sage (ST), linden (LT), and black tea (BT)) and four various fruit teas (bilberry (BBT), rosehip (RT), apple (AT), and pomegranate tea (PT)) were used for Kombucha production. All the tea samples were provided by the Unilever Company in Konya, Turkey.

The extraction process was realized by mixing 1 L of boiled pure water with 10 g tea and waiting for 15 min to obtain tea extracts [29]. The mix was filtered by using roughing filter paper (cellulosic filter paper) to separate the insoluble materials. After filtration, different amounts of sucrose (10 g/L, 40 g/L, or 70 g/L) were immediately added. After the sugar was completely dissolved, the mixture was transferred into 250 mL flasks (100 mL working volume) and cooled to room temperature. It was stored in appropriate conditions until inoculation.

After pre-culture and fermentation media were prepared, the flasks were inoculated with 10 mL of pre-culture. Inoculated sugared tea mixtures were incubated at 24 °C for 10 days with no agitation, and samples were taken daily under aseptic conditions and stored at 4 °C [30].

2.4. Analysis

The total acidity was determined by adding 0.1 N NaOH to samples until the pH was 8.2 [31]. The pH values of fermented teas were measured with an electronic pH meter (Thermo Scientific Orion 4 Star, Singapore). The total biomass of fermented samples was gravimetrically determined. The collected samples during fermentation were filtered by using pre-weighed filter paper (Whatman No.: 1), and the fermented broth was removed. The filter cake (biomass) was then dried at 60 °C in the oven until constant weight [32]. The residual sugar concentration was spectrophotometrically determined using the 3,5-dinitrosalicylic acid method [33]. The Folin–Ciocalteu method was used to determine the total phenolic substance concentration in samples. The results were given as milligrams of gallic acid equivalents per liter (mg GAE/L) of Kombucha [34]. The antioxidant analysis was determined with the α , α -diphenyl- β -picrylhydrazyl (DPPH) free radical scavenging method, and the antioxidant capacity was determined as % inhibition [19].

2.5. Kinetic Parameters

Kinetic parameters including substrate consumption (ΔS , g/L), maximum substrate consumption rate (Q_S , g/L/d), substrate utilization yield (η , %), biomass production (ΔX , g/L), maximum biomass production rate (Q_X , g/L/d), biomass yield ($Y_{X/S}$, g biomass/g substrate), total acidity (TA, %), maximum total acidity production rate (Q_{TA} , %/d), phenolics production (ΔPH , mg/L), maximum phenolics production rate (Q_{PH} , mg/L/d), and phenolics yield ($Y_{PH/S}$, mg phenolics/g substrate) were calculated. The details regarding how kinetic parameters are calculated can be found in previous similar studies [28].

2.6. Kinetic Modeling

The LM (Equation (1)) and LPM (Equation (2)) were utilized to estimate the experimental substrate consumption and total acidity data of Kombucha fermentation. Microsoft Office Excel 2013 was used. Traditionally, LM is used to describe cell growth. However, in this work, the model was modified to define sugar consumption and independently employed cell growth data because there is no sigmoid growth of biomass because of high acidity or low pH values.

$$\frac{-dS}{dt} = \mu_{m,S} \left[1 - \frac{S}{S_m} \right] S \quad (1)$$

where $-dS/dt$ is the substrate consumption rate (g/L/d), $\mu_{m,S}$ is the specific sugar consumption rate (1/d), S is the residual substrate concentration at the time "t" (g/L), and S_m is the maximum substrate concentration (g/L).

The LPM is utilized to define the metabolite production rate (dP/dt) related to cell growth. However, dP/dt is also thought to be contingent on both momentary S and dS/dt linearly [35].

$$\frac{dP}{dt} = \alpha \frac{dS}{dt} + \beta S \quad (2)$$

where dP/dt is the total acidity rate (%/d) and α and β are the empirical constants that vary based on fermentation conditions and are determined with the best appropriate real data. Moreover, the determination of coefficient (R^2) was utilized to comprehend whether modeling is accomplished or not [28].

2.7. Statistical Analysis

The SAS version 7 program (Statistical Analysis System, TS P1, Cary, NC, USA) was used for the statistical evaluation of the data obtained from the study, and variance analysis was performed. Significant differences were evaluated by the Duncan Multiple Comparison Test at a confidence level of 95%.

3. Results and Discussion

3.1. Sugar Consumption and Biomass Production

Three ISCs were used to determine the fermentation performance of the commercial Kombucha culture. It was determined that all the sugar in the fermentation medium is consumed by the Kombucha culture in fermentations performed with AT-10, RT-10, PT-10, and BT-10. However, when the fermentation medium contains high sugar concentration, all the substrate in the medium is not consumed by the Kombucha culture at the end of the fermentation (Figure 1A and Supplementary Materials). The highest sugar consumption value is 55.40 g/L for LT-70 herbal Kombucha tea, whereas its highest value is 48.39 g/L for AT-70 fruit Kombucha tea (Figure 1A and Table 2). These sugar consumption values also affect biomass formation. In Figure 1B and the Supplementary Materials, biomass production curves from different medium compositions are given. The difference in the medium used, amount of sugar, the composition of culture, fermentation conditions, and applied period are effective in the chemical composition of Kombucha [36]. Moreover, ISC affects total sugar consumption. High sugar consumption is observed in fermentations with high ISCs (Table 2). It is determined that residual sugar concentration decreases

during fermentation. Furthermore, the highest biomass productions for herbal and fruit Kombucha teas are determined as 6.46 g/L for GT-70 and 8.77 g/L for PT-70 (Figure 1B). These results show that biomass formation increases with an increase in sugar consumption (Table 2). In work conducted by Muhialdin et al. [37], the amount and yield of biomass were associated with the sugar source.

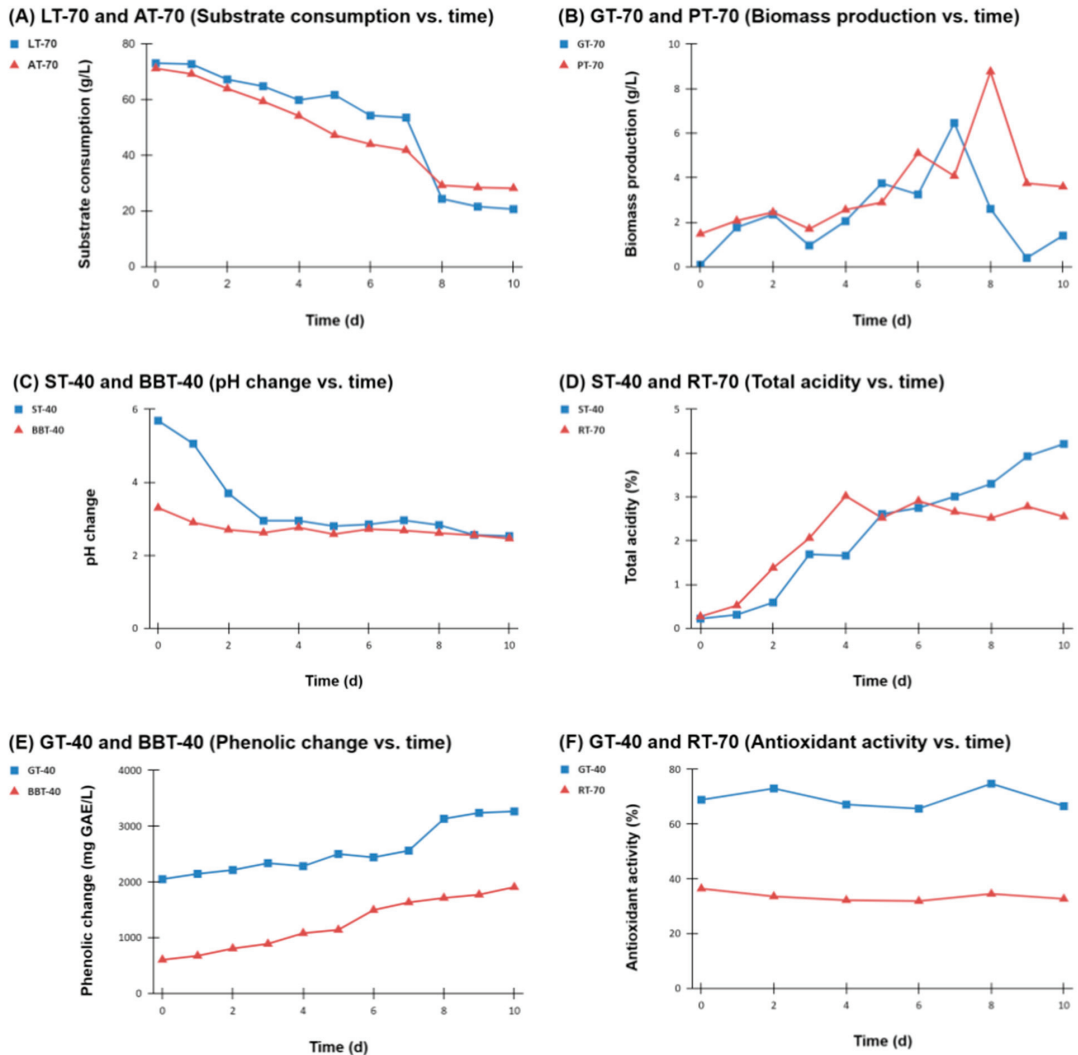


Figure 1. Change of substrate concentration, biomass production, pH, total acidity, phenolic, and antioxidant activity during Kombucha fermentation performed on media containing different initial sugar concentrations. (A) Substrate consumption vs. time with sage tea (ST-70) and linden tea (LT-70). (B) Biomass production vs. time with green tea (GT-70) and pomegranate tea (PT-70). (C) pH change vs. time with sage tea (ST-40) and blueberry tea (BBT-40). (D) Total acidity vs. time with sage tea (ST-40) and rosehip tea (RT-70). (E) Phenolic change vs. time with green tea (GT-40) and blueberry tea (BBT-40). (F) Antioxidant activity vs. time with green tea (GT-40) and rosehip tea (RT-70).

Table 2. Kinetic parameters of Kombucha fermentation performed with extracts from different types of tea with various initial sugar concentrations.

		Kinetic Parameters										
Tea	[Substrate]	ΔS (g/L)	Q_S (g/L/d)	η (%)	ΔX (g/L)	Q_X (g/L/d)	$Y_{X/S}$ (g/g)	ΔTA (%)	Q_{TA} (%/d)	ΔPH (mg/L)	Q_{PH} (mg/L/d)	$Y_{PH/S}$ (mg/g)
ST	10 g/L	8.52	1.29	79.48	0.72	0.12	0.08	0.17	0.08	445.96	97.18	52.34
	40 g/L	13.10	3.71	29.39	1.74	0.51	0.13	4.10	0.60	883.17	169.75	67.42
	70 g/L	26.62	4.05	32.71	3.96	0.94	0.15	1.51	0.28	900.31	189.07	33.82
LT	10 g/L	11.66	2.72	97.25	1.02	0.22	0.09	0.59	0.17	242.12	26.80	20.77
	40 g/L	19.85	4.00	47.40	2.72	1.20	0.14	1.04	0.27	399.65	49.54	20.13
	70 g/L	55.40	11.28	72.78	3.80	0.14	0.07	1.63	0.31	227.06	48.14	4.10
GT	10 g/L	12.13	2.40	88.80	0.74	0.26	0.06	0.35	0.15	1217.60	410.68	100.38
	40 g/L	32.43	4.90	56.65	2.52	0.78	0.08	0.87	0.33	1215.90	345.69	37.49
	70 g/L	44.07	6.34	53.72	6.46	1.22	0.15	1.42	0.37	1268.40	264.16	28.78
AT	10 g/L	15.75	2.82	100.00	1.09	0.34	0.07	0.34	0.15	321.98	64.14	20.44
	40 g/L	18.61	3.07	39.89	3.76	1.39	0.20	1.18	0.27	785.45	159.90	42.21
	70 g/L	48.39	5.28	63.15	4.28	1.37	0.09	1.64	0.41	466.38	74.71	9.64
RT	10 g/L	15.43	3.65	100.00	2.01	0.23	0.13	1.07	0.36	130.66	21.39	8.47
	40 g/L	28.74	6.37	54.33	4.71	2.17	0.16	1.61	0.49	295.36	76.28	10.28
	70 g/L	45.66	8.32	51.38	5.60	1.31	0.12	2.77	0.82	255.86	56.83	5.60
PT	10 g/L	10.33	2.47	100.00	2.20	0.91	0.21	0.39	0.20	549.89	95.36	53.23
	40 g/L	21.04	3.67	44.69	3.25	1.43	0.15	1.30	0.30	800.04	101.66	38.02
	70 g/L	42.92	6.36	50.61	8.77	1.66	0.20	2.18	0.34	930.94	166.20	21.69
BBT	10 g/L	12.67	2.54	95.62	0.81	0.31	0.06	0.44	0.18	655.20	95.51	51.71
	40 g/L	16.05	3.07	32.56	2.07	0.70	0.13	1.52	0.39	1311.92	187.92	81.74
	70 g/L	21.41	3.24	26.02	3.55	1.40	0.17	1.73	0.41	782.90	178.13	36.57

ΔS , substrate consumption (g/L); Q_S , maximum substrate consumption rate (g/L/d); η , substrate utilization yield (%); ΔX , biomass production (g/L); Q_X , maximum biomass production rate (g/L/d); $Y_{X/S}$, biomass yield (g biomass/g substrate); ΔTA , total acidity (%); Q_{TA} , maximum total acidity production rate (%/d); ΔPH , phenolic production (mg/L); Q_{PH} , maximum phenolic production rate (mg/L/d); and $Y_{PH/S}$, phenolic yield (mg phenolic/g substrate).

3.2. pH and Total Acidity

Kombucha fermentation was performed with herbal and fruit tea extracts for 10 days, and pH changes are shown in Figure 1C and the Supplementary Materials. Herbal and fruit tea extracts' initial pH values range from 4.86 to 5.90 and from 3.12 to 3.53, respectively. Differences between initial and final values of pH are higher for herbal tea samples than for fruit tea samples (Figure 1C and Supplementary Materials). The lowest final pH values of herbal and fruit teas are measured to be 2.53 for ST-40 and 2.46 for BBT-40 (Figure 1C), and their highest values are 3.73 for ST-10 and 3.57 for AT-10 (Supplementary Materials). It is seen that a slight pH increase at the end of Kombucha fermentation in AT supplemented with 10 g/L sucrose (Supplementary Materials). This may be due to the breakdown of dead cells in the fermentation medium [38]. All pH values, except for that of AT-10, decrease during fermentation because microorganisms metabolize sugar into different metabolites, such as organic acids and by-products (Figure 1C and Supplementary Materials). For all samples, a significant decrease in pH is noticed between days 0 and 5, and changes in pH are statistically insignificant after day 5 ($p < 0.05$). Total acidity values in all herbal and fruit tea samples are below 0.30% acetic acid at the beginning of fermentation. Initial total acidity values differ from 0.04% to 0.22% for herbal tea extracts and 0.15% to 0.27% for fruit tea extracts (Figure 1D and Supplementary Materials). The highest and lowest total acidity values for herbal and fruit teas are determined to be 4.21% (ST-40) (Figure 1D), 0.15% (GT-10) (Supplementary Materials), and 2.55% (RT-70) (Figure 1D), 0.23% (AT-10) (Supplementary Materials). In general, when examining Figure 1D and the Supplementary Materials, an increase in total acidity values is observed as a result of organic acid production and dead cell fragmentation during fermentation [26]. These results show that organic acid production and microbial by-products, which occur in

parallel with sugar consumption during fermentation, decrease pH and increase total acidity (Figure 1D and Supplementary Materials).

3.3. Total Phenolic Compounds and Antioxidant Activity

The changes in total phenolic compounds for herbal and fruit Kombucha teas are given in Figure 1E and the Supplementary Materials. The phenolic concentration increases in almost all herbal (except for those of BT-40 and BT-70) and fruit Kombucha tea experiments at the end of fermentation. The highest total phenolic compound values are determined to be 1522.90 mg GAE/L in ST-40, 1061.55 mg GAE/L in LT-10, and 3266.05 mg GAE/L in GT-40 (Figure 1E), and 1025.67 mg GAE/L in BT-10 for herbal Kombucha teas after 10 days fermentation (Supplementary Materials). For fruit Kombucha teas, the highest total phenolic compound values are calculated to be 1041.21 mg GAE/L in AT-40, 1016.99 mg GAE/L in RT-40, 1420.44 mg GAE/L in PT-40 (Supplementary Materials), and 1907.53 mg GAE/L in BBT-40 (Figure 1E) after 10 days fermentation. When considering all fermentations, the highest increase in total phenolic substance concentration is yielded as 215.44% with BBT-40. An increase in phenolic content with fermentation may be related to the enzymes of mixed Kombucha culture, the acidic environment of Kombucha tea, the synergistic effect of different components in tea, and the breakdown of complex phenolic compounds [39]. Moreover, the fact that phenolic components are more stable at acidic pH may cause differences in the total amount of phenolic substances during fermentation [40]. The decline in total phenolic concentration in black Kombucha tea samples (BT-40 and BT-70) might be due to the characteristics of black tea of that season. The total amount of phenolic substances in green tea is higher than in black tea [40]. Moreover, the percentage increase in total phenolic concentration in fruit Kombucha teas (average 112.49%) is higher than in herbal Kombucha teas (average 49.14%) (Figure 1). In summary, the total amount of phenolic compounds increased.

The antioxidant activity results are given in Figure 1F and the Supplementary Materials. The final DPPH scavenging ability decreases except for GT-70 (+4.46%), AT-10 (+5.99%), and AT-40 (+38.08%) assays. Decline values change from 0.86% to 31.97% for herbal Kombucha teas and 2.92% to 17.50% for fruit Kombucha teas. The maximal decrease is calculated to be 31.97% for LT-40. This decline could be about substrate and starter culture types. Because of research about the influence of starter culture on Kombucha fermentation, results show that DPPH scavenging ability is slightly increased in the first 3 days and decreased after day 3 of fermentation [15]. The final antioxidant values are lower than the initial values of this research. The highest final DPPH scavenging ability value is 66.59% for the GT-40 at the end of the fermentation (Figure 1F). In a study [19], half of eight different Kombucha samples showed a regular increase in antioxidant activity, while the rest of them had irregular and variable results. It was predicted that Kombucha is affected by different environments, sugar quantity, fermentation conditions, and ionization change that occurs during fermentation may cause this variability. The highest initial and final DPPH scavenging ability results are calculated in green tea samples (Figure 1F). All other herbal and fruit tea Kombucha samples are lower than green tea samples (Figure 1F and Supplementary Materials). It is also reported that the highest DPPH scavenging ability is generally obtained from green tea samples [41]. Moreover, the change in antioxidant activity is affected by tea type and fermentation temperature. DPPH scavenging ability, despite decreases and increases during fermentation, generally increases at the end of fermentation [41].

3.4. Kinetic Characterization

Based on the kinetic results given in Table 2, the minimum and maximum ΔS are determined as 8.52 g/L in ST-10 and 55.40 g/L in LT-70, respectively. As the sugar concentration in the fermentation medium increases, ΔS increases. However, this is not alone as an indicator that indicates the success of fermentation. Therefore, other kinetics regarding substrate depletion, Q_s , and η , were estimated. The results indicate that the lowest and

highest values of Q_S are 1.29 g/L/d in ST-10 and 11.28 g/L in LT-70, which are the same as ΔS . Moreover, as the substrate concentration increases, Q_S increases. The η was also determined, and the values of η range from 26.02 in BBT-70 to 100% in AT-10, RT-10, and PT-10. When the sugar amount added into the fermentation medium was minimum, almost all the sugar was consumed by the Kombucha culture. However, when the substrate concentrations in the fermentation medium are 40 g/L and 70 g/L, the η varies from 29.39% in ST-40 to 56.65% in GT-40 and 26.02% in BBT-70 to 72.78% in LT-70, respectively. Therefore, we can say that as the substrate concentration in the fermentation environment increases, η decreases in general.

Similar to the kinetics regarding substrate consumption, when the fermentation medium is enriched with 10 g/L sucrose, the minimum ΔX is 0.72 g/L for ST-10, whereas its maximum value is 2.20 g/L for PT-10. When 40 g/L sucrose is added into the fermentation medium, the lowest and highest values of ΔX are 1.74 g/L and 4.71 g/L in ST-10 and RT-40, respectively. Similarly, when the substrate concentration in the medium is 70 g/L, the ΔX varies from 3.55 to 8.77 g/L in BBT-70 and PT-70. Therefore, as the substrate concentration increases, ΔX increases. As for the Q_X , when the fermentation medium is supplemented with 10 g/L, 40 g/L, and 70 g/L of sucrose, the lowest and highest values of Q_X are calculated as 0.12 g/L/d and 0.91 g/L/d (ST-10 and PT-10), 0.51 g/L/d and 2.17 g/L/d (ST-40 and RT-40), and 0.14 g/L/d and 1.66 g/L/d (LT-70 and PT-70), respectively. Between both the minimum and maximum Q_X values, the highest Q_X values are yielded when 40 g/L substrate is added into the medium. Moreover, when the fermentation medium is supplemented with 10 g/L, 40 g/L, and 70 g/L, the lowest values of $Y_{X/S}$ are 0.06 g/g, 0.08 g/g, and 0.07 g/g, whereas their highest values are 0.21 g/g, 0.20 g/g, and 0.20 g/g, respectively. The minimum and maximum values of $Y_{X/S}$ at different substrate concentrations are highly close to each other. Although ΔX increases depending on the substrate concentration, this situation is not valid for the $Y_{X/S}$.

Regarding the kinetic results related to the total acidity, the minimum and maximum ΔTA values are determined as 0.17% and 1.07%, 0.87% and 4.10%, and 1.42% and 2.77% of ST-10 and RT-10, GT-40 and ST-40, and GT-70 and RT-70 when 10 g/L, 40 g/L, and 70 g/L sucrose are inserted into the medium, respectively. Except for the ΔTA values of the Kombucha fermentation of ST, as the substrate concentration increases, ΔTA values increase (Table 2). The lowest and highest Q_{TA} values are found as 0.08%/d and 0.36%/d (ST-10 and RT-10), 0.27%/d and 0.60%/d (LT-40 and ST-40), and 0.28%/d and 0.82%/d (ST-70 and RT-70) with 10 g/L, 40 g/L, and 70 g/L of sucrose concentration added into the medium. As it is in the values of ΔTA , except for Q_{TA} values of ST, Q_{TA} values increase with an increase in substrate concentration (Table 2).

The lowest values of ΔPH are 130.66 mg/L, 295.36 mg/L, and 227.06 mg/L with 10 g/L, 40 g/L, and 70 g/L sucrose concentrations inserted into the RT-10, RT-40, and LT-70 media, respectively. Contrarily, its maximum values are yielded as 1217.60 mg/L from GT-10, 1311.92 mg/L from BBT-40, and 1268.40 mg/L from GT-70. Except for the ΔPH values of ST, GT, and BT, the highest ΔPH values are obtained when 40 g/L sucrose is used in the medium (Table 2). Additionally, the minimum and maximum values of Q_{PH} are 21.39 mg/L/d and 410.68 mg/L/d, 49.54 mg/L/d and 245.69 mg/L/d, and 48.14 mg/L/d and 264.16 mg/L/d for RT-10 and GT-10, LT-40 and GT-40, and LT-70 and GT-70, respectively. It is realized that the Kombucha teas from GT supplemented with 10 g/L, 40 g/L, and 70 g/L sucrose give the highest phenolic substance amounts. As the substrate concentration in the GT-based medium increase, the values of Q_{PH} decrease. Conversely, the Q_{PH} increase with an increase in substrate concentration added into the ST- and PT-based media. For the rest of Q_{PH} , the maximum peak values of Q_{PH} are yielded when 40 g/L substrate concentration is added into the fermentation medium. Concerning the $Y_{PH/S}$, its lowest values are obtained to be 8.47 mg PH/g, 10.28 mg PH/g, and 4.10 mg PH/g substrate when the fermentation media are RT-10, RT-40, and LT-70, respectively. Maximum $Y_{PH/S}$ values are also calculated as 100.38 mg PH/g, 81.74 mg PH/g, and 36.57 mg PH/g substrate for GT-10, BBT-40, and BBT-70, respectively. As the sugar concentration in the

medium increases, the maximum $Y_{PH/S}$ value decreases. Moreover, it is determined that $Y_{PH/S}$ values decrease with an increase in the substrate levels of GT- and PT-based media. For the remaining media, except for that of the LT, the highest $Y_{PH/S}$ peak values are yielded when the media are enriched with 40 g/L sucrose (Table 2).

3.5. Kinetic Modeling

The observed values of total acidity were estimated by the LPM, while the actual values related to sugar depletion were predicted by the LM (Figure 2). Concerning the prediction of sugar depletion values, the observed and estimated sugar depletion curves are plotted vs. time in Figure 2. As indicated in Figure 2, ST, LT, GT, AT, RT, PT, and BBT, the experimental and estimated sugar depletion values are generally in good agreement, except for that of the Kombucha fermentation performed with ST supplemented with 40 g/L sucrose because its R^2 value (0.6038) is lower than 0.75 (Table 3). Indeed, the experimental data on days 4–7 of fermentation are overestimated by the LM (Figure 2, ST). Additionally, if the R^2 value is higher than 0.75, meaning that the model can be used to estimate the fermentation experimental data [42]. Therefore, the yielded R^2 values are found between 0.7731 and 0.9750, except for $R^2 = 0.6038$, demonstrating that the proposed model for substrate depletion adequately fits the actual data of substrate depletion. Additionally, the values of $\mu_{m,s}$, and S_f are between 0.17 and 1.14 d^{-1} and 0.34 and 9.64 g/L, respectively. The minimum and maximum values of $\mu_{m,s}$ are obtained when the BBT supplemented with 40 g/L and 10 g/L sucrose is used in the production of Kombucha tea, respectively. The highest $\mu_{m,s}$ values are achieved when 10 g/L sucrose is added to the fermentation media (Table 3). The lowest and highest S_f values are also yielded with ST supplemented with 10 g/L sucrose and RT supplemented with 70 g/L sucrose, respectively. Nevertheless, the values of S_f increase with an increase in sucrose concentration added into the fermentation media in general (Table 3). Mahdinia et al. [35] predicted the observed substrate depletion data of Menaquinone-7 fermentation in the biofilm reactor with glucose- or glycerol-based medium using the LM. Based on the modeling results, it was declared that the R^2 values of the process were determined between 0.953 and 0.991, indicating that the suggested models fit well with the experimental substrate consumption data. The values of $\mu_{m,s}$ for glucose- and glycerol-based media were 0.059 h^{-1} and 0.054 h^{-1} , respectively [35], which are all higher than those of this study (Table 3). Ilgin et al. [43] estimated the substrate consumption data of *Aspergillus niger* inulinase fermentation from carob extract under shake flask fermentation circumstances using the LM. From the calculations, it was reported that the values of $\mu_{m,s}$, and S_f were found to be 0.062 h^{-1} and 0.93 g/L, respectively, showing that the $\mu_{m,s}$ value is greater than the results yielded from the current study while the S_f value is compatible with those of this study (Table 3). In another study in which *A. niger* inulinase fermentation of sugar beet molasses in the large-scale stirred tank bioreactor was taken place [44], the experimental data of substrate consumption were forecasted by using the LM; thus, the $\mu_{m,s}$, and S_f values are computed as 0.042 h^{-1} and 1.18 g/L, respectively. It is determined that the computed $\mu_{m,s}$, and S_f values are highly consistent with the present study (Table 3). It was reported that the proposed model successfully fitted the experimental data of substrate depletion with a high R^2 value ($R^2 = 0.9778$) [44].

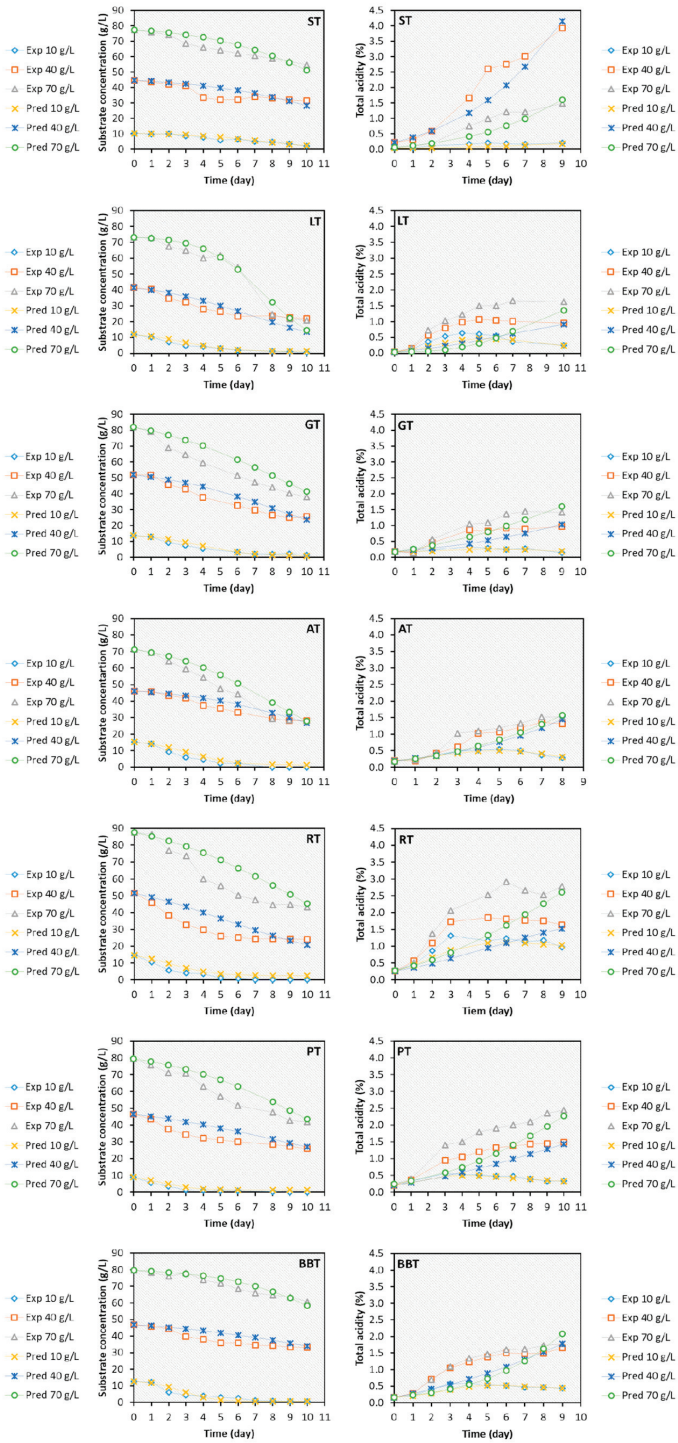


Figure 2. Substrate consumption and total acidity curves fitted by the LM and LPM.

Table 3. The model parameters calculated for kinetically modeling the Kombucha fermentation.

Tea	[Substrate]	Kinetics for Substrate Consumption				Kinetics for Acidity			
		$\mu_{m,s}$ (1/d)	S_m (g/L)	S_f (g/L)	R^2	β (%/gS.d)	α (%/gS)	A > β Fold	R^2
ST	10 (g/L)	0.4738	10.24	0.34	0.9438	0.0001	0.0201	360.19	0.5675
	40 (g/L)	0.2752	44.58	1.87	0.6038	0.0076	0.2584	34.00	0.9064
	70 (g/L)	0.2864	77.45	2.54	0.8572	0.0013	0.0662	49.85	0.8481
LT	10 (g/L)	0.7821	11.99	1.19	0.9672	−0.0058	0.0631	10.91	0.8060
	40 (g/L)	0.3462	41.42	3.89	0.8055	−0.0006	0.0343	60.27	0.5337
	70 (g/L)	0.5947	73.16	0.83	0.9655	0.0004	0.0211	55.41	0.4809
GT	10 (g/L)	0.7168	13.62	0.84	0.9487	−0.0024	0.0142	5.87	0.7586
	40 (g/L)	0.2909	52.03	4.44	0.9185	0.0005	0.0315	63.17	0.7220
	70 (g/L)	0.2503	82.03	9.18	0.9413	0.0001	0.0394	282.80	0.8259
AT	10 (g/L)	0.7798	15.34	1.24	0.9636	−0.0075	0.0468	6.24	0.9228
	40 (g/L)	0.2757	46.12	2.46	0.9012	0.0019	0.0863	45.75	0.8479
	70 (g/L)	0.3324	71.27	5.07	0.9563	0.0015	0.0365	23.65	0.8251
RT	10 (g/L)	0.7978	14.64	2.49	0.9671	−0.0030	0.0876	29.15	0.8465
	40 (g/L)	0.2765	51.46	9.47	0.7731	−0.0003	0.0475	145.00	0.6153
	70 (g/L)	0.2459	87.58	9.64	0.8645	−0.0006	0.0671	110.88	0.7225
PT	10 (g/L)	1.0969	8.94	1.39	0.9750	−0.0039	0.0554	14.30	0.9526
	40 (g/L)	0.2011	46.40	6.97	0.8137	0.0008	0.0568	75.30	0.8141
	70 (g/L)	0.2589	79.37	6.13	0.9332	0.0013	0.0493	39.13	0.8193
BBT	10 (g/L)	1.1422	12.71	0.52	0.9166	−0.0023	0.0371	16.34	0.7676
	40 (g/L)	0.1671	46.97	4.90	0.8257	0.0010	0.1349	129.31	0.7937
	70 (g/L)	0.3043	79.67	1.49	0.9088	0.0008	0.1122	135.44	0.6790

$\mu_{m,s}$, specific sugar consumption rate (1/d); S_m , maximum substrate concentration (g/L); S_f , final substrate concentration (g/L); R^2 , determination of coefficient; β , empirical constant (%/gS.d); α , empirical constant (%/gS); ST, sage tea; LT, linden tea; GT, green tea; AT, apple tea; RT, rosehip tea; PT, pomegranate tea; and BBT, bilberry tea.

The actual and estimated total acidity values are also plotted vs. time and shown in Figure 2. It is detected that the values of R^2 range from 0.4809 to 0.9526. It can be said that those with R^2 values higher than 0.75 (in this case, they are ST-40, ST-70, LT-10, GT-10, GT-70, AT-10, AT-40, AT-70, RT-10, PT-10, PT-40, PT-70, BBT-10, and BBT-40) are adequately fitted by the LPM (Table 3). Therefore, most of the Kombucha fermentation from different tea extracts supplemented with different concentrations of sucrose is satisfactorily fitted by the LPM with the R^2 value greater than 0.75. Moreover, α and β values, which can change based on the fermentation circumstances, were estimated (Table 3). If $\alpha \neq 0$ and $\beta = 0$, then the total acidity is associated with substrate consumption. If $\alpha = 0$ and $\beta \neq 0$, then the total acidity is non-associated with substrate consumption. The values of β vary from −0.0075 to 0.0076%/gS.d, which are so close to zero, while the values of α range from 0.0142 and 0.2584%/gS. The values of α are 5.87 to 360.19 times greater than those of β (Table 3). Therefore, we can say that the total acidity is associated with substrate consumption. Mahdinia et al. [35] studied the kinetic modeling of Menaquinone-7 fabrication from glucose and glycerol in the biofilm reactor using the LPM. The model parameters of the LPM, which are α and β , were calculated to be −0.138 mg/g and 0.00010 mg/g/h for the production in the glucose-based medium and −0.089 mg/g and 0.00301 mg/g/h for the production in glycerol-based medium, respectively. Therefore, the values of α were 1380- and 29.57-fold higher than those of β , respectively, showing that Menaquinone-7 fabrication was associated with substrate consumption [35], as it is in the current study. To the best of our knowledge, there is no study regarding the kinetic modeling of Kombucha fermentation using different tea extracts enriched with different concentrations of sucrose as a carbon source. Therefore, this study is important in terms of contributing to science because of the information it contains.

4. Conclusions

In conclusion, the study focused on the fermentation performance of a commercial Kombucha culture using different herbal and fruit tea extracts with varying sugar concentrations. The results showed that the Kombucha culture effectively consumed all sugar in the fermentation medium when supplemented with AT-10, RT-10, PT-10, and BT-10, but when higher sugar concentrations were present, not all substrate was consumed. The highest sugar consumption value was 55.40 g/L for LT-70 herbal Kombucha tea, while AT-70 fruit Kombucha tea had the highest value at 48.39 g/L. These sugar consumption values were correlated with biomass production, showing an increase with higher sugar consumption. The pH and total acidity of the Kombucha teas changed during fermentation, with herbal teas showing more significant fluctuations than fruit teas. The organic acid production and microbial by-products during fermentation decreased pH and increased total acidity. Additionally, the total phenolic compounds and antioxidant activity increased during fermentation, with higher increases observed in fruit kombucha teas compared to herbal teas. Kinetic characterization revealed the relationships between sugar depletion, biomass production, total acidity, and phenolic compounds during fermentation. The values of different kinetic parameters varied depending on the sugar concentration in the fermentation medium. However, this study had some limitations, such as the lack of detailed analysis of the specific enzymes involved in the breakdown of complex phenolic compounds and the influence of environmental factors on fermentation variability. Furthermore, only a specific commercial Kombucha culture was used, which may not fully represent the diversity of Kombucha cultures available. Despite these limitations, this study provides valuable insights into the fermentation performance of Kombucha cultures under different conditions, which could be beneficial for further research and industrial applications.

Supplementary Materials: The following supporting information can be downloaded at: <https://www.mdpi.com/article/10.3390/pr11072100/s1>, Figure S1: Change of substrate concentration, biomass production, pH, total acidity, phenolic, and antioxidant activity during Kombucha fermentation performed on media containing different initial sugar concentrations. (A, H, and O): Sage tea (ST); (B, I, and Q): Linden tea (LT); (C, J, and P): Green tea (GT); (D, K, and R): Apple tea (AT); (E, L, and S): Rosehip tea (RT); (F, M, and T): Pomegranate tea (PT); and (G, N, and U): Bilberry tea (BBT).

Author Contributions: K.T.K. conceptualization, investigation, methodology, project administration, and writing—original draft preparation; G.A. conceptualization, investigation, methodology, project administration, and writing—original draft preparation; S.T. conceptualization, investigation, methodology, project administration, and writing—original draft preparation; E.Y. writing—review and editing, project administration, supervision, and formal analysis; M.G. writing—review and editing, formal analysis, software, and modeling; I.Y. writing—review and editing, formal analysis, software, and modeling; I.T. writing—review and editing, resources, supervision, conceptualization, and methodology. All authors have read and agreed to the published version of the manuscript.

Funding: This research received no external funding.

Data Availability Statement: Not applicable.

Acknowledgments: This study was supported by the TUBITAK 2209-University Student Research Project Support Program.

Conflicts of Interest: The authors declare no conflict of interest.

Abbreviations

Abbreviations	Full Name
ISC	Initial sucrose concentration
AAB	Acetic acid bacteria
R ²	Determination of coefficient
α and β	Empirical constants
N	Normal
HCl	Hydrochloric acid
LPM	Luedeking–Piret model
LM	Logistic model
GT	Green tea
ST	Sage tea
LT	Linden tea
BT	Black tea
BBT	Bilberry tea
RT	Rosehip tea
AT	Apple tea
PT	Pomegranate tea
NaOH	Sodium hydroxide
GAE	Gallic acid equivalents
DPPH	α , α -diphenyl- β -picrylhydrazyl
ΔS	Substrate consumption, g/L
Q _S	Maximum substrate consumption rate, g/L/d
η	Substrate utilization yield, %
ΔX	Biomass production, g/L
Q _X	Maximum biomass production rate, g/L/d
Y _{X/S}	Biomass yield, g biomass/g substrate
TA	Total acidity, %
Q _{TA}	Maximum total acidity production rate, %/d
ΔPH	Phenolic production, mg/L
Q _{PH}	Maximum phenolic production rate, mg/L/d
Y _{PH/S}	Phenolic yield, mg phenolic/g substrate
$-dS/dt$	Substrate consumption rate, g/L/d
$\mu_{m,S}$	Specific sugar consumption rate, 1/d
S	Residual substrate concentration at the time "t", g/L
S _m	Maximum substrate concentration, g/L
S _f	Final substrate concentration, g/L
dP/dt	Total acidity rate, %/d
SAS	Statistical Analysis System

References

- Dutta, H.; Paul, S.K. Kombucha drink: Production, quality, and safety aspects. In *Production and Management of Beverages*; Elsevier: Amsterdam, The Netherlands, 2019; pp. 259–288.
- Jayabalan, R.; Malbasa, R.V.; Loncar, E.S.; Vitas, J.S.; Sathishkumar, M. A review on kombucha tea: Microbiology, composition, fermentation, beneficial effects, toxicity, and tea fungus. *Compr. Rev. Food Sci. Food Saf.* **2014**, *13*, 538–550. [CrossRef] [PubMed]
- Teoh, A.L.; Heard, G.; Cox, J. Yeast ecology of Kombucha fermentation. *Int. J. Food Microbiol.* **2004**, *95*, 119–126. [CrossRef] [PubMed]
- Malbaša, R.; Lončar, E.; Djurić, M. Comparison of the products of Kombucha fermentation on sucrose and molasses. *Food Chem.* **2008**, *106*, 1039–1045. [CrossRef]
- Şafak, S.; Mercan, N.; Aslim, B.; Beyatli, Y. A study on the production of poly- β -hydroxybutyrate by some eukaryotic microorganisms. *Turk. Electron. J. Biotechnol.* **2002**, *1*, 11–17.
- Mayser, P.; Fromme, S.; Leitzmann, G.; Gründer, K. The yeast spectrum of the 'tea fungus Kombucha'. *Mycoses* **1995**, *38*, 289–295. [CrossRef]
- Tsilo, P.H.; Basson, A.K.; Ntombela, Z.G.; Maliehe, T.S.; Pullabhotla, R.V. Isolation and optimization of culture conditions of a bioflocculant-producing fungi from Kombucha tea SCOBY. *Microbiol. Res.* **2021**, *12*, 950–966. [CrossRef]
- Greenwalt, C.; Steinkraus, K.; Ledford, R. Kombucha, the fermented tea: Microbiology, composition, and claimed health effects. *J. Food Prot.* **2000**, *63*, 976–981. [CrossRef]

9. Kurtzman, C.P.; Robnett, C.J.; Basehoar-Powers, E. *Zygosaccharomyces kombuchaensis*, a new ascosporegenous yeast from 'Kombucha tea'. *FEMS Yeast Res.* **2001**, *1*, 133–138. [CrossRef]
10. Liu, C.-H.; Hsu, W.-H.; Lee, F.-L.; Liao, C.-C. The isolation and identification of microbes from a fermented tea beverage, Haipao, and their interactions during Haipao fermentation. *Food Microbiol.* **1996**, *13*, 407–415. [CrossRef]
11. Chakravorty, S.; Bhattacharya, S.; Chatzinotas, A.; Chakraborty, W.; Bhattacharya, D.; Gachhui, R. Kombucha tea fermentation: Microbial and biochemical dynamics. *Int. J. Food Microbiol.* **2016**, *220*, 63–72. [CrossRef]
12. Morales-de la Peña, M.; Miranda-Mejía, G.A.; Martín-Belloso, O. Recent Trends in Fermented Beverages Processing: The Use of Emerging Technologies. *Beverages* **2023**, *9*, 51. [CrossRef]
13. Nummer, B.A. Kombucha brewing under the Food and Drug Administration Model Food Code: Risk analysis and processing guidance. *J. Environ. Health* **2013**, *76*, 8–11. [PubMed]
14. Villarreal-Soto, S.A.; Beaufort, S.; Bouajila, J.; Souchard, J.P.; Taillandier, P. Understanding kombucha tea fermentation: A review. *J. Food Sci.* **2018**, *83*, 580–588. [CrossRef] [PubMed]
15. Malbasa, R.V.; Loncar, E.S.; Vitas, J.S.; Canadanovic-Brunet, J.M. Influence of starter cultures on the antioxidant activity of kombucha beverage. *Food Chem.* **2011**, *127*, 1727–1731. [CrossRef]
16. Greenwalt, C.J.; Ledford, R.A.; Steinkraus, K.H. Determination and characterization of the antimicrobial activity of the fermented tea kombucha. *LWT-Food Sci. Technol.* **1998**, *31*, 291–296. [CrossRef]
17. Battikh, H.; Bakhrouf, A.; Ammar, E. Antimicrobial effect of kombucha analogues. *LWT-Food Sci. Technol.* **2012**, *47*, 71–77. [CrossRef]
18. Bhattacharya, D.; Bhattacharya, S.; Patra, M.M.; Chakravorty, S.; Sarkar, S.; Chakraborty, W.; Koley, H.; Gachhui, R. Antibacterial activity of polyphenolic fraction of kombucha against enteric bacterial pathogens. *Curr. Microbiol.* **2016**, *73*, 885–896. [CrossRef]
19. Chu, S.C.; Chen, C.S. Effects of origins and fermentation time on the antioxidant activities of kombucha. *Food Chem.* **2006**, *98*, 502–507. [CrossRef]
20. Malbasa, R.; Loncar, E.; Djuric, M.; Dosenovic, I. Effect of sucrose concentration on the products of kombucha fermentation on molasses. *Food Chem.* **2008**, *108*, 926–932. [CrossRef]
21. Zubaidah, E.; Yurista, S.; Rahmadani, N. Characteristic of physical, chemical, and microbiological kombucha from various varieties of apples. In *IOP Conference Series: Earth and Environmental Science*; IOP Publishing Ltd.: Bristol, UK, 2018; Volume 1, p. 012040.
22. Tarhan, K. Use of Different Substrate Resources in the Production of Kombucha Tea. 2017. Available online: <https://agris.fao.org/agris-search/search.do?recordID=TR2019000120> (accessed on 18 February 2023).
23. Tamer, C.E.; Temel, Ş.G.; Suna, S.; Karabacak, A.Ö.; Özcan, T.; Ersan, L.Y.; Kaya, B.T.; Çopur, Ö.U. Evaluation of bioaccessibility and functional properties of kombucha beverages fortified with different medicinal plant extracts. *Turk. J. Agric. For.* **2021**, *45*, 13–32.
24. Jayabalan, R.; Marimuthu, S.; Swaminathan, K. Changes in content of organic acids and tea polyphenols during kombucha tea fermentation. *Food Chem.* **2007**, *102*, 392–398. [CrossRef]
25. Battikh, H.; Chaieb, K.; Bakhrouf, A.; Ammar, E. Antibacterial and antifungal activities of black and green kombucha teas. *J. Food Biochem.* **2013**, *37*, 231–236. [CrossRef]
26. Lončar, E.S.; Kanurić, K.G.; Malbaša, R.V.; Đurić, M.S.; Milanović, S.D. Kinetics of saccharose fermentation by Kombucha. *Chem. Ind. Chem. Eng. Q.* **2014**, *20*, 345–352. [CrossRef]
27. Ismaiel, A.A.; Bassyouni, R.H.; Kamel, Z.; Gabr, S.M. Detoxification of patulin by kombucha tea culture. *CyTA-J. Food* **2016**, *14*, 271–279. [CrossRef]
28. Germec, M.; Karhan, M.; Demirci, A.; Turhan, I. Kinetic modeling, sensitivity analysis, and techno-economic feasibility of ethanol fermentation from non-sterile carob extract-based media in *Saccharomyces cerevisiae* biofilm reactor under a repeated-batch fermentation process. *Fuel* **2022**, *324*, 124729. [CrossRef]
29. Alboreadi, M.A.; Al-Najdawi, M.M.; Jarrar, Q.B.; Moshawih, S. Evaluation of hair growth properties of topical kombucha tea extracts. *Adv. Tradit. Med.* **2021**, *22*, 155–161. [CrossRef]
30. Kruk, M.; Trzaskowska, M.; Ścibisz, I.; Pokorski, P. Application of the “SCOBY” and Kombucha tea for the production of fermented milk drinks. *Microorganisms* **2021**, *9*, 123. [CrossRef]
31. Cemeroglu, B. *Gıda Analizleri, Gıda Teknolojisi Derneği Yayınları*; Bizim Grup Basımevi: Ankara, Turkey, 2010.
32. Germec, M.; Karahalil, E.; Yatmaz, E.; Tari, C.; Turhan, I. Effect of process parameters and microparticle addition on polygalacturonase activity and fungal morphology of *Aspergillus sojae*. *Biomass Convers. Biorefin.* **2021**, *12*, 5329–5344. [CrossRef]
33. Miller, G.L. Use of dinitrosalicylic acid reagent for determination of reducing sugar. *Anal. Chem.* **1959**, *31*, 426–428. [CrossRef]
34. Škerget, M.; Kotnik, P.; Hadolin, M.; Hraš, A.R.; Simonič, M.; Knez, Ž. Phenols, proanthocyanidins, flavones and flavonols in some plant materials and their antioxidant activities. *Food Chem.* **2005**, *89*, 191–198. [CrossRef]
35. Mahdinia, E.; Mamouri, S.J.; Puri, V.M.; Demirci, A.; Berenjian, A. Modeling of vitamin K (Menaquinone-7) fermentation by *Bacillus subtilis natto* in biofilm reactors. *Biocatal. Agric. Biotechnol.* **2019**, *17*, 196–202. [CrossRef]
36. Watawana, M.I.; Jayawardena, N.; Gunawardhana, C.B.; Waisundara, V.Y. Health, wellness, and safety aspects of the consumption of kombucha. *J. Chem.* **2015**, *2015*, 591869. [CrossRef]
37. Muhialdin, B.; Osman, F.; Muhamad, R.; Che Wan Sapawi, C.; Anzian, A.; Voon, W.; Hussin, A. Effects of sugar sources and fermentation time on the properties of tea fungus (kombucha) beverage. *Int. Food Res. J.* **2019**, *26*, 481–487.

38. Kallel, L.; Desseaux, V.; Hamdi, M.; Stocker, P.; Ajandouz, E. Insights into the fermentation biochemistry of kombucha teas and potential impacts of kombucha drinking on starch digestion. *Food Res. Int.* **2012**, *49*, 226–232. [CrossRef]
39. Bhattacharya, S.; Gachhui, R.; Sil, P.C. Effect of kombucha, a fermented black tea in attenuating oxidative stress mediated tissue damage in alloxan induced diabetic rats. *Food Chem. Toxicol.* **2013**, *60*, 328–340. [CrossRef]
40. Emiljanowicz, K.E.; Malinowska-Pańczyk, E. Kombucha from alternative raw materials—The review. *Crit. Rev. Food Sci. Nutr.* **2020**, *60*, 3185–3194. [CrossRef] [PubMed]
41. Fu, C.L.; Yan, F.; Cao, Z.L.; Xie, F.Y.; Lin, J. Antioxidant activities of kombucha prepared from three different substrates and changes in content of probiotics during storage. *Food Sci. Technol.* **2014**, *34*, 123–126. [CrossRef]
42. Carlson, H.A. Check your confidence: Size really does matter. *J. Chem. Inf. Model.* **2013**, *53*, 1837–1841. [CrossRef]
43. İlgin, M.; Germec, M.; Turhan, I. Statistical and kinetic modeling of *Aspergillus niger* inulinase fermentation from carob extract and its partial concentration. *Ind. Crops Prod.* **2020**, *156*, 112866. [CrossRef]
44. Germec, M.; Turhan, I. Kinetic modeling and sensitivity analysis of inulinase production in large-scale stirred tank bioreactor with sugar beet molasses-based medium. *Biochem. Eng. J.* **2021**, *176*, 108201. [CrossRef]

Disclaimer/Publisher’s Note: The statements, opinions and data contained in all publications are solely those of the individual author(s) and contributor(s) and not of MDPI and/or the editor(s). MDPI and/or the editor(s) disclaim responsibility for any injury to people or property resulting from any ideas, methods, instructions or products referred to in the content.

Article

Fermentation of Menaquinone-7: The Influence of Environmental Factors and Storage Conditions on the Isomer Profile

Neha Lal¹, Mostafa Seifan¹ and Aydin Berenjian^{1,2,*}¹ School of Engineering, The University of Waikato, Hamilton 3240, New Zealand² Department of Chemical and Biological Engineering, Colorado State University, Fort Collins, CO 80523, USA

* Correspondence: aydin.berenjian@waikato.ac.nz

Abstract: Menaquinone-7 (MK-7) provides significant health gains due to its excellent pharmacokinetic properties. However, MK-7 occurs at low concentrations in mainstream foods, heightening the demand for nutritional supplements. MK-7 exists as geometric isomers, and only all-*trans* MK-7 is bioactive. Exposure to certain environments impacts the isomer profile. Knowledge of these factors and their influence on the isomer composition is important, as the efficacy of fermented MK-7 end products is solely determined by the all-*trans* isomer. This investigation aimed to evaluate the short- and long-term effect of atmospheric oxygen, common temperatures, and light on the isomer profile. From the short-term study, it was ascertained that MK-7 is moderately heat-stable but extremely light-sensitive. The stability of all-*trans* MK-7 was then examined during 8 weeks of storage at a low temperature with minimal oxygen exposure in the absence of light. Negligible change in the all-*trans* MK-7 concentration occurred, suggesting it is reasonably stable during prolonged storage in this environment. These findings will aid the development of optimal storage conditions to preserve bioactive MK-7 in fermented nutritional supplements, the large-scale availability and consumption of which will help compensate for the dietary deficit of this essential vitamin and provide consumers with better health outcomes.

Keywords: menaquinone-7 isomer profile; bioactivity; fermentation; environmental factors; storage conditions

Citation: Lal, N.; Seifan, M.; Berenjian, A. Fermentation of Menaquinone-7: The Influence of Environmental Factors and Storage Conditions on the Isomer Profile. *Processes* **2023**, *11*, 1816. <https://doi.org/10.3390/pr11061816>

Academic Editor: Ibrahim M. Abu-Reidah

Received: 24 May 2023
Revised: 9 June 2023
Accepted: 13 June 2023
Published: 15 June 2023



Copyright: © 2023 by the authors. Licensee MDPI, Basel, Switzerland. This article is an open access article distributed under the terms and conditions of the Creative Commons Attribution (CC BY) license (<https://creativecommons.org/licenses/by/4.0/>).

1. Introduction

The vitamin K family consists of a set of fat-soluble vitamins, namely vitamin K1 (phylloquinone), vitamin K2 (menaquinones), and vitamin K3 (menadiolone). The various K vitamers are structurally similar, as they all contain a 2-methyl-1,4-naphthoquinone group [1]. However, they differ in the nature of an isoprenoid side chain at the 3-position, the length and degree of unsaturation of which confers unique properties to each kind of vitamin K [2]. Phylloquinone (PK) and menaquinones (MK) are the natural forms of the vitamin and play an essential role in human health and nutrition [3]. PK has one unsaturated and three saturated isoprenoid units in its side chain. It is ubiquitous within the chloroplasts of photosynthetic plants and algae, where it functions as an electron carrier during photosynthesis [2,4]. Therefore, PK can be consumed from a selection of everyday foods, including leafy greens, vegetable oils, and products resulting from such plant oils, and is the most abundant type of dietary vitamin K [4,5]. Conversely, MK are a series of compounds with isoprenoid chains of various lengths and degrees of unsaturation. The structure of the side chain can be represented by the format MK-*n*, where *n* is generally between four and thirteen and signifies the number of unsaturated isoprenoid residues in the chain [2]. MK are typically of microbial origin and are present in small quantities in specific animal, dairy, and fermented goods [2,5–8].

It is well-known that all vitamin K subtypes perform essential functions in the coagulation cascade and haemostasis. However, recent research has uncovered numerous other

roles and health gains of vitamin K. The intake of vitamin K2, in particular, has been related to the maintenance of bone and cardiovascular health, the suppression of neurological conditions, the prevention of cancer, aiding the functional recovery of the liver, reducing the likelihood of many health disorders, and decreasing the morbidity and mortality linked to coronavirus disease 2019 (COVID-19) [2,9–17].

MK-7 is the most notable vitamin K2 isoform due to its superior physicochemical characteristics and long plasma half-life (72 h), which enhance its extrahepatic bioavailability and therapeutic value [17–19]. Despite the significant health gains associated with MK-7, obtaining sufficient levels of the vitamin from regular food products is challenging for most consumers, as it is present in insufficient concentrations in limited foods. Natto, a Japanese fermented soybean containing nearly 800–1000 µg of MK-7 per 100 g of natto, is the richest source of MK-7 [6,8,20]. However, owing to its strong flavour and pungent aroma, most individuals perceive natto as unappetising and, hence, it tends to be a niche product that is not universally consumed by all populations. The MK-7 concentration in other dietary sources that appeal to mainstream consumers is inadequate. Consequently, meeting the daily intake requirements without the aid of nutritional supplements is not achievable for most populations, as it would require the consumption of unfeasibly large amounts of MK-7-containing foods [6]. This has increased the demand and created a lucrative market for MK-7 dietary supplements and enriched foods to complement natural sources, and the availability of such products has become progressively widespread [21].

It must be acknowledged that MK-7 demonstrates *cis-trans* isomerism, a feature that is common to most biomolecules. The all-*trans* isomer is the naturally occurring and bioactive form of the vitamin, whereas the various *cis* isomers are biologically ineffectual [7,22,23]. The bioactivity of MK-7 is related to its shape and structure, which depend on the arrangement of unsaturated bonds in the side chain. All-*trans* MK-7 has a straight isoprenoid chain (Figure 1), as all double bonds have the *trans* organisation [24]. In contrast, one or more unsaturated bonds in the *cis* conformation deform the linear molecular structure (Figure 1), and different numbers and combinations of *cis* double bonds can give rise to several *cis* MK-7 isomers [24]. The shape of MK-7 molecules determines their capacity to engage with subcellular components, and the non-linear configuration of the *cis* isomers impairs their ability to perform their biological role [25]. The *cis* isomers of vitamin K only sustain 1% of the biological significance of the all-*trans* form [26–28]. More recently, it has been established that *cis* MK-7 isomers have considerably diminished carboxylative potential and compromised bioactivity compared to all-*trans* MK-7 [25]. It is anticipated that the presence of *cis* MK-7 does not diminish the activity of the all-*trans* isomer. When the geometric isomers of the vitamin co-exist in a formulation, it is unlikely for interaction with the *cis* isomer to change the structure and bond arrangement of all-*trans* MK-7. As a result, the shape and, thus, the biological function of the all-*trans* isomer is expected to be unaffected. However, the remedial value of the preparation is only determined by the quantity of the biologically important isomer. Therefore, while the presence of *cis* MK-7 does not explicitly impact the activity of the all-*trans* isomer, its presence in the formulation is essentially an impurity, which decreases the biological function and therapeutic efficacy of all-*trans* MK-7 end products. In this regard, the isomer profile of MK-7 functional foods and dietary supplements is noteworthy, as their effectiveness is fundamentally governed by the proportion of the all-*trans* isomer.

MK-7 can be synthesised via chemical methods or microbial fermentation. The isomer composition of the MK-7 product is determined by various factors, primarily the manufacturing process and the techniques used to purify the post-reaction mixture [7,23]. Although chemical approaches are likely to be cost-effective, fermentation is more favourable from the perspective of both consumers and the environment. This is predominantly due to the recent consumer market trend promoting natural alternatives over synthetic formulations and the call for sustainable production methodologies. Fermentation is not only a natural approach for the synthesis of MK-7, but it is also more eco-friendly for the industrial

production of the vitamin. Hence, microbial fermentation can fulfil both consumer demand and environmental sustainability goals [29].

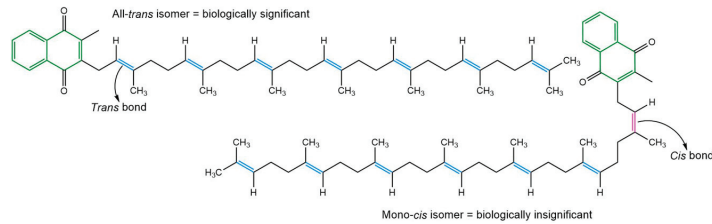


Figure 1. Chemical structure and bond organisation of MK-7 isomers.

The MK-7 isomer composition achieved from MK-7 fermentation has not been widely examined, and it is generally believed that MK-7 resulting from fermentation-based synthesis exclusively occurs in the all-*trans* conformation. However, it has been proposed that exposure to particular factors may induce the transformation of the all-*trans* isomer to *cis* MK-7, and our previous studies were the first to ascertain the existence of *cis* MK-7 in fermented samples [30,31]. The occurrence of a *cis* isomer in samples obtained from fermentation implies that although the bacterium produces the naturally occurring all-*trans* isomer intracellularly, secretion into the fermentation broth exposes all-*trans* MK-7 to the extracellular milieu, which can promote its isomerisation to the *cis* form. It is important to appreciate that the exact structural identity (the number and location of *cis* double bonds in the isoprenoid side chain) of the *cis* MK-7 isomer produced from fermentation under the investigated conditions cannot be established in the absence of nuclear magnetic resonance (NMR) spectroscopy methods. It has been suggested that all-*trans* MK-7 is most likely to isomerise to the mono-*cis* isomer under certain conditions [32]. Therefore, it is anticipated that the *cis* MK-7 observed is a mono-*cis* isomer, which contains a single *cis* double bond in its isoprenoid chain. Nevertheless, complete structure determination is not essential when considering the bioactivity of fermented MK-7 end products, as all *cis* isomers, irrespective of the number and location of *cis* bonds in their isoprenoid side chain, have significantly reduced biological efficacy compared to the all-*trans* isomer.

Although our prior investigations have focused on optimising the extracellular environment, specifically the fermentation media [30] and key fermentation parameters [31], to increase the synthesis of the all-*trans* isomer and reduce the production of *cis* MK-7 during fermentation, it is crucial to guarantee that the quantity of the bioactive isomer is maintained in the final product. Hence, not only is it necessary to achieve a high concentration of all-*trans* MK-7 from fermentation, but its quantity must also be preserved in dietary supplements and functional foods to develop effective fermented MK-7 consumer end products. It has been postulated that exposure to light (especially ultraviolet (UV) light), atmospheric oxygen, and elevated temperatures may encourage the geometric isomerisation of isoprenoid residues in the side chain of MK-7 and result in the formation of *cis* isomers [7,23,25,33,34]. However, this aspect has not been explicitly explored, particularly in the context of MK-7 isomers produced from fermentation. The effect of typical environmental and storage conditions is worthy of consideration from the perspective of fermented MK-7 dietary supplements and fortified or functional foods, as these consumer end products are likely to be subjected to such factors during their manufacture, use, and shelf life, which will influence their effectiveness and therapeutic value.

Therefore, the objective of this study was to assess the effect of various storage conditions on the isomer profile of fermented MK-7 from the perspective of MK-7 end products. Accordingly, factors representing possible conditions and environments that MK-7 dietary supplements and fortified or functional foods may be subjected to during their production, consumption, and general shelf life were selected and examined. These include exposure to atmospheric oxygen, different temperatures, and light. All factors were initially investigated over a short interval, and the conditions that resulted in the least isomerisation

and/or degradation of all-*trans* MK-7 were further evaluated to explore the stability of the all-*trans* isomer in an ideal storage environment over an extended timeframe. The outcomes of this study will offer valuable insights for the development of optimum storage conditions to preserve the quantity of the all-*trans* isomer in fermented MK-7 end products. This will likely be an important progression in improving the accessibility of bioactive fermented MK-7 nutritional supplements and functional foods, as the *cis* isomers of the vitamin are effectively contaminants that have little therapeutic value. The widespread availability and consumption of such products by diverse populations will help boost the dietary intake of MK-7 and offer more significant health benefits to consumers.

2. Materials and Methods

2.1. Chemicals and Materials

The all-*trans* MK-7 reference standard (98.1% purity) was acquired from ChromaDex (Los Angeles, CA, USA). Glucose was obtained from Ajax Finechem Pty Ltd. (Taren Point, NSW, Australia). Yeast extract and tryptone were supplied by Becton, Dickinson and Company (Franklin Lakes, NJ, USA). Soy peptone, methanol, 2-propanol, and *n*-hexane were obtained from Merck Millipore (Burlington, MA, USA). NaCl was acquired from a local supplier, and CaCl₂ was purchased from Sigma-Aldrich Co. (St. Louis, MO, USA). Nutrient agar plates were procured from Fort Richard Laboratories (Auckland, New Zealand). All media components were microbiology grade, and all solvents were analytical grade.

2.2. Microorganism and Inoculum Preparation

Bacillus subtilis natto was selected for the fermentation experiments since it results in a high MK-7 yield and is considered the most suitable strain for industrial MK-7 production. Furthermore, there are no safety issues accompanying the *B. subtilis natto* strain, and it is generally recognised as safe (GRAS). Consequently, it is ideal for synthesising fermented MK-7 end products expected for human consumption. The procedure outlined by Berenjian et al. [20] was used to prepare the *B. subtilis natto* strain. The microbial cells were grown in an aqueous culture medium comprising yeast extract, tryptone, and NaCl and streaked on nutrient agar plates, which were incubated for 48 h at 37 °C. After incubation, the cells were removed from the plates and submerged in a sterile NaCl solution. The mixture was then put in a water bath for 30 min at 80 °C to inactivate the vegetative cells and stimulate the production of spores prior to centrifuging (laboratory centrifuge, Sigma Laborzentrifugen GmbH, Osterode am Harz, Germany) at 3000 rpm for 10 min to remove the cell debris. The resulting bacterial spore suspension functioned as the inoculum for the fermentation studies.

2.3. Fermentation Procedure

MK-7 was synthesised from fermentation using the optimal media and conditions determined from our previous investigations [30,31] to enable maximal all-*trans* and minimal *cis* MK-7 isomer production. The media, containing 1% (*w/v*) glucose, 2% (*w/v*) yeast extract, 2% (*w/v*) soy peptone, 2% (*w/v*) tryptone, and 0.1% (*w/v*) CaCl₂ [30], was prepared in bulk to maintain consistency and sterilised at 121 °C for 20 min by autoclaving (TOMY SX-700E, Tokyo, Japan). Afterwards, the samples were inoculated with 2% (*v/v*) of the *B. subtilis natto* spore suspension and fermented in individual McCartney bottles under aerobic conditions at 40 °C and 200 rpm for 7 days [31].

2.4. MK-7 Extraction

Following fermentation, MK-7 was extracted from the samples with 2-propanol and *n*-hexane, which were mixed in a ratio of 1:2 (*v/v*), and the liquid-to-organic ratio was 1:4 (*v/v*) [20]. The solution was vortexed for 2 min, and phase separation was achieved by centrifugation (laboratory centrifuge, Sigma Laborzentrifugen GmbH, Osterode am Harz, Germany) at 3000 rpm for 10 min. Due to the fat-soluble nature of MK-7, it favourably

dissolves in non-polar solvents, such as *n*-hexane. Thus, the hexane layer was isolated from the mixture and evaporated in another set of McCartney bottles under a vacuum to obtain the extracted MK-7.

2.5. Exposure Studies

The extracted MK-7 samples (contained in transparent McCartney bottles) were then exposed to various environmental and storage conditions to explore the short- and long-term impact of these factors on the MK-7 isomer composition. Different temperature (low (4 °C), ambient (20 °C), and high (100 °C)), light (no light/dark, ambient light, and UV light), and oxygen (exposed to atmospheric oxygen and not exposed to atmospheric oxygen) conditions were selected to simulate likely storage environments for fermented MK-7 consumer end products, such as MK-7-enriched fortified or functional foods and dietary supplements. Possible conditions that fermented MK-7 could be exposed to during the manufacture of these products were also considered.

The effect of short-term exposure to the different temperature, light, and oxygen conditions on the isomer profile of fermented MK-7 was initially assessed. As a part of this process, samples were subjected to the factors outlined in Table 1 for 0, 3, 6, and 9 days to investigate the variation in the isomer composition over a brief timeframe for all conditions.

Table 1. Environmental and storage conditions for the short-term exposure study.

Sample	Conditions
1	Low temperature (4 °C) and exposed to atmospheric oxygen = stored in the fridge with the lid off
2	Low temperature (4 °C) and not exposed to atmospheric oxygen = stored in the fridge with the lid on (purged with nitrogen)
3	High temperature (100 °C) and exposed to atmospheric oxygen = stored in the oven with the lid off
4	High temperature (100 °C) and not exposed to atmospheric oxygen = stored in the oven with the lid on (purged with nitrogen)
5	No light and exposed to atmospheric oxygen = stored in the dark with the lid off at ambient temperature (by default)
6	No light and not exposed to atmospheric oxygen = stored in the dark with the lid on (purged with nitrogen) at ambient temperature (by default)
7	Ambient light and exposed to atmospheric oxygen = stored in ambient light (lamp) with the lid off at ambient temperature (by default)
8	Ambient light and not exposed to atmospheric oxygen = stored in ambient light (lamp) with the lid on (purged with nitrogen) at ambient temperature (by default)
9	UV light and exposed to atmospheric oxygen = stored in UV light (lamp) with the lid off at ambient temperature (by default)
10	UV light and not exposed to atmospheric oxygen = stored in UV light (lamp) with the lid on (purged with nitrogen) at ambient temperature (by default)

The optimum storage conditions, which resulted in the least deterioration of all-*trans* MK-7, determined from the short-term investigation, were further analysed in a monitoring study to explore the stability of the all-*trans* isomer and variation in the isomer profile over an extended period. Accordingly, samples were prepared in triplicates and stored at a low temperature (4 °C) with minimal oxygen exposure in the absence of light for 8 weeks. The MK-7 isomer composition was analysed after 0, 1, 2, 3, 4, 5, 6, 7, and 8 weeks of storage.

2.6. MK-7 Analysis

At the conclusion of the exposure period, the MK-7 isomer composition of all samples was analysed, as discussed in our earlier study [30]. The all-*trans* and *cis* MK-7 concentrations were determined using a Dionex high-performance liquid chromatography (HPLC) instrument (Thermo Fisher Scientific, Waltham, MA, USA) composed of four P680 pumps, an ASI-100 automated sample injector, a TCC-100 thermostatted column compartment,

and a UVD340U photodiode array UV detector. A packed column (COSMOSIL Cholester, 100 mm × 2 mm × 2.5 μm; Nacalai Tesque Inc., Kyoto, Japan) was used to separate the compounds at 40 °C. Pure methanol constituted the mobile phase, and the compounds were eluted isocratically at a flow rate of 0.2 mL/min. The run-time, analytical wavelength, autosampler temperature, and injection volume were 30 min, 248 nm, 10 °C, and 10 μL, respectively. The Chromeleon 7 program (Thermo Fisher Scientific, Waltham, MA, USA) was used for data collection, and a relative retention time (RRT) of 1.12 was used to ascertain the *cis* isomer.

Liquid chromatography–mass spectrometry (LC–MS) methods were employed to verify the identity and corroborate the retention times of all-*trans* and *cis* MK-7, using the approach described in our previous investigation [30]. The LC–MS platform comprised a Dionex Ultimate 3000 ultra-high-performance liquid chromatography (UHPLC) system and a QExactive mass spectrometer with a HESI II source (Thermo Fisher Scientific, Waltham, MA, USA). The Thermo XCalibur 4.3 package (Thermo Fisher Scientific, Waltham, MA, USA) was used to operate the equipment, and data were obtained using the Chromeleon 7.3 application (Thermo Fisher Scientific, Waltham, MA, USA). The conditions summarised above were implemented for liquid chromatography; however, the injection volume was modified to 5 μL, and the run-time was increased to 37 min to suit the LC–MS system. Data were collected in the positive ionisation mode with a resolution of 70,000, a MS1 scan range of 150–1000 *m/z*, a maximum injection time of 200 ms, and an AGC target of 3×10^6 . The Thermo FreeStyle 1.6 software (Thermo Fisher Scientific, Waltham, MA, USA) was utilised to evaluate the mass spectrometry (MS) data.

The MK-7 concentration of the samples was determined using a calibration curve (linear between 0.1 mg/L and 50 mg/L ($R^2 = 0.99$)), which was created with reference to the peak area corresponding to known concentrations of the analytical standard.

2.7. Statistical Methods

Statistical significance was determined by analysis of variance (ANOVA), and a two-sample *t*-test was used to compare the mean values of different groups. The data were reported as the mean ± standard deviation (SD) of three replicates, and significance was accepted at $p < 0.05$.

3. Results and Discussion

The various factors explored were selected to represent the likely storage environments for fermented MK-7 supplements and fortified or functional foods, together with potential conditions to which fermented MK-7 may be exposed during the manufacture of such products. For example, fermented MK-7-enriched dairy goods or supplements requiring cold temperature storage will probably be stored in the fridge at a low temperature (4 °C). In comparison, most other supplements and MK-7-enriched foods are likely to be stored and consumed at ambient temperature (20 °C). The packaging material and design for MK-7 products can influence the amount of light that MK-7 supplements and functional foods are exposed to, as dark, opaque, and transparent materials all permit the passage of variable amounts of light. Additionally, exposure to atmospheric oxygen is inevitable in the case of all MK-7 end products. High temperature (100 °C) conditions and exposure to UV light are likely to represent conditions that fermented MK-7 may be exposed to during the production, transportation, and storage of certain MK-7-enriched supplements and fortified or functional foods. All variables were first considered over a short timeframe. The optimal conditions that promoted minimal degradation and/or isomerisation of bioactive MK-7 were further explored to evaluate the stability of all-*trans* MK-7 over a longer period.

3.1. Effect of Environmental Factors and Storage Conditions on the MK-7 Isomer Composition

3.1.1. Light

The MK-7 isomer profile resulting from short-term storage in the dark at room temperature is outlined in Figure 2. Approximately 61% and 39% of the all-*trans* isomer and

87% and 67% of the *cis* isomer remained in the presence and absence of oxygen after 9 days of exposure. In addition, there is also no statistically significant difference in the all-*trans* and *cis* MK-7 isomer concentrations for the dark samples between days 3, 6, and 9 when assessing the presence and absence of oxygen independently ($p = 0.652$ and $p = 0.115$ for all-*trans* MK-7 in the presence and absence of oxygen and $p = 0.785$ and $p = 0.797$ for *cis* MK-7 in the presence and absence of oxygen). These findings indicate that no considerable reduction in the all-*trans* and *cis* MK-7 concentration occurs during short-term storage in the dark at ambient temperature, both with and without exposure to atmospheric oxygen.

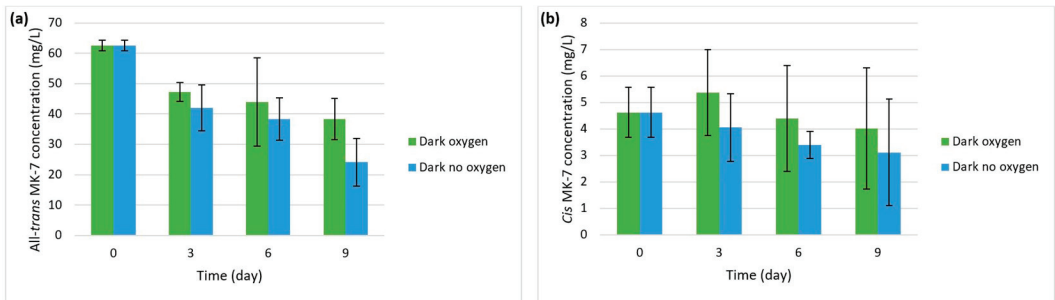


Figure 2. MK-7 isomer composition following short-term storage in the dark at ambient temperature in the presence and absence of oxygen for (a) all-*trans* MK-7 and (b) *cis* MK-7.

Figure 3 illustrates the effect of ambient light at room temperature on the all-*trans* and *cis* MK-7 concentration, and it is evident that exposure to ambient light has a detrimental impact on the isomer concentration. Over 99% of all-*trans* and 100% of *cis* MK-7 were degraded to undetectable levels within 3 days of exposure to ambient light with and without oxygen, implying that contact with oxygen does not have a noticeable effect on MK-7 stability in the presence of ambient light. The influence of UV light exposure on the MK-7 isomer concentration is displayed in Figure 4. It is apparent that MK-7 is very unstable in UV light, as both all-*trans* and *cis* MK-7 were not detected over the entire exposure period, regardless of the presence or absence of atmospheric oxygen.

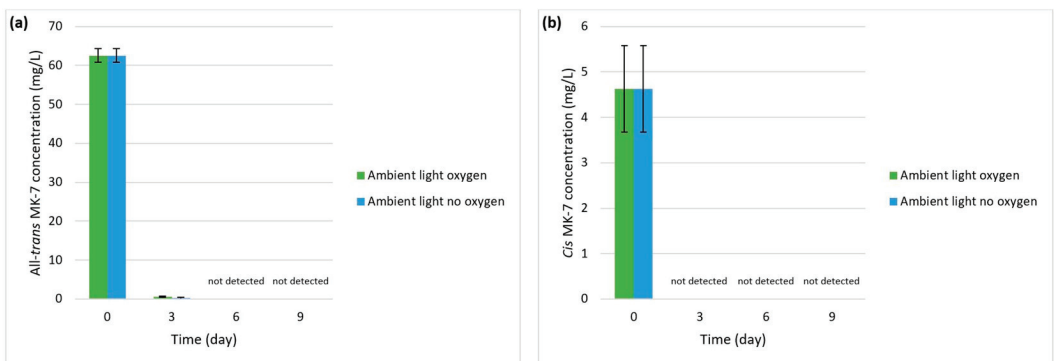


Figure 3. MK-7 isomer profile resulting from short-term exposure to ambient light at room temperature in the presence and absence of oxygen for (a) all-*trans* MK-7 and (b) *cis* MK-7.

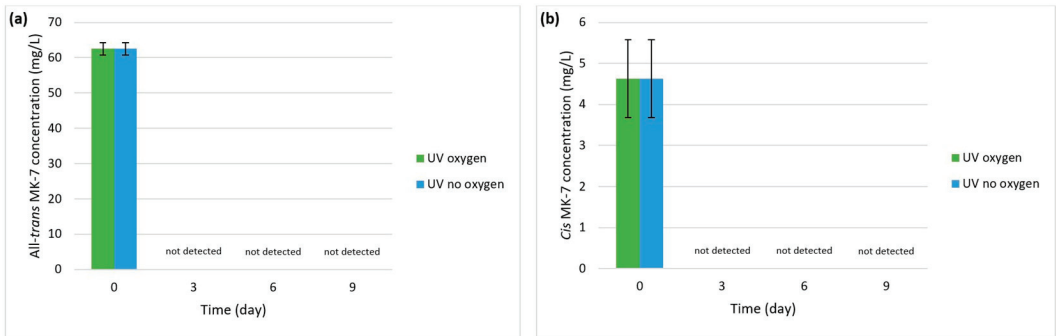


Figure 4. MK-7 isomer composition obtained from short-term exposure to UV light at ambient temperature in the presence and absence of oxygen for (a) all-*trans* MK-7 and (b) *cis* MK-7.

Fat-soluble vitamins, including vitamin K, tend to be light-sensitive and are degraded by exposure to various forms of light, such as ambient light, daylight, and UV light [35–38]. It has been suggested that light exposure may promote photoisomerisation, which refers to the conversion of one isomer of a molecule to another by light. Transformation of all-*trans* MK-7 to one or more *cis* forms of the vitamin may potentially occur due to light; however, there are no specific reports in the literature [7,23,34]. Geometric isomerisation of all-*trans* MK-7 as a result of exposure to ambient or UV light was not observed in the current study. Instead, the concentration of all-*trans* and *cis* MK-7 was quickly reduced to undetectable levels in the presence of both types of light. It is also worth noting that the degree of photosensitivity of all-*trans* MK-7 might vary depending on the intensity and wavelength of light. Additionally, only particular intensities or wavelengths of light may induce the isomerisation of all-*trans* MK-7. Therefore, it could be that the light sources used in this investigation were not of the appropriate intensity or wavelength to promote this effect.

While it has been established that K vitamins are destroyed by light, limited research has been conducted to explore the stability of MK in the presence of different light sources. Moreover, studies explicitly considering MK-7 and its isomers in this context are absent. Ferland and Sadowski [39] assessed the PK content of several vegetable oils and evaluated the effect of light (daylight and fluorescent light) exposure on the stability of vitamin K1 in rapeseed and safflower oils over 22 days. It was determined that after only 2 days of exposure, the PK content of rapeseed and safflower oils was reduced by 46% and 59%, respectively, in the presence of fluorescent light and by 87% and 94%, respectively, when exposed to daylight. The effect of the type of storage container was also examined for rapeseed oil. It was ascertained that after 36 h of daylight and fluorescent light exposure, the PK content decreased by 93% and 44% for oil stored in clear bottles, respectively. In contrast, storage in amber bottles did not have a significant impact. Despite consideration of different types of light and vitamin K compounds, the results of this research are similar to the present study and demonstrate that vitamin K forms are highly vulnerable to light.

Collectively, these observations illustrate the destructive effect of various light sources on MK-7 and emphasise the importance of using dark or amber bottles and opaque packaging materials for the storage of fermented all-*trans* MK-7 dietary supplements and fortified or functional foods to preserve the quantity of the vitamin over its shelf life. UV exposure must also be avoided and is unsuitable for the manufacture of all-*trans* MK-7-containing supplements, milk, and other products that may require UV treatment as a means of processing or sterilisation. Strategies such as encapsulation, especially for dietary supplements, can also be implemented to further protect the all-*trans* isomer from exposure to light. Furthermore, it would be worthwhile to increase the awareness of consumers and state that exposure to light should be avoided on the product packaging to ensure the optimal performance of fermented all-*trans* MK-7 nutraceuticals.

3.1.2. Temperature

The impact of low (4 °C) and high (100 °C) temperatures on the MK-7 isomer composition was investigated in the presence and absence of oxygen. The results are depicted in Figures 5 and 6 for storage in the fridge (4 °C) and oven (100 °C), respectively. Around 68% and 61% of all-*trans* MK-7 and 79% and 61% of *cis* MK-7 remained in the presence and absence of oxygen at the end of the exposure period under low temperature conditions. There is also no statistically significant difference in the all-*trans* and *cis* MK-7 concentration for the fridge samples between days 3, 6, and 9 when considering the presence and absence of oxygen separately ($p = 0.997$ and $p = 0.944$ for all-*trans* MK-7 in the presence and absence of oxygen and $p = 0.749$ and $p = 0.098$ for *cis* MK-7 in the presence and absence of oxygen). This indicates that there is no notable decrease in the all-*trans* and *cis* isomer concentration over short-term exposure to low temperature conditions, both with and without contact with atmospheric oxygen. In comparison, approximately 17% and 33% of the all-*trans* isomer and 43% and 43% of *cis* MK-7 remained in the presence and absence of oxygen after 9 days of storage at a high temperature. Furthermore, there is no statistically significant difference in the all-*trans* and *cis* isomer concentrations for the oven samples between days 3, 6, and 9 when individually examining the effect of atmospheric oxygen ($p = 0.062$ and $p = 0.488$ for all-*trans* MK-7 in the presence and absence of oxygen and $p = 0.830$ and $p = 0.689$ for *cis* MK-7 in the presence and absence of oxygen). However, there is a statistically significant difference in the all-*trans* isomer concentration for the oven samples in the presence of oxygen between days 3 and 9 ($p = 0.002$). These observations suggest that although there is no appreciable difference in the isomer concentrations with and without contact with atmospheric oxygen between all three days of exposure holistically, there is a substantial decrease in the all-*trans* MK-7 concentration in the presence of oxygen between days 3 and 9. Thus, oxygen seems to accelerate the decomposition of the biologically active isomer at high temperatures. Although the effect of heat treatment and oxygen exposure has not been previously investigated for MK-7 isomers, it has been observed that during heating, oxygen increases the rate of degradation of all-*trans*- β -carotene, a precursor of vitamin A, which, similar to MK-7, is a lipid-soluble vitamin [40].

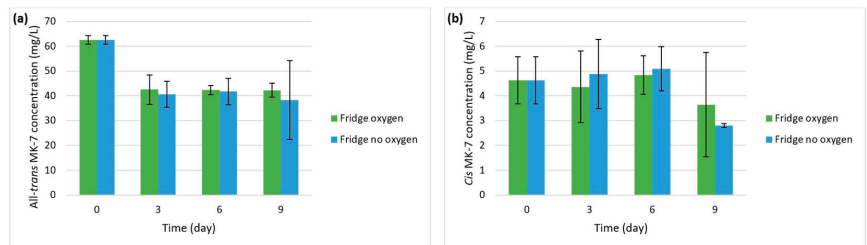


Figure 5. MK-7 isomer profile arising from short-term storage in the fridge at a low temperature in the presence and absence of oxygen for (a) all-*trans* MK-7 and (b) *cis* MK-7.

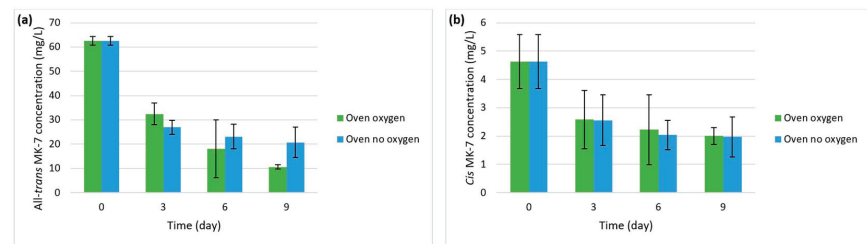


Figure 6. MK-7 isomer composition occurring from short-term storage in the oven at a high temperature in the presence and absence of oxygen for (a) all-*trans* MK-7 and (b) *cis* MK-7.

The stability of vitamin K compounds is only slightly affected by heat exposure; hence, they are regarded as fairly heat-stable [35,36,41]. While there are no prior studies assessing the influence of heat on the stability of MK-7 isomers specifically, Ferland and Sadowski [39] have investigated the thermal stability of vitamin K1 in different vegetable oils at temperatures between 185 and 190 °C over 20 and 40 min. A slight loss of PK was observed, and approximately 7% and 11% of the original vitamin K was lost over 20 and 40 min of exposure, respectively. The findings of this research are largely comparable with the present study. Despite the differences in the investigated K vitamins, temperatures, and exposure times between the two studies, they both demonstrate a moderate loss of vitamin K upon heating, suggesting that MK-7 is relatively stable when exposed to reasonably high temperatures over a short period.

These observations imply that thermal sterilisation and manufacturing processes involving high temperatures, such as milling and drying for the synthesis of MK-7 dietary supplements and extrusion cooking for the production of cereals and other foods fortified with MK-7, may not reduce the MK-7 content significantly. Although such technological processes could require greater temperatures than that investigated in the current study (100 °C), the exposure times are expected to be much shorter (over a few minutes or hours rather than for 3, 6, or 9 days), which will likely mitigate the detrimental effect of higher temperatures. Additionally, encapsulation methods could be used to protect all-*trans* MK-7 in processes involving extreme temperatures and/or long handling times.

It is also evident that storage of MK-7 at ambient temperature is acceptable. This is demonstrated by the relatively high MK-7 content remaining after 9 days for the samples that were stored in the dark at room temperature (Figure 2). Moreover, there is no statistically significant difference in the all-*trans* and *cis* MK-7 concentrations between the dark and fridge conditions in the presence and absence of oxygen following short-term exposure ($p = 0.498$ for all-*trans* MK-7 and $p = 0.832$ for *cis* MK-7 from the overall ANOVA analysis of the dark and fridge groups). These outcomes also indicate that the negligible MK-7 isomer concentrations observed for both the ambient and UV light samples were due to exposure to the different light conditions and did not result from storage at room temperature.

The amount of light exposure was similar between the samples kept in the dark, fridge, and oven, as closure of the fridge and oven doors also eliminated light exposure in the low and high temperature conditions. This allows the effect of temperature to be meaningfully assessed between these groups. The ANOVA results indicate that there is a statistically significant difference in the all-*trans* isomer concentration between the dark, fridge, and oven conditions in the presence and absence of oxygen over the entire exposure period ($p = 2.201 \times 10^{-4}$). However, there is no statistically significant difference in the *cis* MK-7 concentration between these three groups in the presence and absence of oxygen over the investigated timeframe ($p = 0.149$). This suggests that while exposure to high temperatures negatively impacts the concentration of the bioactive isomer, it does not considerably affect the concentration of the biologically insignificant isomer.

3.1.3. Atmospheric Oxygen

Vitamin K is slowly affected by exposure to atmospheric oxygen [35,41]. It has been proposed that contact with atmospheric oxygen during the storage of MK-7 dietary supplements may lead to autoxidation processes, which adversely impact the concentration of the all-*trans* isomer and promote its isomerisation to *cis* MK-7 [7,23,34]. Nevertheless, this phenomenon has not been explicitly assessed, particularly for MK-7 isomers produced from fermentation.

The experimental observations from the present investigation suggest that contact with atmospheric oxygen does not have a substantial negative effect on the stability of MK-7 over a short period. The statistical analysis for the dark, fridge, and oven conditions (Table 2) indicates that there is no statistically significant difference ($p > 0.05$) in the all-*trans* and *cis* MK-7 concentrations between the samples that were and were not in contact with atmospheric oxygen for each day of the exposure period. For the ambient and UV light

conditions, all-*trans* MK-7 was only noted in the presence and absence of oxygen for the ambient light samples on day 3 of exposure, and there was no statistically significant difference in the all-*trans* isomer concentration between these two groups ($p = 0.109$). Furthermore, since all-*trans* and *cis* MK-7 were essentially undetectable following short-term exposure to ambient and UV light, it is evident that both isomers are rapidly degraded due to the different light exposures, irrespective of contact with atmospheric oxygen.

Table 2. Comparison of the MK-7 isomer concentrations between the oxygen and no oxygen samples on each day of the exposure period for the dark, oven, and fridge conditions using a two-sample *t*-test.

DARK		FRIDGE		OVEN	
All- <i>trans</i> MK-7 concentration		All- <i>trans</i> MK-7 concentration		All- <i>trans</i> MK-7 concentration	
Groups compared	<i>p</i> -value	Groups compared	<i>p</i> -value	Groups compared	<i>p</i> -value
Day 3 oxygen and no oxygen	0.416	Day 3 oxygen and no oxygen	0.754	Day 3 oxygen and no oxygen	0.212
Day 6 oxygen and no oxygen	0.653	Day 6 oxygen and no oxygen	0.893	Day 6 oxygen and no oxygen	0.610
Day 9 oxygen and no oxygen	0.125	Day 9 oxygen and no oxygen	0.748	Day 9 oxygen and no oxygen	0.085
<i>Cis</i> MK-7 concentration		<i>Cis</i> MK-7 concentration		<i>Cis</i> MK-7 concentration	
Groups compared	<i>p</i> -value	Groups compared	<i>p</i> -value	Groups compared	<i>p</i> -value
Day 3 oxygen and no oxygen	0.416	Day 3 oxygen and no oxygen	0.736	Day 3 oxygen and no oxygen	0.984
Day 6 oxygen and no oxygen	0.454	Day 6 oxygen and no oxygen	0.772	Day 6 oxygen and no oxygen	0.852
Day 9 oxygen and no oxygen	0.699	Day 9 oxygen and no oxygen	0.603	Day 9 oxygen and no oxygen	0.960

Therefore, oxygen exposure is unlikely to significantly influence the all-*trans* MK-7 concentration of products that are consumed quickly and have a short shelf life, such as fortified or functional dairy products containing bioactive MK-7. However, it may adversely affect the all-*trans* MK-7 content of dietary supplements and products that are consumed over a longer period and have an extended shelf life. Encapsulation may be an effective technique to minimise the oxygen exposure of MK-7 contained in dietary supplements. Including labels on products to lessen their contact with oxygen (by closing the bottle lid or securing the packaging material) is also advisable for MK-7-enriched goods with a long shelf life.

3.1.4. Geometric Isomerisation of All-*trans* MK-7

It is interesting to notice that although it has been proposed that vitamin K, particularly all-*trans* MK-7, is susceptible to isomerisation upon exposure to various conditions, such as light, atmospheric oxygen, and elevated temperatures [7,23,34], conversion of the all-*trans* isomer to the *cis* form was not observed in the current study (only degradation of the vitamin and reduction in the concentration of both isomers was noted). A decrease in the concentration of the biologically effective isomer and a concurrent increase in the concentration of the *cis* isomer over time would denote the geometric isomerisation of all-*trans* MK-7. The *cis* MK-7 isomer concentration fluctuated considerably over the different days of exposure. While a slight increase in the concentration of *cis* MK-7 was observed for the fridge and dark storage conditions, there is no statistically significant difference in the *cis* isomer concentration in the presence and absence of oxygen between days 0 and 9 for the fridge and dark samples ($p = 0.850$). Moreover, a general downward trend in the *cis* isomer concentration can be noted over the entire exposure period for not only the fridge and dark samples but for all investigated storage conditions. This indicates a gradual decline, rather than an increase, in the *cis* isomer concentration over the 9-day storage period. Hence, it can be concluded that geometric isomerisation of all-*trans* MK-7 did not occur during the short-term exposure study. A potential explanation for the lack of isomerisation observed in this investigation could be that the conditions explored were reasonably mild and may not be sufficient to stimulate the isomerisation of all-*trans*

MK-7 over the timeframe explored. However, it may be possible for isomerisation to occur following longer periods of exposure to the same conditions. Alternatively, different conditions and/or harsher and more extreme environments may be required to promote the geometric isomerisation of the all-*trans* isomer.

3.2. Stability of All-*trans* MK-7 in an Optimal Storage Environment

A monitoring study was conducted to assess the stability of all-*trans* MK-7 and variation in the isomer composition over an extended timeframe during storage at a low temperature (4 °C) with minimal oxygen exposure in the absence of light.

In the short-term exposure study, the smallest decline in the concentration of the bioactive isomer was observed for the samples stored in the fridge at a low temperature and in the dark at ambient conditions. As previously outlined, the results obtained for the dark and fridge samples were comparable over a short span (no statistically significant difference in the MK-7 isomer concentration existed between these two groups). However, it is recognised that heat has a negative impact on the stability of MK-7 over a longer interval. Therefore, it was decided to consider storage at low rather than ambient temperature conditions over an extended period. The samples were also stored in dark/opaque bottles to further eliminate any light exposure, as it was determined from the short-term study that light has a detrimental effect on the stability of MK-7. In addition, no statistically significant difference in the MK-7 isomer concentration was noted between the samples that were and were not in contact with atmospheric oxygen during the short-term exposure investigation. Although oxygen is known to slowly impact the stability of MK-7, the effect of which is only likely to be observed after a prolonged period, the samples for the long-term study were just stored with the lid on (to decrease oxygen exposure) and not purged with nitrogen. This was done to simulate the potential environmental conditions that bioactive fermented MK-7 consumer end products will likely be subjected to during their manufacture, consumption, and overall shelf life, as, in reality, it would not be feasible to avoid exposure to atmospheric oxygen completely.

The samples were kept in an optimum storage environment for an extended timeframe. Figure 7 illustrates the variation in the all-*trans* and *cis* isomer concentrations over the long-term storage investigation. There was no appreciable change in the concentration of both isomers during 8 weeks of storage at a low temperature in the dark with minimal oxygen exposure. This implies that all-*trans* MK-7 is reasonably stable in this environment and is not susceptible to geometric isomerisation under optimal conditions.

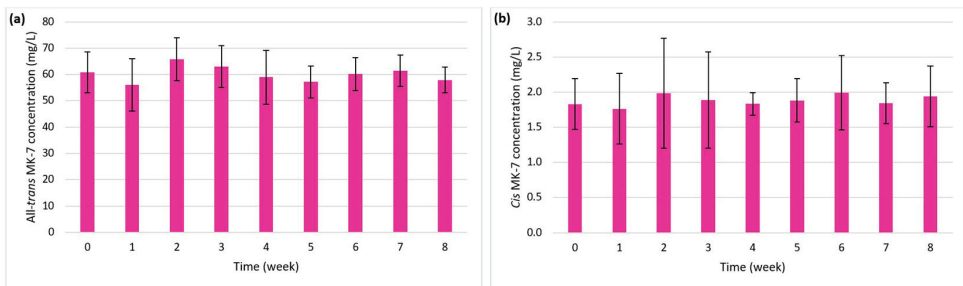


Figure 7. Variation in the isomer concentration over 8 weeks of storage at a low temperature with minimal oxygen exposure in the absence of light for (a) all-*trans* MK-7 and (b) *cis* MK-7.

These observations are supported by the ANOVA assessment, which indicates no statistically significant difference in the all-*trans* and *cis* isomer concentrations between the different weeks of exposure ($p = 0.951$ for all-*trans* MK-7 and $p = 1.00$ for *cis* MK-7). Additionally, a comparison of the MK-7 isomer concentration for every week of storage (weeks 1–8) with the control (week 0) via a *t*-test revealed that both the all-*trans* and *cis*

MK-7 concentration for each week of storage did not differ significantly from that of the control ($p > 0.05$).

Overall, the results of the long-term monitoring study demonstrate that low temperature conditions, reduced oxygen exposure, and the absence of light constitute the ideal storage environment for fermented MK-7. These conditions prevent the deterioration and preserve the concentration of the bioactive isomer, thereby retaining the therapeutic value of fermented MK-7 products.

3.3. Study Limitations

The findings of this investigation offer key insights into the effect of typical environmental and storage conditions that fermented MK-7 supplements and fortified or functional foods are likely to be subjected to on the MK-7 isomer profile and have shed light on the stability of the all-*trans* isomer over an extended period in an optimal storage environment. The ideal conditions to preserve the concentration of fermented all-*trans* MK-7 constituted the absence of light, low temperatures, and minimal oxygen exposure. Therefore, it is proposed that, where appropriate, fermented MK-7 products are packaged in dark/opaque bottles or materials and stored with the lid on or packaging tightly secured in the fridge at low temperature conditions (around 4 °C) to ensure that they retain their biological efficacy.

Although the impact of these factors on the isomer composition has been considered from the perspective of fermented MK-7 consumer end products, they have been examined in isolation. Thus, the experimental observations are restricted, and the conclusions drawn may differ slightly when the fermented MK-7 is actually formulated into supplements and fortified or functional foods.

It has been established that MK-7 is liable to degradation during storage, and the rate at which this occurs is accelerated in certain environments. Whilst exposure to specific storage conditions has been investigated in this study, it only covers a subset of the many factors that may be encountered during the manufacture and overall shelf life of a particular product. In addition, different preparations of bioactive fermented MK-7 may be exposed to unique storage environments depending on the characteristics of the final product (tablets, capsules, or fortified/functional foods).

For instance, fermented all-*trans* MK-7 formulated into tablets or capsules is likely to be exposed to various excipient compounds and active ingredients (in the case of multi-nutrient supplements), such as magnesium oxide (MgO), calcium carbonate (CaCO₃), calcium citrate (Ca₃(C₆H₅O₇)₂), cellulose, gelatine, and other vitamins and minerals. Certain compounds, including MgO, may also promote alkalisation, and since MK-7 is vulnerable to alkaline conditions, such additives can create an unfavourable milieu that may enhance its deterioration. Hence, the inclusion of additional compounds and ingredients and their different combinations can create and expose the vitamin to different environments, which can affect the isomer profile and stability of all-*trans* MK-7 in different preparations. In contrast, fermented bioactive MK-7-enriched fortified or functional foods will likely be subjected to a different set of environmental factors specific to the selected food matrix and its storage requirements. For example, fresh dairy products require refrigeration at low temperatures and have a relatively short shelf life compared to cereals and other dry goods, commonly stored at ambient conditions over a longer period. Therefore, the isomer composition and stability of all-*trans* MK-7 will likely vary with the nature of the end product. Consequently, future research efforts need to be directed towards exploring and comprehensively understanding the effect of different environmental factors and storage conditions on the isomer composition and stability of all-*trans* MK-7 in context rather than independently of the desired application.

While prior studies have examined the stability of commercially available MK-7 dietary supplements and similar preparations, there have been no attempts thus far to explore the stability and isomer profile of fermented MK-7 in different types of formulated products. Furthermore, since the therapeutic benefits of fermented MK-7 nutritional supplements and fortified or functional foods solely result from the quantity of all-*trans* MK-7, it is essential

to ensure that they contain the bioactive isomer almost exclusively or in the most significant proportion following their manufacture, during their consumption, and throughout their overall shelf life. Therefore, in subsequent investigations, it would be advantageous to consider formulating fermented all-*trans* MK-7 into various consumer end products, such as tablets, capsules, and fortified or functional foods, to develop a deeper understanding of the effect of different production processes, preparations, and foods matrices on the MK-7 isomer profile.

In future work, it would also be valuable to carry out shelf life or degradation studies to explore both the short- and long-term stability of fermented all-*trans* MK-7 when formulated in various dietary supplement preparations and fortified or functional foods. This will allow the impact of a range of environmental and storage conditions, including product-specific features and those relating to the proposed packaging materials and design, on the quantity of bioactive MK-7 and the isomer composition resulting from different end uses to be elucidated. Factors often governed by commercial pressures also contribute to the overall shelf life of a product, and these include the time it takes for it to reach the consumer, the range of temperatures and climates that it is likely to be subjected to between production and consumption, and the rate at which it is expected to be consumed. Thus, such aspects also need to be considered in future research when assessing the stability of fermented all-*trans* MK-7 over its shelf life after it has been formulated into a diverse range of consumer products. Additionally, it is vital to ensure that a therapeutically significant concentration of the vitamin remains in the product at the end of its shelf life after taking into account the impact of the many factors that contribute to its holistic storage environment.

Essentially, the outcomes of appropriate shelf life and degradation studies examining the stability of fermented all-*trans* MK-7 in different product formulations will aid the estimation of a realistic shelf life and initial content (overage) of the vitamin in various end products in the future. This will also inform decisions regarding the product packaging and its recommended storage conditions to preserve the quantity of the bioactive isomer in specific applications.

4. Conclusions

This investigation presents unique insights into the impact of various environmental factors and storage conditions that fermented MK-7 consumer end products, such as dietary supplements and fortified or functional foods, may be subjected to during their production, consumption, and overall shelf life. The selected parameters included exposure to atmospheric oxygen, different temperature conditions, and light. These factors were first considered over a short interval to determine the optimal storage conditions. Essentially, there appeared to be no discernible differences in the degradation profiles of all-*trans* and *cis* MK-7 under the studied conditions, as, despite minor dissimilarities (possibly due to experimental variation), the overall trends in the reduction of both isomers with exposure to the various factors were comparable. Storage in the absence of light at a low temperature with minimal oxygen exposure preserved the quantity of the all-*trans* isomer to the greatest extent and was the ideal storage environment for fermented MK-7. The stability of the biologically significant MK-7 isomer under the optimal conditions was then evaluated over an extended period, and negligible change in the concentration of all-*trans* MK-7 occurred after 8 weeks of storage. This implies that the all-*trans* isomer is reasonably stable and not prone to substantial degradation during long-term storage in this environment. The findings of this study are significant, as they will facilitate the development of suitable storage conditions to maintain the concentration of the all-*trans* isomer in fermented MK-7 end products. The results will also aid the estimation of suitable overage levels of the vitamin in different products to account for its deterioration during storage, which will ensure that the amount of the biologically important isomer remaining at the end of a product's shelf life is not below the required or stated quantity. Collectively, this will be a significant advancement in improving the availability of bioactive fermented MK-7 nutritional supplements and fortified or functional foods, as the *cis* isomers

have considerably compromised biological function and therapeutic value. The broad consumption of such efficacious products by a range of populations will boost the dietary intake of MK-7 and help decrease the risk and progression of several age-related disorders and diseases of global relevance.

Author Contributions: Conceptualisation, A.B. and M.S.; methodology, N.L., M.S. and A.B.; validation, N.L.; formal analysis, N.L.; investigation, N.L.; data curation, N.L., M.S. and A.B.; writing—original draft preparation, N.L.; writing—review and editing, N.L., M.S. and A.B.; supervision, A.B. and M.S. All authors have read and agreed to the published version of the manuscript.

Funding: This research received no external funding.

Data Availability Statement: All relevant data that support the findings of this study are included in this article.

Conflicts of Interest: The authors declare no conflict of interest.

References

1. Shearer, M.J. Vitamin K. *Lancet* **1995**, *345*, 229–234. [CrossRef] [PubMed]
2. Beulens, J.; Booth, S.; van Den Heuvel, E.; Stoecklin, E.; Baka, A.; Vermeer, C. The role of menaquinones (vitamin K2) in human health. *Br. J. Nutr.* **2013**, *110*, 1357–1368. [CrossRef]
3. Azuma, K.; Inoue, S. Multiple Modes of Vitamin K Actions in Aging-Related Musculoskeletal Disorders. *Int. J. Mol. Sci.* **2019**, *20*, 2844. [CrossRef] [PubMed]
4. Basset, G.; Latimer, S.; Fatihi, A.; Soubeyrand, E.; Block, A. Phylloquinone (vitamin K1): Occurrence, biosynthesis and functions. *Mini-Rev. Med. Chem.* **2017**, *17*, 1028–1038. [CrossRef] [PubMed]
5. Booth, S.L. Vitamin K: Food composition and dietary intakes. *Food Nutr. Res.* **2012**, *56*, 5505. [CrossRef]
6. Berenjian, A.; Mahanama, R.; Talbot, A.; Regtop, H.; Kavanagh, J.; Dehghani, F. Designing of an intensification process for biosynthesis and recovery of menaquinone-7. *Appl. Biochem. Biotechnol.* **2013**, *172*, 1347–1357. [CrossRef]
7. Szterk, A.; Zmysłowski, A.; Bus, K. Identification of cis/trans isomers of menaquinone-7 in food as exemplified by dietary supplements. *Food Chem.* **2018**, *243*, 403–409. [CrossRef]
8. Walther, B.; Karl, P.J.; Booth, S.L.; Boyaval, P. Menaquinones, bacteria, and the food supply: The relevance of dairy and fermented food products to vitamin K requirements. *Adv. Nutr.* **2013**, *4*, 463–473. [CrossRef]
9. Anastasi, E.; Ialongo, C.; Labriola, R.; Ferraguti, G.; Lucarelli, M.; Angeloni, A. Vitamin K deficiency and COVID-19. *Scand. J. Clin. Lab. Investig.* **2020**, *80*, 525–527. [CrossRef]
10. Berenjian, A.; Sarabadani, Z. How menaquinone-7 deficiency influences mortality and morbidity among COVID-19 patients. *Biocatal. Agric. Biotechnol.* **2020**, *29*, 101792. [CrossRef]
11. Dofferhoff, A.S.M.; Piscaer, I.; Schurgers, L.J.; Visser, M.P.J.; van den Ouweland, J.M.W.; de Jong, P.A.; Gosens, R.; Hackeng, T.M.; van Daal, H.; Lux, P.; et al. Reduced vitamin K status as a potentially modifiable risk factor of severe COVID-19. *Clin. Infect. Dis.* **2021**, *73*, 4039–4046. [CrossRef] [PubMed]
12. Fusaro, M.; Gallieni, M.; Porta, C.; Nickolas, T.L.; Khairallah, P. Vitamin K effects in human health: New insights beyond bone and cardiovascular health. *J. Nephrol.* **2020**, *33*, 239–249. [CrossRef] [PubMed]
13. Karamzad, N.; Maleki, V.; Carson-Chahhoud, K.; Azizi, S.; Sahebkar, A.; Gargari, B.P. A systematic review on the mechanisms of vitamin K effects on the complications of diabetes and pre-diabetes. *BioFactors* **2020**, *46*, 21–37. [CrossRef] [PubMed]
14. Mehta, D.; de Souza, A.; Jadhav, S.S.; Kuret, T.; Sodin-Šemrl, S.; Ünal, M.; Fini, E.H.; Ayat, S.; Pahlavan, F.; Bhatti, M.Z. Menaquinone-7: Wide Ranging Physiological Relevance in Muscle and Nerve Health. In *Vitamin K-Recent Topics on the Biology and Chemistry*; Kagechika, H., Shirakawa, H., Eds.; IntechOpen: London, UK, 2021; Volume 27, pp. 57–76.
15. Tarkesh, F.; Jahromi, B.N.; Hejazi, N.; Tabatabaee, H. Beneficial health effects of Menaquinone-7 on body composition, glycemic indices, lipid profile, and endocrine markers in polycystic ovary syndrome patients. *Food Sci. Nutr.* **2020**, *8*, 5612–5621. [CrossRef]
16. Xv, F.; Chen, J.; Duan, L.; Li, S. Research progress on the anticancer effects of vitamin K2. *Oncol. Lett.* **2018**, *15*, 8926–8934. [CrossRef] [PubMed]
17. Vik, H. Vitamin K2: A Clinically Proven Cardio-Protective Powerhouse: Known for bone-support benefits, vitamin K2 as MK-7 has also been recognized as vital for heart health. *Nutraceuticals World* **2020**, *23*, 44.
18. Brugè, F.; Bacchetti, T.; Principi, F.; Littarru, G.P.; Tiano, L. Olive oil supplemented with menaquinone-7 significantly affects osteocalcin carboxylation. *Br. J. Nutr.* **2011**, *106*, 1058–1062. [CrossRef]
19. Stafford, D.W.; Roberts, H.R.; Vermeer, C. Vitamin K supplementation during oral anticoagulation: Cautions. *Blood* **2007**, *109*, 3607. [CrossRef]
20. Berenjian, A.; Mahanama, R.; Talbot, A.; Biffin, R.; Regtop, H.; Valtchev, P.; Kavanagh, J.; Dehghani, F. Efficient media for high menaquinone-7 production: Response surface methodology approach. *New Biotechnol.* **2011**, *28*, 665–672. [CrossRef]
21. Lal, N.; Seifan, M.; Ebrahiminezhad, A.; Berenjian, A. The Effect of Iron Oxide Nanoparticles on the Menaquinone-7 Isomer Composition and Synthesis of the Biologically Significant All-Trans Isomer. *Nanomaterials* **2023**, *13*, 1825. [CrossRef]

22. Bus, K.; Sitkowski, J.; Bocian, W.; Zmysłowski, A.; Ofiara, K.; Szterk, A. Separation of menaquinone-7 geometric isomers by semipreparative high-performance liquid chromatography with silver complexation and identification by nuclear magnetic resonance. *Food Chem.* **2022**, *368*, 130890. [CrossRef]
23. Szterk, A.; Bus, K.; Zmysłowski, A.; Ofiara, K. Analysis of Menaquinone-7 Content and Impurities in Oil and Non-Oil Dietary Supplements. *Molecules* **2018**, *23*, 1056. [CrossRef] [PubMed]
24. Lal, N.; Berenjian, A. Cis and trans isomers of the vitamin menaquinone-7: Which one is biologically significant? *Appl. Microbiol. Biotechnol.* **2020**, *104*, 2765–2776. [CrossRef] [PubMed]
25. Cirilli, I.; Orlando, P.; Silvestri, S.; Marcheggiani, F.; Dłudla, P.V.; Kaesler, N.; Tiano, L. Carboxylative efficacy of trans and cis MK7 and comparison with other vitamin K isomers. *BioFactors* **2022**, *48*, 1129–1136. [CrossRef] [PubMed]
26. Knauer, T.E.; Siegfried, C.; Willingham, A.K.; Matschiner, J.T. Metabolism and biological activity of cis-and trans-phyloquinone in the rat. *J. Nutr.* **1975**, *105*, 1519–1524. [CrossRef]
27. Lowenthal, J.; Rivera, G.V. Comparison of the activity of the cis and trans isomer of vitamin K1 in vitamin K-deficient and coumarin anticoagulant-pretreated rats. *J. Pharmacol. Exp. Ther.* **1979**, *209*, 330–333.
28. Matschiner, J.T.; Bell, R.G. Metabolism and vitamin K activity of cis phyloquinone in rats. *J. Nutr.* **1972**, *102*, 625–629. [CrossRef]
29. Kang, M.-J.; Baek, K.-R.; Lee, Y.-R.; Kim, G.-H.; Seo, S.-O. Production of Vitamin K by Wild-Type and Engineered Microorganisms. *Microorganisms* **2022**, *10*, 554. [CrossRef]
30. Lal, N.; Seifan, M.; Berenjian, A. Optimisation of the fermentation media to enhance the production of the bioactive isomer of vitamin menaquinone-7. *Bioprocess. Biosyst. Eng.* **2022**, *45*, 1371–1390. [CrossRef]
31. Lal, N.; Seifan, M.; Berenjian, A. The impact of key fermentation parameters on the production of the all-trans isomer of menaquinone-7. *Biocatal. Agric. Biotechnol.* **2022**, *46*, 102548. [CrossRef]
32. Marles, R.J.; Roe, A.L.; Oketch-Rabah, H.A. US Pharmacopeial Convention safety evaluation of menaquinone-7, a form of vitamin K. *Nutr. Rev.* **2017**, *75*, 553–578. [CrossRef] [PubMed]
33. Huang, B.; Zheng, F.; Fu, S.; Yao, J.; Tao, B.; Ren, Y. UPLC-ESI-MS/MS for determining trans- and cis-vitamin K-1 in infant formulas: Method and applications. *Eur. Food Res. Technol.* **2012**, *235*, 873–879. [CrossRef]
34. Sitkowski, J.; Bocian, W.; Szterk, A. The application of multidimensional NMR analysis to cis/trans isomers study of menaquinone-7 (vitamine K2MK-7), identification of the (E,Z3,E2, ω)-menaquinone-7 isomer in dietary supplements. *J. Mol. Struct.* **2018**, *1171*, 449–457. [CrossRef]
35. Camire, M.E.; Camire, A.; Krumhar, K. Chemical and nutritional changes in foods during extrusion. *Crit. Rev. Food Sci. Nutr.* **1990**, *29*, 35–57. [CrossRef] [PubMed]
36. Orlando, P.; Silvestri, S.; Marcheggiani, F.; Cirilli, I.; Tiano, L. Menaquinone 7 Stability of Formulations and Its Relationship with Purity Profile. *Molecules* **2019**, *24*, 829. [CrossRef] [PubMed]
37. Mladěnka, P.; Macáková, K.; Kujovská Krčmová, L.; Javorská, L.; Mrštná, K.; Carazo, A.; Protti, M.; Remião, F.; Nováková, L.; Researchers, O.; et al. Vitamin K—sources, physiological role, kinetics, deficiency, detection, therapeutic use, and toxicity. *Nutr. Rev.* **2022**, *80*, 677–698. [CrossRef] [PubMed]
38. Zhou, S.; Mehta, B.M.; Feeney, E.L. A narrative review of vitamin K forms in cheese and their potential role in cardiovascular disease. *Int. J. Dairy Technol.* **2022**, *75*, 726–737. [CrossRef]
39. Ferland, G.; Sadowski, J.A. Vitamin K1 (phyloquinone) content of edible oils: Effects of heating and light exposure. *J. Agric. Food Chem.* **1992**, *40*, 1869–1873. [CrossRef]
40. Yoon, S.H. Effect of oxygen on isomerization of β -carotene during thermal treatment. *Biocatal. Agric. Biotechnol.* **2015**, *4*, 555–558. [CrossRef]
41. Ottaway, P.B. Stability of vitamins in food. In *The Technology of Vitamins in Food*; Ottaway, P.B., Ed.; Springer: Cornwall, UK, 1993; pp. 90–113.

Disclaimer/Publisher’s Note: The statements, opinions and data contained in all publications are solely those of the individual author(s) and contributor(s) and not of MDPI and/or the editor(s). MDPI and/or the editor(s) disclaim responsibility for any injury to people or property resulting from any ideas, methods, instructions or products referred to in the content.

Review

Production of Value-Added Products as Food Ingredients via Microbial Fermentation

Attia Iram ¹, Ali Ozcan ², Irfan Turhan ² and Ali Demirci ^{1,*}

¹ Department of Agricultural and Biological Engineering, 221 Agricultural Engineering Building, Pennsylvania State University, University Park, PA 16802, USA; axi52@psu.edu

² Department of Food Engineering, Akdeniz University, Konyaaltı, Antalya 07070, Turkey; ozzcanali@gmail.com (A.O.); iturhan@akdeniz.edu.tr (I.T.)

* Correspondence: Author: demirci@psu.edu

Abstract: Humankind has been unknowingly utilizing food fermentations since the first creation of bread, cheese, and other basic foods. Since the beginning of the last century, microbial fermentation has been extensively utilized for production of commodity chemicals. It has also gained substantial interest in recent decades due to its underlying applications in the preparation of natural and safe food ingredients including enzymes, antimicrobial agents, vitamins, organic acids, sweeteners, stabilizers, emulsifiers, oligosaccharides, amino acids, and thickening agents. In addition, some novel food ingredients that were conventionally made from some other sources such as plant tissue cultures or animals are now being introduced in the industry as ‘fermentation products.’ Some examples of such novel fermentation food ingredients include flavonoids, cultured meat products, food colorants, antioxidants, lipids, and fatty acids. This review summarizes some of the most prominent food ingredients and novel fermentation food products currently being produced via microbial fermentation as well as the strategies to enhance such fermentation processes. Additionally, economical feedstocks are discussed with their potential to be converted into value-added products with the help of microbial fermentations.

Keywords: enzymes; food ingredients; microbial fermentation; value-added products; vitamins

Citation: Iram, A.; Ozcan, A.; Turhan, I.; Demirci, A. Production of Value-Added Products as Food Ingredients via Microbial Fermentation. *Processes* **2023**, *11*, 1715. <https://doi.org/10.3390/pr11061715>

Academic Editor: Francesca Raganati

Received: 3 May 2023

Revised: 26 May 2023

Accepted: 31 May 2023

Published: 3 June 2023



Copyright: © 2023 by the authors. Licensee MDPI, Basel, Switzerland. This article is an open access article distributed under the terms and conditions of the Creative Commons Attribution (CC BY) license (<https://creativecommons.org/licenses/by/4.0/>).

1. Introduction

Fermentation is used for foods to provide flavor, preservation, enriching, and improving textural quality by humans over thousands of years. Although it has appeared as a production method of fermented foods, fermentation has also become an important process for the food industry with the development of bioprocess technologies and biotechnology. Furthermore, consumers worry about unsafe chemical food additives, and they tend to consume natural foods or natural additives as far as possible. Therefore, natural food ingredients, obtained by fermentation processes, are becoming preferable option [1].

Food ingredients, which are produced by fermentation such as enzymes, sweeteners, vitamins, organic acids, stabilizers, thickening agents, and amino acids, interest many manufacturers and researchers for the improvement of food quality. In addition, another of the main reasons to produce these ingredients by fermentation is to reduce costs and improve sustainability. For example, enzymes are widely used in different processes in the food industry, such as cheesemaking, baking, brewing, etc. Moreover, the market size of the enzyme industry reached more than USD 6.1 billion annually [2]. Industrial-scale fermentation processes have become increasingly important to meet the growing demand for enzymes. Similarly, microbial fermentation processes are essential to increase the production of valuable organic acids, especially lactic acid and citric acid. On the other hand, some ingredients, such as vitamins, can be produced by the chemical process, which can cause toxic impact for environment. However, microbial fermentation could be an environmentally friendly alternative to the traditional production of vitamins by means

of green “cell factories” [3]. Moreover, due to the preference for microbial fermentation, different types of wastes, such as agricultural and food wastes, can be evaluated in the production of food ingredients. Therefore, improvement in the fermentation process can contribute to overcoming many environmental problems.

However, there are some challenges for the production of these ingredients including high production costs, increasing energy consumption, low productivity, and sustainability of feedstocks. There is extensive research in the literature to overcome these challenges to the production of value-added food products by improving fermentation strategies. Various ingredients are basically produced by submerged batch fermentation. Nevertheless, fed-batch or continuous fermentation modes are frequently used by researchers to enhance production yield [4]. On the other hand, solid-state fermentation can be preferred to produce some food ingredients, especially those obtained from fungi. This can be explained by features of solid-state fermentation such as low-energy requirement, less wastewater generation, and environment friendliness [5]. In addition, regardless of submerged or solid-state fermentation, studies about optimization of fermentation conditions should be carried out to improve efficiency [6]. Other strategies studied by researchers include various approaches related to microorganisms. The most used microorganisms in food industry can be mentioned as *Aspergillus*, *Penicillium*, *Kluyveromyces*, *Rhizopus*, etc. (fungi); *Saccharomyces*, *Pichia*, *Candida*, *Yarrowia*, etc. (yeast); *Lactobacillus*, *Bacillus*, recombinant *Escherichia coli*, etc. (bacteria) (Table 1). Although food ingredients can be produced by almost of all type of microorganisms, some studies, such as the utilization of genetically engineered microorganisms [7], co-cultured processes [8], and cultivation with newly isolated microorganisms [9], may be required.

Table 1. Microbial products as value-added food ingredients.

Category	Product	Microorganisms	Fermentation Mode	Productivity	Fermentation Conditions	Refs.
Enzymes	Proteases	<i>Bacillus subtilis</i> B22	Submerged	334 ± 1.8 U/mL	40 °C with pH: 8 and Agricultural waste materials	[10]
	Proteases	<i>Rhodotorula mucilaginosa</i> CBMAI 1528	Submerged	280 ± 1.7 U/mL	20 °C and a culture medium containing both glucose and casein peptone (20 and 10 g/L, respectively)	[11]
	Proteases	<i>Geobacillus ther- moglucosidasius</i> SKF4	Submerged	175 U/mL	60 to 65 °C, pH 7 to 8, >1% NaCl with casein and yeast extract	[12]
	Proteases	<i>Aspergillus sydowii</i> URM5774	Submerged	352.0 U/mL	pH 8.0 at 45 °C with coffee ground residues	[13]
	Proteases	<i>Bacillus mojavensis</i>	Submerged	78.7%	pH 9.08, temperature 39.74 °C with eggshells and membrane-based substrates	[14]

Table 1. Cont.

Category	Product	Microorganisms	Fermentation Mode	Productivity	Fermentation Conditions	Refs.
	Lipase	<i>A. niger</i>	Submerged	1.55 U/mL	soluble starch 4%, (NH ₄) ₂ SO ₄ 0.1%, K ₂ HPO ₄ 0.1%, MgSO ₄ ·7H ₂ O 0.05%, peptone 3%, olive oil 1.05%. pH 7. Temperature 30 °C, agitation 213 rpm	[15]
	Lipase	<i>Penicillium fellutanum</i>	Submerged	1038.86 U/gds	pH 5.0, incubation time 24 h, temperature 35 °C	[16]
	Glucoamylase	<i>Aspergillus niger van Tieghem</i>	Submerged	274.4 U/mL	51.82 g L ⁻¹ malt extract, 9.27 g L ⁻¹ CaCl ₂ ·2H ₂ O and 0.50 g L ⁻¹ FeSO ₄ ·7H ₂ O 30 °C and 150 rpm	[17]
	α-amylase	<i>Aspergillus oryzae</i>	Solid-State	10,994.74 U/gds	edible oil cakes, temperature of 32.5 °C, pH of 4.5, moisture content of 64%	[18]
	Cellulase	<i>A. niger</i> (NRRL 330)	Submerged	0.54 ± 0.02 IU/mL	pH: 5, Temperature: 30 °C, Peptone: 5 g/L, Yeast extract: 16.5 g/L and Ammonium sulfate: 1.9 g/L	[19]
	Hemicellulase	<i>A. niger</i> (NRRL 330)	Submerged	48.71 ± 2.05 IU/mL	pH: 5, Temperature: 30 °C, Peptone: 5 g/L, Yeast extract: 16.5 g/L and Ammonium sulfate: 1.9 g/L	[19]
Antimicrobials	Nisin	<i>Lactococcus lactis</i>	Submerged	523.5 ± 256.7 IU/mL	D-glucose (80 g/L), peptone (10 g/L), YE (10 g/L), KH ₂ PO ₄ (10 g/L), NaCl (2 g/L), and MgSO ₄ ·7H ₂ O (0.2 g/L), at 32 °C	[20]
	lysozyme	<i>Kluyveromyces lactis</i> K7	Submerged	141 U/mL	25 °C, pH 4, no aeration	[21]
	lysozyme	<i>Kluyveromyces lactis</i> K7	Submerged	173 U/mL	16.3% lactose, 1.2% casamino acid, 0.8% yeast nitrogen, no pH control, 25 °C, 150 rpm, and no aeration	[22]
	lysozyme	<i>Pichia pastoris</i> GS115	Submerged	14,680 ± 300 U/mL	28 °C Temperature, 250 rpm agitation	[23]

Table 1. Cont.

Category	Product	Microorganisms	Fermentation Mode	Productivity	Fermentation Conditions	Refs.
Vitamins	Vitamin B12	<i>Propionibacterium freudenreichii</i> DSM 20271 and <i>Levilactobacillus brevis</i>	Submerged	742 ng/g dw	200 rpm at 25 °C	[24]
	Vitamin K	<i>Bacillus subtilis natto</i>	Submerged	12.09 mg/L	temperature (35 °C), agitation (200 rpm) and pH (6.58)	[25]
	Vitamin K	<i>Bacillus subtilis natto</i> (NF1)	Submerged	28.7 ± 0.3 mg/L	aeration (1 vvm), agitation (200 rpm for glycerol and 234 rpm for glucose), pH (6.48 for glucose and 6.6 for glycerol), and temperatures (30 °C for glucose and 35 °C for glycerol)	[26]
Organic acids	Lactic acid	<i>Lactobacillus casei</i>	Submerged	59.27 g/L	yeast extract was 31.35 (g/L)	[27]
	Lactic acid	<i>Lactobacillus plantarum</i> 23	Submerged	14.2 g/L/h	pH 5.0 and 200 rpm agitation	[28]
	Propionic acid	Mixed bacterial culture	Submerged	26.5 g/L	pH 6, 30 °C	[29]
Sweeteners	Arabitol	<i>Candida parapsilosis</i> SK26.002 Mutant A6	Submerged	32.92 g/L	30 °C, pH: 4.0, 4% initial inoculum and 200 rpm in shake flask with medium containing 200 g/L glucose and 30 g/L yeast extract	[30]
	Arabitol	<i>Yarrowia lipolytica</i> ARA9	Submerged	118.5 g/L	30 °C, pH: 5.0, 600 rpm agitation speed and 1.0 vvm aeration rate. Medium containing 200 g/L crude glycerol, 3.7 g/L (NH ₄) ₂ SO ₄ and 2 g/L yeast extract	[31]

Table 1. Cont.

Category	Product	Microorganisms	Fermentation Mode	Productivity	Fermentation Conditions	Refs.
	Erythritol	<i>Yarrowia lipolytica</i> M53-S	solid state fermentation	190.5 mg/gds	30 °C, 70% initial moisture content, pH: 4.0, 7.5×10^4 cells/gds inoculum size and supplemented with 0.02 g/gds NaCl. Medium containing 60% peanut press cake and 40% sesame meal supplemented with 4% biochar and 20% concentrated enzymatic hydrolysate of the defatted <i>Schizochytrium</i> residue	[32]
	Erythritol	<i>Moniliella pollinis</i> MUCL 40570	Submerged	106.40 ± 0.42 g/L	30 °C, pH: 5.5, 3% (v/v) initial inoculum and 200 rpm in shake flask. Sugarcane molasses media: 300 g/L total sugar conc. and 5 g/L yeast extract. Beet molasses media: 200 g/L total sugar and 0.67 g/L yeast extract. Grape musts media: 200 g/L total sugar and 6.7 g/L yeast extract.	[33]
	Erythritol	<i>Moniliella pollinis</i> CBS 461.67	Submerged Fed-Batch	94 g/L	30 °C, initial pH: 6.5–6.8 (not controlled during fermentation), 150 rpm agitation speed and 1.0 vvm aeration rate. Sugarcane juice medium: 175 g/L total sugar and 1.63 g/L <i>Moniliella</i> culture lysate. Molasses medium: 219.8 g/L total sugar and 1.63 g/L <i>Moniliella</i> culture lysate	[34]

Table 1. Cont.

Category	Product	Microorganisms	Fermentation Mode	Productivity	Fermentation Conditions	Refs.
	Mannitol	<i>Leuconostoc citreum</i> TR116	Submerged	61.6 g/L	30 °C, initial pH: 6.5, 1.0% (v/v) initial inoculum and 120 rpm agitation speed. MRS5 medium containing 100.0 g/L fructose and 50.0 g/L glucose. Apple juice medium supplemented with 2.0 g/L yeast extract	[35]
	Mannitol	<i>Lactobacillus intermedius</i> NRRL B-3693	Submerged	80 g/L	37 °C, initial pH: 6.0 and 100 rpm agitation speed. Red must medium containing 155.3 g/L sugar, 7.48 g/L yeast extract and 0.047 g/L MnSO ₄ ·H ₂ O and white must medium containing 175.7 g/L sugar, 7.54 g/L yeast extract and 0.088 g/L MnSO ₄ ·H ₂ O	[36]
Oligosaccharides	Fructooligosaccharides	<i>Aspergillus oryzae</i> DIA–MF	Solid state fermentation	7.64 g/L	30 °C, pH: 4.5, 70% initial moisture content and 2.0 × 10 ⁷ spores/g substrat inoculum size. Different fermentation medium including sugarcane bagasse, coffee husk, pineapple peel, prickly pear peel and banana peel waste supplemented with aguamiel	[37]
	Fructooligosaccharides	<i>Bacillus aryabhatai</i> GYC2-3	Submerged	26 g/L	30 °C, pH: 8.0, 5% (v/v) inoculum containing 1 × 10 ⁶ CFU/mL and 150 rpm in shake flask with medium containing 250 g/L sucrose	[38]

Table 1. Cont.

Category	Product	Microorganisms	Fermentation Mode	Productivity	Fermentation Conditions	Refs.
	Fructooligosaccharides	Mutant strain of <i>Aspergillus oryzae</i> S719 (overexpressed FTase genes)	Submerged	586 ± 4.7 g/L	50 °C, pH: 6.0, 160 rpm agitation speed and 1.0 g/L mycelium as inoculum. Medium containing 900 g/L sucrose	[39]
	Mannooligosaccharide	recombinant <i>Aspergillus sojae</i> AsT3	solid state fermentation	983.53 U/mg	30 °C, pH: 7.0, 1:3 (w/v) solid-to-liquid ratio and 7.0% inoculum size. Different fermentation medium including 5 g of wheat bran, rye bran, oat husk, barley husk supplemented with 4 g/L yeast extract	[5]
Polysaccharides	Glucan	<i>Lasiodiplodia theobromae</i> CCT 3966	Submerged	0.047 g/g	28 °C, pH: 7.0, 105 CFU/m inoculum and 200 rpm in shake flask. Fermentation medium including Sugarcane straw hydrolysate (40 g/L glucose concentration)	[40]
	Glucan	<i>Candida utilis</i> ATCC 9950	Submerged	82%	28 °C, 10.0% (v/v) inoculum, 200 rev/min agitation and 2.5 vvm aeration. Medium containing Deproteinated Potato Juice Water (pH 5.0 ± 0.2) supplemented with 10% of glycerol	[41]
	Glucan	<i>Lasiodiplodia theobromae</i> MMPI	Submerged	1.06 g/L	28 °C, pH: 5.5, 10.0 mL inoculum and 150 rpm in shake flask. Medium including soybean molasses (20 g/L total sugar)	[42]

Table 1. Cont.

Category	Product	Microorganisms	Fermentation Mode	Productivity	Fermentation Conditions	Refs.
	Glucan	<i>T-DNA</i> – based mutant <i>Aureobasidium pullulans</i> CGMCC 19650	Submerged	78.6%	30 °C, pH: 3.8, 10.0% (v/v) inoculum, 400 rpm agitation speed and 1.0 vvm aeration rate. Medium containing 50 g/L glucose, 3.0 g/L yeast extract	[43]
	Pullulan	<i>Aureobasidium pullulans</i> MTCC 2013	Submerged	24.77 ± 1.06 g/L	28 °C, pH: 6.5, 5.0% of 1 × 10 ⁸ cells inoculum and 150 rpm in shake flask. Medium including hydrolyzed kitchen waste supplemented with 0.25% peptone and yeast extract	[44]
	Pullulan	<i>Aureobasidium pullulans</i> CCTCC M 2012259	Submerged	50 g/L	30 °C, pH: 3.8, 10.0% (v/v) inoculum, 400 rpm agitation speed and 1.0 vvm aeration rate. M1 containing 51.59 g/L cassava starch and 4.40 g/L corn steep liquor powder. M2 containing 51.75 g/L cassava starch and 9.47 mL/L soybean meal hydrolysate	[45]
	Pullulan	<i>Aerobasidiom pullulans</i> KY 767024	Submerged	19.45 ± 0.40 g/L	28 °C, pH: 5.5, 10.0% inoculum in shake flask. Medium including corn bran hydrolysates 20% (w/v) yeast extract 0.2% (w/v)	[46]
	Pullulan	<i>Aureobasidium pullulans</i> FB-1	Submerged	4.8%, w/v	30 °C, pH: 6.5 5.0% (v/v) inoculum, 300 rpm agitation and 0.75 vvm aeration. Medium containing 50 g/L sucrose, 2.0 g/L yeast extract	[47]

Table 1. Cont.

Category	Product	Microorganisms	Fermentation Mode	Productivity	Fermentation Conditions	Refs.
Amino Acids	Glutamic acid	<i>Corynebacterium glutamicum</i> NCIM 2168	Submerged	16.49 g/L	30 °C, 5.0% (v/v) inoculum and 200 rpm in shake flask. Medium containing 50 g/L glucose, 10 g/L urea and 19.24% of salt solution	[48]
	Glutamic acid	<i>Corynebacterium glutamicum</i> PTCC 1532	Submerged	19.84 mg/mL	30 °C, pH: 7.0, 10 mL of the overnight culture inoculum, 180 rpm in shake flask. Medium containing 90 g/L glucose, 9 µg/L biotin and 3 g/L urea	[49]
	methionine	Genetically engineered <i>Escherichia coli</i> W3110-BL	Submerged	1.48 g/L	37 °C, 5.0% (v/v) inoculum, 1.4 vvm aeration rate and agitation controlled DO 20%. Medium containing 120 g/L glucose, 50 mg/L L-lysine, 100 mg/mL Amp, and 0.1 mmol/L isopropyl b-d-1-thiogalactopyranoside	[7]
	methionine	Recombinant <i>Escherichia coli</i>	Submerged (Fed-Batch)	3.22 g/L	30 °C, pH: 7.0, 10 mL of the overnight culture inoculum, 180 rpm in shake flask. Medium containing 20 g/L glucose, 2 g/L yeast extract, 0.01 g/L L-lysine and 1.0 mL/L salt solution	[50]
	tryptophan	Genetically engineered <i>Escherichia coli</i> TS-10	Submerged	1.710 g/L	Tryptophan fermentation was carried out in shake flask with lysogeny broth medium for 48 h	[51]

Table 1. Cont.

Category	Product	Microorganisms	Fermentation Mode	Productivity	Fermentation Conditions	Refs.
	tryptophan	<i>Pediococcus acidilactici</i> TP-6	Submerged	68.05 mg/L	30 °C, 10.0% (v/v) inoculum in shake flask. Medium containing 14.06 g/L molasses, 23.68 g/L meat extract, 5.56 g/L urea 0.024 g/L and FeSO ₄	[52]
	tryptophan	Genetically modified <i>Escherichia coli</i> CCTCC M20211388	Submerged	52.1 g/L	35 °C, pH: 7.0, 20 mL (OD600: 1.0) inoculum, aeration rate and agitation controlled DO 20–30%. Medium containing 20 g/L glucose, 1 g/L yeast extract and 2 g/L sodium citrate	[53]
	Lysine	Metanolic engineered <i>C. glutamicum</i>	Submerged (Fed-Batch)	221.3 ± 17.6 g/L	fermentation was carried out in bioreactor with 10% (v/v) inoculum. Medium containing 80 g/L glucose, 40 g/L beet	[54]

This review focusses on the production of food ingredients produced via microbial fermentations by utilizing novel approaches as well as low-cost feedstocks. Furthermore, the utilized microbial strains, fermentation conditions, alternative substrates, and the properties of each ingredient were also discussed.

2. Food Ingredients as the Fermentation Products

Food ingredients are significant factors for human health and lifestyle and could be produced through different ways. Fermentation is one of production methods, and it has some advantages such as sustainability, flexibility, and productivity. Therefore, using fermentation to produce food ingredients has become a significant option for researchers and manufacturers. In this section of review, critical points of fermentative production of food ingredients are summarized.

2.1. Enzymes

Enzymes are the biological catalysts that can accelerate the corresponding reactions [55]. Since their discovery, enzymes have become a crucial part of many industrial sectors due to their accelerated mode of action under operable conditions such as temperature and pH [55]. Based on one estimate, the enzyme industry comprised more than USD 6.1 billion annually, which is expected to increase to at least USD 8.5 billion [2]. For the food industry, proteases, lipases, and carbohydrases are some of the enzymes that can be expanded into many different applications based on their mode of action and market size along with their novel fermentation strategies in the food industry. While most of these enzymes are produced with the help of microbial fermentations at industrial scales, the new and innovative technologies such as biofilm reactors, cell-immobilization techniques,

and the use of economical feedstock are also continuously evaluated to enhance the overall enzyme production process (Tables 1 and 2).

Among a broad spectrum of microbial enzymes in the food industry, proteases can be considered as one of the most prominent ones as they approximately represent more than 60% of the hydrolytic enzyme production in the world [56]. There are many applications of proteases in the food industry, specifically in the coagulation of milk to produce cheese, meat tenderization, brewing, and baking processes (Table 3). All such applications require specific operating conditions especially related to the optimum pH, and proteases can be categorized according to their optimum pH into acidic, neutral, and alkaline proteases [56]. The mechanism of action of proteases can be generalized according to their catalytic types based on the types of amino acids present at their active sites. Proteases can be divided into aspartate proteases, serine proteases, cysteine proteases, and metalloproteases [57]. Aspartate proteases cleave a peptide bond between two hydrophobic amino acid residues [57]. Cysteine proteases have a thiol group which upon activation by binding to the substrate attacks the peptide bond as a nucleophile. Serine proteases act in a similar way with the nucleophilic serine at the active site. On the other hand, metalloproteases use the nucleophilic action of water as the steps for peptide bond hydrolysis. On the other hand, protease can also operate under a wide temperature range (20 to 65 °C). The production of protease, therefore, has been a topic of interest for the past few decades because of their chemical nature and culture conditions as shown in Table 1. Owing to their wide range of functional parameters, they have been found in many food processing applications. For example, in case of cheesemaking, their function to digest casein through peptide hydrolysis is imperative for operating at the required pH [58].

Numerous studies are showing the potential of many microbial strains that can be used to produce proteases under different cultural conditions. Among various microbial species for enzyme production, fungal strains represent more than 60% of the total enzyme productions, while other species such as bacteria (24%), *Streptomyces* (4%), and yeast (4%) are also prominent [55]. Table 1 also shows that most of the new research is happening to replace the current solid-state fermentations process by submerged fermentations which are more easily adaptable at the industrial scales. For example, in the research by Elumalai et al. [14], it was observed that agricultural wastes can be used as the feedstock for protease production under submerged conditions at 40 °C and pH 8 [10]. In another submerged fermentation approach, *Rhodotorula mucilaginosa* CBMAI 1528 was used to produce protease by using glucose and casein peptone [11]. The temperature for the growth of this strain was only 20 °C. On the other hand, 60 to 65 °C was evaluated as the optimum temperature by Suleiman et al. showing a wide range of temperature for the production and action of this enzyme [12]. Many other examples of such studies are given in Table 1.

Lipases, on the other hand, are needed in many food industries mainly to enhance or modify the flavors [59]. Lipases help in the hydrolysis of ester linkages [60]. Lipases belong to the α/β hydrolase family with an active serine residue at the active site. Most of the microbial lipases are the esterases that are activated by binding to the lipid–water interface [61]. The cleaving of ester linkages is carried out through a variety of reactions such as esterification, acidolysis, alcoholysis, and hydrolysis [62]. Microbial lipases are prominent in biotechnology for their applications in the lipid–water interface [62]. Among various applications in the food industry, the prominent ones are the obtaining the desirable flavors and the production of modified acylglycerols with the help of interesterification processes carried out by lipases [62]. Lipases can be classified according to the specificity in the substrates and sources of the lipids. There are many different classification systems and microbial lipases are generally classified into fungal, yeast, and bacterial lipases.

The optimum production temperature for lipases is around 30 to 40 °C and the optimum pH can be from 5 to 7 (Table 1). Lipases are produced by many different types of microbial species, but most of the research focus is on fungal strains due to their potential for high enzyme productions (Table 1). While fungal strains are used in solid-state fermentation conditions because of their adaptability to low moisture environments, the submerged

fermentation techniques are being explored at accelerated rates due to their realization at large industrial scales [59]. *A. niger* and *P. fellutanum* are explored under submerged fermentation for lipase production with a temperature range from 30 to 35 °C and pH from 5 to 7 [15,16]. The novelty of such studies is their optimization approach through statistical designs such as response surface methodology. Through such optimization approaches not only optimum fermentation conditions but the optimum concentrations of media components are also determined hence giving an ideal fermentation mode for the specific product and microbial strain.

Many different types of carbohydrases are currently prevalent in the food industry. Carbohydrases are the enzymes that catalyze polysaccharides into oligo- and monosaccharides. Prominent examples include amylases, glucosidases, cellulases, and hemicellulases (Table 1). Among various applications of such enzymes in the food industry, the most prominent ones are the breakdown of starch by amylases and glucosides to produce simple sugars and clarification of juices by cellulases and hemicellulases (Table 3).

For cellulase and hemicellulase production, economical feedstocks, which are high in fiber, can be used. Economical feedstocks are agricultural wastes such as food waste or the byproducts of an industrial process. One example, in this regard, is the use of the byproduct of the corn ethanol industry, which is known as distillers dried grains with solubles or DDGS [19]. These inexpensive feedstocks can provide the essential carbon sources, while additional media elements such as nitrogen sources can further increase enzyme production. For most of these enzymes, *A. niger* strains are being employed and researched for high enzyme activities. Fungal strains especially *A. niger* and *Trichoderma reesei* can produce a wide array of such enzymes in a single fermentation batch [63,64]. This is the main reason that these two strains are researched more extensively for their optimum enzyme production conditions [63,64]. Overall, the production of enzymes through microbial fermentation has been adapted in various industries including the food industry for the last several decades. There are also recent advancements in the field of microbial enzyme productions, and it is important to mention that the market size of enzymes is increasing with every passing year.

Table 2. Some examples of inexpensive feedstocks with their pretreatment methods.

Inexpensive Feedstock	Products	Examples	Pretreatment Conditions	Refs.
Agricultural waste	Enzymes	Crop straw, Poplar wood, sawdust	Grinding	[65,66]
	Other value-added products	Cattle dung, rice straw, wheat straw	Hydrothermal treatment, Mild chemical treatment	[67,68]
Food waste	Enzymes	Banana skin, bagasse	Sulfuric acid hydrolysis	[65,69]
	Monosaccharides	Wheat bran, coffee waste	Mild chemical treatment, Hydrothermal treatment	[70]
	Other value-added products	Cucumber, tomato, lettuce, lemon peel	ultrasonic and ozone pretreatment	[71]
Oceanic seaweed	Lactic acid	Brown, red or green alga	Acid and/or enzymatic hydrolysis	[72]
	Other value-added products	Brown seaweed	Ethanol extraction	[73]

Table 3. Applications of value-added food ingredients from microbial fermentations.

Category	Value-Added Ingredient	Application in Food Industry	Refs.
Enzymes	Protease	Coagulation of milk, Bread quality enhancement, Meat tenderization, Brewing	[74]
	Amylase	Baking, Brewing, Clarification of fruit juices	[74]
	Cellulase	Clarification of fruit juices, Animal feed	[74]
	Hemicellulase	Beer improvement	[75]
Antimicrobials	Nisin	Shelf-life extension	[76]
	Lysozyme	Decreasing the microbial population in food	[76]
	Natamycin	Inhibiting the growth of harmful mold	[77]
Vitamins	B2, B12, K	Improve food quality	[3]
Sweeteners	Sugar Alcohols	Improve the flavor, health concerns, diabetic food industry	[78]
Cultured meat	Non-animal-based meat	Vegetarian/vegan industry	[79]
Stabilizers	Xanthan gum	Shelf-life extension	[80]
	Gellan		[80]
	Curdlan		[80]

2.2. Antimicrobials

For decades, the food industry has been using chemical and physical methods for the preservation to inactivate the harmful pathogenic and spoilage microorganisms, which have contributed to the loss of thousands of lives and billions of dollars [76]. On the other hand, some microorganisms and their natural metabolic products can prevent the growth of other microorganisms. There are many antimicrobial agents such as nisin, natamycin, and lysozymes that can be produced by the microbial fermentation process. Such antimicrobial agents have been approved by Food and Drug Administration (FDA) and the European Food Safety Authority (EFSA) for their safe use in the food preservation industry [76]. The improvement in the fermentation processes for the production of such antimicrobials is an ongoing research area as summarized on Table 1.

Among all of such antimicrobials, nisin is considered one of the most prominent antimicrobials in terms of its ability to improve food safety, quality, and increasing shelf-life [81]. Nisin is an antimicrobial peptide with bactericidal properties by binding to the bacterial cell wall through electrostatic interactions [82]. Then, nisin generates pores in the cell membrane and interrupts cell wall biosynthesis through specific lipid interactions [82].

This microbial peptide has been used in the food industry for many years as a natural and safe preservative. Nisin is effective against a wide array of Gram-positive bacteria and endospores. Therefore, it has been used in the dairy and canned food productions [81]. It is mainly produced by *Lactococcus lactis*, and there are many recent developments in the fermentation process to enhance nisin production (Table 1). One example is the development of biofilms reactors to immobilize *L. lactis* [20]. It has been demonstrated that high level of microbial cells bound to a solid matrix of porous material can result in higher nisin production as compared to the suspended cells reactors [20].

Among various other novel fermentation strategies to enhance the production of nisin, online recovery of nisin during fermentation, foam fractionation, addition of hemin to induce cell respiration, aeration with variable feeding rate, and co-culturing with other microorganisms are most prominent. Zheng et al. [83] reported the increase in the fermentation efficiency with the help of online recovery and foam fractionation. On the other hand, media optimization strategies such as the addition of hemin to stimulate the cell respiration have also been reported [84]. Culture condition optimization such as variable feeding and aeration rates has also proven to be effective in the increase of nisin production [85]. Microbial strains *Yarrowia lipolytica* ATCC18942 and *L. lactis* UTMC106 are co-cultured to enhance nisin production as well [86].

Natamycin is another antimicrobial peptide produced mainly by Actinomycetes including *Streptomyces chattanogenesis* and *Streptomyces natalensis* [77]. Natamycin acts by binding to ergosterol which is a primary sterol in fungal cell wall [87]. Among various food preservations applications, cheese is the most common [77]. Natamycin has low solubility, and therefore it is ideal to apply over the cheese surface. While simple sugars such as glucose can be used as the carbon source, natamycin can be produced at industrial scales by using molasses or soybean meal with the most commonly used microbial strains of *S. natalensis* or *Streptomyces gilvosporeus* [77]. The optimum temperature for this antibiotic production can be between 26 to 30 °C, and pH can be between 6 and 8. All such temperature and pH ranges are determined over the period of extensive research on the increase of this antibiotic production using novel fermentation strategies [77].

Lysozyme is found in many of the organisms in this world including humans. The enzyme acts as the protective mechanism in these organisms against Gram-positive bacteria by breaking the glycosidic bonds in the cell wall, which causes the cell lysis [88]. Lysozyme has been attributed to the extension of shelf life of meat products under refrigerated conditions [89]. Microbial lysozymes can be produced from different strains of *Pichia pastoris* (Table 1). Furthermore, the human lysozyme can be produced by genetically modified strain of *K. lactis* K7, and its production has been greatly enhanced by using biofilm reactors [21]. Strain selection and biofilm reactors are some of the fermentation strategies used recently to enhance lysozyme production. In conclusion, antimicrobial production through microbial fermentation is gaining interest at both research and industrial scales. The potential of using fermentation processes to produce antimicrobials has been explored extensively in recent years, as summarized on Table 1.

2.3. Vitamins

Vitamins are the essential nutrient components that are required for the growth and health of humans. There are more than 30 vitamins, and at least 20 of them are essential for the metabolic functions [3]. Vitamins can either be produced from the chemical process, which can be energy-intensive and toxic for the environment. Microbial fermentation processes, on the other hand, have been recognized as the green “cell factories” for the low-cost production of vitamins [3]. In addition, microbial fermentations result in lesser intensive waste management strategies. Vitamins can be categorized into water-soluble or fat-soluble, and they each have a specific function in almost all the metabolic processes. Therefore, their deficiency can cause serious health problems in humans. Typically, different biotechnological techniques such as genetic engineering, metabolic engineering, media, and culture optimization with the development of special types of bioreactors have been developed and explored for the production of vitamins at industrial scales.

Production of most of the vitamins such as various types of Vitamin B and K takes place in submerged fermentation (Table 1). The majority of the carbon sources are simple sugars such as glucose or other monosaccharides with minerals and nitrogen sources, as mentioned in Table 1. Technical parameters such as optimized temperature, pH, and aeration rates are also mentioned in Table 1. As can be seen in the table, these fermentation parameters can have different ranges for different types of vitamins and microbial strains.

Therefore, it is crucial to know the optimized value according to every vitamin and other microbial products.

A recent trend that is gaining more interest due to the relative applications in scale-up is the development of biofilm reactors for vitamin production [25,26,90]. These biofilm reactors are equipped with plastic composite support (PCS) where the bacterial species can form biofilms and enhance the production of vitamins. In a recent study, Vitamin K was produced successfully under agitated conditions by using biofilm reactors, which will enable the fermentation scale-up easily for commercial production of Vitamin K as opposed to the currently used static fermentation [26]. The fed-batch bioreactors are another type of product enhancement strategy where the media is supplemented at regular intervals for the maximum production of the microbial product. Both of these strategies are being explored for vitamin production especially vitamin K [26].

2.4. Organic Acids

Organic acids are one of the most important platform chemicals that are needed for the production of several products in food and many other industries [91]. For example, lactic acid is used as an acidifier with antimicrobial agent in foods and in packing material. On the other hand, acetic acid is crucial in the production of vinegar, pickles, and some flavors. All such applications make organic acids important in the food industry. Citric acid is another important organic acid in the food industry. According to one estimate, organic acids had a market size of USD 6.94 billion in 2016 which is projected to increase to USD 12.54 billion by 2026 [91]. The overall impact of the increase in the demand for organic acids entails different research strategies to enhance the production through various improvement techniques in microbial fermentation (Table 1). The fermentation conditions are usually within the pH of 5 to 6 and temperature from 30 to 37 °C (Table 1). Among various microbial species, *Lactobacillus*, *Acetobacter*, *Gluconoacetobacter*, and *Gluconobacter* species are the most common for the production of organic acids. Most of these microbial species have been optimized for maximum production of organic acids under optimized culture parameters.

2.5. Sweeteners

Low calories alternatives of sugars in human diet become more attractive for food manufacturers and scientists, with the increasing of diseases and dependance on sugar consumption [78]. Polyols, such as sorbitol, mannitol, maltitol, lactitol, xylitol, and erythritol, are mostly used as a sweetener substitute of sugars, due to their low caloric, cariogenic properties with no effect on insulin resistance features. On the other hand, synthetic sweeteners (thaumatin and aspartame) are also widely used as a food ingredient in various industries [78,92]. Synthetic sweeteners are produced by chemical, enzymatic, and microbial techniques. There has been extensive research in the literature about enhancing the production of sweeteners, and most sweeteners, produced by fermentation, are notably erythritol [93,94]. Table 1, including recent research about fermentative production of sweeteners, shows that fungi, yeast, and bacteria are used for sweetener production. Considering producer microorganisms in Table 1, *Yarrowia lipolytica* and *Moniliella* spp., *Rhodosporidium toruloides* and *Candida* spp., and *Lactobacillus* spp. are preferred for erythritol, arabitol, and mannitol production, respectively [36,95]. Moreover, genetically modified microorganisms are also used for boosting yield by researchers. On the other hand, evaluating different fermentation strategies (Batch, fed-batch, and solid-state fermentation) and the low-cost fermentation media ingredients (Crude glycerol, okara-buckwheat husk, waste oil, peanut press cake, sugarcane molasses, etc.) are also prominent strategies for increasing yield and reducing production costs as summarized in Tables 1 and 2.

2.6. Flavonoids

Flavonoids such as flavones, chalcones, flavanols, and isoflavones are bioactive compounds found in plants that play an active role in many health-promoting properties such as antitumor, antifungal, antiviral, and antibacterial attributes [96]. Therefore, research efforts have been promoted to develop different variations of such compounds. While the major source of such compounds is plants which possess the difficulty of large-scale culture, specific culture requirements, and low abundance of molecules of interest, the increasing demands for such chemical compounds are now met with the idea of producing such compounds in the microbial systems [96]. Various microorganisms have been genetically modified to produce flavonoids with the help of microbial fermentation. Traditional examples include *Escherichia coli* and *Yarrowia lipolytica* [96].

2.7. Cultured Meat Products

The current global population of 7.3 billion is expected to increase to 10 billion by 2050, which will result in the doubling of the demand for proteins which are currently met by an unsustainable meat industry [79]. While plant proteins are proposed as the alternative protein source, they also possess various issues including allergic reactions and low protein content. To solve such problems, a new technology employs cultured muscle cells as an alternative to real meat. This is a relatively a new technique, which is a type of in vitro cell culture technology where the skeletal muscle-derived cells are grown and used as meat for human consumption. The original source of the cells is from the slaughterhouse [79]. While it is still in its infancy stages, various bioreactor techniques can be used to enhance the production of cultured meat products with the help of various optimization strategies [79]. Products such as bio-artificial muscles (BAMs) can be produced using skeletal muscle resident stem cells or satellite cells, but much research is needed to develop technologies where such products can be used as the cultured meat products [97].

2.8. Oligosaccharides and Polysaccharides

Oligosaccharides are generally formed by 2–10 monosaccharides unit such as pentose and hexose and can be defined as an intermediate polymeric carbohydrate between monosaccharides and polysaccharides. They are naturally found in animals, microorganisms and plants [98]. These carbohydrates are commercially obtained from lignocellulosic biomass by physical, chemical, biological, or enzymatic pretreatment methods, and they supplement food products as a prebiotic due to their functional properties [98–100]. Biological pretreatment is known as the degradation of polysaccharides by microbial enzymes or using microorganisms directly (in situ) for producing oligosaccharides [101]. Because of requiring less energy, being eco-friendly, and being an efficient method, biological pretreatment is also used to produce well known oligosaccharides like fructooligosaccharides (FOSs), xylooligosaccharides (XOSs), and manooligosaccharides (MOSs) [98]. In addition to these most used oligosaccharides, galactooligosaccharides (GOSs), pectic oligosaccharides, and human milk oligosaccharides (HMOs) are also produced by biological pretreatment [101,102]. FOSs are produced with sucrose bioconversion, which catalyzed by β -fructofuranosidase and fructosyltransferase enzymes, generally. This bioconversion process begins with enzyme production by fermentation and ending with enzymatic degradation [103]. In recent years, FOS production was carried out with different fermentation strategies such as submerged, solid-state, and co-cultured by using *Aspergillus* sp., *Lactobacillus* sp., *Bifidobacterium longum*, *Leuconostoc mesenteroides*, *Aureobasidium pullulans*, and a mutant strain of *Aspergillus oryzae* (Table 1). Moreover, cashew apple juice, aguamiel, sugarcane bagasse, coffee husk, pineapple peel, prickly pear peel, and banana peel waste were evaluated as alternative substrates (Table 1). XOSs, one of the other important attracted oligosaccharides, can be obtained from xylan and alternative substrates by using enzymes, which are produced by fermentation. Generally, microorganisms, able to produce endo-1,4- β -xylanase enzyme, such as *Aspergillus*, *Fusarium*, *Penicillium*, and *Trichoderma* are main XOS fermentation fungi [104]. Nevertheless, using recombinant enzymes, pro-

duced by *Bacillus subtilis*, and adding an alternative carbon source instead of xylan are promising alternatives (Table 1). MOSs are non-digestible and water-soluble dietary fiber and are used as a nutrient for human intestinal microflora in daily nutrition. MOSs can be produced by enzymatic hydrolysis of mannan and different plant sources. Production of these oligosaccharides is carried out by using of β -mannanase or directly cultivating the β -mannanase producer microorganism, which is *Aspergillus* sp. [5].

Texture properties of food products affect consumer perception, considerably. Accordingly, the production of quality foods in terms of visual and sensory perception is related with the controlling and characterization of rheological properties by some ingredients [105]. Quite a few polymers like exopolysaccharides are used as stabilizers, emulsifiers, and thickening agents in the food industry. This section focused on these polymers, which are produced by fermentation such as β -glucan, pullulan, xanthan gum, bacterial cellulose, gellan, dextran, and curdlan [80]. β -glucans, which are generally used as emulsifier and thickening agents, consist of D-glucose units linked by β -glycosidic linkages [40,106]. Despite bacteria, fungi, and yeast being able to produce β -glucans, fungi (*Aspergillus niger*, *Rhizopus oryzae*, and *Lasiodiplodia theobromae*) were mostly used in recent research (Table 1). The main substrate of β -glucan fermentation is glucose, but alternative substrates such as oat bran, sugarcane straw, soybean molasses, and potato juice were also evaluated (Table 1). Pullulan, produced by *Aureobasidium pullulans* substantially, is composed of repeated maltotriose units. Due to its characteristic properties, Pullulan is used in food products as an additive for stabilization and thickening. Carbon sources of pullulan fermentation include widely alternatives like glucose, fructose, sucrose, and some agro-wastes. Nevertheless, some studies, about the use of genetic modification techniques and/or low-cost medium component, appear in literature for lowering production cost of pullulan [101,107] (Table 1). Unlike β -glucans and pullulans, xanthan gum, consisting of D-glucose, D-mannose, D-glucuronic acid, and pyruvic acid, is a heteropolysaccharide. Xanthan gum is naturally produced by Gram-negative bacteria *Xanthomonas* sp. Through major properties of this polymer such as high viscosity, water solubility, and stability, market size reached about USD 23 million per year and was used for contributing to stabilization and thickening of food products. Using expensive substrates like glucose and sucrose is significantly responsible for high production cost [108,109]. Some studies present strategies in Table 1 for avoiding of fermentation outgoings, which are regarding using alternative carbon sources, optimization of conditions, and using genetical tools.

2.9. Amino Acids

Since the production of monosodium glutamate, amino acids have been evaluated in the food industry as additives to be a flavorant [110]. The market size of amino acids reached nearly USD 25.6 billion, and amino acids, used for animal feed, are the largest part of demand at USD 10.4 billion [111]. This value-added compound can be produced by different methods such as extraction of proteins, chemical synthesis, enzymatic reactions, and fermentation. Fermentation processes can be used for amino acid production in two different ways: one, for production of enzymes to catalyze amino acid synthesis and second for direct amino acid production through fermentation using microorganisms. A great number of different amino acids can be produced by *Corynebacterium glutamicum*, *Brevibacterium* spp., and *Escherichia coli*. Moreover, the most commercially known amino acids, such as glutamic acid, methionine, tryptophan, lysine, tyrosine, phenylalanine, leucine, valine, arginine, histidine, and others, can be produced by these microorganisms (Table 1). Moreover, *C. glutamicum* and *E. coli* can utilize different type of carbon sources, and these bacteria are easily modified by metabolic engineering [112]. Due to those advantages of *C. glutamicum* and *E. coli*, several amino acid production studies were carried out in recent years (Table 1). On the other hand, agricultural biomass was used to boost the yield of amino acid production by genetically modified *C. glutamicum*. For instance, Han et al. extracted biotin from corn leaves to enrich the fermentation medium of glutamic acid. Glutamic acid fermentation was carried out in a bioreactor by using genetically engineered

several studies in the literature on increasing the efficiency of microbial lipid production. Chen et al. studied the effect of methanol addition to the medium on lipid production. Crude glycerol was used as a carbon source in non-sterilized fed-batch fermentation. They showed that methanol could be used to control the growth of contaminants in non-sterilized fermentation while achieving 20.42 g/L of lipid production [123]. On the other hand, the effect of different dissolved oxygen concentrations on lipid production by *Trichosporon oleaginosus* was investigated in order to improve lipid production and reduce energy consumption. It was reported that energy consumption was reduced by 41%, and 11.77 g/L of lipids were produced [124]. Definition and usefulness of fatty acids vary according to length of hydrocarbon chain including double bonds and the location of those bonds. For example, polyunsaturated fatty acids like arachidonic acid, γ -linolenic acid, and eicosapentaenoic acid or lipids, involving these fatty acids, are commonly used in food industry to enrich of foods or to form stabile emulsions [125]. Microbial production of polyunsaturated fatty acids has been trending upward in the last decade in furtherance of meeting the demand and sustainable production. Consequently, there is a lot of research in the literature to improve production by different ways, such using alternative substrate [126,127], isolating new microorganisms [128,129], trying different fermentation techniques [130–132], and metabolic engineering [133–135].

2.13. Alcohols

Alcohols, which refer generally to ethyl alcohol or ethanol, are commonly used biotechnological products in the beverage industry and as bioethanol to reduce fossil fuel consumption. Global alcoholic beverages are beer, wine, and spirits, and especially beer and spirits are the most preferred drinks after water and tea. Ethanol is a product of alcoholic fermentation and can be mainly produced by yeasts [136,137]. Although *Saccharomyces cerevisiae* is the main producer of alcohol, other yeasts such as *Pichia*, *Torulasporea*, *Hanseniaspora*, *Candida*, *Metschnikowia*, *Lachancea*, *Schizosaccharomyces*, and *Brettanomyces* are used in brewing and winemaking fermentations. Mixed culture fermentation is another preferred application for alcoholic fermentation [138]. Moreover, while genetic engineering techniques and recombinant DNA technologies are proven methods for improving production yield, synthetic biology applications such as the *Yeast 2.0 Project* are also promising technologies. On the other hand, some bacteria such as *Zymomonas* spp. can produce ethanol with a different metabolic pathway (the Entner–Doudoroff pathway) [136]. Glycerol, a yeast metabolism byproduct, can be used as a food additive in the food industry. Although it is commonly produced by recovering from byproducts of fat and oil industries, many researchers have become interested in fermentation methods to produce glycerol. Apart from its use as a thickening agent, it is an important compound for the winemaking process. Glycerol may affect sensorial properties of red wine, which is produced by *Saccharomyces* and non-*Saccharomyces* yeast [139,140]. Glycerol can be produced by wide variety of microorganisms such as *Zygosaccharomyces*, *Candida*, and *Kluyveromyces* as yeast; *Rhizopus*, *Aspergillus*, and *Debaryomyces* as fungi; *Bacillus* spp., *Bacterium* spp., and *Lactobacillus* spp. as bacteria; and *Dunaliella* as algae [139].

3. Inexpensive Substrates for Such Fermentations

Only the nutritional need of humans is not sufficient as it is estimated that four billion tons of agricultural and food processing waste will be generated by 2050 [141]. For example, 88 million tons of food waste are generated in only Europe according to the European Commission [142]. Moreover, agricultural and food wastes cause many environmental problems and greenhouse gas emissions. Due to these reasons, management of agricultural and food wastes and evaluation of the production of value-added products are important in terms of a sustainable economy and prevention of environmental pollution. In this section, some agricultural and food wastes, which are used as carbon or nitrogen sources for food ingredient fermentation, are summarized.

3.1. Agricultural Wastes

Agricultural wastes can be categorized as crop residues, livestock wastes, poultry wastes, agro-industrial wastes, pulps, and oil-seed cakes, in general. Some of these materials could be mentioned as leaves, corn stover, rice, wheat, oat, and barley straws (crop residues); eggshells and farm animal skins (poultry wastes); wastewaters of farms (livestock wastes); molasses, sugarcane bagasse, rice husk, vegetables, and pomaces (agro-industrial wastes); and cotton, safflower, sesame, palm kernel, and soybean (oil-seed cakes) (Figure 1). Agricultural wastes require physical, chemical, or biological pretreatment, generally [143]. Much of the research present in the literature is about value-added food ingredient fermentation by using agricultural wastes, which include lignocellulosic structure. Some of these ingredients are erythritol (sugarcane and beet molasses) [33], FOSs (cashews and apple juice) [144], MOSs (wheat bran, rye bran, oat husk, and barley husk) [5], inulinase (sugar beet molasses) [145], β -mannanase (carob pods) [4], Pullulan (corn bran) [46], and microbial lipids (wastepaper enzymatic hydrolysates) [146].

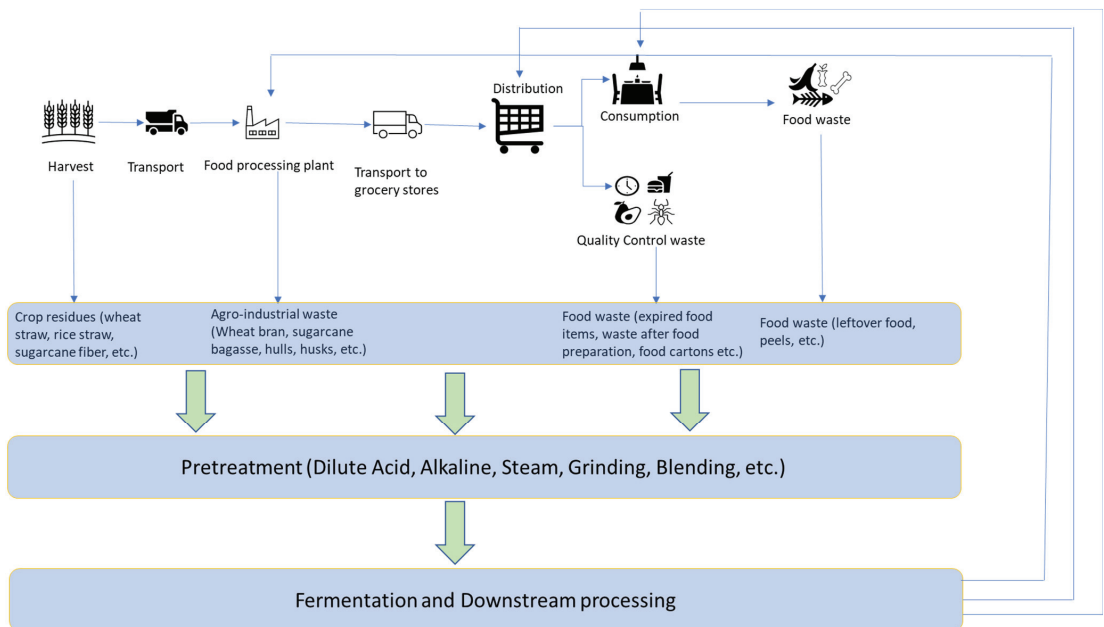


Figure 1. Supply chain of inexpensive feedstock for microbial fermentations.

For instance, by-products of sugar factories and wineries were evaluated in erythritol production by Valsero et al. [33]. Sugar cane molasses, beet molasses, and grape musts were added to the fermentation medium as carbon sources, and 106 g/L of erythritol was produced by shake-flask fermentation with sugar cane molasses medium. Dried and milled agro-industrial wastes, such as sugarcane bagasse, coffee husk, pineapple peel, prickly pear peel, and banana peel waste, were used as substrate for FOS production by solid-state fermentation. It was found that sugar cane bagasse was the most promising substrate [103]. In another study, MOSs were produced by solid-state fermentation from dried and chopped wheat bran, rye bran, oat husk, barley husk, and spent coffee grounds. According to this, the highest MOS production was achieved in the fermentation of spent coffee grounds [5]. Gürler et al. studied the large-scale production of β -mannanase from carob extract. Broken and seedless carob pods were used in fed-batch fermentation after pre-treatment with water extraction. They reported that microparticle-added carob extract is a promising carbon source to produce β -mannanase [4]. Corn bran, an agricultural by-product, was enzymatically pretreated to produce pullulan by shake-flask fermentation. It was found

that more than 19 g/L of pullulan can be produced from hydrolyzed corn bran [46]. Apart from these, fermentation strategies, pretreatment conditions, and productivity of some ingredients produced from wastes are shown in Table 1.

3.2. Food Wastes

Food wastes consist of food processing wastes and kitchen wastes (Figure 1). While processing wastes are generated from the dairy industry, meat processing, vegetable and oil processing, and cereal processing, kitchen wastes are generated from dairies, meats, cereals, fruits, and vegetables at homes, restaurants, and cafeterias [146,147]. Food wastes are mostly rich content sources owing to their inclusion of carbohydrates, proteins, fats, lipids, and inorganic components. Thus, they could be evaluated for bioconversion to energy and production of value-added products by fermentation. Many of food ingredient could be produced by different fermentation strategies with or without using pretreatment [146,148]. Table 2 includes some of these studies about enzymes, monosaccharides, and other value-added products produced by using various food wastes such as cucumber, tomato, lettuce, and lemon peel. Food processing and kitchen wastes can be utilized for food ingredient production as carbon sources. However, more research is needed to find economically feasible and productive methods of this promising bioconversion process [146].

4. Conclusions and Future Perspective

Current advancements in the field of microbial fermentation to produce value-added food ingredients have been discussed with the help of specific examples of enzymes (proteases in cheese making industry, lipases in flavor modification and carbohydrases in juice and baking industries, etc.), antimicrobial agents (nisin, natamycin, lysozyme, etc.), vitamins (Vitamin B, K, etc.), organic acids (citric acid, acetic acid, etc.), sweeteners, flavonoids (flavones, chalcones, flavonols, and isoflavones), cultured meat products (BAMs), stabilizers, emulsifiers, oligosaccharides, amino acids, food colorants (Astaxanthin, carotene, Canthaxanthin, Lycopene, etc.), antioxidants, lipids, fatty acids, thickening agents, and alcohols. While microorganisms can produce many of such food ingredients efficiently and abundantly, the improvement in the basic fermentation processes with the help of genetic engineering, metabolic editing, and optimization is still an ongoing research topic. The future holds many possibilities to produce microbial products as food ingredients which will be safe, natural, and environmentally friendly. More studies should be performed to optimize the microbial production process parameters such as temperature, pH, and aeration at larger scales. The design of new bioreactor techniques such as biofilm reactors should also be a focus to cause the adaptation of microbial production at larger scales. In addition, the design of new bioreactors for innovative research products such as cultured meats should be researched. The fermentation sector also promises to utilize organic waste of food industries thus recycling most of the resources back into value-added products.

Author Contributions: Conceptualization, A.D. and I.T.; validation, A.I., A.O., A.D., and I.T.; formal analysis, A.D. and I.T.; investigation, A.I. and A.O.; resources, A.D.; writing—original draft preparation, A.I. and A.O.; writing—review and editing, A.D. and I.T.; supervision, A.D. and I.T.; project administration, A.D.; funding acquisition, A.D. All authors have read and agreed to the published version of the manuscript.

Funding: This research was funded by USDA National Institute of Food and Agriculture Federal Appropriations under Project PEN04671 and Accession number 1017582.

Data Availability Statement: Data can be provided as needed.

Acknowledgments: This work was supported in part by FULBRIGHT Student Program by providing scholarship to Attia Iram.

Conflicts of Interest: The authors declare no conflict of interest.

References

- Marti-Quijal, F.J.; Khubber, S.; Remize, F.; Tomasevic, I.; Roselló-Soto, E.; Barba, F.J. Obtaining antioxidants and natural preservatives from food by-products through fermentation: A review. *Fermentation* **2021**, *7*, 106. [CrossRef]
- Zhang, Y.; He, S.; Simpson, B.K. Enzymes in food bioprocessing—Novel food enzymes, applications, and related techniques. *Curr. Opin. Food Sci.* **2018**, *19*, 30–35. [CrossRef]
- Wang, Y.; Liu, L.; Jin, Z.; Zhang, D. Microbial Cell Factories for Green Production of Vitamins. *Front. Bioeng. Biotechnol.* **2021**, *9*, 473. [CrossRef]
- Gürler, H.N.; Erkan, S.B.; Ozcan, A.; Yilmazer, C.; Karahalil, E.; Germec, M.; Yatmaz, E.; Ogel, Z.B.; Turhan, I. Scale-up processing with different microparticle agent for β -mannanase production in a large-scale stirred tank bioreactor. *J. Food Process. Preserv.* **2021**, *45*, e14915. [CrossRef]
- Yilmazer, C.; Germec, M.; Turhan, I. Solid-state fermentation for the production of a recombinant β -mannanase from *Aspergillus fumigatus* expressed in *Aspergillus sojae* grown on renewable resources. *J. Food Process. Preserv.* **2021**, *45*, e14584. [CrossRef]
- Liu, X.; Yu, X.; Zhang, T.; Wang, Z.; Xu, J.; Xia, J.; He, A.; Yan, Y.; Xu, J. Novel two-stage solid-state fermentation for erythritol production on okara-buckwheat husk medium. *Bioresour. Technol.* **2018**, *266*, 439–446. [CrossRef]
- Zhou, H.Y.; Wu, W.J.; Xu, Y.Y.; Zhou, B.; Niu, K.; Liu, Z.Q.; Zheng, Y.G. Calcium Carbonate Addition Improves L-Methionine Biosynthesis by Metabolically Engineered *Escherichia coli* W3110-BL. *Front. Bioeng. Biotechnol.* **2020**, *8*, 300. [CrossRef] [PubMed]
- Nobre, C.; Gonçalves, D.A.; Teixeira, J.A.; Rodrigues, L.R. One-step co-culture fermentation strategy to produce high-content fructo-oligosaccharides. *Carbohydr. Polym.* **2018**, *201*, 31–38. [CrossRef] [PubMed]
- Guo, Q.; Zaved, H.; Zhang, H.; Wang, X.; Yun, J.; Zhang, G.; Yang, M.; Sun, W.; Qi, X. Optimization of fermentation medium for a newly isolated yeast strain (*Zygosaccharomyces rouxii* JM-C46) and evaluation of factors affecting biosynthesis of D-arabitol. *LWT* **2019**, *99*, 319–327. [CrossRef]
- Elumalai, P.; Lim, J.-M.; Park, Y.-J.; Cho, M.; Shea, P.J.; Oh, B.-T. Agricultural waste materials enhance protease production by *Bacillus subtilis* B22 in submerged fermentation under blue light-emitting diodes. *Bioprocess Biosyst. Eng.* **2020**, *43*, 821–830. [CrossRef]
- Lario, L.D.; Pillaca-Pullo, O.S.; Sette, L.D.; Converti, A.; Casati, P.; Spampinato, C.; Pessoa, A. Optimization of protease production and sequence analysis of the purified enzyme from the cold adapted yeast *Rhodotorula mucilaginosa* CBMAI 1528. *Biotechnol. Reports* **2020**, *28*, e00546. [CrossRef]
- Suleiman, A.D.; Rahman, A.; Mohd Yusof, H.; Mohd Shariff, F.; Yasid, N.A. Effect of cultural conditions on protease production by a thermophilic *Geobacillus thermoglucosidasius* SKF4 isolated from Sungai Klah hot Spring Park, Malaysia. *Molecules* **2020**, *25*, 2609. [CrossRef]
- Rocha, F.T.B.; Brandão-Costa, R.M.P.; Neves, A.G.D.; Cardoso, K.B.B.; Nascimento, T.P.; Albuquerque, W.W.C.; Porto, A.L.F. Purification and characterization of a protease from *Aspergillus sydowii* URM5774: Coffee ground residue for protease production by solid state fermentation. *An. Acad. Bras. Cienc.* **2021**, *93*. [CrossRef] [PubMed]
- Mumecha, T.K.; Zewde, F.T. Alkaline protease production using eggshells and membrane-based substrates: Process modeling, optimization, and evaluation of detergent potency. *Eng. Appl. Sci. Res.* **2021**, *48*, 171–180.
- Ma, X.; Kexin, Z.; Yonggang, W.; Ebadi, A.G.; Toughani, M. Optimization of Low-Temperature Lipase Production Conditions and Study on Enzymatic Properties of *Aspergillus Niger*. *Iran. J. Chem. Eng.* **2021**, *40*, 1364–1374.
- Amin, M.; Bhatti, H.N.; Sadaf, S.; Bilal, M. Optimization of lipase production by response surface methodology and its application for efficient biodegradation of polyester vylon-200. *Catal. Letters* **2021**, *151*, 3603–3616. [CrossRef]
- Izmirlioglu, G.; Demirci, A. Strain selection and medium optimization for glucoamylase production from industrial potato waste by *Aspergillus niger*. *J. Sci. Food Agric.* **2016**, *96*, 2788–2795. [CrossRef] [PubMed]
- Balakrishnan, M.; Jeevarathinam, G.; Kumar, S.K.S.; Muniraj, I.; Uthandi, S. Optimization and scale-up of α -amylase production by *Aspergillus oryzae* using solid-state fermentation of edible oil cakes. *BMC Biotechnol.* **2021**, *21*, 33. [CrossRef] [PubMed]
- Iram, A.; Cekmecelioglu, D.; Demirci, A. Salt and nitrogen amendment and optimization for cellulase and xylanase production using dilute acid hydrolysate of distillers' dried grains with solubles (DDGS) as the feedstock. *Bioprocess Biosyst. Eng.* **2022**, *45*, 527–540. [CrossRef]
- Bastarrachea, L.J.; Britt, D.W.; Demirci, A. Development of Bioactive Solid Support for Immobilized *Lactococcus lactis* Biofilms in Bioreactors for the Production of Nisin. *Food Bioprocess Technol.* **2022**, *15*, 132–143. [CrossRef]
- Ercan, D.; Demirci, A. Production of human lysozyme in biofilm reactor and optimization of growth parameters of *Kluyveromyces lactis* K7. *Appl. Microbiol. Biotechnol.* **2013**, *97*, 6211–6221. [CrossRef] [PubMed]
- Ercan, D.; Demirci, A. Enhanced human lysozyme production in biofilm reactor by *Kluyveromyces lactis* K7. *Biochem. Eng. J.* **2014**, *92*, 2–8. [CrossRef]
- He, H.; Wu, S.; Mei, M.; Ning, J.; Li, C.; Ma, L.; Zhang, G.; Yi, L. A combinational strategy for effective heterologous production of functional human lysozyme in *Pichia pastoris*. *Front. Bioeng. Biotechnol.* **2020**, *8*, 118. [CrossRef]
- Xie, C.; Coda, R.; Chamlagain, B.; Edelmann, M.; Varmanen, P.; Piironen, V.; Katina, K. Fermentation of cereal, pseudo-cereal and legume materials with *Propionibacterium freudenreichii* and *Levilactobacillus brevis* for vitamin B12 fortification. *LWT* **2021**, *137*, 110431. [CrossRef]
- Mahdinia, E.; Demirci, A.; Berenjian, A. Optimization of *Bacillus subtilis* natto growth parameters in glycerol-based medium for vitamin K (menaquinone-7) production in biofilm reactors. *Bioprocess Biosyst. Eng.* **2018**, *41*, 195–204. [CrossRef] [PubMed]

26. Mahdinia, E.; Demirci, A.; Berenjian, A. Implementation of fed-batch strategies for vitamin K (menaquinone-7) production by *Bacillus subtilis* natto in biofilm reactors. *Appl. Microbiol. Biotechnol.* **2018**, *102*, 9147–9157. [CrossRef]
27. Turhan, I.; Bialka, K.L.; Demirci, A.; Karhan, M. Enhanced lactic acid production from carob extract by *Lactobacillus casei* using invertase pretreatment. *Food Biotechnol.* **2010**, *24*, 364–374. [CrossRef]
28. Chen, P.-T.; Hong, Z.-S.; Cheng, C.-L.; Ng, I.-S.; Lo, Y.-C.; Nagarajan, D.; Chang, J.-S. Exploring fermentation strategies for enhanced lactic acid production with polyvinyl alcohol-immobilized *Lactobacillus plantarum* 23 using microalgae as feedstock. *Bioresour. Technol.* **2020**, *308*, 123266. [CrossRef]
29. Ali, R.; Saravia, F.; Hille-Reichel, A.; Gescher, J.; Horn, H. Propionic acid production from food waste in batch reactors: Effect of pH, types of inoculum, and thermal pre-treatment. *Bioresour. Technol.* **2021**, *319*, 124166. [CrossRef]
30. Zheng, S.; Jiang, B.; Zhang, T.; Chen, J. Combined mutagenesis and metabolic regulation to enhance d-arabitol production from *Candida parapsilosis*. *J. Ind. Microbiol. Biotechnol.* **2020**, *47*, 425–435. [CrossRef]
31. Yang, L.B.; Kong, W.; Yang, W.; Li, D.; Zhao, S.; Wu, Y.; Zheng, S. High D-arabitol production with osmotic pressure control fed-batch fermentation by *Yarrowia lipolytica* and proteomic analysis under nitrogen source perturbation. *Enzyme Microb. Technol.* **2022**, *152*, 109936. [CrossRef] [PubMed]
32. Liu, X.; Dong, X.; Chen, S.; Yan, Y.; He, J.; Xu, J.; Xu, J. Enhancing erythritol production by wheat straw biochar-incorporated solid-state fermentation of agricultural wastes using defatted *Schizochytrium* sp. biomass as supplementary feedstock. *Ind. Crops Prod.* **2021**, *170*, 113703. [CrossRef]
33. Hijosa-Valsero, M.; Garita-Cambronero, J.; Paniagua-García, A.I.; Díez-Antolínez, R. By-products of sugar factories and wineries as feedstocks for erythritol generation. *Food Bioprod. Process.* **2021**, *126*, 345–355. [CrossRef]
34. Deshpande, M.S.; Kulkarni, P.P.; Kumbhar, P.S.; Ghosalkar, A.R. Erythritol production from sugar based feedstocks by *Moniliella pollinis* using lysate of recycled cells as nutrients source. *Process Biochem.* **2022**, *112*, 45–52. [CrossRef]
35. Rice, T.; Sahin, A.W.; Lynch, K.M.; Arendt, E.K.; Coffey, A. Isolation, characterisation and exploitation of lactic acid bacteria capable of efficient conversion of sugars to mannitol. *Int. J. Food Microbiol.* **2020**, *321*, 108546. [CrossRef]
36. Hijosa-Valsero, M.; Garita-Cambronero, J.; Paniagua-García, A.I.; Díez-Antolínez, R. Mannitol bioproduction from surplus grape musts and wine lees. *LWT* **2021**, *151*, 112083. [CrossRef]
37. de la Rosa, O.; Muñoz-Marquez, D.B.; Contreras-Esquivel, J.C.; Wong-Paz, J.E.; Rodríguez-Herrera, R.; Aguilar, C.N. Improving the fructooligosaccharides production by solid-state fermentation. *Biocatal. Agric. Biotechnol.* **2020**, *27*, 101704. [CrossRef]
38. Nasir, A.; Sattar, F.; Ashfaq, I.; Lindemann, S.R.; Chen, M.H.; Van den Ende, W.; Öner, E.T.; Kirtel, O.; Khaliq, S.; Ghauri, M.A.; et al. Production and characterization of a high molecular weight levan and fructooligosaccharides from a rhizospheric isolate of *Bacillus aryabhatai*. *LWT* **2020**, *123*, 109093. [CrossRef]
39. Han, S.; Pan, L.; Zeng, W.; Yang, L.; Yang, D.; Chen, G.; Liang, Z. Improved production of fructooligosaccharides (FOS) using a mutant strain of *Aspergillus oryzae* S719 overexpressing β -fructofuranosidase (FTase) genes. *LWT* **2021**, *146*, 111346. [CrossRef]
40. Abdeshahian, P.; Ascencio, J.J.; Philippini, R.R.; Antunes, F.A.F.; dos Santos, J.C.; da Silva, S.S. Utilization of sugarcane straw for production of β -glucan biopolymer by *Lasiodiplodia theobromae* CCT 3966 in batch fermentation process. *Bioresour. Technol.* **2020**, *314*, 123716. [CrossRef]
41. Bzducha-Wróbel, A.; Koczko, P.; Błażej, S.; Kozera, J.; Kieliszek, M. Valorization of Deproteinated Potato Juice Water into β -Glucan Preparation of *C. utilis* Origin: Comparative Study of Preparations Obtained by Two Isolation Methods. *Waste Biomass Valorization* **2020**, *11*, 3257–3271. [CrossRef]
42. Acosta, S.B.P.; Marchioro, M.L.K.; Santos, V.A.Q.; Calegari, G.C.; Lafay, C.B.B.; Barbosa-Dekker, A.M.; Dekker, R.F.H.; da Cunha, M.A.A. Valorization of Soybean Molasses as Fermentation Substrate for the Production of Microbial Exocellular β -Glucan. *J. Polym. Environ.* **2020**, *28*, 2149–2160. [CrossRef]
43. Chen, X.; Wang, Y.; He, C.Y.; Wang, G.L.; Zhang, G.C.; Wang, C.L.; Wang, D.H.; Zou, X.; Wei, G.Y. Improved production of β -glucan by a T-DNA-based mutant of *Aureobasidium pullulans*. *Appl. Microbiol. Biotechnol.* **2021**, *105*, 6887–6898. [CrossRef] [PubMed]
44. Rishi, V.; Sandhu, A.K.; Kaur, A.; Kaur, J.; Sharma, S.; Soni, S.K. Utilization of kitchen waste for production of pullulan to develop biodegradable plastic. *Appl. Microbiol. Biotechnol.* **2020**, *104*, 1307–1317. [CrossRef]
45. He, C.; Zhang, Z.; Zhang, Y.; Wang, G.; Wang, C.; Wang, D.; Wei, G. Efficient pullulan production by *Aureobasidium pullulans* using cost-effective substrates. *Int. J. Biol. Macromol.* **2021**, *186*, 544–553. [CrossRef]
46. Haghghatpanah, N.; Khodaiyan, F.; Kennedy, J.F.; Hosseini, S.S. Optimization and characterization of pullulan obtained from corn bran hydrolysates by *Aureobasidium pullulans* KY767024. *Biocatal. Agric. Biotechnol.* **2021**, *33*, 101959. [CrossRef]
47. Singh, R.S.; Saini, G.K.; Kennedy, J.F. Pullulan production in stirred tank reactor by a colour-variant strain of *Aureobasidium pullulans* FB-1. *Carbohydr. Polym. Technol. Appl.* **2021**, *2*, 100086. [CrossRef]
48. Alharbi, N.S.; Kadaikunnan, S.; Khaled, J.M.; Almana, T.N.; Innasimuthu, G.M.; Rajoo, B.; Alanzi, K.F.; Rajaram, S.K. Optimization of glutamic acid production by *Corynebacterium glutamicum* using response surface methodology. *J. King Saud Univ.-Sci.* **2020**, *32*, 1403–1408. [CrossRef]
49. Fahimitabar, A.; Razavian, S.M.H.; Rezaei, S.A. Application of RSM for optimization of glutamic acid production by *Corynebacterium glutamicum* in bath culture. *Heliyon* **2021**, *7*, e07359. [CrossRef]
50. Tang, X.L.; Du, X.Y.; Chen, L.J.; Liu, Z.Q.; Zheng, Y.G. Enhanced production of l-methionine in engineered *Escherichia coli* with efficient supply of one carbon unit. *Biotechnol. Lett.* **2020**, *42*, 429–436. [CrossRef]

51. Li, Z.; Ding, D.; Wang, H.; Liu, L.; Fang, H.; Chen, T.; Zhang, D. Engineering *Escherichia coli* to improve tryptophan production via genetic manipulation of precursor and cofactor pathways. *Synth. Syst. Biotechnol.* **2020**, *5*, 200–205. [CrossRef]
52. Lim, Y.H.; Foo, H.L.; Loh, T.C.; Mohamad, R.; Rahim, R.A. Rapid evaluation and optimization of medium components governing tryptophan production by *Pediococcus acidilactici* tp-6 isolated from Malaysian food via statistical approaches. *Molecules* **2020**, *25*, 779. [CrossRef]
53. Guo, L.; Ding, S.; Liu, Y.; Gao, C.; Hu, G.; Song, W.; Liu, J.; Chen, X.; Liu, L. Enhancing tryptophan production by balancing precursors in *Escherichia coli*. *Biotechnol. Bioeng.* **2022**, *119*, 983–993. [CrossRef]
54. Xu, J.Z.; Ruan, H.Z.; Yu, H.B.; Liu, L.M.; Zhang, W. Metabolic engineering of carbohydrate metabolism systems in *Corynebacterium glutamicum* for improving the efficiency of l-lysine production from mixed sugar. *Microb. Cell Fact.* **2020**, *19*, 39. [CrossRef] [PubMed]
55. Siddiqui, A.J.; Singh, R.; Jahan, S.; Alreshidi, M.; Hamadou, W.S.; Khan, A.; Ahmad, A.; Patel, M.; Abdelmuhsin, A.A.; Sulieman, A.M.E.; et al. Enzymes in Food Fermentations. In *African Fermented Food Products- New Trends*; Elhadi Sulieman, A.M., Adam Mariod, A., Eds.; Springer International Publishing: Cham, Switzerland, 2022; pp. 101–133. ISBN 978-3-030-82902-5.
56. Hyseni, B.; Aytakin, A.Ö.; Nikerel, E. Solid state fermentation for enzyme production for food industry. *J. Microbiol. Biotechnol. Food Sci.* **2021**, *2021*, 615–622. [CrossRef]
57. Shah, M.A.; Mir, S.A.; Paray, M.A. Plant proteases as milk-clotting enzymes in cheesemaking: A review. *Dairy Sci. Technol.* **2014**, *94*, 5–16. [CrossRef]
58. Visser, S. Proteolytic enzymes and their relation to cheese ripening and flavor: An overview. *J. Dairy Sci.* **1993**, *76*, 329–350. [CrossRef]
59. Fatima, S.; Faryad, A.; Ataa, A.; Joyia, F.A.; Parvaiz, A. Microbial lipase production: A deep insight into the recent advances of lipase production and purification techniques. *Biotechnol. Appl. Biochem.* **2021**, *68*, 445–458. [CrossRef] [PubMed]
60. Mala, J.G.S.; Takeuchi, S. Understanding Structural Features of Microbial Lipases—An Overview. *Anal. Chem. Insights* **2008**, *3*, ACI-S551. [CrossRef]
61. Hilton, S.; Buckley, J.T. Studies on the reaction mechanism of a microbial lipase/acyltransferase using chemical modification and site-directed mutagenesis. *J. Biol. Chem.* **1991**, *266*, 997–1000. [CrossRef]
62. Pandey, A.; Benjamin, S.; Soccol, C.R.; Nigam, P.; Krieger, N.; Soccol, V.T. The realm of microbial lipases in biotechnology. *Biotechnol. Appl. Biochem.* **1999**, *29*, 119–131. [PubMed]
63. Iram, A.; Cekmecelioglu, D.; Demirci, A. Screening of bacterial and fungal strains for cellulase and xylanase production using distillers' dried grains with solubles (DDGS) as the main feedstock. *Biomass Convers. Biorefinery* **2020**, *11*, 1955–1964. [CrossRef]
64. Iram, A.; Cekmecelioglu, D.; Demirci, A. Ideal Feedstock and Fermentation Process Improvements for the Production of Lignocellulolytic Enzymes. *Processes* **2021**, *9*, 38. [CrossRef]
65. Wang, F.; Xu, L.; Zhao, L.; Ding, Z.; Ma, H.; Terry, N. Fungal laccase production from lignocellulosic agricultural wastes by solid-state fermentation: A review. *Microorganisms* **2019**, *7*, 665. [CrossRef]
66. Raina, N.; Slathia, P.S.; Sharma, P. Experimental optimization of thermochemical pretreatment of sal (*Shorea robusta*) sawdust by Central Composite Design study for bioethanol production by co-fermentation using *Saccharomyces cerevisiae* (MTCC-36) and *Pichia stipitis* (NCIM-3498). *Biomass Bioenergy* **2020**, *143*, 105819. [CrossRef]
67. Chen, L.; Yang, X.; Raza, W.; Luo, J.; Zhang, P.; Shen, Q. Solid-state fermentation of agro-industrial wastes to produce bioorganic fertilizer for the biocontrol of *Fusarium* wilt of cucumber in continuously cropped soil. *Bioresour. Technol.* **2011**, *102*, 3900–3910. [CrossRef]
68. Kumar, V.; Bahuguna, A.; Ramalingam, S.; Kim, M. Developing a sustainable bioprocess for the cleaner production of xylooligosaccharides: An approach towards lignocellulosic waste management. *J. Clean. Prod.* **2021**, *316*, 128332. [CrossRef]
69. Panakkal, E.J.; Sriariyanun, M.; Ratanapoompinyo, J.; Yasurin, P.; Cheenkachorn, K.; Rodiahwati, W.; Tantayotai, P. Influence of sulfuric acid pretreatment and inhibitor of sugarcane bagasse on the production of fermentable sugar and ethanol. *Appl. Sci. Eng. Prog.* **2022**, *15*. [CrossRef]
70. Javed, U.; Ansari, A.; Aman, A.; Qader, S.A.U. Fermentation and saccharification of agro-industrial wastes: A cost-effective approach for dual use of plant biomass wastes for xylose production. *Biocatal. Agric. Biotechnol.* **2019**, *21*, 101341. [CrossRef]
71. Greses, S.; Tomás-Pejó, E.; Gonzalez-Fernandez, C. Agroindustrial waste as a resource for volatile fatty acids production via anaerobic fermentation. *Bioresour. Technol.* **2020**, *297*, 122486. [CrossRef]
72. Lin, H.-T.V.; Huang, M.-Y.; Kao, T.-Y.; Lu, W.-J.; Lin, H.-J.; Pan, C.-L. Production of lactic acid from seaweed hydrolysates via lactic acid bacteria fermentation. *Fermentation* **2020**, *6*, 37. [CrossRef]
73. Hoffmann, S.L.; Kohlstedt, M.; Jungmann, L.; Hutter, M.; Poblete-Castro, I.; Becker, J.; Wittmann, C. Cascaded valorization of brown seaweed to produce l-lysine and value-added products using *Corynebacterium glutamicum* streamlined by systems metabolic engineering. *Metab. Eng.* **2021**, *67*, 293–307. [CrossRef]
74. Raveendran, S.; Parameswaran, B.; Beevi Ummalyma, S.; Abraham, A.; Kuruvilla Mathew, A.; Madhavan, A.; Rebello, S.; Pandey, A. Applications of microbial enzymes in food industry. *Food Technol. Biotechnol.* **2018**, *56*, 16–30. [CrossRef]
75. Bhat, M.K. Cellulases and related enzymes in biotechnology. *Biotechnol. Adv.* **2000**, *18*, 355–383. [CrossRef]
76. El-Saber Batiha, G.; Hussein, D.E.; Algammal, A.M.; George, T.T.; Jeandet, P.; Al-Snafi, A.E.; Tiwari, A.; Pagnossa, J.P.; Lima, C.M.; Thorat, N.D.; et al. Application of natural antimicrobials in food preservation: Recent views. *Food Control* **2021**, *126*, 108066. [CrossRef]

77. Meena, M.; Prajapati, P.; Ravichandran, C.; Sehrawat, R. Natamycin: A natural preservative for food applications—A review. *Food Sci. Biotechnol.* **2021**, *30*, 1481–1496. [CrossRef] [PubMed]
78. Carochi, M.; Morales, P.; Ferreira, I.C.F.R. Sweeteners as food additives in the XXI century: A review of what is known, and what is to come. *Food Chem. Toxicol.* **2017**, *107*, 302–317. [CrossRef]
79. Hong, T.K.; Shin, D.-M.; Choi, J.; Do, J.T.; Han, S.G. Current issues and technical advances in cultured meat production: A review. *Food Sci. Anim. Resour.* **2021**, *41*, 355. [CrossRef]
80. Yildiz, H.; Karatas, N. Microbial exopolysaccharides: Resources and bioactive properties. *Process Biochem.* **2018**, *72*, 41–46. [CrossRef]
81. Brum, L.F.W.; dos Santos, C.; Zimnoch Santos, J.H.; Brandelli, A. Structured silica materials as innovative delivery systems for the bacteriocin nisin. *Food Chem.* **2022**, *366*, 130599. [CrossRef] [PubMed]
82. Prince, A.; Sandhu, P.; Ror, P.; Dash, E.; Sharma, S.; Arakha, M.; Jha, S.; Akhter, Y.; Saleem, M. Lipid-II independent antimicrobial mechanism of nisin depends on its crowding and degree of oligomerization. *Sci. Rep.* **2016**, *6*, 37908. [CrossRef]
83. Zheng, H.; Zhang, D.; Guo, K.; Dong, K.; Xu, D.; Wu, Z. Online recovery of nisin during fermentation coupling with foam fractionation. *J. Food Eng.* **2015**, *162*, 25–30. [CrossRef]
84. Kördikanhoğlu, B.; Şimşek, Ö.; Saris, P.E.J. Nisin production of *Lactococcus lactis* N 8 with hemin-stimulated cell respiration in fed-batch fermentation system. *Biotechnol. Prog.* **2015**, *31*, 678–685. [CrossRef]
85. Jiang, L.; Liu, Y.; Yan, G.; Cui, Y.; Cheng, Q.; Zhang, Z.; Meng, Q.; Teng, L.; Ren, X. Aeration and fermentation strategies on nisin production. *Biotechnol. Lett.* **2015**, *37*, 2039–2045. [CrossRef]
86. Ariana, M.; Hamed, J. Enhanced production of nisin by co-culture of *Lactococcus lactis* sub sp. *lactis* and *Yarrowia lipolytica* in molasses based medium. *J. Biotechnol.* **2017**, *256*, 21–26. [CrossRef]
87. Davidson, P.M.; Doan, C. Natamycin. In *Antimicrobials in Food*; CRC Press: Boca Raton, FL, USA, 2020; pp. 339–356. ISBN 0429058195.
88. Masschalck, B.; Michiels, C.W. Antimicrobial properties of lysozyme in relation to foodborne vegetative bacteria. *Crit. Rev. Microbiol.* **2003**, *29*, 191–214. [CrossRef]
89. Leśniewski, G.; Yang, T. Lysozyme and its modified forms: A critical appraisal of selected properties and potential. *Trends Food Sci. Technol.* **2021**, *107*, 333–342. [CrossRef]
90. Mahdini, E.; Demirci, A.; Berenjian, A. Utilization of glucose-based medium and optimization of *Bacillus subtilis* natto growth parameters for vitamin K (menaquinone-7) production in biofilm reactors. *Biocatal. Agric. Biotechnol.* **2018**, *13*, 219–224. [CrossRef]
91. Duan, Y.; Mehariya, S.; Kumar, A.; Singh, E.; Yang, J.; Kumar, S.; Li, H.; Kumar Awasthi, M. Apple orchard waste recycling and valorization of valuable product-A review. *Bioengineered* **2021**, *12*, 476–495. [CrossRef]
92. Paulino, B.N.; Molina, G.; Pastore, G.M.; Bicas, J.L. Current perspectives in the biotechnological production of sweetening syrups and polyols. *Curr. Opin. Food Sci.* **2021**, *41*, 36–43. [CrossRef]
93. Rice, T.; Zannini, E.; Arendt, E.K.; Coffey, A. A review of polyols—biotechnological production, food applications, regulation, labeling and health effects. *Crit. Rev. Food Sci. Nutr.* **2020**, *60*, 2034–2051. [CrossRef]
94. Felipe Hernández-Pérez, A.; Jofre, F.M.; De Souza Queiroz, S.; Vaz De Arruda, P.; Chandel, A.K.; Felipe, M.D.G.D.A. Biotechnological production of sweeteners. In *Biotechnological Production of Bioactive Compounds*; Elsevier: Amsterdam, The Netherlands, 2019; pp. 261–292. ISBN 9780444643230.
95. Liu, X.; Yu, X.; Gao, S.; Dong, X.; Xia, J.; Xu, J.; He, A.; Hu, L.; Yan, Y.; Wang, Z. Enhancing the erythritol production by *Yarrowia lipolytica* from waste oil using loofah sponge as oil-in-water dispersant. *Biochem. Eng. J.* **2019**, *151*, 107302. [CrossRef]
96. Goris, T.; Pérez-Valero, Á.; Martínez, I.; Yi, D.; Fernández-Calleja, L.; San Leon, D.; Bornscheuer, U.T.; Magadán-Corpas, P.; Lombo, F.; Nogales, J. Repositioning microbial biotechnology against COVID-19: The case of microbial production of flavonoids. *Microb. Biotechnol.* **2021**, *14*, 94–110. [CrossRef]
97. Post, M.J. Cultured meat from stem cells: Challenges and prospects. *Meat Sci.* **2012**, *92*, 297–301. [CrossRef]
98. Yue, P.; Hu, Y.; Tian, R.; Bian, J.; Peng, F. Hydrothermal pretreatment for the production of oligosaccharides: A review. *Bioresour. Technol.* **2022**, *343*, 126075. [CrossRef]
99. Bhatia, L.; Sharma, A.; Bachheti, R.K.; Chandel, A.K. Lignocellulose derived functional oligosaccharides: Production, properties, and health benefits. *Prep. Biochem. Biotechnol.* **2019**, *49*, 744–758. [CrossRef]
100. Su, Z.; Luo, J.; Li, X.; Pinelo, M. Enzyme membrane reactors for production of oligosaccharides: A review on the interdependence between enzyme reaction and membrane separation. *Sep. Purif. Technol.* **2020**, *243*, 116840. [CrossRef]
101. Mano, M.C.R.; Neri-Numa, I.A.; da Silva, J.B.; Paulino, B.N.; Pessoa, M.G.; Pastore, G.M. Oligosaccharide biotechnology: An approach of prebiotic revolution on the industry. *Appl. Microbiol. Biotechnol.* **2018**, *102*, 17–37. [CrossRef]
102. Bych, K.; Mikš, M.H.; Johanson, T.; Hederos, M.J.; Vigsnaes, L.K.; Becker, P. Production of HMOs using microbial hosts—From cell engineering to large scale production. *Curr. Opin. Biotechnol.* **2019**, *56*, 130–137. [CrossRef]
103. de la Rosa, O.; Flores-Gallegos, A.C.; Muñoz-Marquez, D.; Nobre, C.; Contreras-Esquivel, J.C.; Aguilar, C.N. Fructooligosaccharides production from agro-wastes as alternative low-cost source. *Trends Food Sci. Technol.* **2019**, *91*, 139–146. [CrossRef]
104. Santibáñez, L.; Henríquez, C.; Corro-Tejeda, R.; Bernal, S.; Armijo, B.; Salazar, O. Xylooligosaccharides from lignocellulosic biomass: A comprehensive review. *Carbohydr. Polym.* **2021**, *251*, 117118. [CrossRef] [PubMed]
105. Himashree, P.; Sengar, A.S.; Sunil, C.K. Food thickening agents: Sources, chemistry, properties and applications—A review. *Int. J. Gastron. Food Sci.* **2022**, *27*, 100468. [CrossRef]

106. Horue, M.; Rivero Berti, I.; Cacicedo, M.L.; Castro, G.R. Microbial production and recovery of hybrid biopolymers from wastes for industrial applications- a review. *Bioresour. Technol.* **2021**, *340*, 125671. [CrossRef]
107. Babbar, N.; Dejonghe, W.; Gatti, M.; Sforza, S.; Elst, K. Pectic oligosaccharides from agricultural by-products: Production, characterization and health benefits. *Crit. Rev. Biotechnol.* **2016**, *36*, 594–606. [CrossRef]
108. Singh, R.S.; Kaur, N.; Kennedy, J.F. Pullulan production from agro-industrial waste and its applications in food industry: A review. *Carbohydr. Polym.* **2019**, *217*, 46–57. [CrossRef]
109. Barcelos, M.C.S.; Vespermann, K.A.C.; Pelissari, F.M.; Molina, G. Current status of biotechnological production and applications of microbial exopolysaccharides. *Crit. Rev. Food Sci. Nutr.* **2020**, *60*, 1475–1495. [CrossRef]
110. D'Este, M.; Alvarado-Morales, M.; Angelidaki, I. Amino acids production focusing on fermentation technologies—A review. *Biotechnol. Adv.* **2018**, *36*, 14–25. [CrossRef]
111. Wendisch, V.F. Metabolic engineering advances and prospects for amino acid production. *Metab. Eng.* **2020**, *58*, 17–34. [CrossRef]
112. Zhang, G.; Ren, X.; Liang, X.; Wang, Y.; Feng, D.; Zhang, Y.; Xian, M.; Zou, H. Improving the Microbial Production of Amino Acids: From Conventional Approaches to Recent Trends. *Biotechnol. Bioprocess Eng.* **2021**, *26*, 708–727. [CrossRef]
113. Han, X.; Li, L.; Bao, J. Microbial extraction of biotin from lignocellulose biomass and its application on glutamic acid production. *Bioresour. Technol.* **2019**, *288*, 121523. [CrossRef]
114. Coban, H.B.; Demirci, A.; Patterson, P.H.; Elias, R.J. Enhanced phenylpyruvic acid production with *Proteus vulgaris* in fed-batch and continuous fermentation. *Prep. Biochem. Biotechnol.* **2016**, *46*, 157–160. [CrossRef] [PubMed]
115. Rana, B.; Bhattacharyya, M.; Patni, B.; Arya, M.; Joshi, G.K. The Realm of Microbial Pigments in the Food Color Market. *Front. Sustain. Food Syst.* **2021**, *5*, 54. [CrossRef]
116. Sen, T.; Barrow, C.J.; Deshmukh, S.K. Microbial pigments in the food industry—Challenges and the way forward. *Front. Nutr.* **2019**, *6*, 7. [CrossRef]
117. Lin, Y.; Jain, R.; Yan, Y. Microbial production of antioxidant food ingredients via metabolic engineering. *Curr. Opin. Biotechnol.* **2014**, *26*, 71–78. [CrossRef]
118. Chandra, P.; Sharma, R.K.; Arora, D.S. Antioxidant compounds from microbial sources: A review. *Food Res. Int.* **2020**, *129*, 108849. [CrossRef] [PubMed]
119. Foong, L.C.; Loh, C.W.L.; Ng, H.S.; Lan, J.C.W. Recent development in the production strategies of microbial carotenoids. *World J. Microbiol. Biotechnol.* **2021**, *37*, 12. [CrossRef] [PubMed]
120. Bhanja Dey, T.; Chakraborty, S.; Jain, K.K.; Sharma, A.; Kuhad, R.C. Antioxidant phenolics and their microbial production by submerged and solid state fermentation process: A review. *Trends Food Sci. Technol.* **2016**, *53*, 60–74. [CrossRef]
121. Béligon, V.; Christophe, G.; Fontanille, P.; Larroche, C. Microbial lipids as potential source to food supplements. *Curr. Opin. Food Sci.* **2016**, *7*, 35–42. [CrossRef]
122. Kuttiraja, M.; Dhouha, A.; Tyagi, R.D. Harnessing the Effect of pH on Lipid Production in Batch Cultures of *Yarrowia lipolytica* SKY7. *Appl. Biochem. Biotechnol.* **2018**, *184*, 1332–1346. [CrossRef]
123. Chen, J.; Zhang, X.; Tyagi, R.D.; Drogui, P. Utilization of methanol in crude glycerol to assist lipid production in non-sterilized fermentation from *Trichosporon oleaginosus*. *Bioresour. Technol.* **2018**, *253*, 8–15. [CrossRef]
124. Zhang, X.; Chen, J.; Wu, D.; Li, J.; Tyagi, R.D.; Surampalli, R.Y. Economical lipid production from *Trichosporon oleaginosus* via dissolved oxygen adjustment and crude glycerol addition. *Bioresour. Technol.* **2019**, *273*, 288–296. [CrossRef] [PubMed]
125. Bellou, S.; Triantaphyllidou, I.E.; Aggeli, D.; Elazzazy, A.M.; Baeshen, M.N.; Aggelis, G. Microbial oils as food additives: Recent approaches for improving microbial oil production and its polyunsaturated fatty acid content. *Curr. Opin. Biotechnol.* **2016**, *37*, 24–35. [CrossRef] [PubMed]
126. Laddha, H.; Pawar, P.R.; Prakash, G. Bioconversion of waste acid oil to docosahexaenoic acid by integration of “ex novo” and “de novo” fermentation in *Aurantiochytrium limacinum*. *Bioresour. Technol.* **2021**, *332*, 125062. [CrossRef] [PubMed]
127. Zhang, T.Y.; Wu, Y.H.; Wang, J.H.; Wang, X.X.; Deantes-Espinosa, V.M.; Dao, G.H.; Tong, X.; Hu, H.Y. Heterotrophic cultivation of microalgae in straw lignocellulose hydrolysate for production of high-value biomass rich in polyunsaturated fatty acids (PUFA). *Chem. Eng. J.* **2019**, *367*, 37–44. [CrossRef]
128. Estupiñán, M.; Hernández, I.; Saitua, E.; Bilbao, M.E.; Mendibil, I.; Ferrer, J.; Alonso-sáez, L. Novel *Vibrio* spp. Strains Producing Omega-3 Fatty Acids Isolated from Coastal Seawater. *Mar. Drugs* **2020**, *18*, 99. [CrossRef]
129. Wang, Q.; Ye, H.; Sen, B.; Xie, Y.; He, Y.; Park, S.; Wang, G. Improved production of docosahexaenoic acid in batch fermentation by newly-isolated strains of *Schizochytrium* sp. and *Thraustochytriidae* sp. through bioprocess optimization. *Synth. Syst. Biotechnol.* **2018**, *3*, 121–129. [CrossRef]
130. Du, Z.Y.; Alvaro, J.; Hyden, B.; Zienkiewicz, K.; Benning, N.; Zienkiewicz, A.; Bonito, G.; Benning, C. Enhancing oil production and harvest by combining the marine alga *Nannochloropsis oceanica* and the oleaginous fungus *Mortierella elongata*. *Biotechnol. Biofuels* **2018**, *11*, 174. [CrossRef]
131. Cordova, L.T.; Alper, H.S. Production of α -linolenic acid in *Yarrowia lipolytica* using low-temperature fermentation. *Appl. Microbiol. Biotechnol.* **2018**, *102*, 8809–8816. [CrossRef]
132. Arbter, P.; Sinha, A.; Troesch, J.; Utesch, T.; Zeng, A.P. Redox governed electro-fermentation improves lipid production by the oleaginous yeast *Rhodospiridium toruloides*. *Bioresour. Technol.* **2019**, *294*, 122122. [CrossRef]
133. Santos-Merino, M.; Garcillán-Barcia, M.P.; De La Cruz, F. Engineering the fatty acid synthesis pathway in *Synechococcus elongatus* PCC 7942 improves omega-3 fatty acid production. *Biotechnol. Biofuels* **2018**, *11*, 239. [CrossRef]

134. Liu, H.H.; Wang, C.; Lu, X.Y.; Huang, H.; Tian, Y.; Ji, X.J. Improved Production of Arachidonic Acid by Combined Pathway Engineering and Synthetic Enzyme Fusion in *Yarrowia lipolytica*. *J. Agric. Food Chem.* **2019**, *67*, 9851–9857. [CrossRef] [PubMed]
135. Geng, L.; Chen, S.; Sun, X.; Hu, X.; Ji, X.; Huang, H.; Ren, L. Fermentation performance and metabolomic analysis of an engineered high-yield PUFA-producing strain of *Schizochytrium* sp. *Bioprocess Biosyst. Eng.* **2019**, *42*, 71–81. [CrossRef]
136. Walker, G.M.; Walker, R.S.K. *Enhancing Yeast Alcoholic Fermentations*; Elsevier Ltd.: Amsterdam, The Netherlands, 2018; Volume 105, ISBN 9780128151815.
137. Sahu, L.; Panda, S.K. Innovative Technologies and Implications in Fermented Food and Beverage Industries: An Overview. In *Innovations in Technologies for Fermented Food and Beverage Industries*; Springer: Cham, Switzerland, 2018; pp. 1–23. ISBN 9783319748207.
138. Alperstein, L.; Gardner, J.M.; Sundstrom, J.F.; Sumbly, K.M.; Jiraneck, V. Yeast bioprospecting versus synthetic biology—Which is better for innovative beverage fermentation? *Appl. Microbiol. Biotechnol.* **2020**, *104*, 1939–1953. [CrossRef]
139. Taherzadeh, M.J.; Adler, L.; Lidén, G. Strategies for enhancing fermentative production of glycerol—A review. *Enzyme Microb. Technol.* **2002**, *31*, 53–66. [CrossRef]
140. Ivit, N.N.; Longo, R.; Kemp, B. The Effect of Non-Saccharomyces and Saccharomyces Non-Cerevisiae Yeasts on Ethanol and Glycerol Levels in Wine. *Fermentation* **2020**, *6*, 77. [CrossRef]
141. Duque-Acevedo, M.; Belmonte-Ureña, L.J.; Cortés-García, F.J.; Camacho-Ferre, F. Agricultural waste: Review of the evolution, approaches and perspectives on alternative uses. *Glob. Ecol. Conserv.* **2020**, *22*, e00902. [CrossRef]
142. Celli, I.; Brunori, E.; Eugeni, M.; Cristinariu, C.A.; Zampilli, M.; Massoli, S.; Bartocci, P.; Caldarelli, V.; Saetta, S.; Bidini, G.; et al. Development of a tool to optimize economic and environmental feasibility of food waste chains. *Biomass Convers. Biorefinery* **2022**, *12*, 4307–4320. [CrossRef]
143. Koul, B.; Yakoob, M.; Shah, M.P. Agricultural waste management strategies for environmental sustainability. *Environ. Res.* **2022**, *206*, 112285. [CrossRef]
144. Kaprasob, R.; Kerchoechuen, O.; Laohakunjit, N.; Somboonpanyakul, P. B vitamins and prebiotic fructooligosaccharides of cashew apple fermented with probiotic strains *Lactobacillus* spp., *Leuconostoc mesenteroides* and *Bifidobacterium longum*. *Process Biochem.* **2018**, *70*, 9–19. [CrossRef]
145. Germec, M.; Turhan, I. Kinetic modeling and sensitivity analysis of inulinase production in large-scale stirred tank bioreactor with sugar beet molasses-based medium. *Biochem. Eng. J.* **2021**, *176*, 108201. [CrossRef]
146. Sindhu, R.; Gnansounou, E.; Rebello, S.; Binod, P.; Varjani, S.; Thakur, I.S.; Nair, R.B.; Pandey, A. Conversion of food and kitchen waste to value-added products. *J. Environ. Manage.* **2019**, *241*, 619–630. [CrossRef] [PubMed]
147. Nayak, A.; Bhushan, B. An overview of the recent trends on the waste valorization techniques for food wastes. *J. Environ. Manage.* **2019**, *233*, 352–370. [CrossRef] [PubMed]
148. Kover, A.; Kraljić, D.; Marinaro, R.; Rene, E.R. Processes for the valorization of food and agricultural wastes to value-added products: Recent practices and perspectives. *Syst. Microbiol. Biomanufacturing* **2022**, *2*, 50–66. [CrossRef]

Disclaimer/Publisher’s Note: The statements, opinions and data contained in all publications are solely those of the individual author(s) and contributor(s) and not of MDPI and/or the editor(s). MDPI and/or the editor(s) disclaim responsibility for any injury to people or property resulting from any ideas, methods, instructions or products referred to in the content.

Article

Synergistic Ball Milling–Enzymatic Pretreatment of Brewer’s Spent Grains to Improve Volatile Fatty Acid Production through Thermophilic Anaerobic Fermentation

Can Liu ¹, Ahamed Ullah ¹, Xin Gao ² and Jian Shi ^{1,*}

¹ Biosystems and Agricultural Engineering, University of Kentucky, Lexington, KY 40546, USA; can.liu@uky.edu (C.L.); ahamed.ullah@uky.edu (A.U.)

² Department of Mechanical Engineering, University of Kentucky, Lexington, KY 40506, USA; xin.gao1@uky.edu

* Correspondence: j.shi@uky.edu; Tel.: +859-218-4321

Abstract: Brewer’s spent grain (BSG) as the major byproduct in the brewing industry is a promising feedstock to produce value-added products such as volatile fatty acids (VFAs). Synergistic ball mill–enzymatic hydrolysis (BM-EH) process is an environmentally friendly pretreatment method for lignocellulosic materials before bioprocessing. This study investigated the potential of raw and BM-EH pretreated BSG feedstocks to produce VFAs through a direct thermophilic anaerobic fermentation process without introducing a methanogen inhibitor. The highest VFA concentration of over 30 g/L was achieved under the high-solid loading fermentation (HS) of raw BSG. The synergistic BM-EH pretreatment helps to increase the cellulose conversion to 70%. Under conventional low TS fermentation conditions, compared to the controlled sample, prolonged pretreatment of the BSG substrate resulted in increased VFA yields from 0.25 to 0.33 g/g_{VS}, and butyric acid became dominant instead of acetic acid.

Keywords: brewer’s spent grain; ball mill–enzymatic hydrolysis pretreatment; thermophilic anaerobic fermentation; volatile fatty acid profile

Citation: Liu, C.; Ullah, A.; Gao, X.; Shi, J. Synergistic Ball Milling–Enzymatic Pretreatment of Brewer’s Spent Grains to Improve Volatile Fatty Acid Production through Thermophilic Anaerobic Fermentation. *Processes* **2023**, *11*, 1648. <https://doi.org/10.3390/pr11061648>

Academic Editors: Ali Demirci, Irfan Turhan and Ehsan Mahdinia

Received: 11 May 2023
Revised: 24 May 2023
Accepted: 25 May 2023
Published: 28 May 2023



Copyright: © 2023 by the authors. Licensee MDPI, Basel, Switzerland. This article is an open access article distributed under the terms and conditions of the Creative Commons Attribution (CC BY) license (<https://creativecommons.org/licenses/by/4.0/>).

1. Introduction

Brewer’s spent grain (BSG) is a major byproduct of the brewing industry, with 40 million wet tons produced annually worldwide [1]. Due to its abundance in lignocellulosic fibrous material and relatively high protein content, BSG is commonly used as animal feed for cattle or poultry [2]. However, fresh BSG has a high moisture content and can perish during storage and transportation, while drying the wet BSG can be energy-intensive and costly. Currently, despite being used as animal feed and a small portion for biogas production, over 20% of BSG is not well-utilized and is disposed of in landfills, releasing millions of tons of CO₂ greenhouse gas equivalent and posing a threat to the environment. In recent years, biorefinery has been investigated as an alternative valorization route to convert this cheap and easily accessible biomass into multiple value-added compounds such as volatile fatty acids (VFAs), amino acids, and second-generation biofuels [2].

In recent years, the biosynthesis of VFAs from biomass has gained much interest in the biorefinery area. Acidogenic fermentation, as a part of the anaerobic digestion (AD) process, can be readily accomplished in well-established AD facilities while yielding products with higher value than biogas [3]. VFAs produced from such mixed-culture systems consist mainly of acetic, propionic, isobutyric, butyric, and valeric acids, which are key platform chemicals widely used in various conventional industries and are currently being researched as a C-source for the synthesis of bioproducts such as lipids [4] and bioplastics [5], among others. It has been found that when food waste is used as feedstock in an acidogenesis process, adjusting the initial substrate/inoculum (S/I) ratio to over three

can suppress methane production and achieve the highest VFA yield of 0.8 g/g_{VS} under optimized conditions [6].

Thermophilic conditions (>50 °C) have been found to facilitate a stable system under higher organic loading, as it enables better mass and heat transfer [3]. Furthermore, a higher temperature could lead to the physicochemical solubilization of the feedstock at the beginning and help build a greater population of cellulolytic and xylanolytic microbes that would boost VFA production under short hydraulic retention time (HRT) [7]. Similar conclusions have been drawn in previous research that shortening the sludge retention time and increasing the temperature efficiently converts microbial communities in the AD system towards accumulating specific VFAs instead of producing methane [8].

In recent years, there have been several studies exploring the production of VFA from BSG using mesophilic acidogenic fermentation systems under various conditions [9–11]. The results indicate that raw BSG can be used as a feedstock in fed-batch AD systems to produce VFA, with the main components being propionic, acetic, and butyric acid. However, due to differences in the origin of the BSG samples and AD conditions, the concentration and composition of VFA produced vary. For example, Sarkar and coworkers studied batch acidogenic fermentation of raw BSG and achieved a VFA recovery of 8.9 g/L rich in acetic and butyric acids under alkaline conditions of pH = 9 [10]. To maximize the utilization of lignocellulosic feedstocks such as BSG, efficient pretreatment processes are needed to improve the hydrolysis and biodegradability and to facilitate the release of fermentable sugars [12,13]. For instance, Guarda et al. [9] used sulfuric acid (3%) at 121 °C to pretreat the BSG sample before feeding the resulting supernatant (neutralized with Ca(OH)₂) into an expanded AD granular sludge bed reactor, achieving higher volumetric VFA productivity with a lower HRT of 2.5 d compared to a previous study [11].

In addition to the aforementioned chemical pretreatment methods using acid or alkaline, ball milling (BM) is a physical pretreatment method to reduce the material size to micro or even nano scale. The reduced particle size provides a high specific surface area and easy access for enzymes and microorganisms, thus facilitating the bioconversion process [12,14,15]. Martin-Sampedro et al. demonstrated that smaller lignocellulosic nanofibrils undergo more rapid and complete hydrolysis when incubated in multicomponent enzyme systems [16]. Therefore, a process intensification approach was developed that integrates ball milling and enzymatic hydrolysis (BM-EH) in a one-pot process, providing an environmentally friendly pretreatment process [17]. This BM-EH process was proved to significantly simplify the pretreatment process and enhance the efficiencies for releasing monosaccharides and the fermentation of different feedstocks such as solid digestate, corn stover, switchgrass, and miscanthus [17].

In this research, the synergistic BM-EH method was optimized for BSG pretreatment and compared with EH pretreatment method alone, with respect to polysaccharides' conversion. The raw and pretreated BSG were subjected to a direct thermophilic anaerobic VFA fermentation process without inducing any methanogen inhibitor. Based on the resultant VFAs profiles and yields, a three-cycle fermentation process was proposed to exhaust the VFAs production potentials by replacing the supernatant during fermentation. This research is the first to explore the whole process to produce VFAs from BM-EH pretreated BSG feedstocks in terms of pretreatment efficiency and the effect of different fermentation strategies.

2. Materials and Methods

2.1. Materials

Wet distillery stillage was collected from Wilderness Trail Distillery (Danville, KY, USA), filtered, and dried at 105 °C to obtain the BSG sample. The BSG sample was then grounded using a 0.75 qt food grinder (WARING COMMERCIAL[®], McConnellsburg, PA, USA) and passed through a No. 7 sieve (2.8 mm) before being stored in an airtight glass jar at room temperature. The enzyme used for enzymatic hydrolysis was a mixture of cellulase (CTec2, Cellic[®]) and hemicellulase (HTec2, Cellic[®]). Both enzymes were from

Novozymes North America (Franklinton, NC, USA). A planetary ball mill (MSK-SFM-1S model, MTI corporation, Richmond, CA, USA) was applied for the ball milling process. The enzymatic hydrolysis process took place in an Innova[®] 42 incubator. The activated sludge was the effluent from an anaerobic digester operated by Quasar Energy Group, LLC (Wooster, OH, USA) that was fed with biosolids (sludge from wastewater treatment plant) and food wastes. The activated sludge was stored at 4 °C upon receipt.

2.2. BSG Pretreatment

The BSG sample underwent various processing methods, including enzymatic hydrolysis only (EH), one cycle (BM-EH-1) or two cycles (BM-EH-2) of BM-EH pretreatment, and a control group treated with autoclaving alone (CTRL), as illustrated in Figure 1. In brief, the dried BSG sample was first prepared to 15% paste with citrate buffer (0.1 M, pH = 5.0) in the ball mill jars and added with milling balls to a balls/wet biomass ratio of around 2.25 (*w/w*). Then, the whole jars were autoclaved at 121 °C for 30 min and cooled to room temperature in an ice bucket before adding enzymes. The sealing ring gaskets used to seal the jars were sterilized by wiping with 75% ethanol. The enzymatic hydrolysis process was carried out under control conditions of 50 °C and 150 rpm shaking. An enzyme mixture consisting of CTec2 and HTec2 at a volume ratio of 1:1 (*v/v*) and a protein dosage of 20 mg/g dry biomass was used. In each BM-EH cycle, the BSG paste was ball milled at 600 rpm for 3 h [17]. To prevent overheating at the high ball milling speed, an optimized strategy was implemented where every after 1 min of continuous ball milling, the machine ceased for 1 min to cool down. As a result, each BM-EH cycle lasted for a total of 6 h. The optimized ball milling strategy and enzyme mixture composition was determined based on previous experiments. In these experiments, the temperature of the BSG paste was monitored under different BM-rest settings and a typical enzyme mixture of CTec2: HTec2 = 9:1 (*v/v*) [17] was compared for the EH pretreatment part.

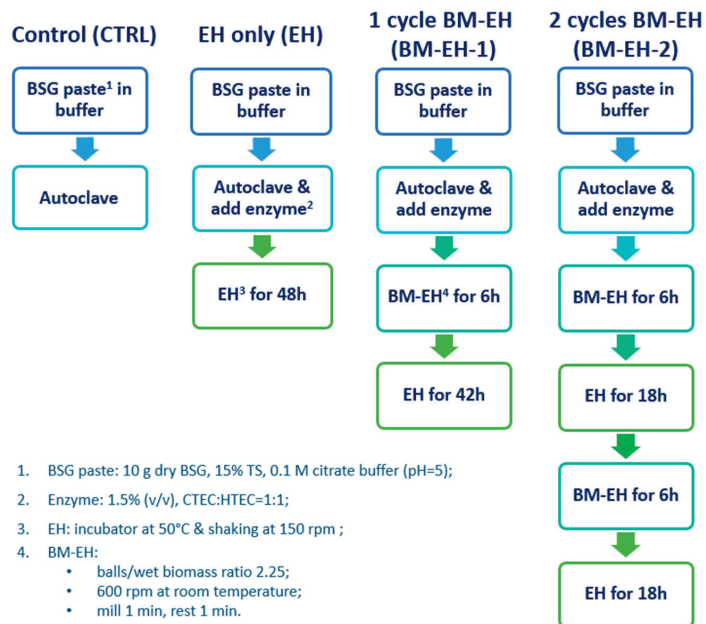


Figure 1. A flowchart of the experiments to pretreat brewer's spent grain (BSG) with an optimized ball milling–enzymatic pretreatment method (EH—enzymatic hydrolysis; BM—ball milling; BM-EH—synergistic ball milling and enzymatic hydrolysis for 1 or 2 cycles).

2.3. Characterization of the Raw and Pretreated BSG Samples

The total solid (TS) content (%) and volatile solid (VS) content (%) of the raw BSG, CTRL sample, and pretreated BSG samples were determined according to the standard methods examination of water and wastewater [18]. The CTRL and pretreated BSG samples were collected and weighed, then the TS weight (g) and VS weight (g) were calculated accordingly. To determine their compositions, a known weight (g) of each sample was centrifuged at 4500 rpm for 40 min, and the supernatant and precipitate were characterized separately. The supernatant was filtered through 0.2 μm nylon filter and the glucose, cellobiose, xylose, and arabinose concentrations were determined using a Dionex Ultimate 3000 HPLC (Dionex Corporation, Sunnyvale, CA, USA) equipped with a refractive index detector and a Biorad Aminex HPX-87H column, applying 5 mM H_2SO_4 as the mobile phase at a flow rate of 0.4 mL/min, and the column temperature was set to 50 $^\circ\text{C}$. The collected precipitate was rinsed four times and dried in a freeze drier before weighing and other characterization. The rest of the samples were frozen at -20 $^\circ\text{C}$ for use in the following fermentation test.

2.3.1. Composition and Proximate and Ultimate Analysis

The structural carbohydrate composition—cellulose, hemicellulose, acid soluble lignin (ASL), and acid insoluble residue (AIR)—of the dried precipitates was measured according to an NREL laboratory analytical procedure [19]. Based on the weight of the wet samples and dried precipitates, the amount of each dissolved or precipitated carbohydrate component was calculated, and the percentage was calibrated accordingly based on raw BSG sample. The calibrated percentage of each component in all samples was calculated by the Equations (1)–(3), where P_i (%), P_j (%), and P_U (%) are the percentage of the precipitating component i (cellulose, hemicellulose, ASL, or AIR), the dissolved component j (glucose, cellobiose, xylose, or arabinose), and the undetected components U , respectively.

$$P_i = \frac{W_{d,s} \times C_{i,s}}{W_{d,r}} \times 100\% \quad (1)$$

$$P_j = \frac{(W_{w,s} - W_{d,s}) \times \frac{C_{j,s}}{F_j}}{W_{d,r}} \times 100\% \quad (2)$$

$$P_U = 1 - P_i - P_j. \quad (3)$$

The subscripts s and r represent the sample s (CTRL, EH, BM-EH-1, or BM-EH-2) and the raw BSG, respectively. W_w (g) is the weight of the wet sample s . W_d (g) is the weight of the freeze-dried sample s or r (raw BSG). C_i (%) is the percentage of component i in the precipitated sample s or r . C_j (g/mL) is the concentration of component j in the supernatant (assuming the density of supernatant to be 1000 kg/m³). F_j is the stoichiometric conversion factor for specific monosaccharides such as glucose, cellobiose, and xylose/arabinose, which are 1.11, 1.055, and 1.14, respectively [17]. The conversion of cellulose and hemicellulose during pretreatment (CTRL, EH, BM-EH-1, or BM-EH-2) was calculated by Equations (4) and (5), respectively, with consistent parameter notation.

$$\text{CNV}_{\text{cellulose},s} = \frac{(W_{w,s} - W_{d,s}) \times (C_{\text{glucose},s}/F_{\text{glucose}} + C_{\text{cellobiose},s}/F_{\text{cellobiose}})}{W_{d,r} \times C_{\text{cellulose},r}} \times 100\%. \quad (4)$$

$$\text{CNV}_{\text{hemicellulose},s} = \frac{(W_{w,s} - W_{d,s}) \times (C_{\text{xylose},s} + C_{\text{arabinose},s})/F_{\text{xylose/arabinose}}}{W_{d,r} \times C_{\text{hemicellulose},r}} \times 100\%. \quad (5)$$

The content of hydrogen, carbon, and nitrogen in the freeze-dried samples, as well as the calibrated volatile matter, fixed carbon, and ash percentage on a dry weight basis, was

measured according to the standard proximate and ultimate analysis procedure (ASTM E870-82) [20].

2.3.2. Surface Morphology Analysis

The surface morphology of the BSG samples subjected to different pretreatment processes was assessed by comparing their respective Scanning Electron Microscopy (SEM) images. To investigate the effect of ball milling alone on the surface morphology, imaging was also performed on the BSG sample treated solely with ball milling. These samples underwent one or two cycles of ball milling, termed as BM-1 and BM-2, respectively (i.e., intermittently milled for 6 or 12 h at the optimized setting). The precipitate of the EH-induced samples (i.e., EH, BM-EH-1, and BM-EH-2) that were rinsed and freeze-dried, as well as the directly freeze-dried BSG samples (i.e., raw BSG, BM-1, and BM-2), was sputter-coated with an ultrathin gold layer and then analyzed using an FEI Quanta 20 FEG instrument at beam accelerating voltages of 5 kV. Furthermore, the surface area of the raw and the only BM-treated BSG samples was analyzed using the Brunauer–Emmett–Teller (BET) method based upon the N₂ adsorption–desorption isotherm. The analysis was conducted at 77 K using a Micrometrics ASAP2020 surface area and porosity analyzer. The raw BSG sample was further ground down to 0.5 mm before use in both morphology analyses to ensure accuracy.

2.3.3. Fourier Transform Infrared Spectroscopy (FTIR) and X-ray Powder Diffraction (XRD)

The impact of ball milling alone and various pretreatment methods on the chemical fingerprinting of the BSG samples was determined using FTIR. Representative samples including the freeze-dried ground raw sample (<0.5 mm) and the sample BM-2, as well as the rinsed and freeze-dried sample CTRL, EH, and BM-EH-2, were selected. FTIR was conducted by a Thermo Nicolet Nexus 870 ATR-FTIR (Thermo Fisher Scientific, Waltham, MA, USA) spectrophotometer, and the spectra were collected using an average of 32 scans over the wavenumber range between 650 and 4000 cm⁻¹ with a spectral resolution of 1.93 cm⁻¹. Baseline correction was performed afterwards using the OMNIC 6.1a software. The powder X-ray diffraction patterns of samples of raw ground BSG (<0.5 mm), BM-1, and BM-2 were collected from 10 to 80° at 0.01°/step using Cu K α X-ray energy produced from a Rigaku SmartLab system.

2.4. Thermophilic AD for VFA Production

The control and pretreated BSG samples were used in an anaerobic fermentation test to produce VFA. To eliminate the pH buffering effect induced by citrate buffer in the CTRL sample and evaluate the actual potential of raw BSG for VFA production, two additional conditions were included: a high-solid fermentation system using dried raw BSG (labeled as 'raw BSG (HS)') and a wet system using raw BSG slurry with the TS adjusted to be in the same range of the pretreated BSG samples (approximately 20% TS, labeled as 'raw BSG') using DI water. The TS and VS of the activated sludge (SLG) and all substrates, as well as the inoculated mixture before and the digestates after the fermentation experiments, were measured according to the standard methods for the examination of water and wastewater [18].

The substrate was inoculated with a fixed substrate/inoculum (S/I) ratio of 3.0 (on VS basis) for all conditions, following acclimation of the SLG inoculum at 55 °C for 1 day. For the raw BSG (HS) condition, 50 mL serum bottles were used, and each bottle was sealed with a rubber stopper and connected to a 1 L gas bag to collect any possibly produced biogas. Since a negligible amount of gas was collected during this test, the subsequent experiments were performed in disposable plastic centrifuge tubes with tightly screwed caps. All containers were placed in an incubator (435 model, Thermo Forma™, Thermo Scientific, Waltham, MA, USA) at 55 °C and were manually vortexed twice a day. This was necessary because the resulting TS values of the mixture after inoculated with sludge remained high, ranging from 12% to 14%, indicating an excessive thickness that impeded

proper flow and mixing under standard shaking conditions. Digestate samples were collected daily to monitor the TS, VS, pH, and VFA concentrations. The samples were centrifuged at 4500 rpm for 10 min, and the pH value and VFA concentrations in the supernatant were measured using the same method as described previously. The VFA concentration contributed by the activated sludge was deducted for all effluent samples.

In order to prevent acid accumulation in the system and enhance the VFA production, a three-cycle fermentation method was evaluated. After 2 days of fermentation and prior to acidification, the supernatant containing the VFAs was separated from the sedimented solids by centrifugation at 4500 rpm for 20 min. The VFA-rich supernatant was then collected, and the precipitate was washed with DI water and refilled with the same amount of DI water for the next two cycles of 2 days' fermentation (6 days in total). The supernatant from the original digestate and the washing effluent after each fermentation cycle were collected and analyzed for the VFA composition to calculate the overall VFA production.

2.5. Statistical Analysis

Statistical analysis was conducted using the data analysis tool in Microsoft Excel or in SigmaPlot 14.0. All experiments were run in replicate ($n = 2$ or 3). An analysis of variance (ANOVA) with a significance level of p -value less than 0.05 was conducted to compare the means.

3. Results and Discussion

3.1. Effects of the BM-EH Pretreatment on BSG to Liberate Monosaccharides

The BM treatment significantly increased the uniformity of the substrate slurry. The milling–rest cycle of either 1 min–1 min or 5 min–5 min strategy was proven to efficiently avoid overheating of the BSG paste, and the temperature remained below 35 °C under both conditions (Figure S1). Compared to the samples that underwent separate BM and EH pretreatment (BM + EH), the samples treated with the synergistic BM-EH process had a darker color and were more liquified. The conversion of cellulose was slightly higher when using the 1 min–1 min milling–rest settings compared to that of 5 min–5 min (Table S1). So, the 1 min–1 min BM strategy was selected for the following experiments.

It is worth noting that when the HTec to CTec ratio was (1:9), the conversion of hemicellulose was relatively low for all conditions (Table S1). Unlike most other raw lignocellulosic biomass or some food waste, the structural carbohydrate analysis of the dry BSG samples revealed that they had a higher hemicellulose content on a weight basis of dry matter ($39.0 \pm 0.5\%$) than cellulose ($28.1\% \pm 0.5\%$). The measured values were consistent with the range of hemicellulose and cellulose content previously reported for BSG by Olszewski et al. [21], which was 21.8–40.2% for hemicellulose and 12.0–25.4% for cellulose. Similar findings were also reported by Zeraatkar Dehnavi [22], where the hemicellulose and cellulose content of the raw BSG samples were found to be in the range of 28.4–32.5% and 15.1–16.8%, respectively. Therefore, to enhance the effectiveness of the BM-EH method in breaking down the hemicellulose-rich BSG substrate, the HTec to CTec ratio was increased to 1:1.

The composition of the raw and pretreated BSG samples were calculated based on the initial total solids and are shown in Figure 2. The slight reduction in the cellulose, hemicellulose, and ASL found in the precipitated CTRL sample was consistent with the decrease in the fixed carbon percentage, which decreased from 16.1% to 9.0% in the precipitate (Table 1). The loss of fixed carbon, as well as the hydrogen, carbon, and nitrogen, contents in the precipitate may be attributed to the soaking process in pH = 5 buffer, which may have converted the mass to small amounts of soluble monosaccharides and other unknown compounds. The reduction in fixed carbon also contributed to the increase in the ash percentage in the precipitate, which was due to the calibration process. Overall, there were limited changes in the overall composition of BSG in the CTRL treatment considering both the solid and leachate.

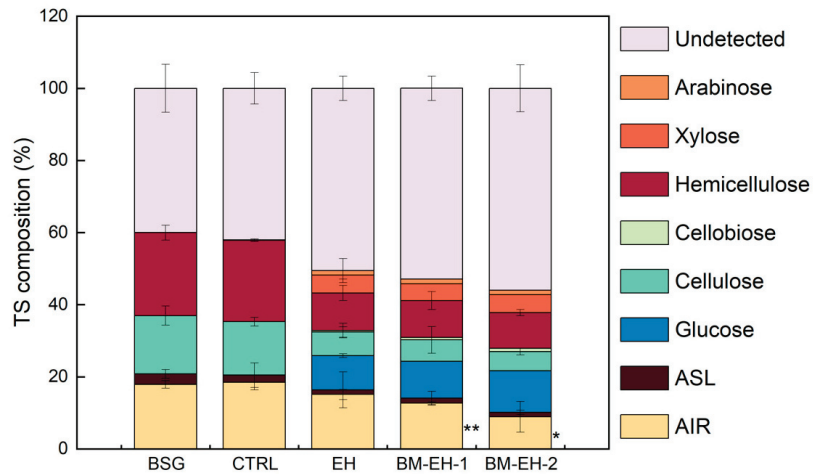


Figure 2. Composition of the BSG samples before and after different pretreatment processes (CTRL—control BSG sample subject with only autoclavation; ASL—acid soluble lignin; AIR—acid insoluble residue). Data are expressed as the mean \pm SD of independent experiments. The statistical significance of the effects of the control and pretreatments on the AIR content was calculated vs. the raw BSG sample (* $p \leq 0.05$, ** $p \leq 0.01$).

Table 1. Characteristics of the raw, control, and pretreated BSG precipitates and the activated sludge (SLG) sample ¹.

Component	BSG	CTRL	EH	BM-EH-1	BM-EH-2	SLG
Volatile Matter, % ²	80.72 \pm 1.18	83.60 \pm 1.68	83.12 \pm 0.81	81.84 \pm 0.93	81.36 \pm 0.70	57.89 \pm 0.58
Fixed Carbon, % ²	16.09 \pm 0.19	8.99 \pm 0.34	10.44 \pm 0.16	11.42 \pm 0.47	11.65 \pm 0.13	1.65 \pm 0.28
Ash, % ²	3.18 \pm 0.33	7.41 \pm 0.49	6.44 \pm 0.51	6.74 \pm 0.09	6.99 \pm 0.28	40.47 \pm 0.48
Hydrogen, %	7.00 \pm 0.10	6.64 \pm 0.04	6.62 \pm 0.17	6.63 \pm 0.08	6.64 \pm 0.06	5.30 \pm 0.16
Carbon, %	47.35 \pm 0.46	45.11 \pm 0.25	44.61 \pm 0.48	44.15 \pm 0.13	43.95 \pm 0.05	28.71 \pm 0.07
Nitrogen, %	4.14 \pm 0.10	3.82 \pm 0.06	3.88 \pm 0.07	3.78 \pm 0.02	3.80 \pm 0.04	4.03 \pm 0.07

¹ Data shown are the average and standard deviation based on replicates. ² All samples were freeze-dried before proximate and ultimate analysis, and the values were calibrated based on dry weight.

As indicated in Figure 3, the conversions of cellulose were 0.3%, 60.2%, 64.9%, and 70.3% for the CTRL, EH, BM-EH-1, and BM-EH-2 conditions, respectively. The cellulose conversion was increased when the synergistic BM-EH process was prolonged from 6 h to 12 h. However, the ball milling had an insignificant effect on the conversion of hemicellulose, as the hemicellulose conversion was around 37% regardless of whether BM was applied or not. The AIR content was lower in the EH sample compared to the CTRL and further decreased with a longer ball milling time. The AIR fraction consists of acid insoluble lignin and ash in BSG, as well as any added insoluble enzymes. The reduction in the AIR content may be attributed to the increased proportion of small-sized AIR particles (e.g., $<1.5 \mu\text{m}$) in the slurry after the more rigorous pretreatment, which could result in a smaller portion being retained on the glass fiber filter and detected.

3.2. Characterization of Materials

The SEM images with lower magnification visually confirmed that the BM-treated samples had significantly smaller particle sizes and decreased density compared to the raw BSG samples (Figure S2a–c). Correspondingly, the BET analysis indicated that the surface area of the samples increased after the BM-1 and BM-2 treatments compared to the raw BSG, with values of 0.714 and 0.994 m^2/g , respectively, compared to 0.541 m^2/g for the

raw BSG. Additionally, the pore volume at a relative pressure of 0.99 also increased from $7.75 \times 10^{-4} \text{ cm}^3/\text{g}$ for the raw BSG to 1.26×10^{-3} and $1.71 \times 10^{-3} \text{ cm}^3/\text{g}$ for the BM-1 and BM-2 treatments, respectively. The BET analysis results also showed that there was a gradual reduction in the BSG particle size as the BM treatment time increased. Nevertheless, it is important to acknowledge that prolonged BM pretreatment results in elevated energy consumption. Ball milling is characterized as an energy-intensive process with high capital investment in mechanical equipment. Therefore, optimizing the operational parameters such as milling time, mode, speed, and other factors becomes vital to minimize the overall costs, particularly in preparation for commercial application [17,23].

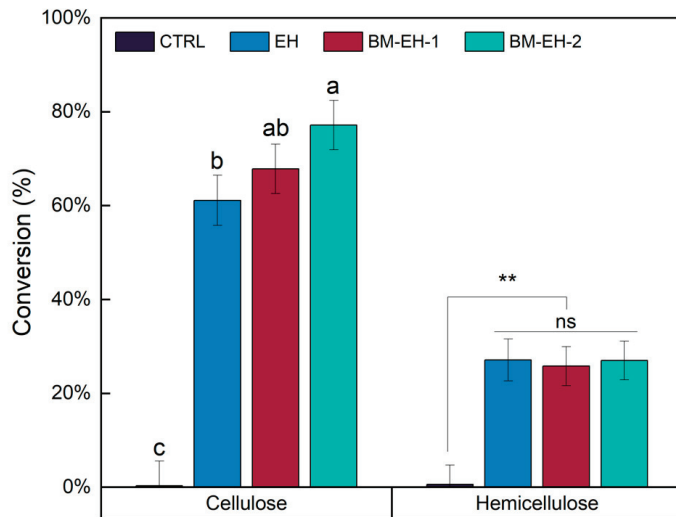


Figure 3. The conversion of cellulose and hemicellulose in the control BSG sample and BSG samples after different pretreatments. Data are expressed as the mean \pm SD of two independent experiments (ns $p > 0.05$, ** $p \leq 0.01$). Different letters on the top of error bars designate significant differences ($p \leq 0.05$) between different pretreatments.

The surface morphology of the materials was more clearly illustrated in the SEM images at higher magnification, as shown in Figure 4. The bulky layer-like structure and rough surface of the raw BSG sample (Figure 4a) were disrupted after BM treatment, resulting in thinner chips with edges that were rich in irregular caves (Figure 4b,c). The small particles on the surface of the raw BSG were not observed in the images of the BM-EH samples, and the structure became less dense after prolonging the ball mill treatment. This finding was in accordance with the loss of the AIR portion, as discussed in the previous section. A simple comparison between the raw and enzymatically hydrolyzed BSG samples (Figure 4a,d) revealed an engraving process of the material surface with the enzymes that resulted in abundant caverns. In addition, when both BM and EH were applied simultaneously (Figure 4e,f), as the pretreatment duration prolonged, the uneven appearance of surface changed from large hollows to numerous tiny holes that formed a sieve-like structure. The change in the surface morphology was expected to provide easier access for acid-producing bacteria and potentially benefit the subsequent fermentation process.

No significant difference was observed in the FTIR spectra between the raw and pretreated BSG samples (Figure S3), suggesting that the chemical structure of the solid residues remained similar after the pretreatment. All the samples showed the characteristic functional group of lignin such as the ester bonds of carboxylic group around 1744 cm^{-1} , C=C bonds in aromatic rings around 1526 cm^{-1} , and aryl-alkyl ether bonds around 1244 cm^{-1} [24]. This observation was consistent with the results from the prox-

imate and ultimate analysis. This is because the lignin component was not specifically removed during the pretreatments. The peaks at 3300 cm^{-1} , 1645 cm^{-1} , and 1036 cm^{-1} in the FTIR spectra are related to polysaccharides, water, and cellulose, respectively, according to previous research [25].

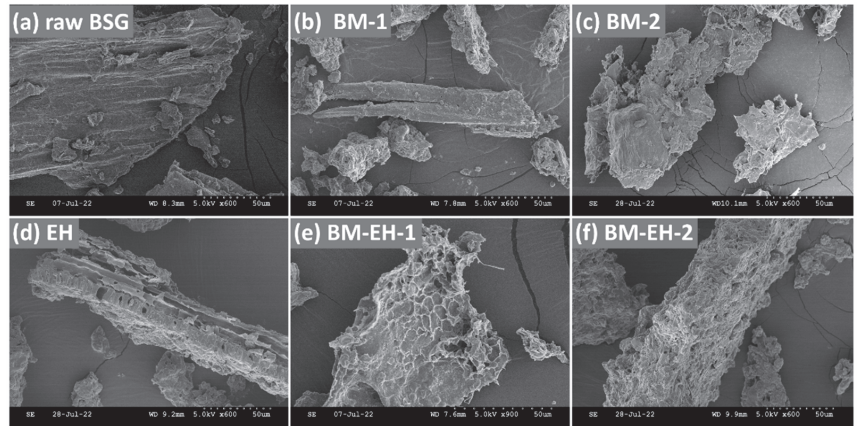


Figure 4. Scanning electron microscopic images at higher magnification for raw BSG and the BSG samples after different pretreatments. BM-1 and BM-2 represent BM for 1 and 2 cycles, respectively.

The XRD spectra of all the untreated and pretreated BSG samples showed no distinct amorphous regions (Figure S4). This result can be explained by the presence of abundant hemicellulose and lignin in the BSG samples, which are amorphous in nature. The crystallinity of plant biomass is primarily contributed by cellulose and is typically determined based on the intensity of the peaks at $2\theta \approx 18^\circ$ and 22° (cellulose crystallinity index (CCI) = $1 - (I_{18}/I_{22})$) [26]. However, in the present study, the combined peaks at around 20° were observed in all samples, which made the conventional calculation method for CCI invalid. Despite this, a reduction in the cellulose crystallinity after BM treatment was still demonstrated by the blunting of the curve of the combined peak for the BM treated BSG samples compared to the raw BSG. This is because the blunting of peaks may be attributed to either the loss of the cellulose partition or the reduction in the cellulose crystallinity, and no cellulose removal process was applied in the tests [27]. This result was consistent with previous studies, which revealed a reduction in the CCI in lignocellulosic biomass and a higher recovery of sugars in the following enzymatic hydrolysis process [28,29].

3.3. VFA Fermentation

The fermentation of the raw BSG (HS) lasted for 10 days, during which a negligible amount of biogas was collected, indicating the successful suppression of methanogenesis. The highest total VFA concentration was obtained within 4 days, reaching a value of 33.7 g/L (i.e., $0.26\text{ g VFA/g substrate VS}$). The rapid accumulation of VFAs and the dramatic drop in the pH from 7.7 to 6.5 indicated an acidification of the system, which was assumed to have inhibited the acidogenic fermentation process. The low pH and increased ionic strength in the system can suppress the dissociation of VFAs, and the un-dissociated species would penetrate into microbial cell and inhibit the metabolic activity [10]. The fermentation process in the other systems also ceased after 4 days, and the change in the pH and VFA composition was determined (Figure 5) to compare the microbial communities' tolerance for VFA accumulation in the acidogenic fermentation systems using the differently pretreated substrates.

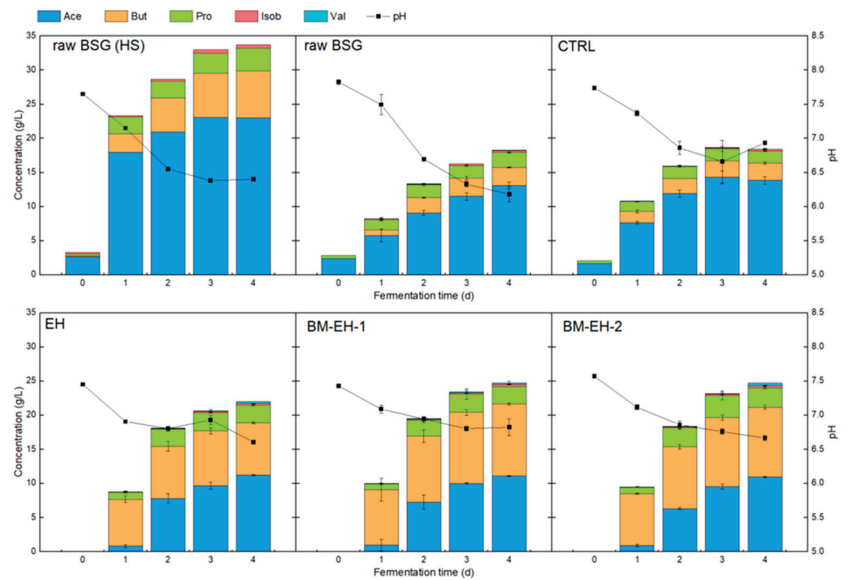


Figure 5. Volatile fatty acid (VFA) composition and pH change in 4 days of thermophilic anaerobic fermentation using raw and various pretreated BSG samples as substrate (raw BSG (HS)—dried raw BSG sample and in high solid fermentation; raw BSG—wet BSG paste (20%) prepared with DI water).

The comparison between the fermentation performance of the raw BSG (HS) and the raw BSG conditions showed that the TS had a significant effect. The fermentation process with a higher TS of 19.5% resulted in a higher maximum overall VFA yield (0.27 g/g VS, Figure 6) than the conventional conditions with a lower TS, demonstrating the acclimation of acid-producing bacteria to higher VFA concentrations under the HS condition. This finding agreed with the suggestion that a high solid condition could enhance the conversion of lignocellulose to VFA [30]. Among the wet systems with a TS of 12~14%, the raw BSG condition had the lowest VFA yield and showed a rapid drop in the pH, which was attributed to the absence of citrate buffer in the system. The citrate buffer induced in the CTRL and pretreated BSG conditions to facilitate the EH process remained in the fermentation system and contributed to maintaining a pH level above 6.5 throughout the fermentation experiment.

The fermentation system utilizing the EH-pretreated BSG substrates (EH, BM-EH-1, and BM-EH-2) outperformed the CTRL system, exhibiting higher VFA concentration and yield. It is noteworthy that all the EH pretreated substrates were converted to a VFA mixture richer in butyric acid than acetic acid, which was the dominant VFA species for the raw BSG and CTRL systems. This result was consistent with a previous study [9] and can be attributed to the elevated concentration of xylose in the hydrolysates [31]. Furthermore, the improved cellulose conversion achieved through the BM-EH pretreatment may have also contributed to the alteration of the VFA profile. The BM-EH-1 and BM-EH-2 conditions achieved VFA concentrations of around 25 g/L and a maximum yield as high as 0.33 g/gVS, which were higher than that obtained with EH pretreatment alone. It is worth noting that the observed increase in the total VFA production was mainly attributed to the increase in the butyric acid concentration. There was no significant difference observed in terms of the VFA concentration and composition between the BM-EH-1 and BM-EH-2 conditions. In all the fermentation systems, the butyric acid was observed to accumulate rapidly within the first day of the experiment, while the production of acetic acid continued and reached its maximum concentration on the third or fourth day.

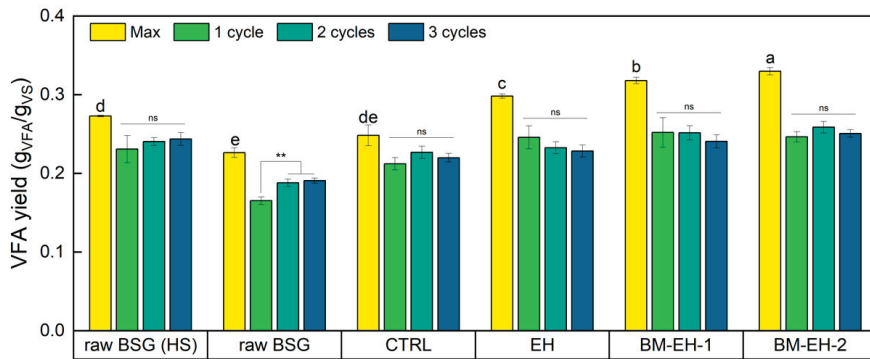


Figure 6. The maximum overall VFA production rate and production rate after 1, 2, and 3 (2d) cycles of fermentation in the thermophilic anaerobic fermentation using raw and various pretreated BSG samples as the substrate. Data are expressed as the mean \pm SD of three independent experiments. The maximum VFA production was compared among different substrates, and the histograms bearing different letters are significantly different ($p \leq 0.05$). The production after 1, 2, and 3 (2d) cycles of fermentation were analyzed for each substrate (ns $p > 0.05$, ** $p \leq 0.01$).

As discussed previously, the accumulation of undissociated acids was considered the primary inhibitor of microbial activity in the systems. Propionic acid, in particular, was identified to have a stronger inhibitory effect at a lower tolerance limit of 1.0–3.2 g/L [32]. The maximum concentration of propionic acid detected in the current research all fell in the same range. Previous research has demonstrated that fermentative microbes can be protected by extracting propionic acid from the digester [33]. So, in the current study, a three-cycle thermophilic anaerobic fermentation method was implemented to remove VFA from the system, aiming to further release the fermentation potential of the organic residues remaining in the precipitate. However, it was found that there was no significant increase in the cumulative VFA yield, as shown in Figure 6. On the contrary, the fermentation process appeared to be interrupted by the direct collecting and washing process. Several reasons may have contributed to this result. Firstly, the removal of alkalinity in the supernatant along with VFA may have led to a reduction in the buffering capacity of the system, which could have contributed to the decrease in acidogenesis activity [34]. Secondly, the collecting and washing process may have broken the anaerobic condition, and the centrifugation step at 4500 rpm and 20 min may also have had a deactivating effect on the microorganisms. Thirdly, the maximum VFA yield was also limited by the nature of the substrate. In comparison to food waste, which can reach a maximum VFA yield of 0.8 g/g_{VS}, BSG is not as easily converted to VFA.

4. Conclusions

BSG was demonstrated to be a suitable substrate to produce short-chain VFAs through anaerobic acid fermentation. Under high solid fermentation condition, the acid-producing bacteria could be acclimated to a higher VFA concentration of over 30 g/L. EH pretreatment helped liberate polysaccharides in the BSG samples, leading to an increased VFA concentration in the fermentation effluent. Furthermore, butyric acid rapidly accumulated and dominated the VFA profile, instead of acetic acid. Simultaneous application of BM and EH resulted in a higher cellulose conversion compared to the EH pretreatment alone, and the conversion increased with the prolonged BM-EH processing time. As a result, the BM-EH pretreatment approach outperformed the EH pretreatment alone and achieved the highest VFA yield of 0.33 g/g_{VS}. Further evaluation is needed to assess the costs and benefits of implementing this approach on a commercial scale, considering the high energy intensity and expenses of BM and EH pretreatments. A direct replacement of the

supernatant containing the accumulated VFAs was found to be an ineffective approach in alleviating VFA inhibition.

Supplementary Materials: The following supporting information can be downloaded at: <https://www.mdpi.com/article/10.3390/pr11061648/s1>, Figure S1: Temperature change of brewer's spent grain (BSG) paste during ball milling with different milling–rest strategies; Figure S2: Scanning electron microscopy images of the raw BSG at lower magnification; Figure S3: Fourier transform infrared spectroscopy spectra of the raw and pretreated BSG samples; Figure S4: X-ray powder diffraction spectra of the raw and ball milled BSG samples; Table S1: BSG composition before and after different pretreatments.

Author Contributions: Conceptualization, C.L. and J.S.; methodology, C.L., A.U. and X.G.; investigation, C.L., A.U. and X.G.; writing—original draft preparation, C.L.; writing—review and editing, J.S., A.U. and X.G.; funding acquisition, J.S. All authors have read and agreed to the published version of the manuscript.

Funding: This work was supported by the USDA National Institute of Food and Agriculture under project accession no. 1018315.

Data Availability Statement: All data generated or analyzed during this study are included in this published article and its Supplementary Information Files.

Acknowledgments: The authors acknowledge Xumeng Ge at Quasar Energy Group for providing activated sludge and Novozymes Inc. for providing enzyme samples.

Conflicts of Interest: The authors declare that they have no known competing financial interest or personal relationships that could have appeared to influence the work reported in this paper.

Abbreviations

EH—enzymatic hydrolysis; BM—ball milling; BM-EH—ball milling and enzymatic hydrolysis; CTRL—control; ASL—acid soluble lignin; AIR—acid insoluble residue; HS—high solid.

References

- Petit, G.; Korbelt, E.; Jury, V.; Aider, M.; Rousselière, S.; Audebrand, L.K.; Turgeon, S.L.; Mikhaylin, S. Environmental Evaluation of New Brewer's Spent Grain Preservation Pathways for Further Valorization in Human Nutrition. *ACS Sustain. Chem. Eng.* **2020**, *8*, 17335–17344. [CrossRef]
- Mitri, S.; Salameh, S.-J.; Khelifa, A.; Leonard, E.; Maroun, R.G.; Louka, N.; Koubaa, M. Valorization of Brewers' spent grains: Pretreatments and Fermentation, a Review. *Fermentation* **2022**, *8*, 50. [CrossRef]
- Wainaina, S.; Lukitawesa; Kumar Awasthi, M.; Taherzadeh, M.J. Bioengineering of anaerobic digestion for volatile fatty acids, hydrogen or methane production: A critical review. *Bioengineered* **2019**, *10*, 437–458. [CrossRef]
- Llamas, M.; Magdalena, J.A.; González-Fernández, C.; Tomás-Pejó, E.J.B. Volatile fatty acids as novel building blocks for oil-based chemistry via oleaginous yeast fermentation. *Biotechnol. Bioeng.* **2020**, *117*, 238–250. [CrossRef] [PubMed]
- Marang, L.; Jiang, Y.; van Loosdrecht, M.C.; Kleerebezem, R.J.B.T. Butyrate as preferred substrate for polyhydroxybutyrate production. *Bioresour. Technol.* **2013**, *142*, 232–239. [CrossRef]
- Lukitawesa; Patinvoh, R.J.; Millati, R.; Sarvari-Horvath, I.; Taherzadeh, M.J. Factors influencing volatile fatty acids production from food wastes via anaerobic digestion. *Bioengineered* **2020**, *11*, 39–52. [CrossRef]
- Shi, J.; Wang, Z.; Stiverson, J.A.; Yu, Z.; Li, Y. Reactor performance and microbial community dynamics during solid-state anaerobic digestion of corn stover at mesophilic and thermophilic conditions. *Bioresour. Technol.* **2013**, *136*, 574–581. [CrossRef]
- Vanwongterghem, I.; Jensen, P.D.; Rabaey, K.; Tyson, G.W. Temperature and solids retention time control microbial population dynamics and volatile fatty acid production in replicated anaerobic digesters. *Sci. Rep.* **2015**, *5*, 8496. [CrossRef]
- Guarda, E.C.; Oliveira, A.C.; Antunes, S.; Freitas, F.; Castro, P.M.L.; Duque, A.F.; Reis, M.A.M. A Two-Stage Process for Conversion of Brewer's Spent Grain into Volatile Fatty Acids through Acidogenic Fermentation. *Appl. Sci.* **2021**, *11*, 3222. [CrossRef]
- Sarkar, O.; Rova, U.; Christakopoulos, P.; Matsakas, L.J.B.T. Influence of initial uncontrolled pH on acidogenic fermentation of brewery spent grains to biohydrogen and volatile fatty acids production: Optimization and scale-up. *Bioresour. Technol.* **2021**, *319*, 124233. [CrossRef]
- Teixeira, M.R.; Guarda, E.C.; Freitas, E.B.; Galinha, C.F.; Duque, A.F.; Reis, M.A.J.N.B. Valorization of raw brewers' spent grain through the production of volatile fatty acids. *New Biotechnol.* **2020**, *57*, 4–10. [CrossRef] [PubMed]
- Kucharska, K.; Rybarczyk, P.; Hołowacz, I.; Łukajtis, R.; Glinka, M.; Kamiński, M.J.M. Pretreatment of lignocellulosic materials as substrates for fermentation processes. *Molecules* **2018**, *23*, 2937. [CrossRef] [PubMed]

13. Zeko-Pivač, A.; Tišma, M.; Žnidaršič-Plazl, P.; Kulisic, B.; Sakellaris, G.; Hao, J.; Planinić, M. The potential of brewer's spent grain in the circular bioeconomy: State of the art and future perspectives. *Biotechnology* **2022**, *10*, 870744.
14. Larsson, S.; Pålsson, B.I.; Parian, M.; Jonsén, P.J.M.E. A novel approach for modelling of physical interactions between slurry, grinding media and mill structure in wet stirred media mills. *Miner. Eng.* **2020**, *148*, 106180. [CrossRef]
15. Sakthivel, S.; Venkatesh, R.P. Solid state synthesis of nano-mineral particles. *Int. J. Min. Sci. Technol.* **2012**, *22*, 651–655. [CrossRef]
16. Martin-Sampedro, R.; Filpponen, I.; Hoeger, I.C.; Zhu, J.Y.; Laine, J.; Rojas, O.J. Rapid and Complete Enzyme Hydrolysis of Lignocellulosic Nanofibrils. *ACS Macro Lett.* **2012**, *1*, 1321–1325. [CrossRef]
17. Zhong, Y.; Frost, H.; Bustamante, M.; Li, S.; Liu, Y.S.; Liao, W.J.R.; Reviews, S.E. A mechano-biocatalytic one-pot approach to release sugars from lignocellulosic materials. *Renew. Sustain. Energy Rev.* **2020**, *121*, 109675. [CrossRef]
18. Rice, E.W.; Baird, R.B.; Eaton, A.D.; Clesceri, L.S. *Standard Methods for the Examination of Water and Wastewater*; American Public Health Association: Washington, DC, USA, 2012; Volume 10.
19. Sluiter, A.; Hames, B.; Ruiz, R.; Scarlata, C.; Sluiter, J.; Templeton, D.; Crocker, D.L.A.P. Determination of structural carbohydrates and lignin in biomass. *Lab. Anal. Proced.* **2008**, *1617*, 1–16.
20. American Society for Testing and Materials. *Standard Test Methods for Analysis of Wood Fuels*; ASTM International: West Conshohocken, PA, USA, 2019.
21. Olszewski, M.; Arauzo, P.; Wądrzyk, M.; Kruse, A.J.J.O.A.; Pyrolysis, A. Py-GC-MS of hydrochars produced from brewer's spent grains. *J. Anal. Appl. Pyrolysis* **2019**, *140*, 255–263. [CrossRef]
22. Zeraatkar Dehnavi, G. *Fractionation of the Main Components of Barley Spent Grains from a Microbrewery*; University of Borås/School of Engineering: Borås, Sweden, 2009.
23. Sitotaw, Y.W.; Habtu, N.G.; Gebreyohannes, A.Y.; Nunes, S.P.; Van Gerven, T. Biorefinery. Ball milling as an important pretreatment technique in lignocellulose biorefineries: A review. *Biomass Convers. Biorefinery* **2021**, 1–24. [CrossRef]
24. Santos, D.M.D.; Bukzem, A.d.L.; Ascheri, D.P.R.; Signini, R.; Aquino, G.L.B.D. Microwave-assisted carboxymethylation of cellulose extracted from brewer's spent grain. *Carbohydr. Polym.* **2015**, *131*, 125–133. [CrossRef] [PubMed]
25. Pereira, P.H.F.; Voorwald, H.C.J.; Cioffi, M.O.H.; Mullinari, D.R.; Da Luz, S.M.; Da Silva, M.L.C.P.J.B. Sugarcane bagasse pulping and bleaching: Thermal and chemical characterization. *BioResources* **2011**, *6*, 2471–2482.
26. Ravindran, R.; Jaiswal, S.; Abu-Ghannam, N.; Jaiswal, A.K. A comparative analysis of pretreatment strategies on the properties and hydrolysis of brewers' spent grain. *Bioresour. Technol.* **2018**, *248*, 272–279. [CrossRef] [PubMed]
27. Mishra, P.K.; Gregor, T.; Wimmer, R. Utilising brewer's spent grain as a source of cellulose nanofibres following separation of protein-based biomass. *BioResources* **2017**, *12*, 107–116. [CrossRef]
28. Lee, J.H.; Kwon, J.H.; Kim, T.H.; Choi, W.I. Impact of planetary ball mills on corn stover characteristics and enzymatic digestibility depending on grinding ball properties. *Bioresour. Technol.* **2017**, *241*, 1094–1100. [CrossRef]
29. Zakaria, M.R.; Fujimoto, S.; Hirata, S.; Hassan, M.A. Ball milling pretreatment of oil palm biomass for enhancing enzymatic hydrolysis. *Appl. Biochem. Biotechnol.* **2014**, *173*, 1778–1789. [CrossRef]
30. Sun, J.; Zhang, L.; Loh, K.C. Review and perspectives of enhanced volatile fatty acids production from acidogenic fermentation of lignocellulosic biomass wastes. *Bioresour. Bioprocess.* **2021**, *8*, 68. [CrossRef]
31. Temudo, M.F.; Mato, T.; Kleerebezem, R.; van Loosdrecht, M.C.M. Xylose anaerobic conversion by open-mixed cultures. *Appl. Microbiol. Biotechnol.* **2009**, *82*, 231–239. [CrossRef]
32. Qiao, W.; Takayanagi, K.; Niu, Q.; Shofie, M.; Li, Y.Y. Long-term stability of thermophilic co-digestion submerged anaerobic membrane reactor encountering high organic loading rate, persistent propionate and detectable hydrogen in biogas. *Bioresour. Technol.* **2013**, *149*, 92–102. [CrossRef]
33. Wang, K.; Chang, Z.; Ma, Y.; Lei, C.; Wang, J.; Zhu, T.; Liu, H.; Zuo, Y.; Li, X. Study on solvent extraction of propionic acid from simulated discharged water in vitamin B12 production by anaerobic fermentation. *Bioresour. Technol.* **2009**, *100*, 2878–2882. [CrossRef]
34. Li, Y.F.; Shi, J.; Nelson, M.C.; Chen, P.H.; Graf, J.; Li, Y.; Yu, Z. Impact of different ratios of feedstock to liquid anaerobic digestion effluent on the performance and microbiome of solid-state anaerobic digesters digesting corn stover. *Bioresour. Technol.* **2016**, *200*, 744–752. [CrossRef] [PubMed]

Disclaimer/Publisher's Note: The statements, opinions and data contained in all publications are solely those of the individual author(s) and contributor(s) and not of MDPI and/or the editor(s). MDPI and/or the editor(s) disclaim responsibility for any injury to people or property resulting from any ideas, methods, instructions or products referred to in the content.

MDPI AG
Grosspeteranlage 5
4052 Basel
Switzerland
Tel.: +41 61 683 77 34

Processes Editorial Office
E-mail: processes@mdpi.com
www.mdpi.com/journal/processes



Disclaimer/Publisher's Note: The title and front matter of this reprint are at the discretion of the Guest Editors. The publisher is not responsible for their content or any associated concerns. The statements, opinions and data contained in all individual articles are solely those of the individual Editors and contributors and not of MDPI. MDPI disclaims responsibility for any injury to people or property resulting from any ideas, methods, instructions or products referred to in the content.



Academic Open
Access Publishing

[mdpi.com](https://www.mdpi.com)

ISBN 978-3-7258-3492-1